VARIABLY SATURATED FLOW BETWEEN STREAMS AND AQUIFERS

by

David M. Peterson

Submitted in Partial Fulfillment of
the Requirements for the Degree of
Doctor of Philosophy

NEW MEXICO INSTITUTE OF MINING AND TECHNOLOGY

Socorro, New Mexico

August, 1988

This dissertation is accepted on behalf of the faculty of the Institute by the following committee:

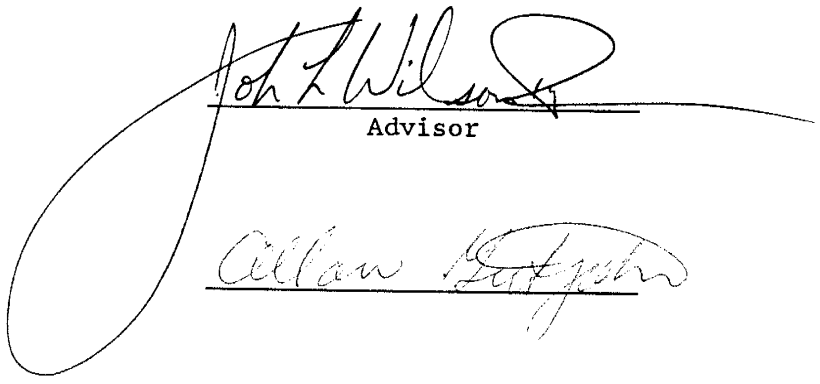

Advisor

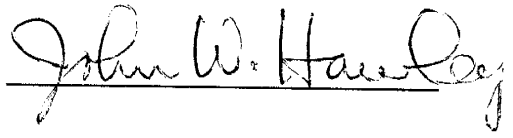

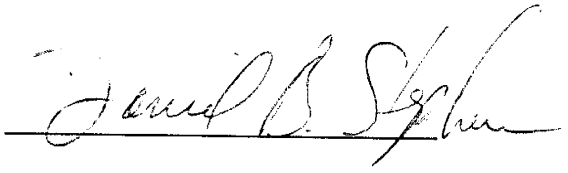

_____

_____

Date

TABLE OF CONTENTS

Table of Contents (con't)

Table of Contents (con't)

Table of Contents (con't)

LIST OF TABLES

LIST OF FIGURES

ABSTRACT

The influence of unsaturated media on stream infiltration has been examined through a series of cross-sectional numerical simulations of combined saturated-unsaturated (variably saturated) flow in simple stream-aquifer systems. System behavior is analyzed largely in terms of response to declines in local water table level, presumably as a result of increased pumping on a regional basis. The simulations, all of which are of a generic nature, are roughly based on existing and possible future conditions in the Mesilla Valley portion of the lower Rio Grande Valley in south-central New Mexico. Several stream-aquifer relationships are considered, with particular emphasis being placed on cases in which a zone of unsaturated aquifer material lies between the streambed and the underlying water table. Under this latter set of conditions, the stream and aquifer are described in this study as being disconnected, although stream water still continues to infiltrate the subsurface and eventually recharges the deeper saturated zones of the aquifer. Factors that strongly influence the disconnection process include streambed clogging by fine-grained materials and aquifer heterogeneity, primarily in the form of stratification. Numerical simulation of infiltration from streams whose beds are unclogged and that overly homogeneous aquifers indicates that the potential for disconnection in such systems increases with decreasing stream width and decreasing saturated hydraulic conductivity. Difficulty in achieving disconnection in these latter types of systems suggests that flow spreading by capillary forces is not always the sole cause of disconnection in real stream-aquifer domains; rather, simulations suggest that aquifer heterogeneity is an equally likely cause of the

flow spreading. When disconnected, a stream-aquifer system with a shallow water table behaves quite differently from one in which the water table is deep. Differences between these two cases, as well as with other stream-aquifer situations, are distinctly manifested in hydraulic head and moisture content distributions, pressure head profiles, system fluxes and water table behavior.

Conventional methods of modeling saturated groundwater flow are largely deficient in capturing the effects of unsaturated flow on stream infiltration, and may, therefore, inaccurately predict hydraulic heads in some stream-aquifer systems. The potential for error with conventional schemes has implications for many applied modeling studies, including those that have been done in the Mesilla Valley. Findings from this research are relevant to stream processes in the Mesilla Valley and to other areas of arid to semiarid climate.

Key words: stream-aquifer system, connection, disconnection, variably saturated, incipient disconnection, incipient maximum flux

ACKNOWLEDGMENTS

Several organizations and individuals played significant roles in bringing this doctoral research to fruition. Financial support by the New Mexico Water Resources Research Institute is gratefully acknowledged. I wish to express my gratitude to Dr. John Wilson for providing continual guidance and insight. His determination, willingness to help, and uncanny ability to cope with my sometimes combative nature are all attributes worthy of praise. A special thank you is also extended to Dr. Peter Huyakorn, Geoff Jones, and GeoTrans, Inc. for the numerical simulator used to conduct this research. Without their contribution, few of the results achieved would have been possible.

The assistance of members of my graduate study committee is also greatly appreciated. Dr. John Hawley and Dr. Raz Khaleel helped acquire funding and were involved with the research since its inception. Dr. Dan Stephens and Dr. Allan Gutjahr had strong interests in the hydraulic and numerical aspects of this work, and were constant sources of encouragement.

I am grateful to fellow students Neil Blandford, Warren Cox, Diana Holford, Bob Knowlton, Warner Losh, Swen Magnuson, Jim McCord, Annette Schafer-Perini and Tony Zimmerman, for assisting with both the theoretical and computational aspects of the research. Dr. Fred Phillips contributed valuable suggestions during my dissertation defense. Debbie Brook typed several versions of the manuscript. Professor Bill Rison and his wife, Carol, gave unwavering encouragement. Thanks is also given to Jeff Billings and his family,

for lending support and for being tremendous friends during the last few years.

These acknowledgements would be incomplete without mention of my own wonderful family. My love to all of you. I dedicate this work to my mother, Anne, who stood solidly behind me from the moment I embarked upon a doctoral program.

VARIABLY SATURATED FLOW BETWEEN STREAMS AND AQUIFERS

I. INTRODUCTION AND SCOPE

Much of the recharge to a groundwater basin is derived from infiltration of surface water in flowing waterways. In many arid areas of the western United States, seepage losses from streams, rivers, canals and occasionally arroyos are significant sources of subsurface water. Because of the importance of stream seepage to maintaining a viable groundwater resource in such regions, a good understanding is needed of the mechanisms by which surface water infiltrates the subsurface and recharges the saturated zone of an aquifer.

In examining the exchange of water between a surface waterway and an adjacent aquifer, hydrologists have traditionally conceptualized the problem using saturated flow concepts. That is, it has not been common to take into account seepage within unsaturated zones lying beneath or beside a stream. Under shallow water table conditions, in which the phreatic surface lies above streambed level, the conventional saturated flow approach has probably been adequate for the purposes to which it has been applied. But, in those cases where the water table lies a few to several feet below a streambed, unsaturated flow can play an important role in the hydraulics of stream infiltration. In fact, the influence of an unsaturated soil can become larger the greater the depth from a stream to an underlying phreatic surface. Such phenomena have implications for our understanding of stream-aquifer processes, particularly for the techniques that might be implemented in describing recharge from surface water bodies in arid to semiarid regions.

This research consists of a numerical simulation study of subsurface water flow in stream-aquifer systems, with particular emphasis on the effects of unsaturated flow on hydraulic processes that occur as a result of stream infiltration. As it is common for both saturated and unsaturated media to simultaneously exist in subsurface domains, the simulations performed as part of the research take into account the concurrent flow in both types of media. Thus, the analyses presented herein comprise a study of "variably saturated" flow in stream-aquifer systems. Likewise, the numerical code employed to conduct the flow simulations is termed a variably saturated flow code, or variably saturated flow simulator.

All of the simulation analyses included herein deal with surface waterways that regularly lose water to the subsurface (i.e., losing streams). However, streams that gain in flow due to groundwater discharging into them (i.e., gaining streams) are also briefly discussed from a theoretical perspective.

The research described in this report is distinctive for several reasons. First, the numerical analyses discussed here have been conducted using a recently developed simulator which utilizes several numerical techniques that permit more efficient modeling of variably saturated flow than has previously been the case. Using an efficient code has in turn made it possible to conduct hundreds of simulations for a large variety of conditions. The simulation results show that variably saturated flow does indeed have a significant effect on stream-aquifer processes, and that the influence of unsaturated media is manifested in numerous ways. Moreover, coincidental examination of traditional methods of representing stream-aquifer processes leads the

authors to speculate as to how existing models, based strictly on saturated flow theory, can be improved to better compute stream losses.

In order that the importance of variably saturated flow in stream-aquifer processes can be described in a straightforward and clear manner, it is helpful to establish a glossary that is appropriate for a study of this nature. Accordingly, a list of terms and expressions frequently utilized in this report, along with their definitions, is provided in Table 1. Further description and explanation of many of these terms is presented in subsequent parts of the report text.

Two of the terms listed in Table 1, namely "connection" and "disconnection", deserve special mention in these early paragraphs, since they are symbolic of two very different forms of stream-aquifer flow and are repeatedly used throughout the report. A stream and its underlying aquifer are said to be hydraulically connected if an uninterrupted zone of saturated material exists to link the water occupying a stream channel to the water table in the aquifer. On the other hand, if an unsaturated zone separates an area of saturated media, located immediately below the streambed, from an underlying water table, the stream and aquifer are described as being disconnected.

As may be surmised, the terms connection and disconnection are used for convenience, and should not be taken literally. If a stream and aquifer become disconnected, it does not mean that flow ceases between the stream and underlying saturated zones of the aquifer. Flow of water from the stream to the water table still takes place, but a zone of unsaturated media separates saturated materials at or near the base of the stream channel from deeper saturated materials. Under steady state conditions, this infers that all of the water seeping into

TABLE 1

Glossary of Terms and Expressions
Used in Stream-Aquifer Study

connection - a state of being in a stream-aquifer system, in which an uninterrupted zone of saturated porous media links water in the stream to the water table in a contiguous unconfined aquifer.

disconnection - a state of being in a stream-aquifer system, in which a zone of unsaturated media separates an area of saturated media, located directly underneath and next to the stream, from the deeper underlying water table in a contiguous unconfined aquifer.

connected gaining stream - a stream-aquifer relationship in which connection exists and groundwater flows from the aquifer to the stream, i.e., stream flow gains due to groundwater discharge.

connected losing stream - a stream-aquifer relationship in which connection exists and water flows from the stream to the aquifer; i.e., the stream loses water to the aquifer.

disconnected stream with a shallow water table - a stream-aquifer relationship in which disconnection exists, and the water table is situated at sufficiently shallow depths, such that changes in its elevation has an effect on the stream loss rate.

disconnected stream with a deep water table - a stream-aquifer relationship in which disconnection exists and the water table is situated at sufficiently great depth, such that changes in its elevation does not have an effect on stream loss rate.

incipient disconnection - (1) in steady state flow simulations, the point at which stream and aquifer first disconnect as hydraulic head in the aquifer underlying the simulation domain is incrementally reduced; (2) in transient flow simulations, the time at which stream and aquifer first disconnect after a period during which connection exists.

incipient maximum flux - (1) in steady state simulations, the point at which a constant maximum stream loss rate is first observed as hydraulic head in the aquifer underlying the simulation domain is incrementally reduced; (2) in transient simulations, the time at which a constant maximum stream loss rate is first observed as water table levels decline from shallow depths.

stage - depth of flow in a stream, measured with respect to the stream bottom in the case of a flat bottom channel.

suction head - negative pressure head

the aquifer from the stream must, at some point or another, pass through unsaturated media.

Based on the above-given descriptions, it is intuitively seen that, under connection conditions, a stream can either be a losing or gaining waterway. In contrast, when disconnected, a stream can only lose water to the aquifer.

Since the inception of this research, it has been recognized that simulation of variably saturated flow is somewhat restricted by the limitations of numerical computer codes used to model this type of flow. Movement of water in unsaturated media is a strongly nonlinear process in the sense that hydraulic conductivities and storage properties of unsaturated soils are heavily dependent on the level to which they are saturated. The degree of nonlinearity is much greater than is typically encountered in conventional saturated groundwater analysis, such as areal, two-dimensional, vertically averaged flow in an unconfined aquifer. Considerable research effort has been expended in this study to analyze and evaluate a variety of numerical schemes that one can apply for simulating such strongly nonlinear processes. Special focus has been placed on the ability of the various numerical approaches to handle conditions representative of stream-aquifer systems.

Initial thinking regarding subsurface seepage in stream-aquifer systems might suggest that the influence of unsaturated flow is most noticeable in the case of transient flow, rather than under steady state conditions. However, this work shows that the influence of variably saturated media on stream-aquifer processes can be equally strong for cases of hydraulic equilibrium. Consequently, both types of simulations are included.

Perhaps some justification is needed for conducting steady state analyses of stream-aquifer processes, as it is questionable as to whether such conditions are representative of real systems. Obviously, no large scale hydrologic domain technically exists in a state of absolute equilibrium. Therefore, the term "steady-state" is used liberally here to represent a stream-aquifer system in which a "dynamic equilibrium" (e.g., Freeze, 1969) exists. That is, hydraulic potentials as well as fluxes into and out of the system fluctuate with season and from year to year; yet, over the long term, average conditions are observed which show no significant change with time.

The original motivation for conducting general numerical simulations of stream-aquifer interaction stems from a groundwater modeling investigation (Peterson et al., 1984) of the Mesilla Bolson, located in south-central New Mexico. Infiltration from the Rio Grande and appurtenant irrigation canals in the Mesilla Valley is observed to be a major (and possibly the most important) source of subsurface water in this agriculturally developed region. Inspection of hydraulic data collected in the basin indicates that most irrigation canals continually remain disconnected from an underlying flood-plain aquifer. In contrast, many portions of the Rio Grande fluctuate between states of connection and disconnection, depending on seasonal and long-term changes in stream flow. Moreover, it is commonly observed (Peterson et al., 1984) that, at a given time, a reach of the river may exist in a state of disconnection while upstream and downstream segments remain fully connected to the regional aquifer system. From these observations, it is inferred that unsaturated flow may strongly affect stream infiltration processes in the Mesilla Valley. The effect is clearly multidimensional and thought to be largely transient in nature.

In light of this study's relevance to the Mesilla Bolson, numerical simulations are to some extent based on hydrologic conditions found in this region. However, it is not the author's intent to model a specific portion of the Mesilla Valley; lack of detailed data prohibits modeling of any one area. Rather, the simulations included in this study are of a generic nature, results from which can be used to interpret general phenomena recorded in the Mesilla hydrologic system.

It should be stressed that the results of the numerical simulations are not only expected to have relevance to the Mesilla region, but also to several alluvial aquifer systems throughout the western United States. Although much of this study deals with cases in which the surface water supply is perennial, much of what is observed also has implications for recharge processes thought to occur as a consequence of sporadic runoff in ephemeral water courses, such as arroyos.

Research Scope

In order that the stream-aquifer analyses could be considered relevant to real stream-aquifer systems it was a fundamental goal of this research to conduct reliable numerical simulations on the same scale as occurs naturally. Therefore, considerable effort was made to develop accurate representations of variably saturated processes on a scale that far exceeds those normally used in a laboratory setting. To achieve this goal, it has been necessary to test the accuracy of numerical codes for various discretization schemes and time step durations under a range of possible cases. In addition, the codes were

also assessed for their relative efficiency in solving nonlinear problems involving large numbers of nodes.

Objectives of the research were:

(1) Select and test a variably saturated flow numerical code for simulating processes associated with groundwater-surface water interaction, including infiltration, exfiltration (excluding evaporation), multidimensional seepage through unsaturated and saturated media, and groundwater mound formation resulting from recharge by infiltrating surface water.

(2) Conduct several generic cross-sectional (two-dimensional) simulations of stream-aquifer interaction in unconfined aquifers; analyze the spatial and temporal behavior of subsurface water flow and groundwater recharge, and the manner in which these processes are affected by depth to water table, hydraulic disconnection, aquifer geometry, aquifer material properties, streambed clogging and system boundary conditions.

(3) Relate phenomena observed from the above simulations to similar occurrences near surface waterways in the Mesilla Valley, and in other stream-aquifer systems.

In addition to performing the cross-sectional simulations mentioned in Objective 2, it was hoped at the outset of the research that some three-dimensional simulations might also be accomplished. However, in the process of testing numerical codes per Objective 1, the authors realized that three-dimensional analyses of large, disconnected stream-aquifer systems would not be practical. The major impediment to achieving reliable three-dimensional simulations of stream-aquifer systems was the virtual nonexistence of efficient, non-proprietary, three-dimensional flow codes capable of simulating large domains under highly nonlinear, predominantly dry conditions. In fact, the inability of three-dimensional numerical codes to handle the needs of this study was somewhat symptomatic of more universal problems encountered in applying most flow simulators, including one-dimensional and two-dimensional codes, to large scale variably saturated flow problems. To that end, a product of this investigation has been an evaluation of some of the codes that have been tested (see Appendix A).

In addition to illustrating the general influence of unsaturated media on subsurface flow of water, the variably saturated simulations have also been compared with those from conventional saturated flow codes to help highlight the potential shortcomings of traditional approaches to stream-aquifer modeling. A benefit derived from such comparisons has come in the form of a specific recommendation for augmenting saturated flow codes to enhance their ability to compensate for unsaturated flow effects.

II. HYDROGEOLOGIC FACTORS AFFECTING STREAM-AQUIFER INTERACTION

There exists numerous combinations of porous media properties, aquifer geometries and boundary conditions that could be potentially examined in a numerical simulation exercise of this type. However, practicalities dictate that the cases examined be limited to a few of the more notable situations. Focus is placed on cases in which the influence of variably saturated flow on groundwater-surface water interchange is evident, and on schemes that are not prohibitive in terms of computer cost and capabilities. This in turn suggests that one must have some idea of what to expect from various types of simulations prior to their execution. With such thinking in mind, this chapter is devoted to a discussion of factors affecting stream-aquifer processes, with emphasis placed on conditions in which the effect of unsaturated subsurface seepage is most pronounced.

It is important to note that the simulations deal only with liquid water flow aspects of the stream-aquifer problem. In other words, any other potential effects on groundwater-surface water interaction, such as chemical processes or vapor transport, are omitted from consideration. Accordingly, the numerical codes used deal only with single phase flow of water and totally ignore any possible influence of the air phase. The following discussion of subsurface hydraulic processes is, therefore, similarly limited.

Most situations described in this chapter depict steady state flow behavior. Except where it is explicitly stated that transient flow is involved, the reader should assume that steady state conditions prevail.

General Factors

Physical factors affecting movement of subsurface water either to or from a stream can be grouped into three categories:

(1) the soil comprising the aquifer, lying underneath and adjacent to a stream, and its associated hydraulic properties;

(2) hydraulic characteristics of flow in the stream channel, especially stage (or depth) of flow; and

(3) streambed properties, particularly the existence of a so-called "clogging layer", which is a layer of soil of lower saturated permeability than that of the underlying aquifer.

The degree to which ground and surface waters can be exchanged strongly depends on the occurrence of a streambed clogging layer. Its existence is not a prerequisite for disconnection of stream and aquifer, but it can play a very important role in bringing about such a phenomenon. Because processes associated with semipermeable streambeds differ from those taking place near waterways without a clogging layer, each situation is discussed separately.

Stream Channels With Clogging Layers

Clogging layers, which are found on the beds and banks of surface waterways, usually consist of fine-grained soils in the form of silt and clay. For that reason, these semipermeable units are also frequently called "silt" layers. However, it is not necessary that clogging materials be comprised solely of fine-grained sediment, as it is also possible that biologically generated organic deposits at the base of a surface water channel may help to render the channel bed semipermeable.

Rather than being a rare occurrence, there is evidence (e.g., Matlock, 1965; Brockway and Bloomsburg, 1968) to suggest that streambed clogging is probably more common than is the case of no clogging.

Factors that lead to the formation of a semipermeable channel bed are only partially understood. Field and laboratory studies (Schumm, 1961; Harms and Fahnestock, 1965; Matlock, 1965; Stephens et al., 1987) suggest that properties such as flow velocity, stream gradient, the sediment load normally carried by a stream, and stream water chemistry, all help to determine when and where clogging takes place. Clogging is surely a spatially dependent process, varying both laterally across a channel and longitudinally along a stream's length. As it is normal that stream flow characteristics show temporal fluctuations, it is also probable that clogging is a transient phenomenon, with clogging layers existing in some streams during portions of a year, and temporarily disappearing at other times.

It is easy to envision that a fine-grained streambed impedes infiltration (and discharge to a stream for that matter), for, as its name implies, a clogging layer is normally of much lower permeability than the aquifer material that underlies it. The thickness of the layer need not be substantial in order that infiltration rates be lowered significantly. Behnke (1969), through laboratory studies, found that clogging is essentially a surface sealing process, with layers as thin as 0.50 centimeters being capable of markedly reducing infiltration rates. Matlock (1965) found that clogging layers with thicknesses of only one or two millimeters could decrease seepage rates to as little as one-hundredth of the seepage rate prior to the actual occurrence of clogging. The potential for promoting drier subsurface conditions, and consequently disconnection, when infiltration from a surface water source is reduced to such an extent, is apparent.

The rate at which water moves to or from a stream whose bed and banks are clogged is directly proportional to the difference in

hydraulic potentials found directly above and immediately below the clogging layer. As is frequently the case in constant density, isothermal subsurface flow, potential can be expressed in terms of hydraulic head, in which case the rate of flow is then determined by the difference in hydraulic heads across the clogging layer. Like most analyses of subsurface flow, the velocity component of hydraulic head in the fine-grained materials comprising a clogging layer is small enough to be ignored; consequently, only the combined values of elevation (z) and pressure head (ψ) are used to determine seepage direction and magnitude.

Figures 1a through 1d are cross-sectional illustrations of four separate steady state flow situations that can potentially exist in a stream-aquifer system wherein the streambed is blanketed by a semipermeable clogging layer. Figures 1a and b show shallow water table conditions in which stream and aquifer are connected. In the first of these cases, the water table lies above the elevation of the stream surface, and the stream is gaining in flow due to discharge of groundwater across the semipermeable streambed. For convenience purposes, this stream-aquifer relationship is called a "connected gaining stream." Figure 1b, on the other hand, depicts a losing stream, from which water infiltrates into the aquifer. In this case, the local water table now lies below the stream surface and some of the stream water seeps into unsaturated aquifer media along the stream banks. Yet, stream and aquifer are still considered to be connected, since at least a portion of the aquifer material on the underside of the clogging layer remains saturated, and at least some of the infiltration from the stream takes place solely through saturated soil.

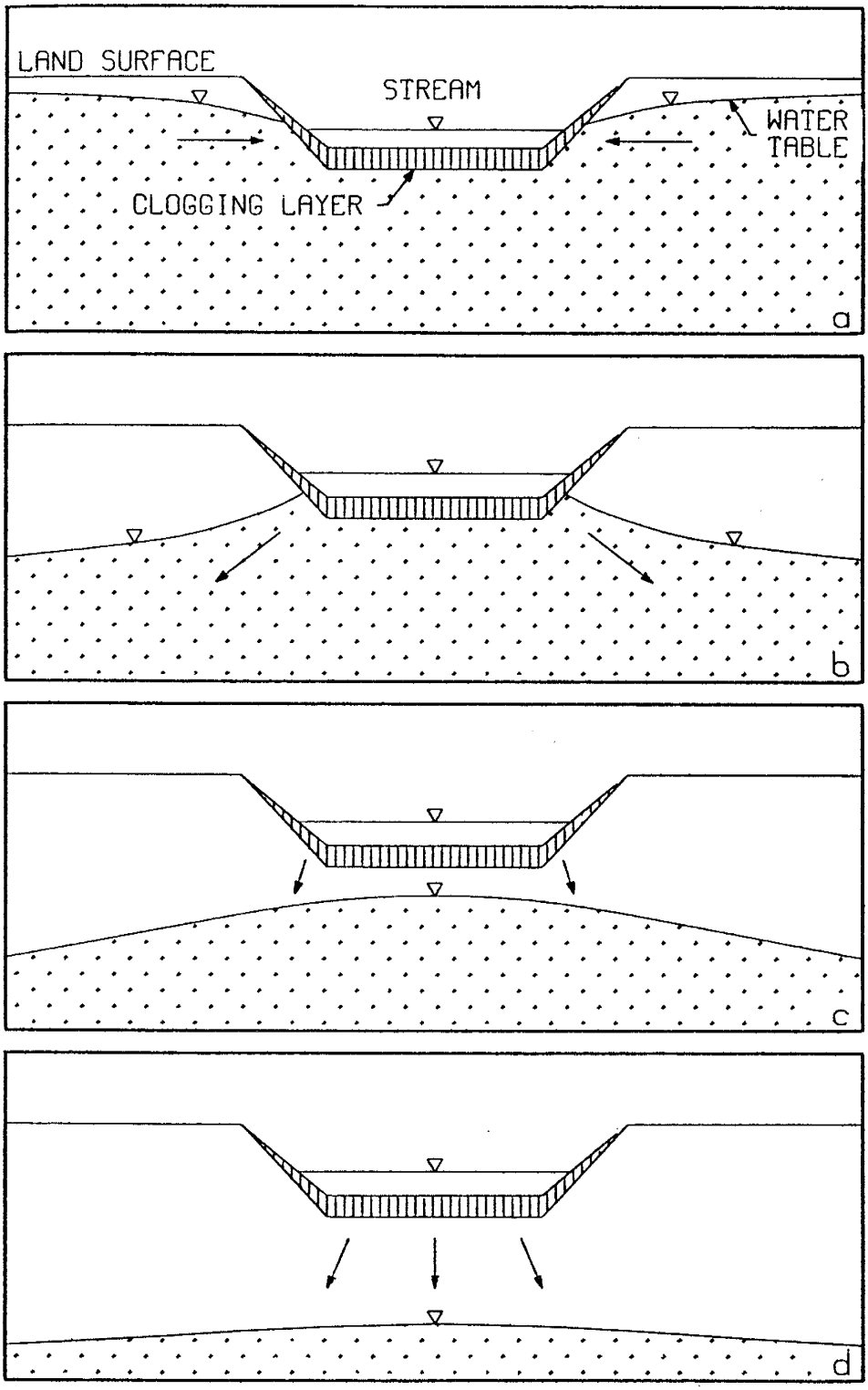

Fig. 1. Stream-aquifer relationships for the case of a clogged streambed: (a) connected gaining stream, (b) connected losing stream, (c) disconnected stream with a shallow water table, and (d) disconnected stream with a deep water table.

This relationship is appropriately labeled as a "connected losing stream."

In the connected losing stream situation of Figure 1b, most of the soil at the base of the clogging layer and located below the stream surface is saturated. However, as the local water table drops, the percentage of streambed and bank area that becomes unsaturated along the base of the clogging layer increases. Obviously, the effect of unsaturated flow processes on stream loss rates also increases. It is important, therefore, to realize that the expression "connected losing stream" is used primarily for convenience of description, and should not be interpreted to mean that saturated flow in the aquifer necessarily dominates stream loss processes in this case.

Under the connected conditions of Figures 1a and b, rate of seepage into or out of the stream is roughly proportional to the height difference between the stream surface and the ambient water table. In other words, if the stream stage remain constant, the seepage rate responds directly to changes in the local water table level. Such a response is expected as hydraulic heads on the underside of the clogging layer are directly affected by local water table levels.

If the water table drops even further, and yet the infiltration rate is diminished by the presence of the streambed silt layer, a situation may eventually occur in which disconnection takes place. This is the case in both Figures 1c and 1d. However, these last two situations differ from each other with respect to the height of the water table relative to the base of the clogging layer.

Figure 1c illustrates a shallower water table condition, in which the water table is located within a few feet of the streambed. As long as the short distance between water table and silt layer is maintained,

the seepage rate from the stream will continue to respond to changes in water table level. This is due to the fact that the head configuration within the saturated portion of aquifer continues to affect heads at the base of the clogging layer, even when all soils below the streambed become unsaturated. Under steady state flow, and within this shallow water table realm, suction is greater the deeper the water table. This case is described as a "disconnected stream with a shallow water table."

As the top of the saturated flow zone is lowered even further, a level is eventually reached at which the pressure head at the base of the clogging layer can no longer be reduced. When this level is reached, presuming the stream stage remains constant, the head difference across the silt layer, and, consequently the seepage rate, also become constant. The constant infiltration rate reached in this case is a maximum value for a given combination of stream, clogging layer and aquifer properties. Therefore, as a phreatic surface deepens even more, it no longer has an effect on stream seepage. This case of a "disconnected stream with a deep water table" is depicted in Figure 1d. The extent to which a water table must drop in order to bring about this stream-aquifer relationship depends on both stream and aquifer properties. In some instances, a few feet of unsaturated material separating the base of the clogging layer from the underlying water table is all that is necessary to induce maximum stream loss rate conditions. Other situations may require the water table to be much deeper.

Using the above-given descriptions of four possible stream-aquifer relationships, as they occur with a progressively declining water table, two additional expressions presented earlier in the glossary of

Table 1 can now be better explained. First, "incipient disconnection" is defined as the point at which conversion from a connected losing stream to a disconnected stream with a shallow water table takes place as the water table drops. Secondly, "incipient maximum flux" is the expression used to demarcate the conversion from disconnected stream/shallow water table conditions to those of a disconnected stream with a deep water table.

When a stream is disconnected from the adjacent aquifer, the seepage across the semipermeable streambed layer occurs, at least to some degree, as saturated flow. A diagram of two possible pressure head (ψ) profiles resulting from one-dimensional, steady state flow across a low permeability clogging layer for disconnected cases, such as that shown in Figure 2, helps to explain the manner in which saturated seepage occurs.

Two separate steady state water table conditions are illustrated in Figure 2: a shallow water table (WATER TABLE 1), and a deep water table (WATER TABLE 2). In both cases the pressure head (ψ) at the top of the clogging layer is the same, being equal to the static pressure head created by the overlying surface water. However, the pressure head profiles for the two situations diverge from each other across the clogging layer. Specifically, the decline in pressure associated with the shallow water table is much more gradual with depth than in the deeper water table situation. Accordingly, pressure at the base of the clogging layer is considerably less (more negative) with the deep water table (ψ_{b2}) than with the shallow water table case (ψ_{b1}).

Profiles of negative pressure heads existing below the base of the clogging layer also differ considerably. The head profile corresponding to WATER TABLE 1 changes with depth throughout the entire

depth ($DEPTH_1$) of unsaturated aquifer material. In contrast, pressures in the second case decrease gradually from the free surface (WATER TABLE 2) upward until such point that an essentially constant negative pressure is reached. Consequently, for some distance below the clogging layer, the pressure head gradient ($d\psi/dz$) is zero. For the given set of stream stage, clogging layer and aquifer properties, pressure head cannot be decreased below the constant value found on the underside of the clogging layer in this deep water table situation. Accordingly, steady state flow across the clogging layer is a maximum value for the given conditions. The deeper water table situation in Figure 2 corresponds to conditions previously associated with Figure 1d, whereas the shallow water table case corresponds to Figure 1c.

Given that pressures are negative in the lower portion of the semipermeable streambed, what then determines the degree to which saturated flow occurs across the clogging layer? Obviously, partially saturated conditions can only occur if pressures within this zone are negative enough to allow the entry of air into the soil pores. It is well documented that fine grained materials tend to remain saturated at pressures considerably less than atmospheric. If pressures are gradually reduced in a soil, the pressure head at which air is first capable of entering the pores of the soil is called the air-entry pressure head (ψ_a). Commonly, ψ_a is more negative the finer grained the soil. Because clogging layers are typically comprised of fine grained material, and are characteristically quite thin, the potential exists for the entire clogging layer thickness (B) to remain saturated when surface water infiltrates into a disconnected aquifer.

In the case of the shallow water table in Figure 2, pressure heads are not less than the clogging layer air entry value (ψ_a) and seepage

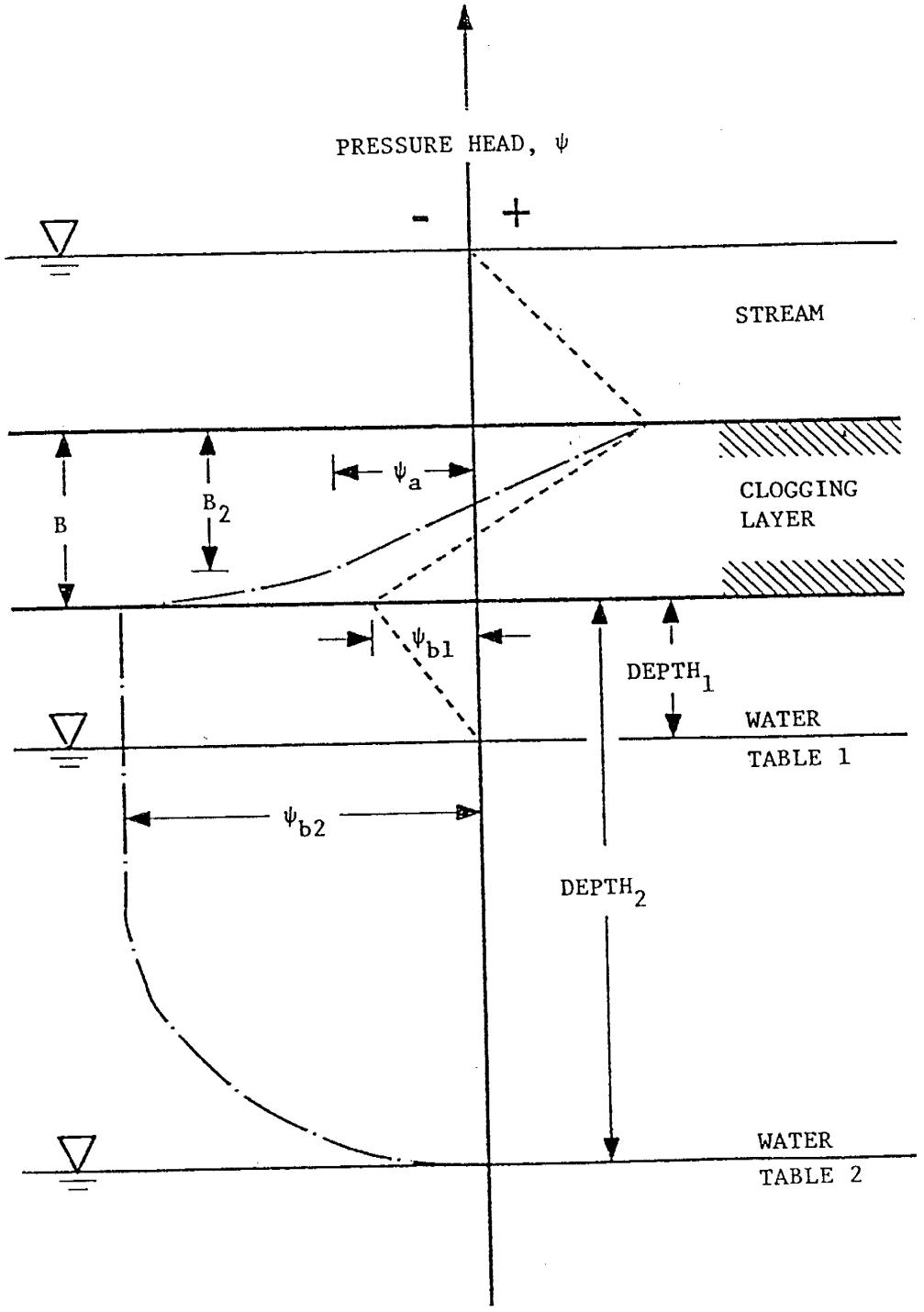

Fig. 2. Pressure head distributions from one-dimensional steady state flow across a streambed clogging layer in disconnected cases.

across the entire thickness (B) of semipermeable material is fully saturated. In contrast, the saturated portion of the fine-grained layer for the deeper water table is limited to a shorter length (B_2), as the pressure head is less than ψ_a near the base of the layer. These two examples should not be construed to mean that the clogging layer always remains saturated when the water table is shallow, nor that some air always enters the base of the clogging layer in the case of a deep water table. Other situations are equally possible. For instance, it is possible that the seepage across the entire thickness of the clogging layer will be totally saturated even for deep water table situations, since some clays and silts have been known to exhibit air entry pressure heads approaching -3 to -5 feet. Similarly, even when the phreatic surface lies at a shallow enough depth below the streambed to still have an effect on infiltration, there is a chance that the basal segment of the clogging layer may be unsaturated.

In this discussion of flow across a clogging layer for disconnected conditions, it has been assumed that the free surface (consisting of the line along which $\psi = 0$) on the underside of the streambed lies entirely within the clogging layer. It is possible, however, that portions or the entire length of this "inverted water table" can be located beneath the base of the clogging layer. Factors that can possibly lead to such an occurrence include irregular channel cross-sections and spatially non-uniform clogging layer properties (e.g., thickness and hydraulic conductivity). It is because of the uncertainty of the free surface location that demarcation of the inverted water table is intentionally omitted from Figures 1c and d. However, the reader should be aware that it does indeed exist and that its location is variable both spatially and temporally.

In summary, it can be said that the type of seepage across the clogging layer, whether fully saturated or combined saturated-unsaturated, is determined by several factors, including channel shape, stream stage, water table depth, aquifer properties and the characteristics of materials comprising the semipermeable streambed. The exact nature of the stream seepage cannot be determined until all of these factors are examined.

Stream Channels Without Clogging Layers

Stream-aquifer domains in which streambed clogging is absent are also common. Studies (Schumm, 1961; Harms and Fahnestock, 1965; Matlock, 1965) suggest that stream channels devoid of a clogging layer often exist along reaches where flow velocities are high, and the quiescent conditions required for settling of fine grained suspended sediment are not present.

When the bed and banks of a surface waterway consist of the same material as found in the contiguous aquifer, stream and aquifer can theoretically exhibit the same connection/disconnection relationships shown in Figure 1. However, the behavior of such a system is somewhat different from that with a clogged streambed. Because seepage is no longer impeded by a low permeability zone, the stream and aquifer are capable of exchanging water at a faster rate in response to changing water table levels. Consequently, one of the four previously mentioned stream/aquifer relationships, namely a "connected losing stream", tends to be maintained over a larger range of local water table levels.

With infiltration rates no longer reduced by fine grained sediment on the stream bottom and banks, the question may arise as to how disconnected conditions, if they are possible, are actually brought

about. Part of the answer to such a concern lies in the dimensionality of the problem. In multidimensional subsurface seepage, capillary forces within unsaturated areas tend to "pull" water away from saturated zones. The overall effect on a stream-aquifer system wherein the stream loses water via infiltration is that seepage paths diverge below the streambed. If the effect of capillarity is strong enough, flow divergence can occur to such an extent that the area between adjacent flowlines becomes quite wide. This width may be incapable of conveying the incoming water with the same hydraulic conductivity as exists upgradient under saturated conditions. Thus, downgradient seepage becomes unsaturated. Since the width of a given streamtube is larger in its downgradient unsaturated portions than it is in the saturated portions located closer to the streambed, the specific discharge is lower in the unsaturated portions. Consequently, the unsaturated zone ends up acting like a zone of flow resistance that limits the seepage rate from the stream.

Disconnection phenomena in stream-aquifer systems without streambed clogging can be somewhat better understood by observing the cross-sectional diagram in Figure 3. Shown is a surface waterway losing water via steady state infiltration, which subsequently spreads out within a bulb of saturated flow. Indeed, it is the spreading of flow that brings about the transition from a saturated to an unsaturated medium along the outer fringe of the saturated bulb. In the earlier discussion of seepage from a semipermeable streambed, it was assumed that the equivalent to this saturated bulb (i.e., inverted water table), when clogging existed, was found solely within the clogging layer itself. The main difference between the clogging and non-clogging situations is that divergence, or spreading, of flow is a

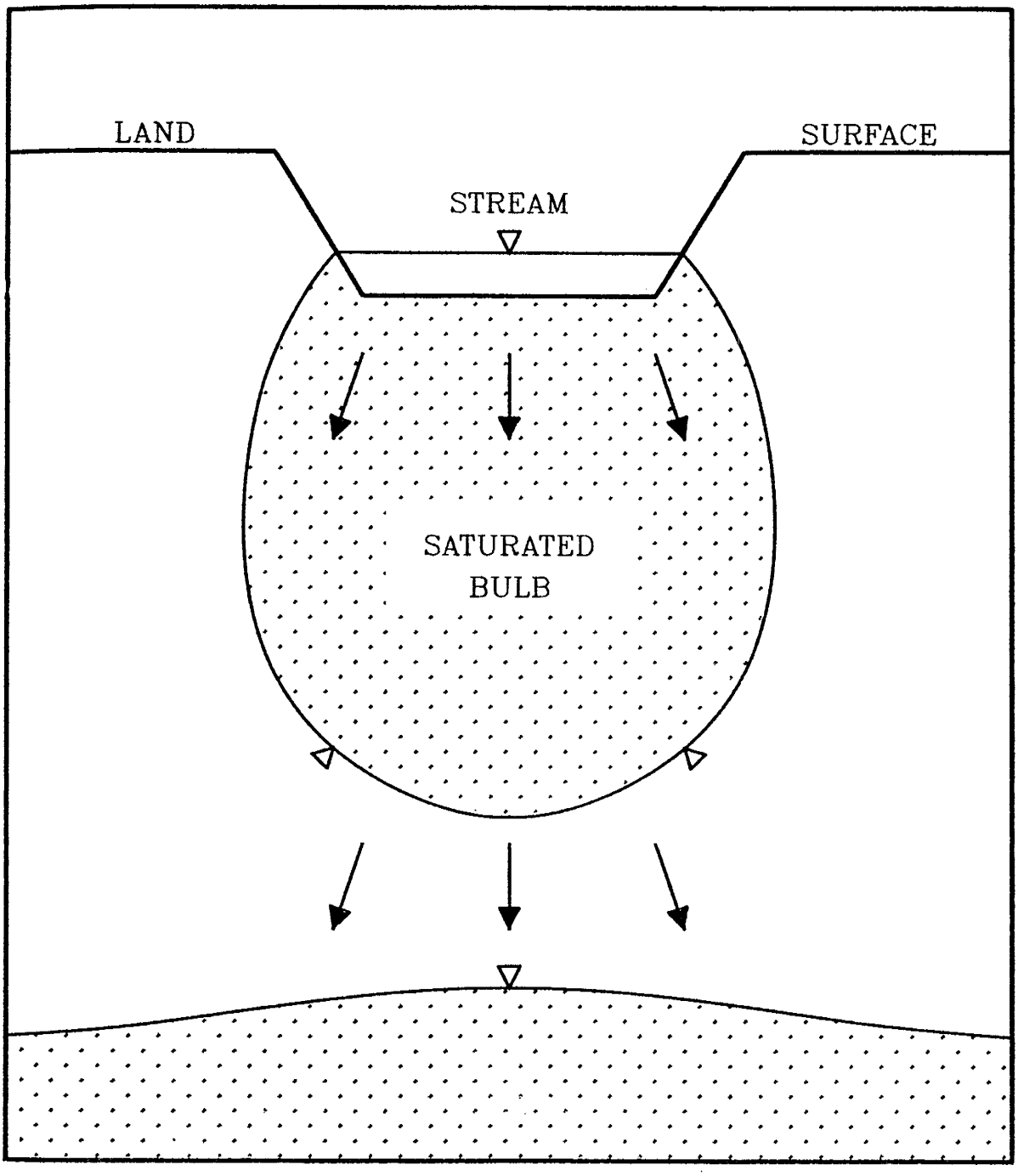

Fig. 3. Disconnection below a stream unaffected by clogging.

requirement for disconnection in a homogeneous aquifer if clogging does not exist, yet may not be necessary when a streambed silt layer is present.

The effects of capillarity, and, consequently, the potential for disconnection, become greater as dimensionality increases. Disconnection in one-dimensional seepage is possible only if a clogging layer exists, and/or if low permeability materials impede the downward flow of water. Flow spreading and disconnection without a clogging layer is more prevalent for three-dimensional seepage than for two-dimensional flow (e.g., Reisenauer, 1963; Philip, 1984; Waechter and Philip, 1985). Accordingly, vertical penetration of the saturated bulb beneath a stream, with its virtually unlimited length, would be deeper than that beneath a surface water body of equal width yet finite length (e.g., a pond). Therefore, it is important to consider the dimensionality of a model when attempting to simulate variably saturated subsurface flow affected by groundwater/surface water interaction. Results from a two-dimensional model may be of limited utility if applied to systems where three-dimensional flow is predominant. Similarly, use of a one-dimensional simulator for analyzing connection/disconnection processes in a stream-aquifer problem is also quite limiting, since disconnection with a one-dimensional flow code is possible only in the event that a clogging layer or some other form of medium heterogeneity is present.

As with the case of streambed clogging, conversion to disconnected conditions as the water table drops below an unclogged stream occurs for a single water table configuration, i.e., the point of incipient disconnection. After disconnection has taken place, water table levels continue to affect stream infiltration rates as long as the distance

between water table and the base of the saturated bulb remains relatively small. Naturally, as the water table deepens, a point is eventually reached where the saturated bulb can no longer expand; i.e., pressure heads at the base of the bulb reach constant values and the infiltration rate is at its maximum level for a given stream stage. The water table depth at which this point of incipient maximum flux is attained again depends on aquifer properties, depth of flow in the stream and stream channel shape.

For most streams unaffected by clogging, flow conditions conducive to disconnection solely by capillary spreading are uncommon. The reason for this can be seen by considering the factors that influence seepage from the stream and ultimately determine flow patterns and head configurations beneath it.

The volumetric seepage rate from a losing stream will be lower the narrower the stream and the shallower the depth of water in it. In addition, the plume of saturated water movement beneath a losing waterway will generally be less wide where its channel is relatively narrow than in locales where it tends to broaden. Correspondingly, capillary forces would have a greater chance of spreading a narrow plume, rather than a very wide one, to the point where it may eventually transform into unsaturated flow at a greater depth (Jeppson and Nelson, 1970). But most natural streams in alluvial systems are usually characterized by substantial width. Man-made canals may be constructed such that their widths are narrow relative to their depth, but such designs are uncommon. Furthermore, nearly all waterways, including irrigation canals that convey water only seasonally, must at least maintain a minimum depth of flow; otherwise, their classification as waterways is dubious. As a consequence, it can be seen that the

stream channel geometries that are most conducive to the creation of disconnection conditions where streambed clogging is not a factor are not common.

Even if a channel is uncharacteristically narrow and the stream stage is low, it is doubtful that the underlying aquifer remains effectively homogeneous to a great enough depth such that capillarity is the only cause of disconnection. Fluvial aquifers are typically characterized by heterogeneity over their vertical extents. Several examples are found in the literature of field studies that document spatial variability of unconsolidated materials over relatively short distances (e.g., Warrick and Nielsen, 1980; Byers and Stephens, 1983). Such variability in the vertical direction tends to promote horizontal spreading of water that has infiltrated from a stream. Even in relatively homogeneous soil profiles, minor variability of soil properties with depth can help bring about enhanced lateral flow (e.g., McCord and Stephens, 1986). Thus, there is reason to believe that it is the combined effects of capillary forces and aquifer heterogeneity, rather than capillarity by itself, that are often the causes of sufficient flow spreading such that disconnection takes place when the streambed is not clogged. Further consideration is given to the mechanisms by which aquifer heterogeneity can lead to disconnection in the next section concerning aquifer stratification.

Effects of Aquifer Stratification

Alluvial sediments are commonly deposited in layers, or beds. Alluvial aquifers comprised of layered deposits are said to be stratified. Generally, stratification affects groundwater seepage by increasing lateral movement of subsurface water, and reducing vertical

movement, more so than would be observed if the aquifer were effectively homogeneous in the vertical direction. If, in the case of disconnection, stratified sediments lie in the unsaturated zone that separates the stream from the water table, the tendency for increased lateral water movement can be even more pronounced than observed in the case of saturated sediments (e.g., Mualem, 1984).

A few of the hydraulic effects of stratification can be analyzed in a simple fashion by examining multidimensional flow across a three layer system such as that given in Figure 4a. Note in this example that a fine-grained material (silt) is overlain by and also overlies a coarser grained soil (sand). Furthermore, flow in this three layer system is assumed to largely result from infiltration from a source located above, such as a stream.

Hydraulic continuity principles require that pressures throughout the system in Figure 4a be continuous. Thus, between the three units, at the interfaces, pressure head in both sand and silt should be equal. Because the elevation at an interface is the same in each material, the continuity requirement establishes that hydraulic heads need also be equal. Yet it is possible, and likely, that the moisture contents of the two dissimilar soils will not be continuous at the interfaces. And, because the hydraulic conductivity of each material varies differently with changing moisture content, two very different types of flow can simultaneously exist in each.

In the first case, let us assume that part of the sand overlying the silt has been saturated (Figure 4b) due to incoming infiltration from above. Therefore, the pressure head at the upper interface (INTERFACE 1) is positive. But, as the graph of hydraulic conductivity vs. pressure head graph of Figure 4e indicates, the saturated hydraulic

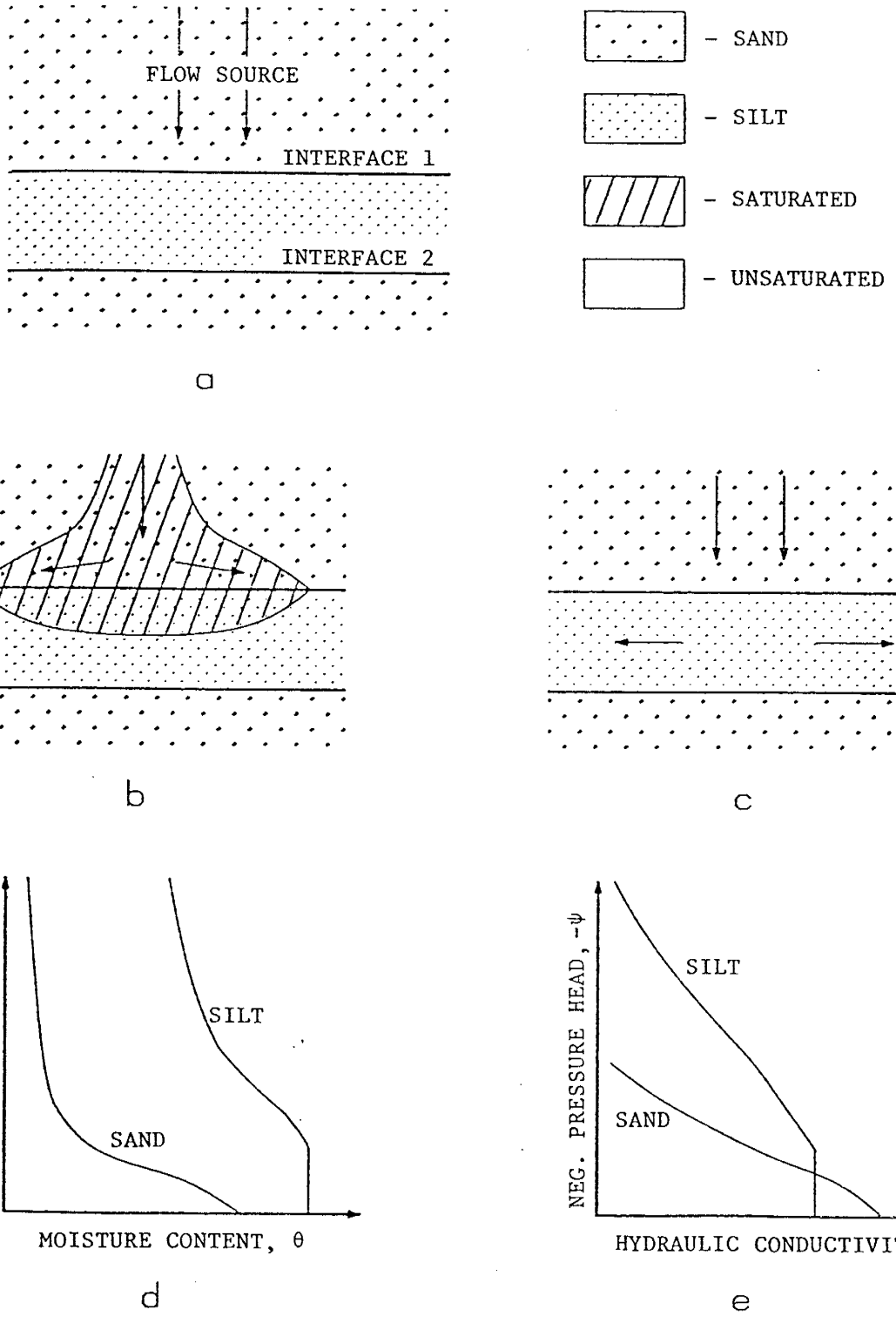

Fig. 4. Effects of aquifer stratification on downward flow: (a) three-layered system, (b) groundwater perching, (c) enhanced lateral flow in silt layer under unsaturated conditions, (d) soil moisture characteristic behavior of layered materials, and (e) unsaturated hydraulic conductivity behavior of layered materials.

conductivity of the sand far exceeds that of the silt when it is saturated. Therefore, assuming that flow in each individual unit is isotropic, the rate of seepage through the fine-grained silt may be considerably less than the rate at which downward moving water is fed into the upper sand unit. Consequently, water in the sand tends to spread out laterally atop the silt rather than pass through it, as depicted in Figure 4b. If saturated flow is prevented from taking place in the lower sand unit, the water in the upper unit is said to be "perched", a phenomenon that has long been recognized. Indeed, under the perching phenomenon, it is possible that the fine-grained silt may be saturated at the lower interface (INTERFACE 2), while the sand at this depth remains unsaturated. Tagaki (1960) presents a detailed mathematical explanation for such an occurrence. In any event, whether groundwater perching exists or not, the overall effect is that horizontal flow is enhanced and vertical movement is impeded.

As a somewhat different example, let us assume that moderate to extremely dry conditions exist over the entire system (Figure 4c). Consider the hydraulic properties of the silt and sand at the lower interface (INTERFACE 2). Once again, despite the fact that the pressure head in either unit at this point is the same, it is likely that moisture contents within each differ (see soil moisture characteristic curves in Figure 4d). Consequently, large differences in the hydraulic conductivities of each might also be expected. If, in fact, the suction head at the interface is very large (i.e., pressure head is very negative), it is quite possible that the water transmitting capabilities of the sand are less than those of the silt. This is visually demonstrated by Figure 4e, where hydraulic conductivities in the sand are shown to be much less than those in the

silt as pressure heads are reduced to very low values. If this is the case the sand now acts to impede downward flow and lateral movement within the silt is promoted. Figure 4c provides an illustration of this case.

Both of the foregoing examples (Figures 4b and 4c) serve to simply illustrate how a stratified system, promotes horizontal flow while impeding vertical seepage. Yet an important distinction needs to be made between the two examples. In the system in which the upper interface is saturated, the ratio of hydraulic conductivities in the two material types, at least within the saturated portions of the two upper layers, remains constant. In contrast, the hydraulic conductivity ratio in the wholly unsaturated flow system is totally dependent on moisture content levels. As a consequence, the degree to which horizontal flow is promoted in the silt layer is not known until the unsaturated flow conditions themselves are known.

Aquifer Anisotropy

The preceding examples (Figure 4) used to illustrate the effects of soil layering on downward flow of subsurface water are quite simple in that they involve only two materials and three layers. But over the vertical extent of most aquifers, numerous interstratified units of different materials are often found. The scope of this investigation does not warrant detailed analyses of the kinds of complex layering schemes that may be observed in actual field situations; instead, the reader is referred to the work of others (e.g., Hillel and Talpaz, 1976; Yeh et al., 1985c; Heermann, 1986) for more thorough explanations of the influence of soil layering. Yet, the foregoing discussion of this topic is sufficient for introducing the concept of layer induced

anisotropy, and how anisotropic flow in soils can affect stream infiltration.

Frequently, it is impractical to characterize each layer comprising a stratified formation. In such cases, hydrologists often choose to treat a heterogeneous layered system as an equivalent homogeneous one. However, the hydraulic conductivity tensor representing the equivalent system is necessarily anisotropic, since the soil layers tend to promote horizontal flow while diminishing vertical flow. In order for the concept of a homogeneous anisotropic medium to be meaningful, the thickness of the individual layers must be much smaller than the size of the domain selected for representation in this manner.

Given that it is possible to characterize layered domains as being anisotropic, it is important to realize that two very different types of anisotropy may occur depending on whether a system is fully saturated or not. In a fully saturated case, the ratio of horizontal hydraulic conductivity to vertical hydraulic conductivity remains constant since saturated hydraulic conductivity is usually considered constant for a given medium. On the other hand, hydraulic conductivities in the unsaturated portions of a variably saturated domain will vary with changing moisture content. Accordingly, the anisotropy ratio used to characterize the unsaturated layered system will vary depending on the system's moisture content distribution. Understandably, researchers sometimes refer to this phenomenon as moisture dependent anisotropy (e.g., Yeh et al., 1985c).

Failure to take into account the effects of moisture dependent anisotropy when predicting seepage of water from a surface water body into stratified soils can lead to erroneous results. In particular,

the classic isotropic or anisotropic models may predict more vertical movement of the infiltrating water than actually occurs. Accordingly, classic models may fail to simulate the enhanced lateral movement of water brought on by the moisture dependent influences. Figure 5 provides a simple example of how classic models may give very different results from those theories that take into account moisture dependent anisotropy. This particular example is based on assumed seepage from a disposal pond, and the moisture dependent anisotropy results are determined using the stochastic model of Yeh and Gelhar (1983).

The potential effects of anisotropy on stream-aquifer interaction near a losing waterway can be generally deduced. First, increased horizontal movement of water, along with resultant diminished vertical flow, increases the potential for disconnection at depths below the stratification, even if the streambed is not clogged. The interbedded materials of variable texture serve to do much of what a clogging layer does in terms of inhibiting the downward flux of water. Secondly, the stream infiltration rate, as well as the vertical penetration and shape of the saturated bulb beneath a stream, depends heavily on properties of the layered soils beneath the stream channel, including their thicknesses and varying hydraulic conductivities under unsaturated conditions.

Characteristics of Materials Comprising Stream-Aquifer Systems

Recognizing the potential effects of stratification on stream infiltration processes, with what frequency does aquifer heterogeneity in the form of stratification actually play an important role in real alluvial aquifers affected by stream seepage? The answer is that stratification is very influential in an abundance of cases.

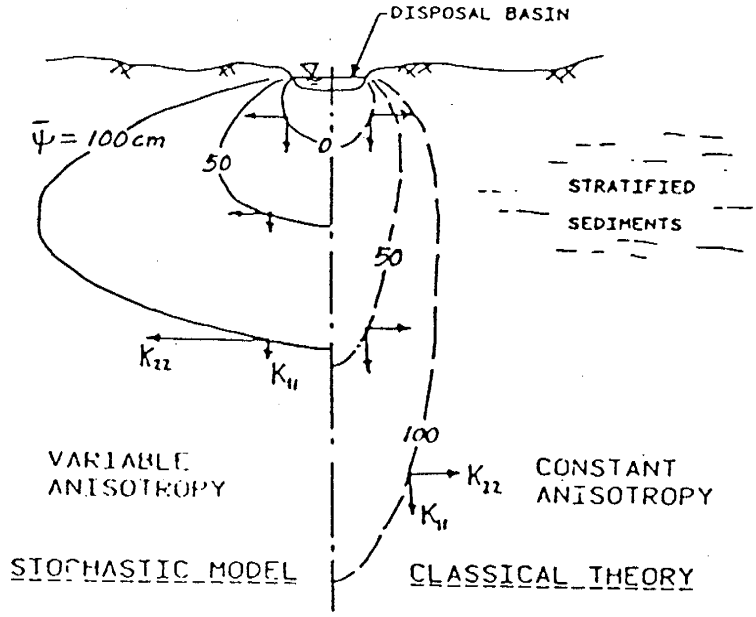

Fig. 5. Soil suction distribution beneath a disposal basin (after Yeh and Gelhar, 1983).

Sharp (1977) has summarized the work of others with regard to the typical sedimentary makeup of fluvial aquifers. As he has pointed out, many natural waterways in the United States are underfit - that is, the stream or river appears too small for the valley in which it flows. Such underfit streams are mostly caused by the fact that past discharges on the stream were much higher during earlier geologic times than observed today. Distinct trends in the spatial distribution of sedimentary materials within alluvial aquifers are commonly observed as a consequence of this major change in stream discharge with time.

Sharp (1977) has found that the vertical variation in hydraulic properties of aquifers associated with underfit streams is quite consistent. In general, grain size of the alluvial sediments coarsens downwards. Materials at the base of the unconfined alluvial aquifers often consist of clean gravels and well sorted, coarse to medium grained sand. Shallower sediments, however, are commonly much more fine-grained. As expected, vertical gradation in grain sizes also signifies an increase in saturated permeability with depth. Indeed, Sharp (1977) has demonstrated that saturated hydraulic conductivity increases exponentially with depth in three major stream-aquifer systems of the United States. In addition, in a few of the alluvial systems included in his analysis, he has been able to divide the aquifer into three distinctly different units, ranging from very coarse sands and gravels at the base, to medium grained sands at intermediate depths, and finally to the least permeable material near the stream and land surface levels.

The explanation for a consistent vertical variation in grain size and permeability in underfit systems found in North America is relatively simple. The coarser material near the aquifer base in most

cases was deposited during the last glacial stage, 10 to 25 thousand years ago. Stream discharges were naturally larger during such wetter periods, and were thus capable of transporting and subsequently depositing large grained sediment. As climates have gradually become drier since the glacial period, suspended and bed loads have naturally become more fine grained. The sediments laid down in more recent times reflect this transition to current climatological conditions. Using this hydraulic explanation, it might also be expected that the deepest alluvial materials are well sorted, effectively homogeneous and relatively isotropic. Accordingly, the most shallow sediments, deposited mostly by a meandering underfit stream, tend to consist of fine and medium grained channel sands interbedded with silty and clayey flood plain deposits. The shallow sediments are less homogeneous and more stratified than their deeper counterparts.

A logical conclusion to be reached from Sharp's (1977) work is that aquifer anisotropy at shallow to moderate depths, resulting primarily from stratification, can be an enormous factor in stream-aquifer processes. In domains where the water table lies well below streambed levels, moisture dependent anisotropy within unsaturated media is also expected to come into play.

The effects of gradually increasing hydraulic conductivity with depth below an unclogged stream channel were discussed in a modeling study by Jeppson and Nelson (1969). Their analysis included an explanation as to how the rate of increase of hydraulic conductivity with depth can markedly affect the depth of the saturated bulb located below a disconnected stream.

Transient Effects

The preceding comments regarding connection/disconnection relationships is based mostly on steady state flow considerations. Yet, some of the most significant effects of variably saturated flow on stream-aquifer interchange can be manifested as transient phenomena.

The temporal influence of variably saturated flow on a subsurface hydrologic system is fundamentally related to the nonlinear nature of unsaturated flow. When not fully saturated, the hydraulic conductivity of a soil can be severely decreased below its saturated value. As a consequence, the propagation of pressure pulses in an unsaturated soil is considerably slower than is observed within saturated portions of an aquifer. In addition to reduced hydraulic conductivity, the availability of air filled pore space for water storage in an unsaturated soil also helps to slow the response to pressure pulses. Using terminology that assists in describing the phenomenon of relative flow rates, it can be said that the "time constants" for unsaturated soils are larger than their saturated equivalents. In other words, the time needed for an unsaturated system to effectively reach a new equilibrium, after being stressed in some manner, is substantially longer than would be needed in a domain that is identical in every way except for its being saturated.

As an example of the transient effects of variably saturated flow on a stream-aquifer system, consider the case in which the stage in a stream is rapidly raised several feet. If the streambed is not clogged, and stream and aquifer are connected, the likelihood is strong that the effects of increased seepage are quickly manifested as increased water table levels. If, however, the streambed is blanketed by a low permeability material, and the phreatic surface is located

tens of feet below the stream channel, unsaturated seepage is plausible. Propagation of the pressure pulse from increased stream infiltration to the underlying water table is then not automatic, and may not take place until a sizable period of time has elapsed after the new infiltration rate has commenced. Actual movement of the newly infiltrated water is also slowed. In fact, it is conceivable that several weeks to months may pass before water that has seeped from an arroyo, for instance, reaches a water table lying 100 feet or greater below ground level.

The time lag between start of infiltration and the first occurrence of recharge can be even longer if the sediments lying within an unsaturated zone below the streambed are stratified. Enhancement of horizontal water movement relative to downward flow in zones exhibiting moisture dependent anisotropy likely impedes the downward movement of infiltrated water to slower rates than those observed when the unsaturated zone is homogeneous.

Summary

A number of factors believed to have influence on stream-aquifer processes have been discussed. It has been argued that streambed clogging is quite pervasive in many streams, and that clogging is frequently instrumental in helping to bring about hydraulic disconnection of stream and aquifer. Yet clogging is not the sole mechanism for creating disconnection; other factors leading to the same phenomenon include flow spreading induced by soil capillarity and effectively anisotropic flow resulting from aquifer heterogeneity.

Disconnection induced by capillarity alone seems unlikely. Even in situations where the streambed remains unclogged, flow conditions in

most stream-aquifer systems are not conducive to capillary spreading being the sole means by which an unsaturated zone is created below a stream. The width of most streams, typical depths of flow in stream channels, and presence of material heterogeneity in most unconfined fluvial aquifers are factors that lead to such thinking.

Four separate stream-aquifer relationships, within the two major classifications of connection and disconnection, have been presented for the case of a stream whose streambed is clogged. The four, listed in the order in which they are observed with a declining water table, are: (a) connected gaining stream, (b) connected losing stream, (c) disconnected stream with a shallow water table, and d) disconnected stream with a deep water table. Based on the definitions for connection and disconnection used in this study, these same relationships can potentially exist in systems where streambed clogging is not present.

Vertical profiles of pressure head resulting from one-dimensional steady state flow have been used to illustrate different types of stream seepage that can take place across a clogging layer when stream and aquifer are disconnected. Both shallow and deep water table conditions have been examined. The two cases differ, most notably because a shallow water table has an effect on the stream infiltration rate, whereas the deep water table does not. In the deep water table instance, the seepage rate is constant, and is equal to a maximum value for a given set of clogging layer and aquifer properties, and a constant depth of flow in the stream.

Aquifer stratification, particularly at shallow depths in an unconfined aquifer, is expected to promote horizontal flow of water infiltrated from a stream, and impede its downward movement. Because

of this, the shallow depths of an aquifer are often effectively anisotropic. When saturated flow exists throughout the stratified zone, the ratio of horizontal and vertical hydraulic conductivities for a composite medium used to represent that zone is a constant. However, when that zone becomes largely unsaturated, the degree of anisotropy varies with the moisture contents occurring in the individual units comprising the stratified system. Anisotropic effects in general, and especially moisture dependent anisotropy, are likely to play a major role in affecting stream losses. Because aquifer stratification produces a similar effect to that of a clogging layer, in that the downward flow of water from the stream is impeded, it is also likely that stratification helps lead to hydraulic disconnection as well. The influences of unsaturated flow, and, therefore, of moisture dependent anisotropy, on stream-aquifer processes, are obviously much greater when stream and aquifer are disconnected.

Fluvial aquifer systems associated with underfit streams appear to be particularly susceptible to the effects of unsaturated flow and moisture dependent anisotropy when groundwater levels drop below streambed elevations. Aquifers in this category are commonly characterized by texturally nonuniform, relatively fine-grained, and highly stratified materials at shallow depths, which ultimately grade into coarser and more texturally uniform sediments at greater depths. A distinct trend from generally low saturated hydraulic conductivities at shallow levels to relatively high saturated hydraulic conductivities at greater depths (Sharp, 1977) is commonly observed of these systems. Such vertical variations in the material makeup and water transmitting capabilities of the alluvium can be explained by an aquifer's evolutionary history.

Most discussions presented in this chapter regarding hydrogeologic influences on stream-aquifer systems have dealt with steady state flow situations. However, it is important to emphasize that transient phenomena in these systems are of equal, if not greater importance. Unsaturated media in disconnected aquifers have a significant effect on the temporal response of a stream-aquifer domain to stresses such as changes in stream stage. Response time of unsaturated materials to pressure pulses is slower than when those materials are saturated. Propagation of a pressure pulse, due to an increase in stream stage, down to a disconnected deep water table, is an example of a situation in which unsaturated flow plays a significant role in affecting system response.

III. MESILLA VALLEY STREAM-AQUIFER HYDROLOGY

As stated earlier, the impetus for making this study stems from a groundwater modeling investigation (Peterson et al., 1984) of the Mesilla Bolson in south-central New Mexico. Many of the variably saturated simulations discussed in subsequent chapters are roughly based on hydro-geologic conditions observed in that basin. Therefore, this chapter is included to provide the reader with a basic understanding of important stream-aquifer processes in the Mesilla region. As the following text demonstrates, discussion of this area helps corroborate many of the assertions outlined in the previous chapter regarding hydraulic and geologic influences on stream-aquifer interaction.

Many recorded observations relevant to stream-aquifer processes in the Mesilla Valley are summarized at length in the groundwater modeling study by Peterson et al. (1984). Some of the more salient features from that summary are briefly discussed here, with emphasis placed on those observations that have the greatest relevance to numerical simulations included in this study. In addition, some mention is made of factors pertinent to the variably saturated flow simulations, but that are inadvertently omitted from the earlier modeling study.

Aquifers in the Mesilla Valley

The Rio Grande, which travels through the Mesilla Valley along its entire length, provides the most dominant hydrologic control on the occurrence of groundwater in a shallow aquifer that underlies the valley (Leggat et al., 1963; Wilson et al., 1981; Wilson and White, 1984). Composed mostly of alluvium deposited by the river during the

Pleistocene and Holocene Epochs, this aquifer is commonly referred to as the flood-plain alluvium. Recharge to the shallow aquifer from the Rio Grande and the numerous irrigation canals that divert water from the river varies both seasonally and from year to year. Stream losses are largely dependent on surface water availability and reservoir operations upstream.

The flood-plain alluvium, varying in thickness from about 50 to 125 feet, is typical of an aquifer associated with an underfit stream. Commonly, the alluvium consists of a basal unit of coarse sand and gravel, which is overlain at shallow depths by interbedded silts, sands and clay (Wilson et al., 1981; Wilson and White, 1984). Consequently, the aquifer appears to be more intensely stratified in its upper 20 to 30 feet, and tends to be more homogeneous in its lower portions. The vertical variation in material types is explained by the reconstructed geologic evolution of the flood plain alluvium (see, for instance, King et al., 1971).

An extensive and deep basin-fill aquifer, comprising part of the Santa Fe Group, underlies the flood-plain alluvium. Numerous clay layers and lenses, interstratified with sands, are found in the intervening depths separating the two aquifers. Vertical leakage across these confining materials is the major means of exchange of water between the Santa Fe Group and the river alluvium (Wilson et al., 1981). The extent of the vertical leakage is largely controlled by the amount of pumping that occurs in the deeper aquifer. Because the largest historic use of groundwater in the region is for supplementation of surface water irrigation, pumping in the Santa Fe Group increases during years of low runoff in the Rio Grande, and is moderately low to nonexistent in years of plentiful water supply.

Accordingly, leakage of groundwater from the flood-plain alluvium to the Santa Fe Group is larger in dry years than in periods of abundant surface water flow.

Seepage from Surface Waterways

Infiltration of surface water in the numerous waterways of the Mesilla Valley is a major, if not the largest, source of modern groundwater recharge to the entire Mesilla Bolson. The majority of stream seepage appears to occur under conditions of hydraulic disconnection. The preponderance of disconnection stems largely from the fact that most of the water conveyed through the valley is in irrigation canals, which are typically elevated above surrounding land, primarily for the purpose of providing hydraulic head sufficient to drive irrigation water the full length of irrigated fields. This fact, combined with evidence of extensive clogging of canal beds, provides plausible explanation for the fact that water tables are sometimes observed to lie as much as ten to fifteen feet below canal bed levels (Peterson et al., 1984).

Connection/disconnection phenomena on the Rio Grande, on the other hand, seem to be spatially variable and also change with season. The attached Figure 6 is a map of the Mesilla Valley area, showing locations that facilitate a summary of connection/disconnection behavior along the river.

Peterson et al. (1984) surmised that the groundwater levels nearly always lie above river stages in the first few miles downstream of Leasburg Dam; thus the river is a gaining waterway in its uppermost reaches within the valley. Below this initial hydraulically connected section, along a 25 to 32 mile stretch that includes the Mesilla Dam

and extends to the vicinity of Vado (see Figure 6), the river is mostly a losing stream. During the non-irrigation months of winter, disconnection also seems to predominate in this area. However, as spring and summer water table levels rise in response to infiltration of irrigation waters, connection at some locations is probably observed over periods spanning several months.

Along the next 10-13 miles of river located downstream of Vado, evidence for connection of the Rio Grande and the underlying flood-plain alluvium, at least during the better part of the irrigation season, is quite strong. However, it is still believed (Peterson et al., 1984) that the river mostly loses water to the subsurface along this stretch during an average year. In the next section downstream, near the town of Canutillo, the groundwater system is affected by pumping from several wells used to augment the municipal water supply of El Paso, Texas. Disconnection appears to prevail here, and large seepage losses are commonly observed along a 10 to 15 mile reach lying both upstream and downstream of the municipal field.

Finally, in the southernmost part of the valley, from an area 3-6 miles upstream of the Courchesne Bridge to the El Paso Narrows, it is likely that the river and the shallow aquifer are connected throughout most of each year. A constricted section of valley fill in the vicinity of the Narrows is thought to back up southward moving groundwater, thus raising local water table levels. Discharge to the river from the alluvial aquifer in the area immediately upstream of the Narrows also seems likely.

Results from a quasi three-dimensional (quasi 3-D) groundwater flow model by Peterson et al. (1984) indicate that mean annual losses from the Rio Grande and canals in the Mesilla Valley amount to roughly

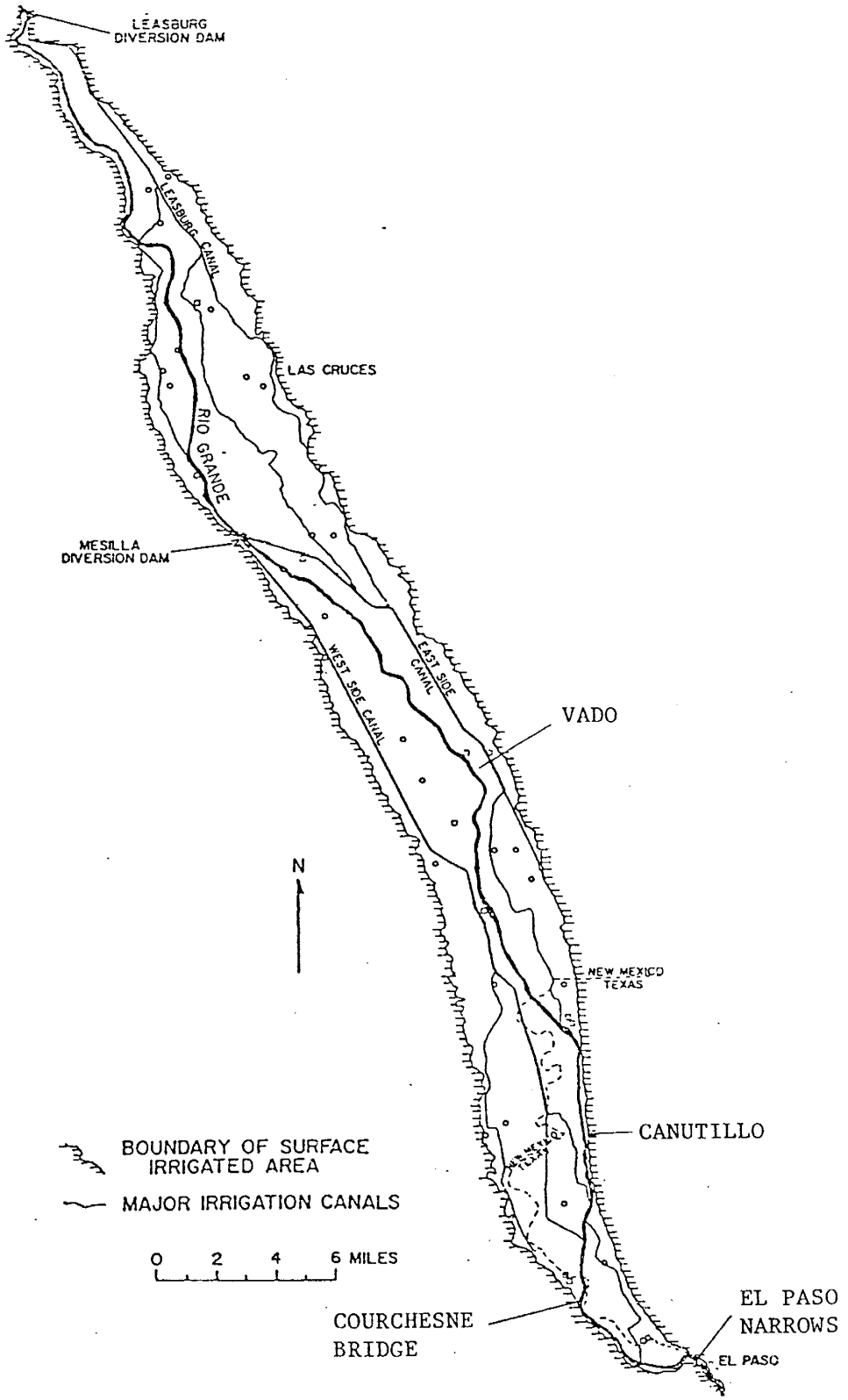

Fig. 6. Map of the Mesilla Valley (after McLin, 1981).

116,000 acre-feet. Such large losses, along with applied irrigation water, counteract the effects of pumping and help to maintain the Mesilla Bolson groundwater system in a state of "dynamic equilibrium" (e.g., Freeze, 1969). Estimates of discharge to gaining portions of Rio Grande in the uppermost and downstream ends of the valley appear to be minor compared to total river losses.

Stream Channel Properties

Most Rio Grande water used for irrigation is diverted into three large canals, namely the Leasburg Canal, the East Side Canal and the West Side Canal. Distribution of surface water to the various agricultural lands located in the valley takes place mostly by diversion of water from these three main waterways to a complex system of laterals. Although much of the total stream conveyance loss occurs along these smaller ditches, some of the more significant seepage losses undoubtedly take place along the main canals.

In their uppermost reaches, the main irrigation canals are characterized by streambed widths approaching 25 to 40 feet. Depths of the channels normally range from 10 to 15 feet. Depths of flow, of course, vary, depending on flow rates and the operation of check gates.

The Rio Grande channel in many locales is quite wide, sometimes exceeding 300 feet. However, normal operation of the surface water system in the valley is such that the river rarely carries discharges that take up the full width of the river channel. During the winter months, for instance, flows in the Rio Grande are regulated because little irrigation water is needed. Consequently, the wetted perimeter of the river in most locales more commonly approaches 50 to 100 feet. Similarly, in spring and summer, most of the river flow is diverted to

the irrigation delivery network; once again flows in the river rarely extend across the full channel width. Vertical distance from the deepest part of the river bed to the top of channel banks is commonly on the order of five to seven feet.

Stratification types found in the bed of the Rio Grande in portions of the Mesilla Valley was extensively investigated by Harms and Fahnestock (1965). Their field study not only demonstrated the pervasiveness of bed stratification, but also illustrated the occurrence of occasional layers of clay- and silt-sized materials deposited by relatively low settling from suspension of such fine-grained matter during low flow periods.

Some field and laboratory data have been collected regarding streambed properties along several irrigation canals by New Mexico State University (NMSU) Civil Engineering Department (1956) as part of a hydrologic investigation of the Mesilla Valley. Although it was found that clogging layer parameters tended to vary depending on the recent history of flow in a given canal, there were some general findings worthy of mention. First, bed materials collected were variously described as clay, clayey silts, sandy silts and compact sands. Secondly, the saturated hydraulic conductivities of streambed materials, determined via laboratory analysis of collected samples, normally ranged in value from about 0.01 to 1 feet per day. Third, the least permeable material was usually found in a thin layer either on the streambed surface or within a foot of the streambed. Finally, thickness of the low permeability layer rarely exceeded a few inches.

Stratification Effects in the Flood-Plain Alluvium

The hydraulic effects of stratification at shallow depths in the Mesilla Valley are not usually noticed during years of average water supply. In such normal years, recharge by stream seepage and irrigation maintains the water table at relatively high levels, and the increased anisotropy effects brought on by unsaturated media are diminished. However, during drought periods spanning a few or more years, the effects of moisture dependent anisotropy become more evident.

One of the more obvious ways in which the moisture dependent anisotropy is manifested is observed in the reported flows of numerous agricultural drains in the region. Gunaji (1961) reported that drain discharges during an extended drought in the early and mid 1950's declined to low levels at a much slower rate than measured water table levels would seem to indicate. Indeed, even during the driest periods, some drain flow was always present. This seemed somewhat unlikely since water table elevations were in many cases reduced below normal levels by as much as ten feet or greater (see King et al., 1971; White, 1983). A feasible explanation for the sustained drain activity was enhanced lateral movement of infiltrating stream and irrigation water, owing largely to increased anisotropy effects in unsaturated, stratified soils.

Potential Effects of Future Pumping

Predictive runs have been made with the quasi 3-D groundwater flow model of Peterson et al. (1984) to assess the potential effects of increased pumping in the Mesilla Valley. The predictive simulations were based on (1) possible larger withdrawals in the Las Cruces area to

meet expected municipal supply demands and (2) proposed pumping from a large well field west of Mesilla Valley (Lee Wilson and Associates, 1981) to help augment the water needs the city of El Paso, Texas. Model results indicated that the state of "dynamic equilibrium" that now exists within the Mesilla Bolson would be upset if the increases in pumping were implemented. The simulations also showed that increased pumping in the Santa Fe Group could possibly lead to a three-fold increase in downward leakage from the flood-plain alluvium to the deeper aquifer. Model predictions suggested that water table levels in some areas might be as much as 40 to 50 feet deeper than currently exists (Peterson et al., 1984) in the Mesilla Valley.

The potential for severely declined water table levels in the Mesilla Valley raises questions as to the future behavior of stream-aquifer processes in this region. The possible greater depths of unsaturated media separating stream channel beds from underlying saturated materials suggest that suction heads beneath stream channels may become larger. Accordingly, increased stream losses may result. Existing models of groundwater flow in the Mesilla Valley flood-plain alluvium (e.g., Peterson et al., 1984; Gates et al., 1984) have been based on saturated flow principles, which ignore the effects of unsaturated flow on stream infiltration rate. Consequently, it is possible that the existing models, which have been calibrated for today's relatively shallow water table conditions, incorrectly estimate stream losses as regional groundwater levels drop.

IV. PREVIOUS WORK

Because this research draws on an a variety of subjects, a summary of relevant work performed under several diverse disciplines is in order. Therefore, much of the following discussion dealing with the findings of foregoing researchers is not specifically related to stream-aquifer processes. Rather, each piece of literature that is referenced usually only deals with one particular facet of the problem being investigated.

Analytical Solutions in the Saturated Flow Domain

Hydrologists have normally limited their attention to the saturated portion of the subsurface domain when attempting to analyze large-scale water flow in an unconfined, or phreatic, aquifer. The methods that have typically been applied, and that continue to be used today, are commonly said to be based on the "free surface" approach. Under this approach, the phreatic surface is assumed to be the upper boundary of the flow domain. Transport of water in unsaturated media has most usually been a subject of study for soil scientists, and research in that field has often been limited to problems of a small scale. It is only during the last 15 to 20 years that significant attempts have been made to analyze the concurrent flow of water in the unsaturated and underlying saturated zones. Application of these variably saturated flow analyses to large scale problems have been limited.

The governing equation of two-dimensional "saturated" groundwater flow in a phreatic aquifer, wherein vertical as well as horizontal seepage is taken into account, and in which a source of recharge such

as that from stream seepage is included, is well documented (e.g., Bear, 1979). In and of itself, this equation, when applied to a homogeneous and isotropic aquifer characterized by simple boundary conditions, would not appear to present serious mathematical hurdles to its being solved analytically. However, because the location and shape of the phreatic (or free) surface boundary is not known a priori, their solutions become part of the problem. The resulting nonlinear boundary condition that describes the phreatic surface often makes unconfined saturated flow problems stated in their "exact" form quite difficult to solve.

Despite the difficulties encountered with the unknown free surface boundary, some exact analytical solutions for two-dimensional (cross-section) steady flow have been developed (e.g., Harr, 1962; Polubarinova-Kochina, 1962) using the hodograph method. In addition, some approximate solutions of transient multidimensional flow, based on the exact statement of unconfined conditions, have been formulated (e.g., Polubarinova-Kochina, 1962; DeWiest, 1962) by utilizing the method of small perturbations.

To avoid the problem of a nonlinear boundary condition inherent in the exact statement of unconfined groundwater flow, investigators often utilize the Dupuit approximation. Problems formulated on Dupuit approximation recast the governing equation and boundary conditions of phreatic aquifer flow into a form wherein the free surface becomes the state variable for which solutions are sought. Inherent in the Dupuit approach are the assumptions that:

(1) the slope of the phreatic surface is small; consequently

(2) equipotential surfaces are essentially vertical; thus

(3) the head at any given location within the saturated zone is equal to the elevation of the water table along a vertical line passing through the given location, and

(4) flow is essentially in the horizontal direction.

Even with the Dupuit assumptions, the governing equation of unconfined groundwater flow is a nonlinear one. Therefore, the usual methods of analytically solving this type of problem are based on techniques which linearize the continuity equation (e.g., Bear, 1972).

Stream Depletion by Wells

Analytical solutions are available to describe saturated groundwater movement in the vicinity of a pumping well located near one or more recharge boundaries. Commonly, such solutions incorporate image well theory to predict the rate at which a pumping well depletes flow in a nearby stream.

Examples of these types of solutions are found in the work of Theis (1941), Glover and Balmer (1954) and Hantush (1965). The mathematical equations developed from these approaches are based on numerous simplifying assumptions, e.g., (1) the aquifer is at all times connected to the stream by fully saturated soil media, (2) the stream recharging the aquifer is straight, infinitely long, and fully penetrates the aquifer, (3) the aquifer is isotropic and of semi-infinite extent, and (4) flow in the aquifer is essentially horizontal. To account for vertical flow to streams that only partially penetrate the full aquifer thickness and the boundary effects created by a semipermeable streambed, the method of additional seepage resistances (e.g., Streltsova, 1974) is often applied (see Hantush, 1965). This technique extends the actual distance between well and aquifer by a supplemental length, horizontal flow through which results in head losses equivalent to the additional losses created by partial penetration and semipermeable bed effects.

The numerous simplifications utilized for analytical solutions to the stream depletion problem often make these techniques inappropriate for application to real situations. Stream losses in pumping areas rarely occur under conditions that are ideal. For example, natural streams are seldom fully penetrating and usually do not act as infinitely long and straight sources of water. Nor do the soils underlying a stream exhibit perfect isotropy and homogeneity of hydraulic conductivity. Often, the streambed infiltration over a given reach is induced by more than one well, and complex boundaries noticeably different from an otherwise semi-infinite flow domain will frequently be found. Moreover, pumping rates in wells that affect a river are not constant or continuous, and in fact, are likely to be somewhat irregular. Jenkins (1968) discusses techniques for analyzing stream depletion under irregular pumping schedules by incorporating the method of temporal superposition into analytical solutions.

Recently, Spalding (1985) conducted a critical evaluation of several analytical methods designed to estimate drawdowns and stream depletions by nearby pumping wells. In addition to pointing out many of the inherent problems with each of the techniques, he also made suggestions for improving the widely used analytical methods.

The preceding investigations on stream depletion by wells are based on an assumed initial condition of a completely horizontal phreatic surface (i.e., hydrostatic conditions). Although some stream-aquifer systems may approximate such an assumed condition, it is likely that most deviate significantly from this idealized condition. Wilson (1981) developed a series of analytical solutions for pumping wells near streams that take into account ambient subsurface inflow to a stream. The inflow was oriented 90 degrees to the stream axis. His

work went a step beyond the traditional methods based on semi-infinite domains by including additional boundary types located on the other side of the well. This approach has been even further enhanced by Newsom and Wilson (1987), who have developed stream depletion solutions for situations in which the ambient flow pathlines lie at an angle, other than 90°, to the stream axis.

Perhaps the largest drawback to analytical methods of computing pumping-induced stream depletion is that the various established techniques assume that stream and aquifer are always hydraulically connected by saturated soils. It is possible that hydraulic connection may not even exist prior to withdrawal of groundwater or that disconnection may occur after lengthy periods of pumping. Severance of saturated hydraulic connection naturally infers the creation of a continuous unsaturated zone adjacent to and underneath the stream channel (i.e., disconnection). As stated earlier, infiltration rates from a surface waterway into an unsaturated medium can be considerably different from those determined for fully saturated seepage.

Groundwater Mounding

Realizing that, under many circumstances, a surface water source may be hydraulically disconnected from the underlying water table, many investigators have developed analytical solutions for relatively simple cases of groundwater mounding. Most of the solutions under this category are based on Dupuit flow theory.

Some of the earliest researchers to produce analytical expressions that describe the growth (and decay) of a groundwater mound below the bed of a surface water recharge source include Baumann (1952), Glover (1960), Marino (1967), Hantush (1967) and Hunt (1971). The

mathematical development of the expressions are based on several simplifying assumptions. These include (Vauclin et al., 1979): (a) transfer of water from the surface source to the saturated domain is instantaneous, (b) spatial distribution of infiltration at the ground surface is equal to the distribution of water flux at the water table (i.e., flow in the unsaturated zone is vertical only), and (c) moisture content is unchanged over the entire vertical extent of the unsaturated zone, and is equal to the residual moisture content.

Of the three preceding assumptions common to "free surface" approaches to groundwater mound simulation, the failure to account for variable moisture content within the unsaturated zone located beneath a surface water body probably provides the most serious drawback in reproducing mound configurations in actual situations. Because of this difficulty, some researchers (e.g., Ortiz et al., 1978) use the concept of effective "permeable height" and effective "saturated height" to account for flow and storage, respectively, in the zone of negative pressure potential. Such an approach utilizes hydraulic conductivity-pressure head-moisture content (K-ψ-θ) information to determine (1) an equivalent depth of saturated soil having the same capacity for horizontal flow as the capillary region, and (2) an equivalent depth of soil having the same value of drainable water as the capillary region. The resulting equations that are solved are still formulated using Dupuit flow theory. Ortiz et al. (1978) report that neglect of capillary effects, particularly the water stored in the zone above the phreatic surface, can lead to serious errors in predicting groundwater mound behavior.

In the interest of evaluating the accuracy of analytical solutions to the groundwater mounding problem, Rao and Sarma (1980) have compared

mound heights predicted by variations of the methods of Hantush (1967) and Baumann (1952) with actual data using a laboratory-scale model. The two tested analytical techniques differ mainly in their methods used to linearize the unconfined aquifer flow equation. Rao and Sarma's (1980) findings indicate that both approaches work reasonably well, with the Hantush (1967) linearization technique being more appropriate over a wider range of situations.

Importance of Unsaturated Flow - Analytical Approach

Distinct properties of flow through the unsaturated zone are ignored in most analytical approaches to the stream depletion problem and groundwater mounding. As has been explained, problems are formulated only in terms of saturated seepage variables. Even when attempts are made to compensate for capillary zone influences (e.g., Ortiz et al, 1978), there are many factors, such as the time lag between incipient infiltration and subsequent recharge of the water table, that cannot be taken into account. It seems intuitive that unsaturated flow should not be ignored in many situations involving analysis of surface-subsurface exchange of water.

As part of an investigation into the influence of unsaturated flow on infiltration processes, Bouwer (1964) has examined methods for computing infiltration across a semipermeable layer into unsaturated media. Bouwer (1969) also applied resulting analytical expressions to compute stream losses. McWhorter and Nelson (1979) utilized the Green and Ampt (1911) technique for vertical unsaturated flow to determine the depth and rate of movement of wetting fronts below uranium mill tailings impoundments. Freyberg et al. (1980) investigated the performance of the Green-Ampt model in estimating open channel losses

for a case in which the channel bed is not clogged. Aside from the fact that analytical techniques based on the Green-Ampt model are specifically used for one-dimensional simulation, other limitations of these methods are assumed conditions of soil homogeneity and isotropy.

Although not directly related to the stream-aquifer problem, some work by soil scientists has bearing on some of the hydraulic processes associated with stream-aquifer interaction. Hillel (1964) and Hillel and Gardner (1969) present formulae for computing seepage rates across low permeability materials resulting crusting on the surface of a soil. Their analyses are analogous to the case of stream seepage across a streambed clogging layer into a disconnected aquifer. Zaslavsky (in Bear, Zaslavsky and Irmay, 1968) presents detailed mathematical models for describing variably saturated flow across two-layered soil systems. In situations where the water table is deep, and a relatively simple constitutive relationship can be used to describe hydraulic conductivity-pressure head (K-ψ) relations of the soils involved, his technique produce a series of equations that can be simultaneously solved for seepage rates and pressure head profiles over the vertical extent of the two-layer domain. Zaslavsky (1963) presents several criteria for determining conditions necessary to produce unsaturated flow beneath a low permeability soil layer with ponded water on its upper surface.

Analytical expressions describing the multidimensional head and moisture content profiles resulting from the steady state infiltration from saturated cavities of various shapes have also been developed. The solutions in most cases apply only to homogeneous soils. If the cavity shape can be interpreted as being similar to a channel cross-section, there may exist an analog between these solutions and that of

a losing stream. Examples of this kind of formulation are found in Philip (1984). It should be noted, however, that few cases examined actually permit the computation of heads within the saturated bulb beneath a water source. Instead, it is common to assume (Waechter and Philip, 1985) that the base of the assumed cavity shape coincides with the underside of the saturated bulb. Thus, most of these types of analytical solutions assume a priori knowledge of the saturated bulb's shape and extent, rather than providing a reliable means of predicting those unknown parameters. These analyses also assume a very deep water table.

Recently, Waechter and Philip (1985) and Philip (1985) have demonstrated that an exact analog exists between infiltration from buried cavities and the scattering of plane-pulses and plane harmonic waves. The analytical solutions derived from the analogs assist greatly in predicting hydraulic potential and moisture content in cases of infiltration where the flow is strongly dominated by gravity, and capillary effects are weak but nonzero. In the event that the scattering analog could be combined with simulation of flow conditions within a saturated bulb (Waechter and Philip, 1985), the possibility may exist that solutions of this nature might aid in predicting seepage from unclogged surface waterways into homogeneous soils.

Day and Luthin (1953) demonstrate that capillarity is capable of bringing about disconnection beneath an irrigation furrow that possesses no clogging layer. The situation that they mathematically analyze involves the presence of a gravel stratum underlying a less permeable soil in which the furrow is located. The inducement of disconnection partly occurs as a result of invoking a zero pressure head condition at the soil-gravel interface. From this standpoint, it

is seen that the disconnection phenomenon in Day and Luthin's (1953) study is the result of media heterogeneity, rather than a natural occurrence in an infinitely deep homogeneous domain.

Field Investigations of Stream-Aquifer Interaction

Studies of alluvial aquifer systems have frequently provided evidence that surface waterways heavily influence the behavior of local groundwater flow (e.g., Stephens et al., 1987). Many investigators (e.g., Kazmann, 1948; Rorabaugh, 1956) have illustrated how pumping induced infiltration can be used to augment groundwater supplies. A field study by Moore and Jenkins (1966) inferred that intense pumping of an alluvial aquifer in the Arkansas River Valley of Colorado created unsaturated soil conditions in the soils below the river bed. Stream seepage calculations indicated that the seepage rate from the river became effectively constant along those reaches where disconnection had apparently occurred (Moore and Jenkins, 1966).

Moisture Dependent Anisotropy

Most investigations of moisture dependent anisotropy have heretofore been of a generic nature, with results being mostly used to interpret the inhibition of downward movement of infiltrating water. Little has been done in the way of simulating the effects of this phenomenon on hydrologic processes occurring in the shallower depths of an aquifer such as stream seepage, evapotranspiration and discharge to drains.

A laboratory study of infiltrating water in multilayered unsaturated media by Palmquist and Johnson (1962) clearly showed that flow parallel to horizontal soil layers was promoted at the expense of

reduced vertical seepage. More recently, Heermann and Stephens (1986) have utilized a point infiltration source in an axisymmetric tank model to illustrate the same effect.

Mathematical descriptions of unsaturated seepage in hypothetical layered domains, (Mualem, 1984; Zaslavsky and Sinai, 1981) have resulted in deterministic expressions of effective anisotropy levels that might be expected in actual soils. Analyzing the problem from a stochastic perspective, Yeh et al. (1985a,b,c) have also mathematically demonstrated the propensity for stratified unsaturated domains to exhibit moisture dependent anisotropy. The studies of Mualem (1984) and Yeh (1985a,b,c) are similar in that both show anisotropy to increase with increasing soil dryness, and that ranges of anisotropy ratios are greatest in soils with high saturated hydraulic conductivities.

Numerical and Analog Models of Saturated Flow

To overcome the limitations of analytical solutions of problems involving porous media seepage, investigators have turned increasingly to analog and numerical models for approximating subsurface water processes. The advantages that these models offer are significant. Perhaps their most useful features are their ability to account for medium heterogeneity and complex boundary conditions.

The mathematical foundation upon which the majority of models have been built stems from saturated flow principles. When simulating two-dimensional areal flow in an unconfined aquifer, the conventional approach has been to base a model on Dupuit approximations. Cross-sectional, numerical models of two-dimensional saturated flow in an unconfined aquifer have been difficult to develop, primarily due to the

nonlinear phreatic surface boundary condition. Despite the potential hurdles, many of the features of the saturated modeling approaches offer a distinct improvement over earlier methods for simulating stream-aquifer processes.

Bouwer (1969) and Jenkins (1968) use electric analogs to describe the transfer of water in a stream channel to the subsurface. A viscous flow (Hele-Shaw) analog for growth of a groundwater mound beneath a surface water body has been developed by Marino (1967). Many existing finite difference numerical simulators of saturated groundwater flow (e.g., Prickett and Lonnquist, 1971; Trescott et al., 1975; McDonald and Harbaugh, 1984) also account for seepage from surface water bodies. Longenbaugh (1967) uses an areal finite difference computer model for a stream-aquifer system in the Arkansas River Valley of eastern Colorado. The quasi three-dimensional numerical model of Peterson et al. (1984) attempts to account for seepage losses on the Rio Grande and irrigation canals in the Mesilla Valley via saturated flow concepts. In these finite difference and analog approaches, however, simulation of flow across unsaturated zones is neglected. The same is true for finite element numerical algorithms that approximate the saturated flow equations (e.g., Townley and Wilson, 1980).

As part of a study of stream-aquifer interchange on the Humbolt River in Nevada, Cooley and Westphal (1974) compare three numerical schemes based on saturated flow with a variably saturated flow model. Their simulations lead them to conclude that differences between fully saturated and variably saturated modeling approaches to the stream-aquifer problem are minimal. However, it is important to note that Cooley and Westphal (1974) only consider systems that are connected.

Examples of finite element models designed to handle two-dimensional, saturated, cross-sectional flow in unconfined materials include Neuman and Witherspoon (1970, 1971) and Taylor and Brown (1967). Included in these numerical schemes are the so-called "adaptive gridding" methods, wherein the shape and location of elements are shifted to accommodate changes in the free surface.

A variation of the finite element technique, called the boundary integral equation method (BIEM) has been utilized (Dillon and Liggett, 1983) to approximate saturated seepage in an aquifer underlying an ephemeral stream whose bed is clogged. Because disconnection is prevalent in this case, attempts are made to incorporate the effects of suction below the streambed, as well as account for the time delay between incipient infiltration and recharge of the water table (Dillon and Ligget, 1983).

Numerical Models of Variably Saturated Flow

Numerical seepage models based on combined saturated-unsaturated (i.e., variably saturated) flow principles have also been applied to groundwater problems. This so-called "unified" approach to groundwater modeling is potentially useful in cases where continuity between unsaturated and saturated systems becomes important (e.g., Freeze, 1971; Cooley, 1971; Neuman, 1973).

Studies indicating the need to include unsaturated flow in hydrologic analyses are numerous. Sophocleus (1985) uses a one-dimensional variably saturated flow model to demonstrate that serious errors in estimating recharge can arise when not accounting for the transient nature of flow across, as well as the water stored within, an unsaturated zone. He is also able to demonstrate that conventional

saturated flow concepts tend to underestimate the rate and total amount of water rise associated with an infiltration event. In a combined laboratory and numerical modeling analysis of groundwater mounding, Vauclin et al. (1979) conclude that proper simulation of transient recharge of the water table should not neglect transfer of water across the unsaturated zone. Reeder et al. (1980) use a one-dimensional finite difference simulator of variably saturated flow to analyze the effect of rapidly varying surface water depths on infiltration rates from unclogged channels.

Several different numerical schemes have been developed to handle multidimensional variably saturated flow problems. Transient finite difference schemes have been used by Freeze (1971) and Cooley (1971). Narasimhan and Witherspoon (1977; 1978) apply an integrated finite difference approach in conjunction with a mixed explicit-implicit procedure (Edwards, 1968) of solving model generated equations. Examples of two-dimensional finite element codes of combined saturated-unsaturated seepage include those of Yeh and Ward (1980) and Neuman (1973).

Accurate numerical simulation of variably saturated flow is often a difficult task due to the strong nonlinearity of seepage processes within the unsaturated zone. The discretization needs of unsaturated media compared to those of the saturated domain, both in space and time, are normally quite incompatible (Frind and Verge, 1978). Block or element sizes in wholly unsaturated problems are usually on the order of centimeters or tens of centimeters. Yet, the range of block sizes that are used in applied work on variably saturated domains is quite large. For example, Freeze (1971) finds it necessary to use vertical block dimensions of 0.33 to 3.5 feet. Winter (1983) finds

vertical element spacings of 2.5 feet in the upper portions of a domain and 400 foot horizontal spacings to be acceptable. In contrast, Rovey (1975) uses vertical spacings as large as 10-25 feet and horizontal block dimensions of up to 1.5 miles. Spatial discretization needs for variably saturated flow problems appear to be influenced not only by the type of problem being addressed, but also by the fundamental numerical scheme used in the variably saturated code and the methods used to solve the equations generated by the code.

Discretization in the time domain is also an important consideration in variably saturated flow modeling. Use of large time steps in problems involving very dry media can lead to highly unstable solutions. Freeze (1971) suggests that appropriate simulation time steps range from 0.01 seconds to a week, whereas Rovey (1975) uses steps of 10 to 30 days. Finlayson (1977) applies eigenvalue analysis to a finite element formulation of unsaturated flow situations to illustrate why solutions in the temporal domain may be difficult to achieve. He demonstrates that most unsaturated seepage problems are "stiff"; that is, the eigenvalues of the coefficient matrix resulting from the numerical solution of the physical problem are widely separated. The net effect is that (Finlayson, 1977) certain variables change rapidly in time, while other variables change slowly and require integration over a large time. Computation times are large since small time steps are used for many time intervals. This problem can be related to the previously discussed issue of discordant "time constants", found in saturated and unsaturated zones, respectively.

Another difficulty seems to arise in finite difference (and integrated finite difference) solutions to unsaturated flow problems when determining mean conductances between grid blocks. The use of

harmonic mean conductances, such as is done in Narasimhan and Witherspoon's (1978) simulator, may fail, for instance, to adequately predict the rate of movement of a wetting front resulting from an infiltration event (see, e.g., Siegel, 1980). To help overcome such inadequacies, upstream weighting techniques, long used for simulation of multiphase flow in petroleum reservoirs, are sometimes applied (e.g. Huyakorn, 1983). One-dimensional, transient simulations by Havercamp and Vauclin (1979) have indicated that a geometric mean conductance, when compared with the harmonic mean, greatly improves the accuracy of finite difference unsaturated flow models. Cooley (1983) suggests that one of the advantages of the finite element procedure over finite difference and integrated finite difference schemes is that it automatically accomplishes the nodal averaging of unsaturated hydraulic conductivity in a manner that produces an accurate approximation of the flow equation.

Up until recently, most finite element models of saturated-unsaturated flow have treated the nonlinearities of this type of flow using standard Picard solution algorithms. However, difficulties often arise when using these relatively simple schemes for certain field problems. To help counteract some of these difficulties, Cooley (1983) has incorporated a Newton-Raphson solution scheme into a two-dimensional finite element simulator. The code, which is formulated upon subdomain collocation principles and uses the strongly implicit procedure to solve resulting numerical equations, is able to handle a variety of variably saturated flow situations. It is also successfully used for large scale applied problems of a steady state nature, which can be computationally burdensome to solve (Cooley, 1983).

A more recent two-dimensional finite element model by Huyakorn et al. (1984) also makes valuable use of the Newton-Raphson algorithm in handling the strong nonlinearities of variably saturated seepage. The code in this case, called SATURN, seems especially adept at simulating steady state conditions using a coarse discretization. Although somewhat indirectly addressed by Huyakorn et al. (1984), SATURN's Newton-Raphson capability also appears very useful for transient cases, particularly since the nonlinear solution strategy helps bring stability to the solution when large time steps are used.

There are numerical simulation studies of variably saturated flow that have bearing on stream-aquifer processes. Reisenauer (1963) and Jeppson and Nelson (1970) analyze various types of subsurface seepage observed beneath surface waterways whose beds and banks are not affected by clogging. In both studies, disconnection of the stream from the underlying water table is achieved with the simulator used. Jeppson and Nelson (1970) show how disconnection is brought about by a gradual increase in saturated hydraulic conductivity with depth. Reisenauer (1963) assumes a priori the water table location and imposes a free surface boundary condition at the base of his model domain.

Siegel (1980), using a two-dimensional saturated-unsaturated numerical model of seepage below lined mill tailings ponds, showed quantitatively that increasing anisotropy causes increased lateral movement of soil moisture and slows the vertical propagation of a wetting front. The McWhorter-Nelson technique (McWhorter and Nelson, 1979) of infiltration analysis (which assumes isotropic conditions) was found to predict seepage front depths that were more than 80 percent greater than numerically computed depths for horizontal to vertical anisotropy ratios of 20 (Siegel, 1980).

Freeze (1971) studied hypothetical settings of saturated-unsaturated flow in groundwater basins affected by a surface water body using a three-dimensional finite difference model. His simulations concentrated on the effects of recharge from rainfall and basin yield determinations, and only addressed gaining streams.

Winter (1983) has demonstrated that variably saturated porous media play a significant role in affecting the interaction of lakes with groundwater. His simulations using Cooley's (1983) model demonstrate that small localized flow systems may form and subsequently dissipate in areas where surface water interacts with variably saturated soils. The complex flow systems, which may take months to totally dissipate, are transient in nature. Reversal of groundwater movement under such conditions is common, the result being that subsurface water alternately flows to and from surface water bodies (Winter, 1983).

Recently, Tracy and Marino (1987) have applied a finite element variably saturated flow simulator to evaluate two-dimensional seepage from a surface water body to an underlying porous medium. They stress two features of their work. First, first order isoparametric (quadrilateral) elements are used, the justification for which is based on the argument that their accuracy is of slightly higher order (Tracy and Marino, 1987) than linear triangular or rectangular elements. Secondly, an algorithm is included in their variably saturated simulator which allows the stage of water in the surface water body to decline in response to losses to the subsurface from the surface water source. Thus, their code is easily applied to cases involving infiltration from a pond of limited volume, which, unlike a stream, may not be continually replenished by external influxes of surface water.

Tracy and Marino's (1987) variably saturated simulation work is useful in that it takes into account the negative pressure heads that may influence seepage from a surface water body. Indeed, disconnected conditions are created in the course of one of their simulations, apparently as a consequence of seepage impedance by a semipermeable streambed. However, the distinct problem they examine appears somewhat limited, primarily because of the relatively small domain (32 meters horizontal by 4 meters vertical) they choose to model. Moreover, the boundary conditions that have been used on this small domain, ranging from prescribed head and zero flow to a designated seepage face, are difficult to relate to any observed field situations. Although such limitations are not directly addressed by the authors (Tracy and Marino, 1985) it is easy to conjecture that the type of simulation they select for study may be limited by the numerical simulation schemes (e.g., Picard iteration, numerical quadrature) that they utilize.

Perhaps the most direct application of saturated-unsaturated flow simulation to the study of stream-aquifer processes was carried out by Rovey (1975). Her approach combined a three-dimensional finite difference algorithm of variably saturated flow over one section of a river valley with a two-dimensional areal saturated flow model in the remaining parts. Rovey's (1975) work aptly demonstrated the application of a unified modeling scheme to a real setting; furthermore, the sensitivities of her model to a variety of hydrologic influences were adequately documented. However, she failed to discuss the accuracy of the three-dimensional model in predicting hydraulic head and the effects of moisture dependent anisotropy were not investigated.

V. METHODOLOGY

Numerical Model Selection

Prior to the execution of any actual simulations of stream-aquifer processes, it was necessary that an appropriate variably saturated flow code be selected and tested for its ability to handle the types of hydraulic conditions expected near losing streams with deep water tables. Of major concern was the code's ability to simulate steady state systems. Similarly, it was important to find a numerical simulator that would not exhibit stability problems due to rapid changes in material properties, such as at material interfaces. Finally, there was some question as to the size of elements (or blocks) that could be used in the simulations; i.e., large element dimensions were desirable, but only to the extent that the nonlinear flow processes within unsaturated zones could be adequately represented.

When first considering the approach to take in selecting a simulator, several alternatives were examined. It was initially felt that the authoring of an original code for this project would be too major a task given the resource constraints of the research. Development of a large code, especially one designed to handle the nonlinear processes in variably saturated flow, can be a drawn-out process that involves excessive amounts of design, development, verification and computer time. A more attractive alternative, therefore, was to utilize an existing code, with perhaps a few modifications designed to meet the specific purposes of the stream aquifer study.

Of the existing variably saturated flow codes, the most appropriate for the project's simulation needs initially appeared to be

those based on the integrated finite difference method (IFDM). The IFDM is particularly attractive due to its adaptability to multidimensional problems. One-dimensional, two-dimensional or three-dimensional problems are usually equally handled with an IFDM code; i.e., specific versions of the code are not needed to handle each of the various levels of dimensionality. The IFDM code TRUST (Reisenauer et al., 1982) was selected for testing in this study.

A number of additional finite difference and finite element codes for multi-dimensional variably saturated flow exist, some of which have been mentioned in the previous chapter on literature review. Unlike the IFDM, many of these codes are limited to simulation in two dimensions, or, at the most, three-dimensions in the form of axisymmetric seepage. Nonetheless, for reasons discussed later, some of these codes were ultimately considered for use in the stream-aquifer simulations.

Selection of codes for detailed evaluation has to a great degree been limited by code accessibility. Although the list of numerical simulators of variably saturated flow is substantial (see Bachmat et al., 1980; Oster, 1982), many of them reported in the literature have not been available to users other than the code authors. In some cases, the codes or their documentation have not been developed to their fully intended extent and are, therefore, not ready for public use. In addition, because private industry is responsible for some of the simulators, the codes fall under a proprietary status and may be available only by purchase.

After extensive testing of various simulators on New Mexico Tech's computing systems (see Chapter VI and Appendix A), the two-dimensional, finite element, flow/transport code called SATURN (Huyakorn et al.,

1984) was finally selected for the stream-aquifer simulations. The most convincing reason for choosing SATURN was that it was the only code, of those tested, that was capable of providing successful steady state solutions to stream-aquifer problems involving deep water tables. This choice limited the simulations to two-dimensional cross-sectional flow. Further discussion of the SATURN code is presented later.

Selection of Simulation Domains

In keeping with the study's original motivation, the generic numerical simulations are to a great extent patterned after conditions observed in the Mesilla Valley. The two-dimensional cross-sections that are analyzed are characterized by stream and porous medium properties that are frequently observed in the unconfined aquifer system of the Rio Grande flood-plain alluvium. Stresses placed on the unconfined systems used in the simulations are in the form of stream infiltration and leakage from the unconfined aquifer to a deeper aquifer. Respective equivalents of these stresses in the Mesilla Valley are found in the seepage from the Rio Grande and its appurtenant canals, and in the leakage from the flood-plain alluvium to the underlying Santa Fe Group aquifer(s).

A pictorial representation of the general type of domain simulated is presented in Figure 7. Note that impermeable boundaries are assumed to lie on either side of the domain, the distance to either of which from the stream centerline is as yet unspecified. The upper boundary (i.e., ground surface), other than at the stream, is also assumed impermeable. By virtue of these zero flow boundaries, all water either entering or leaving the system must do so via the stream and lower boundaries of the domain. Note also that the base of the simulation

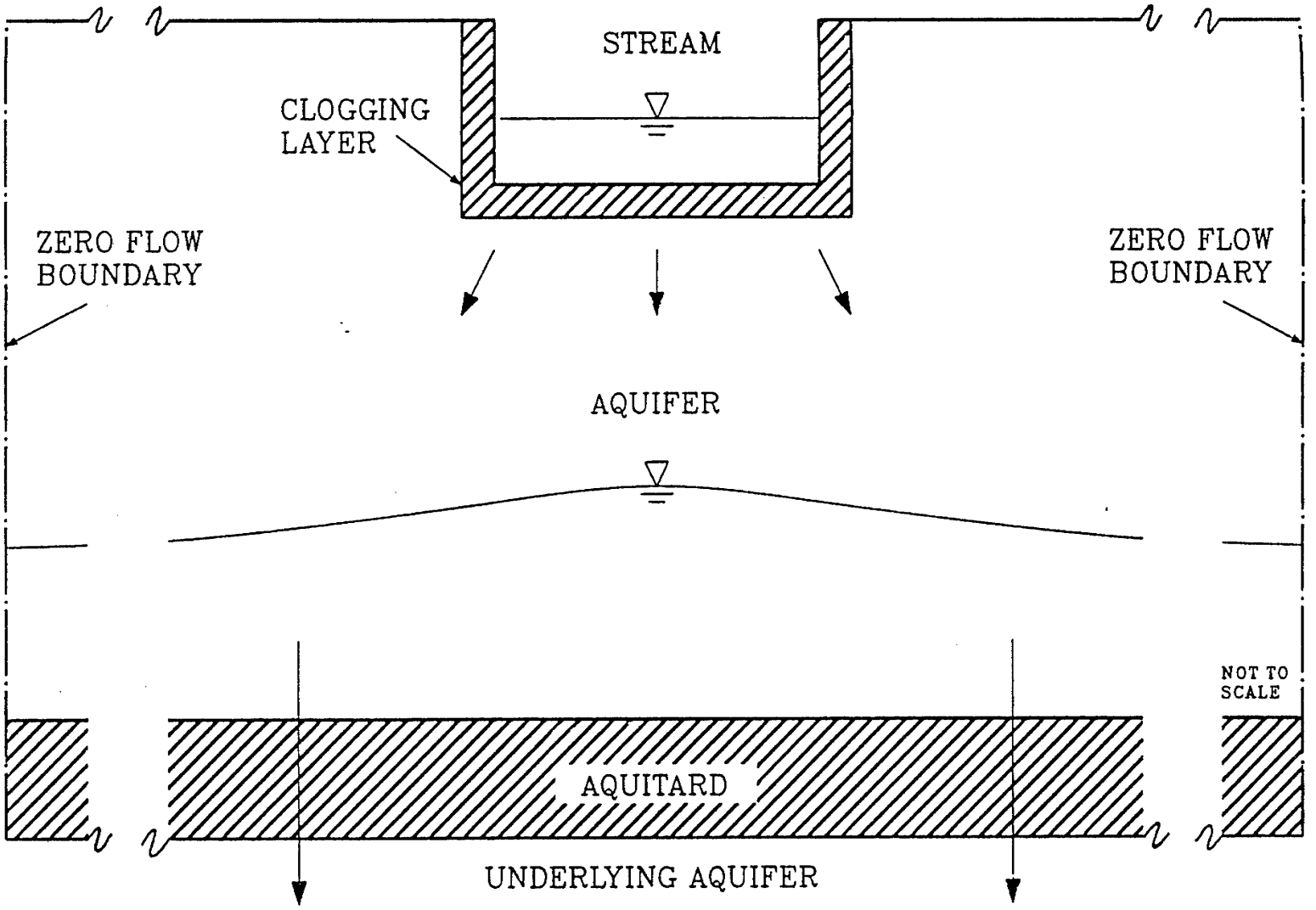

Fig. 7. General stream-aquifer system.

domain is located at the base of the aquitard, or, equivalently, at the top of the so-called underlying aquifer. Similarities between this domain and the Mesilla Valley exist in that (1) the underlying aquifer represents the Santa Fe Group, (2) the shallow aquifer portrays the flood-plain alluvium, and (3) the aquitard is representative of the low permeability units that commonly lie between the two major groundwater producing zones of the region.

In recognition of the fact that variably saturated flow simulation in a large domain of the same nature as that in Figure 7 can be computationally expensive, symmetrical flow conditions are assumed to exist around the centerline of the domain. Thus, simulations are only performed for half the domain shown in Figure 7. As a consequence, the domain centerline (which coincides with the stream centerline) has become an impermeable boundary during actual runs with the variably saturated flow code.

Establishing the upper and lateral domain limits as zero flow boundaries is done primarily in the interest of simplifying the variably saturated flow simulations. Invoking these conditions necessarily makes these boundaries coincide with flow lines, and hydraulic equipotentials are perpendicular to the boundaries. However, certain natural processes are being ignored in making such assumptions. For example, under actual conditions, both evapotranspiration and infiltration normally occur across the ground surface (upper boundary). Evapotranspiration can cause upward flow gradients, and, given a sufficiently shallow water table, will cause water in the saturated zone to move upward. When infiltration across the ground surface occurs, such as during irrigation periods, the flow gradient is then reflective of downward flow. However, even under irrigated conditions,

vegetation along the stream bank can derive water from the stream. Regardless of whether infiltration or evapotranspiration are dominating near the ground surface, flow equipotentials and flow lines will be different from those observed when the upper boundary is assumed impermeable.

Similarly, lateral system borders seldom approximate truly impermeable boundaries. In lieu of the assumed zero flow conditions, the lateral boundaries in Figure 7 might be treated as Dirichlet (prescribed head), Neumann (i.e., prescribed non-zero flux), or Cauchy (head-dependent) boundaries. However, interpretation of these boundary types as to what they represent under actual conditions is as difficult as the case of a zero flow boundary. In any event, selection of an alternative boundary condition would likely bring about greater flow activity near the lateral borders of the stream-aquifer system.

In order to assess the impact of all influences of unsaturated flow within stream-aquifer domains, a variety of possible conditions have been considered. Simulations have been conducted to evaluate model response to variables such as aquifer material properties, material distribution (heterogeneity), clogging layer and aquitard characteristics, and system geometry. To carry out this task in an organized fashion, a "reference" simulation case has been selected, and many of the other stream-aquifer systems examined are considered variations of this reference case. The reference simulation case is comprised of a domain of explicit size and shape, and of specific porous medium materials making up the clogging layer, aquifer and aquitard, respectively. Specifics regarding domain dimensions, material properties and the procedure by which model sensitivity is analyzed are presented later (Chapters VII and VIII).

Steady State and Transient Analyses

Steady state simulations have been made for both shallow and deep water table conditions. The condition of deepening water table levels is created by reducing hydraulic heads in the underlying aquifer (referred to as underlying head). The steady state head configurations arrived at in each case are assumed to represent quasi-equilibrium conditions resulting from gradually increased annual pumping in the underlying aquifer. In addition to examining pressure and hydraulic head profiles, other system properties such as steady state seepage rates and water table levels are inspected.

The number of transient simulations are considerably less than those devoted to steady state analyses. Steady state results are used to determine those situations in which the effect of unsaturated media is most prominent, and therefore worthy of further analysis under temporal influences.

Transient runs have been conducted primarily for the purpose of examining seasonal changes in system response to variations in streamflow over the course of a year. Stream stage is the only variable changed with time, while all other parameters, including hydraulic head beneath the basal aquitard (underlying head), are kept constant. Starting conditions for each transient run are taken from the equivalent steady state simulation in which stream stage was equal to the mean annual value of stream depth used in the transient run.

A more appropriate label for the transient runs might be that of "quasi-steady state" simulations. Although each run catches the behavior of a stream-aquifer system over the course of a year, system response in each case is found to be quick enough such that the same behavior is repeated year after year. This indicates that each

simulated system exists in a state of dynamic equilibrium and lends some justification to the assumption that the steady state simulations are representative of average conditions in a year. Because of the short time response of the simulated stream-aquifer systems, an analysis of long-term response to reductions in head in the underlying aquifer also becomes possible.

Examination of Saturated Flow Modeling

As a further illustration of the importance of unsaturated subsurface seepage in the interchange of ground and surface waters, some comparisons have been made between the variably saturated flow model results and those derived from saturated flow modeling approaches. The numerical code used for comparison with variably saturated results is also a finite element code and is based on commonly applied techniques for simulating saturated subsurface flow.

The greater majority of saturated flow codes used for applied modeling of unconfined aquifers are based on Dupuit theory. As a result, vertical flow within the saturated zone is not fully taken into account. In addition, influxes of water from surface sources, such as from stream seepage, must be simulated in a different manner with saturated, "free surface" schemes than with the "unified" approach taken in variably saturated flow codes. This in turn means that boundary conditions utilized in the two separate approaches are different. Therefore, comparison of the two schemes to single out the significance of unsaturated seepage must be done in a manner such that unsaturated media effects are the predominant factors causing differences in the two approaches. In other words, care must be taken to insure that major differences in results from the two approaches are

not due to peripheral influences such as the dimensionality of problem formulation, or the way in which boundary conditions are handled. Attempts have been made in this study to assure that this latter objective is met. Justification for the comparisons that are made between fully saturated and variably saturated modeling schemes is presented later.

Because the saturated flow modeling schemes examined are based on Dupuit flow theory, the conditions that are included in the comparative simulations are somewhat limited. For example, it is difficult to develop a Dupuit saturated flow model for a heavily stratified phreatic aquifer that can be considered the equivalent of a variably saturated flow model. The determination of an effective saturated hydraulic conductivity to represent a mean value of the permeabilities observed in all of the saturated layers is a subjective process. For that reason, comparative simulations in this report are only made with homogeneous aquifer domains.

VI. NUMERICAL SIMULATOR

Codes Tested

Five separate numerical codes of variably saturated flow were closely examined for the purpose of conducting stream-aquifer simulations. The five, listed by their commonly used acronyms were: (1) TRUST, (2) UNSAT2, (3) FEMWATER, (4) T3FEMWATER and (5) SATURN. The degree to which each code was inspected varied depending on early impressions developed about it from initial runs. It should be noted that several other numerical codes had been considered for examination, but were not actually tested on New Mexico Tech's computing systems, either due to lack of availability or because information regarding them (e.g., Oster, 1984) suggested they would not suit this study's purposes.

As discussed in Appendix A, all but the SATURN code of the five mentioned above possesses properties that limits their applicability to the proposed stream-aquifer simulations. Although SATURN is proprietary, its owner, GEOTRANS Inc., of Herndon, Virginia, has allowed a version of the object code to be used in this research. The primary author of the code is Dr. Peter Huyakorn. The remainder of this section is given to a discussion of the features of SATURN.

Mathematical and Numerical Model

The governing equation of flow (Huyakorn et al., 1984) which the SATURN code approximates is

$$\frac{\partial}{\partial x_i}\left\{(K_s)_{ij}\, k_{rw}\left[\frac{\partial \psi}{\partial x_j} + e_j\right]\right\} = \left\{S_w S_s + \phi \frac{dS_w}{\partial \psi}\right\}\frac{\partial \psi}{\partial t} - q \qquad (1)$$

where

ψ = pressure head [L]

$(K_s)_{ij}$ = saturated hydraulic conductivity tensor [L/T]

k_{rw} = relative permeability with respect to the liquid water phase ($0<k_{rw}\leq 1$) [dimensionless]

x_i = spatial coordinates [L], i=1,2

e_j = unit vector in the vertical (x_2) direction [dimensionless]

S_w = water saturation ($0<S_w\leq 1$) [dimensionless]

S_s = specific storage [1/L]

ϕ = porosity [dimensionless]

$\phi\frac{dS_w}{d\psi}$ = specific moisture capacity (C) [1/L]

t = elapsed time [T]

q = volumetric flow rate, via sources or sinks, per unit volume of the medium [1/T]

Two dimensionless terms in (1), water saturation (S_w) and relative permeability (k_{rw}), deserve further explanation, since neither has as yet been defined, yet both are key variables in variably saturated flow simulation. Water saturation is defined as the ratio of moisture content to medium porosity (i.e. $S_w = \theta/\phi$). Thus, it is possible for S_w in an unsaturated medium to exhibit values ranging from 0 to 1, the latter indicating that the medium is saturated. Relative permeability is the ratio of unsaturated hydraulic conductivity K to saturated hydraulic conductivity K_s (i.e., $k_{rw} = K/K_s$). Consequently, this value also varies between 0 and 1.

It is important to note that anisotropy in SATURN is handled via the saturated hydraulic conductivity tensor $(K_s)_{ij}$ and not with relative permeability. Because horizontal to vertical anisotropy

ratios are constant in a block of material that is saturated, the code (at least the version used in this study) is, therefore, not capable of adjusting for moisture dependent anisotropy in individual elements.

From equation (1) it is clear that the variably saturated seepage problem is posed strictly in terms of liquid water flow, i.e., the role of the air phase is considered insignificant. It can also be seen that both ψ and S_w are considered dependent variables, which can be linked together via a nonlinear constitutive relationship which depends on the type of soil. Relative permeability k_{rw}, also a nonlinear property, can be related by a separate relationship to either water saturation or pressure head.

Equation (1) represents flow in two dimensions. In all further discussion of the code, the x_1 coordinate coincides with what is conventionally thought of as the horizontal, or x direction. Similarly, x_2 stands for the vertical, or z direction with z increasing upwards.

To complete the mathematical formulation of the variably saturated flow problem, boundary conditions need be stated along with an initial condition. In the case of SATURN, the allowed boundary conditions consist of prescribed head (Dirichlet) and prescribed flux (Neumann) conditions. They are written, respectively

$$\psi\ (x_i,t) = \psi_0 \text{ on } \Gamma_1 \tag{2}$$

and

$$V_i n_i = -V_n \text{ on } \Gamma_2 \tag{3}$$

where Γ_1 is the portion of the flow boundary where ψ is prescribed as ψ_0, Γ_2 is the portion of the flow boundary where the outward fluid flux

is prescribed as $-V_n$ and n_i is the outward unit vector normal to the boundary Γ_2.

Equation (1) is solved numerically in SATURN using the Galerkin finite element procedure. A detailed description of the mathematics involved in application of this method to the variably saturated flow equation (1) is not given here. Instead, several features incorporated into the numerical solution scheme are summarized in the following paragraphs. The reader is referred to Huyakorn et al. (1984) if a more rigorous explanation of the techniques involved is needed.

SATURN employs linear rectangular and triangular elements to facilitate its user's discretization needs. The use of these simple types of linear elements is advantageous in two ways: (1) sometimes costly numerical integration involved with nonlinear elements is avoided; necessary integrations involving basis functions can be performed analytically, resulting in the development of relatively simple "influence coefficients" (Huyakorn et al., 1984); (2) combined rectangular and triangular elements are easily applied to flow regions of complex geometry, and are particularly suitable to zones where mesh expansion or contraction is needed.

The Galerkin scheme results in a series of equations, one for each active node, which can be represented by

$$A_{IJ}\psi_J + B_{IJ}\frac{d\psi_J}{dt} - F_I = 0 \qquad I = 1,2...n \qquad (4)$$

where n is the total number of model nodes, A_{IJ} are components of a matrix representing conductance properties of the domain, B_{IJ} are components of a matrix representing storage properties, and F_I are

components of a vector representing source/sink terms, prescribed flux on Γ_2 boundaries, and flow due to gravitational forces.

The system of nonlinear equations given in (4) is solved to find a ψ value at each node. Two techniques are available for carrying out the solution. A summary of the two strategies, Picard and Newton-Raphson iteration, is given in the next several paragraphs.

Picard and Newton-Raphson Schemes

Before applying Picard iteration to (4), the time derivative in this equation is approximated using a standard finite difference expression. Then, after rearrangement of terms, the system of equations for the Picard solution strategy appears as

$$\left[\omega A_{IJ}^{k+\omega} + \frac{B_{IJ}^{k+\omega}}{\Delta t_k}\right]\psi_J^{k+1} = F_I^{k+\omega} + (\omega-1)A_{IJ}^{k+\omega}\psi_J^{k} + \frac{B_{IJ}^{k+\omega}}{\Delta t_k}\psi_J^{k} \qquad (5)$$

where:

k = superscript indicating previous time level

k+1 = superscript indicating current time level

$\Delta t_k = t_{k+1} - t_k$ = the kth time increment

ω = a time weighting factor

In the Picard version of SATURN, only the time-centered Crank-Nicholson time stepping scheme ($\omega = 0.5$) or the fully implicit backward difference option ($\omega = 1.0$) are made available to the user. As with any code designed to handle nonlinear conditions, a given problem is solved iteratively until a stable numerical solution is achieved. Inherent in the Picard scheme is the assumption that, at each iteration, the most recent nodal values, namely $\psi_J^{k+\omega} = (1-\omega)\psi_J^k + \omega\psi_J^{k+1}$,

are used to determine parameters composing the conductance coefficient matrix and the right-hand-side vector.

Following a discussion given by Huyakorn et al. (1984), the Newton-Raphson procedure begins by setting the left hand side of (4) equal to G_I; thus

$$G_I = A_{IJ}\psi_J + B_{IJ}\frac{d\psi_J}{dt} - F_I = 0 \qquad I = 1,2,\ldots,n \qquad (6)$$

The next step in the Newton-Raphson scheme is to develop a Taylor Series expansion of G_I and truncate the expression by eliminating all terms containing second order derivatives or greater. Consequently,

$$G_I^{r+1} \simeq G_I^r + \left(\frac{\partial G_I}{\partial \psi_J}\right)^r \Delta\psi_J^{r+1} = 0 \qquad I = 1,2,\ldots,n \qquad (7)$$

where r and r+1 denote previous and current iteration levels at the present time step, and $\Delta\psi_J^{r+1}$ is defined as

$$\Delta\psi_J^{r+1} = \psi_J^{r+1} - \psi_J^r \qquad (8)$$

Similarly, the so-called sensitivity derivative $\frac{\partial G_I}{\partial \psi_J}$ is given by

$$\frac{\partial G_I}{\partial \psi_J} = A_{IJ} + \psi_L \frac{\partial A_{IL}}{\partial \psi_J} + \frac{B_{IJ}}{\Delta t_k} + \frac{\Delta\psi_L}{\Delta t_k}\frac{\partial B_{IL}}{\partial \psi_J} - \frac{\partial F_I}{\partial \psi_J} \qquad (9)$$

where L is a dummy nodal subscript. Note that in the process of developing the above-given expression for the sensitivity derivative, the finite difference expression for the time derivative has already been applied using a fully implicit time weighting scheme.

Detailed expressions for (9) that are used to evaluate sensitivity derivatives on an element basis, and for both triangular and rectangular elements, are presented in Huyakorn et al. (1984). Substituting these formulae along with (8) into (7), a matrix expression is arrived at which allows the determination of a new value of the state variable ψ_J^{r+1}. Upon conducting this last step the Newton-Raphson cycle is completed. The most notable feature of this algorithm is that sensitivities of the parameters used to build the coefficient matrices to changes in the state variable ψ are taken into account.

The basic structure of the series of equations used to solve for ψ_J^{r+1}, with the Newton-Raphson procedure is similar to those produced by Picard iteration in the sense that a coefficient matrix, multiplied by a vector at the unknowns ψ_J, is equal to another vector of known values located on the right-hand-side of the matrix equation. However, an important difference does exist in that the Picard coefficient matrix is symmetric, while that stemming from the Newton-Raphson approach is asymmetric. A direct solution technique is used to solve the equations in each iterative scheme; therefore, the Newton-Raphson scheme, with its asymmetric coefficient matrix, obviously requires more computer memory. In addition, given a situation in which each method is applied to the same problem, the Newton-Raphson scheme requires more CPU time than does the Picard procedure for the same number of iterations. Distinct advantages of the Newton-Raphson approach, however, are often observed for problems involving highly nonlinear soil properties and/or steady state flow. In such cases, the Newton-Raphson scheme will often converge to a solution in fewer iterations than that required by the Picard scheme (Huyakorn et al., 1984).

Moreover, the Newton-Raphson scheme will frequently yield solutions to variably saturated problems that the Picard algorithm is entirely incapable of solving. In the version of SATURN utilized in this study, the Newton-Raphson scheme can only be implemented with rectangular elements.

Other Enhancements

To enhance convergence of the Picard scheme, SATURN incorporates a chord-slope formula to compute the specific moisture capacity term, $C = \phi \frac{dS_w}{d\psi}$, previously mentioned when presenting equation (1). The chord slope formula for $\frac{dS_w}{d\psi}$ is written

$$\frac{dS_w}{d\psi} = \frac{S_w^{r+1} - S_w^{r}}{\psi^{r+1} - \psi^{r}} \qquad (10)$$

where, as before, r+1 and r denote current and previous iteration levels. Thus, it can be seen that the value of C is determined by a finite approximation to the derivative found in the mathematical expression for this term rather than using a tangent slope of the water saturation versus pressure head curve. This algorithm seems to be particularly suited for, and promotes convergence of, problems in which the material properties used to construct coefficient matrices show an "S-shaped relationship" with the state variable when plotted on graph paper (Huyakorn et al. 1984). Indeed, relations between saturation S_w and pressure head ψ (and, therefore, of θ versus ψ) for unsaturated soils are characterized by S-shaped curves. Apparently, the chord-slope scheme helps avoid oscillations about the true solution, which is frequently the case when the tangent slope approach is used.

Since a chord-slope formula assists in reaching solution convergence when the derivative of saturation level with respect to pressure head is involved, it is intuitive that a similar type of formula would help the solution process for any other cases in which derivatives of a parameter with respect to the state variable are encountered. For this reason SATURN also uses a chord-slope approach to compute sensitivity derivatives resulting from equation (7).

Another feature of the SATURN code that enhances convergence is the use of extrapolation formulae for estimating nodal values ψ_J^{k+1}. At the beginning of a new time level, an estimate of ψ at the new time is obtained from

$$\psi_J^{k+1} = \psi_J^{k} \qquad k = 1 \qquad (11a)$$

$$\psi_J^{k+1} = \psi_J^{k} + \left(\psi_J^{k} - \psi_J^{k-1}\right) \Delta t_k / 2\Delta t_{k-1} \qquad k = 2 \qquad (11b)$$

$$\psi_J^{k+1} = \psi_J^{k} + \left(\psi_J^{k} - \psi_J^{k-1}\right) \frac{\log\,(t_{k+1}/t_k)}{\log\,(t_k/t_{k-1})} \qquad k > 2 \qquad (11c)$$

The above-given extrapolation formulae have also been applied by Cooley (1971) to unsaturated flow problems.

Velocity, Moisture and Boundary Flux Determination

Computation of horizontal and vertical components of Darcy velocity assist the SATURN user in determining flow directions as well as the relative magnitude of seepage in various portions of a flow domain. SATURN utilizes a simple cost-effective means of determining velocities. This is accomplished by evaluating head gradients, and, consequently, velocity parameters, at element centroids. The

simplicity of this scheme derives from the fact that centroidal velocities involve only relatively simple averaging calculations for each element; therefore, there is no need to carry out lengthy matrix computations as is sometimes used in other finite element flow codes (e.g., Yeh and Ward, 1980). For similar reasons, moisture contents are also determined at element centroids.

In the interest of achieving reliable estimates of boundary fluxes, back-substitution of computed pressure heads into the global matrix equation is performed for those matrix rows that correspond to Dirichlet type boundary nodes. Further explanation of the method is provided in Huyakorn and Pinder (1983).

Model Testing

Verification of SATURN's ability to accurately simulate subsurface water flow in various types of variably saturated systems was not the objective of this research. Much of that work has been accomplished and reported on in previous publications (Huyakorn et al., 1983; Huyakorn et al., 1984). However, it was felt necessary to test the code for its ability to handle some of the unique conditions encountered with the proposed stream-aquifer study.

As with many numerical modeling investigations concerned with nonlinear problems like unsaturated flow, analytical solutions to certain boundary value problems are often nonexistent. As a consequence, in such cases, verification of a code by comparison with analytical solutions is impossible. In some instances, therefore, researchers elect to demonstrate the adequacy of numerical solutions by conducting laboratory studies of the nonlinear phenomena and then compare the laboratory results with those from the code (i.e., model

validation). If laboratory results support findings from the numerical modeling approach, it can then be argued that the model code is capable of handling similar yet more complex problems.

Unfortunately, conventional means of code verification and validation are usually not feasible when attempting to demonstrate a model's potential in handling large scale variably saturated flow problems, especially those involving heterogeneous domains and complex boundary conditions. A modeler must then turn to more qualitative means of evaluating a code's appropriateness for a given problem. As a first step, the code user must check the results of test simulations to assure that the physical principles upon which the mathematical model is based are being adhered to. In other words, it is imperative, especially with nonlinear simulators, to confirm that a code is converging to a feasible solution, and not appearing to converge to an answer that cannot be substantiated by physical principles.

A technique that is sometimes applied under situations where code verification is not possible consists of evaluating model results from two or more spatial discretization schemes. With this approach, model runs using a domain based on relatively fine discretization are compared with those from a much coarser discretization scheme (e.g., Winter, 1983). If only minor variations are found between the two sets of results, some justification is derived for using the coarsely discretized domain in all subsequent simulations; thus, computing costs can be kept at a minimum. The degree of allowable mesh coarseness, however, is naturally dependent on the level of accuracy required for the problem at hand. Although this approach does not guarantee that a code is properly and accurately simulating the conditions for which it was designed, it does help to pinpoint the propensity for nonlinear

flow simulators to produce grossly inaccurate results due to numerical errors from large blocks or elements. Similar approaches can be implemented in the time domain to test model sensitivity to time step sizes.

True code verification was infeasible for the domain sizes that were considered in the stream-aquifer analyses. Consequently, like others, this writer had to use indirect techniques for assessing the reliability of SATURN. In addition to routinely confirming model results for their physical plausibility, regular checks were made on other model output, including mass balance calculations and iterative convergence behavior. Some testing was also performed to determine the code's sensitivity to discretization in the vertical direction, particularly in unsaturated zones lying beneath and near to the stream channel. As will be shown in the next chapter, horizontal dimensions of elements situated far from the stream channel were relatively large. However, the authors did not attempt to evaluate their effect on model accuracy. The reason for omitting such evaluations was that the flow activity in these outlying areas was always of much less magnitude than in the more active areas located close to the stream. Consequently, the effect of coarse discretization far from the stream was felt to be of minimal impact on overall model solutions.

To test SATURN's sensitivity to variations in the vertical dimensions of elements, a series of steady state simulations of one-dimensional columnar flow were performed using similar soil properties and conditions to these expected during the final two-dimensional runs. Specifically, the column domain consisted of a thin top layer containing a clogging material, below which a homogeneous aquifer material existed. Prescribed boundary heads above the clogging layer

were varied to simulate the effects of variable stream stages. The pressure head at the base of the domain was maintained at a value of zero. Thus the base of the domain was an assumed phreatic surface, and all flow in the homogeneous aquifer material beneath the clogging layer was forced to be unsaturated.

Several runs were made with the column model using vertical dimensions of elements within the aquifer material of 1, 2, 3 and 5 feet. Head profiles resulting from the 1 and 2 foot element sizes were very good in that the computed vertical head profiles were quite smooth and were physically plausible. When the 3-foot high elements were used, however, significant incongruities began appearing in pressure head profiles in the zone just above the phreatic surface, i.e., pressure head values at a few nodes were more negative than was indicated by the steady state flow rate. Using element heights of 5 feet, computed pressure heads in the unsaturated aquifer materials oscillated strongly around the values that would be expected for the computed flow rate. Similar results to these were reported by Huyakorn et al. (1986).

Information derived from model sensitivities to vertical discretization schemes have played an important role in designing the finite element meshes for the two-dimensional stream-aquifer simulations. Mesh design consider-ations are discussed at some length in the next chapter.

VII. SIMULATION DOMAIN

Dimensions of Simulation Domain

A sketch of the hypothetical cross-section used as the reference case for the variably saturated flow simulations is shown in Figure 8. As discussed previously, in the interest of minimizing computing time and costs, symmetry has been invoked in designing this domain. Consequently, the centerline of the stream constitutes an impermeable boundary as does the other lateral boundary of the system. Neither inflow nor outflow of water are allowed at the upper boundary of the system, other than at the stream. Thus, recharge from irrigation and evapotranspiration is totally omitted from consideration, again for the purpose of simplifying the simulations in this investigation. The lower boundary of the simulation domain is situated at the base of the aquitard along the interface with the underlying regional aquifer. Note that the origin ($x = 0.0$, $y = 0.0$) of the domain is located in the lower left corner of the aquitard. All elevations are determined with respect to this point, as are lateral distances from the stream centerline.

The dimensions of the reference case cross-section are included in Figure 8. Total depth of the aquifer, stream width, channel depth, thickness of the aquitard below the aquifer, and thickness of the clogging layer have been selected as being representative of systems typically observed in the Mesilla Valley flood-plain alluvium. The stream width (full width of 50 feet, half-width of 25 feet) is characteristic of the larger canals of the region, and of the Rio Grande along reaches where its width narrows.

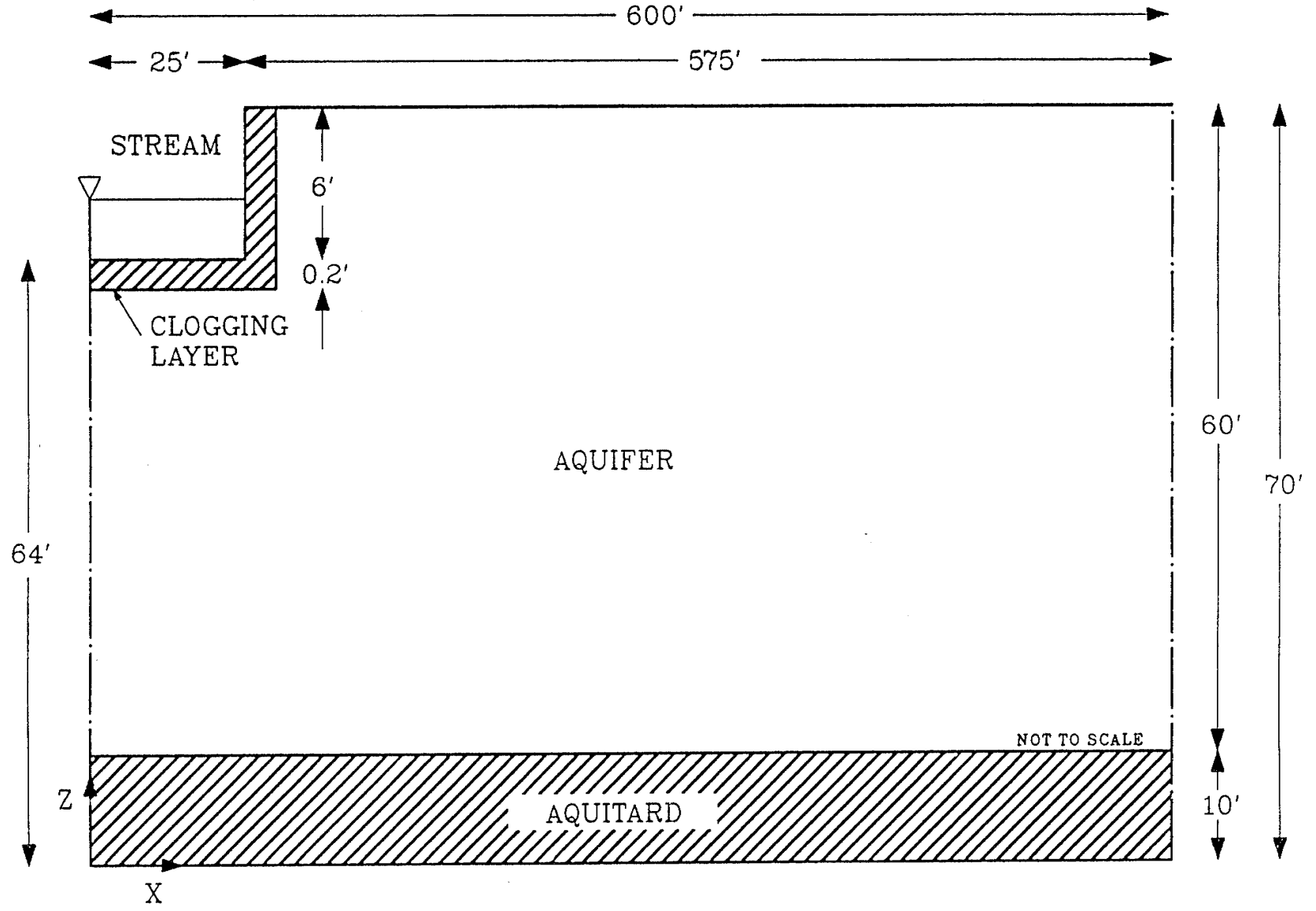

Fig. 8. Dimensions of the reference simulation domain.

The total width of the simulated system, 600 feet, is ten times larger than the aquifer depth. In reality, this width is probably much smaller than is typically observed in the Mesilla area. Nonetheless, the shorter width has been selected so that fewer elements need be used, thus helping to minimize computing time. A larger width is considered later in evaluating system sensitivity to domain dimensions.

The relatively small thickness of the clogging layer (0.2 feet) has been selected on the basis that the semipermeable portions of channel beds in actual surface waterways (e.g., New Mexico State University, 1956; Moore and Jenkins, 1966; Brockway and Bloomsburg, 1968) are frequently of such limited depth. Behnke (1969) has demonstrated that minimal clogging layer thicknesses are the natural result of particle straining mechanisms that prevent suspended sediment from infiltrating more than a few inches below streambed level.

The impermeable boundary condition at the centerline of the stream is easy to conceptualize if it can be assumed that water either leaving or entering the stream does so in a symmetric fashion. Zero flow conditions along the other end of the system, however, are somewhat harder to justify. This latter boundary can be explained, in a physical sense, in two separate ways:

(1) the lateral extent of the alluvial stream-aquifer is limited to the dimensions indicated with effectively impermeable sediments lying to the right (and left) of the system; or

(2) another surface waterway lies to the right of the system being modeled, and the system associated with it is the mirror image of that shown in Figure 8. Thus, the right lateral boundary of the domain that is simulated becomes another line of symmetry, with processes occurring on the other side of it being the mirror equivalents of those in the simulation domain.

Discretization

The reference system presented in Figure 8 is discretized into a model domain consisting of 1704 nodes and 1619 rectangular elements. The discretization scheme is illustrated in Figure 9. Certain features of this scheme reflect some of the authors thoughts and issues dealt with during the discretization procedure, and are worth mentioning:

(1) Only rectangular elements are used, since the Newton-Raphson technique in SATURN is only available for rectangular elements. The Newton-Raphson technique is necessary for achieving solutions under the condition of disconnection with a deep water table.

(2) Use of rectangular elements only forces the channel walls to be vertical. As a consequence, the domain's general shape is that of rectangle with a rectangular notch in the upper left corner.

(3) To help assure that the pressure field is simulated accurately when infiltrating water is moving downward within unsaturated zones below the stream, the largest element height within a depth of 29 feet of the streambed is 1 foot. Below this, elements within the aquifer are given vertical widths of 2 and 2.5 feet, the largest occurring at the aquifer base. Selection of these dimensions is partly based on previously mentioned test simulations of one-dimensional infiltration in partially saturated zones.

(4) For reasons similar to those given in (3) above, and in the interest of handling several different stream depths, element heights for the first 3 feet above the base of the stream is 0.5 feet. Above this zone the vertical dimension of the elements returns to 1 foot.

(5) A single element is used to represent the clogging layer (0.2 feet thick) along each portion of the streambed and stream banks where this layer occurs. Finer discretization of such a thin unit is unwarranted.

(6) In addition, single elements are also used along the entire basal part of the domain to represent the confining layer. Such a step helps minimize the need for more nodes and elements, and thus more costly numerical solutions. By taking this step, the head profile across the aquitard is necessarily assumed to be a steady state one (i.e., a linear head gradient exists across the aquitard). Some question may be raised as to the validity of this approach, since it is well known that a finite length of time is necessary for steady state conditions to occur within a low permeability unit of this type after either the upper or lower surfaces of the aquitard have undergone a change in head. However, calculations for this 10 foot thick unit, using reasonable

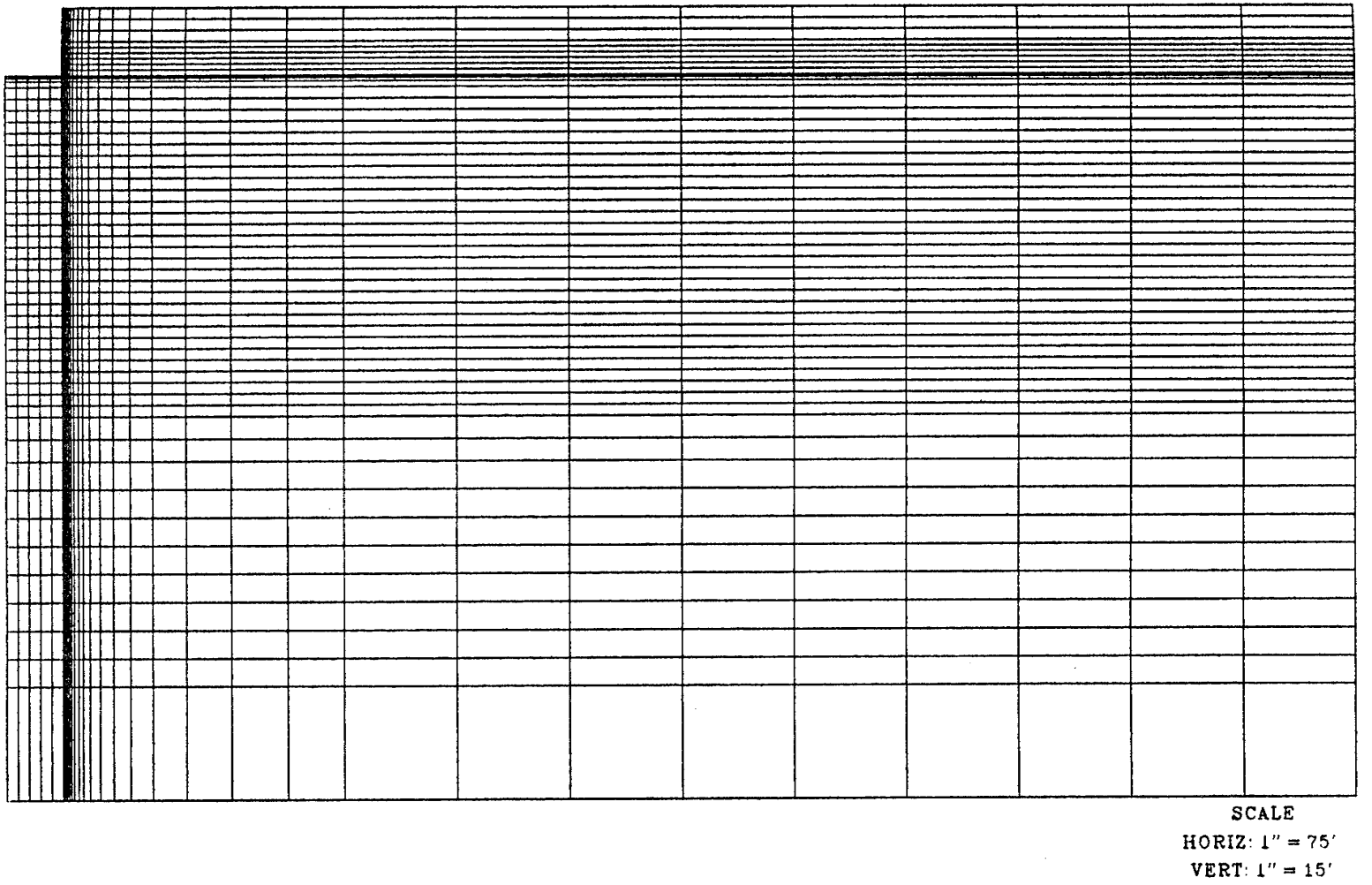

Fig. 9. Finite element mesh for the reference domain.

values for saturated hydraulic conductivity and specific storage in typical semipermeable materials, indicate that the longest time needed to reach equilibrium conditions is on the order of a day. Consequently, it is unlikely that this gross discretization of the basal aquitard will strongly affect transient model runs wherein boundary conditions are maintained for durations approaching several months.

(7) Element lengths beneath the stream are 5 feet. Just to the right of the stream, finer discretization is used, with the horizontal dimensions of rectangles being gradually increased from 0.5 feet to 50 feet. A uniform element length of 50 feet is used for the last 9 columns of elements located just to the left of the right lateral boundary. The possibility of significant numerical errors resulting in this latter zone due to high element length to breadth ratios (in some cases as high as 100 to 1 or larger) appears to be minimal, since most flow in this area is expected to oriented, either perpendicular, or parallel, to the element axes, rather than at odd angles to them.

Media Properties

A total of seven hypothetical soils are developed for use in the computer simulations - three to be used as aquifer materials, and the remaining four for clogging layer and aquitard materials. The hydraulic characteristics for each have been determined using mathematical relationships that interrelate pressure head (ψ), hydraulic conductivity (K) and moisture content (θ). Determination of parameter values used in the relationships is partly based on hydraulic properties reported in the literature; however, final selection of the soil parameters is arbitrary. The three aquifer soils range from a very coarse grained, well sorted sand to a relatively low permeability loamy sand. Streambed clogging and confining (aquitard) materials range from a very low permeability silty clay to a moderately permeable sandy silt. All of these "semipermeable" materials are assumed to contain some clay, with the percentage of clay in the soil matrix decreasing with increasing values of saturated hydraulic conductivity (K_s).

Soil moisture characteristic curves relating moisture content to pressure head are similar to those used by Winter (1983), the constitutive relationship for which is expressed as (Brutsaert, 1966)

$$S_e = \frac{S_w - S_{wr}}{1 - S_{wr}} = \frac{\theta - \theta_r}{\phi - \theta_r} = \frac{A}{A + (\psi - \psi_a)^c} \qquad \psi \geq \psi_a \tag{12}$$

where

S_e = normalized water saturation (dimensionless)

θ = volumetric moisture content (dimensionless)

θ_r = residual moisture content (dimensionless)

ϕ = porosity (dimensionless)

S_w = water saturation, $\frac{\theta}{\phi}$ (dimensionless)

S_{wr} = residual water saturation, $\frac{\theta_r}{\phi}$ (dimensionless)

ψ = pressure head (L)

ψ_a = air entry suction head (L)

A,c = empirical parameters

Similarly, the equation relating hydraulic conductivity to normalized water saturation (and thereby to moisture content as well) is specified in SATURN as (Brooks and Corey, 1966)

$$k_{rw} = S_e^D \tag{13}$$

in which D = an empirical parameter, and remaining parameters are as defined before. In the interest of simplicity, hysteresis is neglected in the above constitutive relationships.

Values for the parameters used to develop hydraulic properties of all seven soils are listed in Table 2. Note that, in addition to being

TABLE 2

Material Properties and Parameter Values

Material Number	Material Type	Saturated Hydraulic Conductivity K_s, ft/d	Porosity ϕ	Residual Moisture Content θ_r	Air Entry Pressure Head ψ_a, ft	A	c	D
			- Aquifer Materials -					
1	coarse sand	800	0.30	0.03	0.0	2.0	4.0	2.25
2	medium sand	100	0.34	0.05	0.0	6.0	2.5	4.00
3	loamy sand	5	0.38	0.15	0.0	10.0	2.0	5.00
			- Clogging Layer and Aquitard Materials -					
4	sandy silt	1	0.40	0.18	4.00	10.0	1.875	4.70
5	silt loam	0.1	0.42	0.22	4.25	10.0	1.75	3.75
6	clay loam	0.05	0.44	0.30	4.50	12.0	1.625	4.00
7	silty clay	0.01	0.46	0.36	4.75	20.0	1.50	4.00

given index numbers, names have been designated for the soils, largely for convenience of description. It is important to stress that the parameters listed in Table 2 have been selected arbitrarily, and that such parameters may not necessarily be characteristic of the soil names with which they have been associated. However, many of the parameters are in the range of values reported for soils bearing these names. For example, the saturated hydraulic conductivities and porosities in Table 2 are of the same magnitude as those reported in McWhorter and Sunada (1977), Clapp and Hornberger (1978), and Freeze and Cherry (1979). Similarly, the residual moisture contents shown in the table have been estimated by subtracting specific yields, on the order of those given in McWhorter and Sunada (1979) and Todd (1980) for the listed materials, from the selected porosities.

The appropriateness of the empirical parameters A, c and D is not as easily evaluated. Coarser grained and more texturally uniform materials such as sands tend to be characterized by smaller values of A (Winter, 1983). Indeed the lowest values of A are assigned to the sandy aquifer materials in Table 2. Similarly, smaller c values are reflective of progressively finer grained and more poorly sorted media. Winter (1983) reported that some of the hypothetical soils he considered exhibited moisture characteristics closely approaching those of silty loams and silty clay loams when a c of 2 was used. The fine-grained soils designated as aquitard and clogging layer materials in this study have c values ranging from 1.5 to 1.875. Finally, the values of D in Table 2 are not taken directly from experimental data; however, Brooks and Corey (1966) report that D values for many materials fall in the range of 3 to 4. Huyakorn et al. (1984) employ a

D of 2 in one of their example simulations. D values for the materials in this study range from 2.25 to 5.0.

Graphical illustrations of the aquifer material properties based on the data in Table 2 are presented in Figures 10a (θ vs. ψ) and 10b (K vs. ψ). The comparable properties for clogging layer and confining units are illustrated in Figures 11a and 11b.

It is noteworthy to point out that saturated hydraulic conductivities of the aquifer materials cover a wide spectrum ranging from a K_s of 5 feet per day (loamy sand) to 800 feet per day (coarse sand). Also of importance is the fact that formation of capillary fringes within any of the three is nonexistent due to the selection of a zero air entry suction head ($\psi_a = 0$) for each. Such a choice is felt to be reasonable inasmuch as air entry pressure heads in coarse-grained soils are commonly of such small magnitude as to be ignored.

Figure 10b also illustrates that moisture dependent effects on hydraulic conductivity can be of significance in areas of unsaturated flow. The three soils depicted in Figure 10b are very nonlinear in the sense that hydraulic conductivity for each varies widely over the range of suctions that might typically exist under unsaturated conditions. Moreover, coarse grained soils that possess high hydraulic conductivities when saturated become less capable of transmitting water than the fine-grained aquifer materials when conditions are very dry.

The materials used for the clogging layer and aquitard are obviously less nonlinear (Figures 11a and 11b) than those used for the aquifer. Saturated hydraulic conductivities are also considerably lower in the case of these "semipermeable" soils. Note that the clogging layer and aquitard materials exhibit air entry pressure heads (ψ_a) ranging from 4.0 (sandy silt) to 4.75 feet (silty clay). Thus,

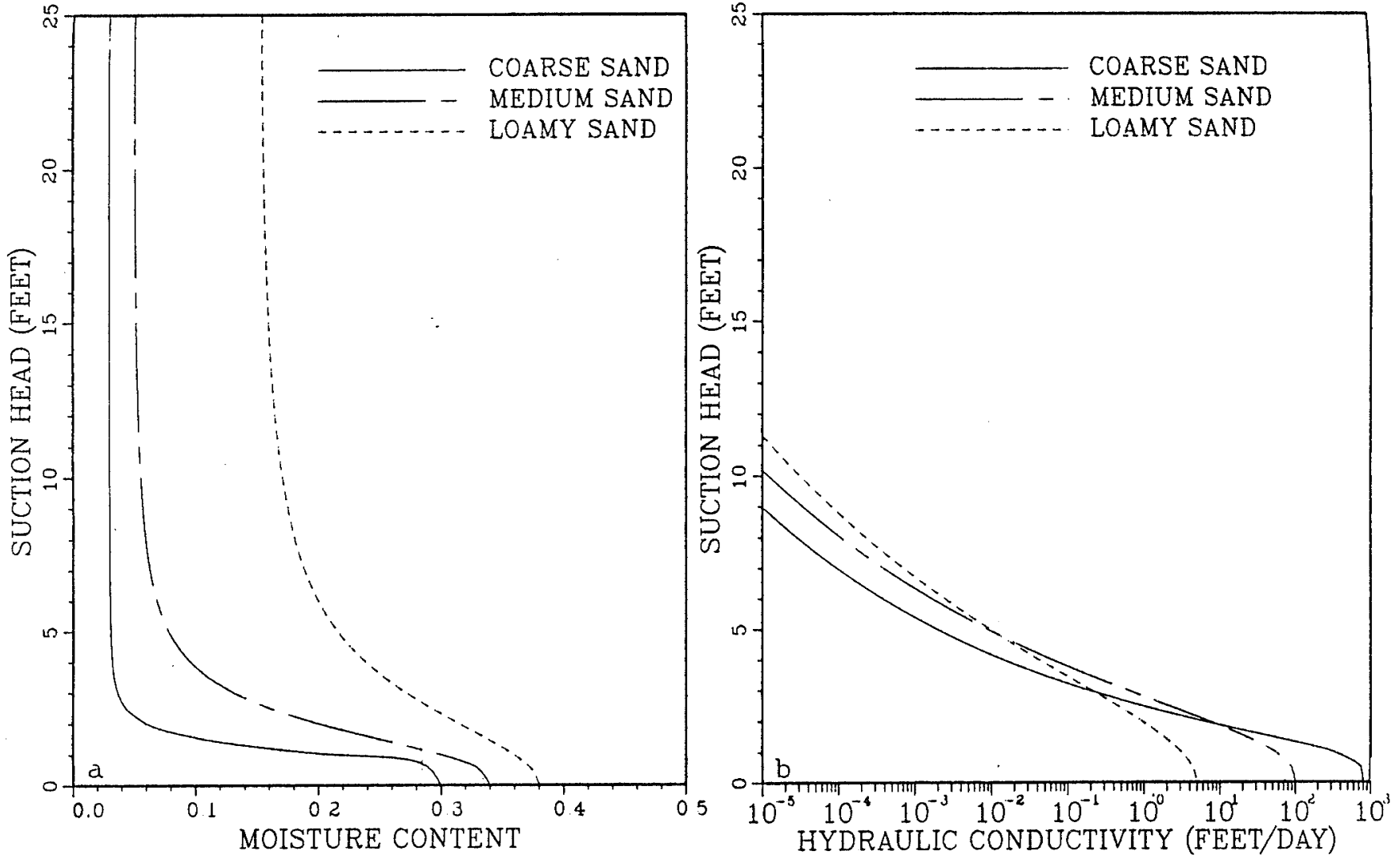

Fig. 10. Properties of aquifer materials: (a) soil moisture characteristics and (b) unsaturated hydraulic conductivities.

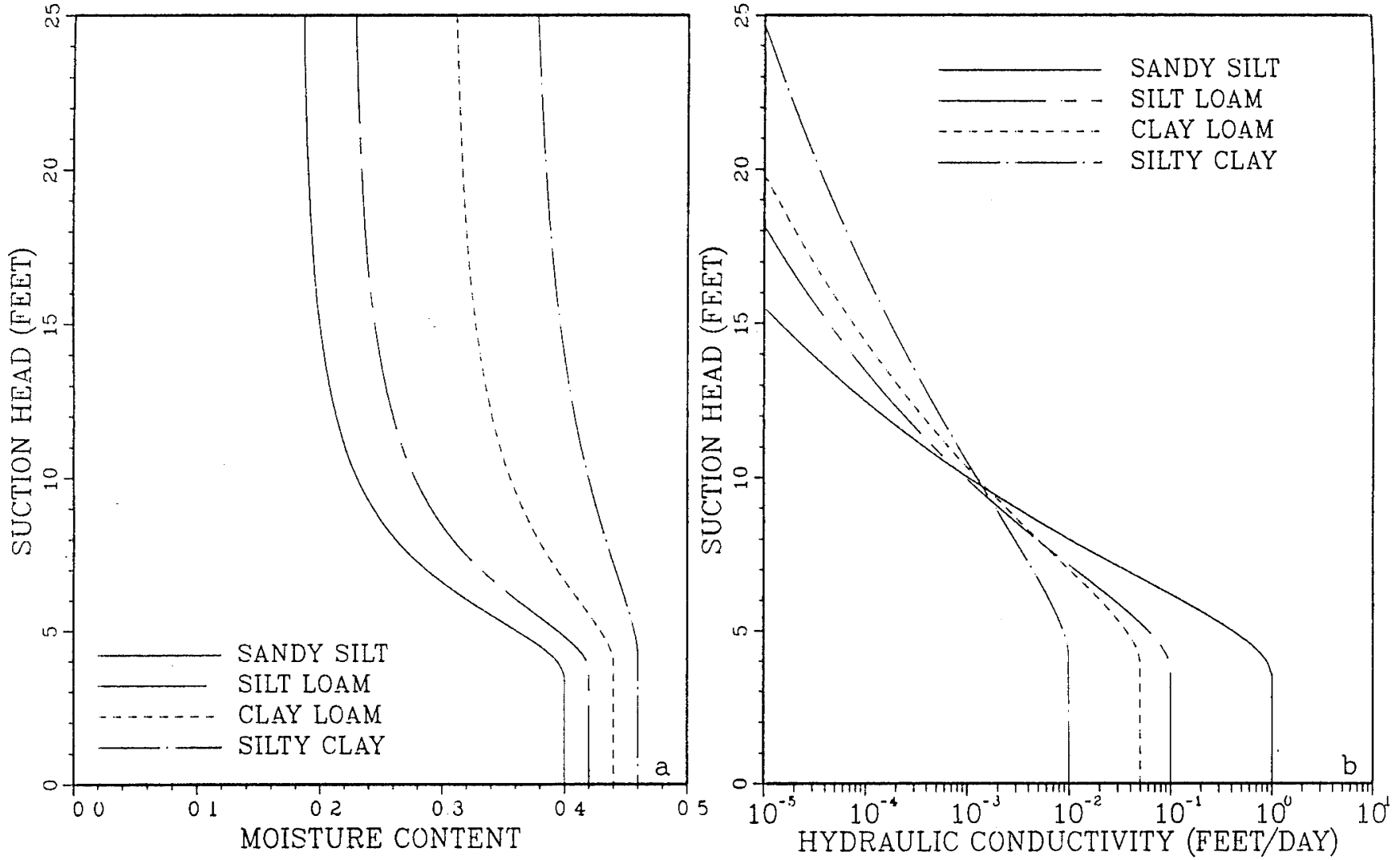

Fig. 11. Properties of aquitard clogging layer materials: (a) soil moisture characteristics and (b) unsaturated hydraulic conductivities.

the potential exists for these materials to remain saturated even when negative pressures occur in the adjacent aquifer. It should be noted that the designated air entry pressure heads are larger than reported values from Brooks and Corey (1966) for fine grained materials, yet fall within the range of magnitudes given by Bouwer (1978) for ψ_a in dispersed clay soils.

Reference Simulation Case

As yet, the geometry, dimensions and discretization of the domain used for the reference simulation case have been outlined, but materials comprising the aquifer, aquitard and clogging layer have not been discussed. In keeping with the study's general approach, those materials have been selected as being somewhat representative of Mesilla Valley conditions. Specifically, the medium sand (Material 2) has been chosen to represent the aquifer, clay loam (Material 6) the clogging layer, and silt loam (Material 5) the aquitard.

Of course, homogeneous units, such as are assumed here, are not really observed in the Mesilla region. Indeed a great deal of heterogeneity is actually present. Nevertheless, because only generic simulations are attempted in this work for the purpose of developing general conclusions on stream-aquifer behavior, the above-selected base case serves well as an initial step toward defining "average" conditions.

VIII. STEADY STATE SIMULATIONS

Steady state simulations of variably saturated flow are conducted for two reasons:

(1) to help determine the average conditions that might be expected over the course of a year in a system existing in a state of dynamic equilibrium, and

(2) to develop head configurations that can be utilized as starting conditions for subsequent transient (year-long, quasi steady state) simulations.

Clearly, steady state analyses are fundamental to this study, as it is impractical to carry out transient simulations without first having an idea as to what the general head distribution will look like for a given set of system properties and boundary conditions. By using a steady state head profile as a starting condition in a transient run, a modeler removes much of the possibility of forcing biased, and perhaps largely unrealistic, influences on the problem. Yet, as necessary as steady state analyses are to a numerical exercise of this kind, it is this kind of simulation that is probably the most difficult to achieve for variably saturated flow in large domains. Consequently, a major hurdle to overcome prior to accomplishing any of the research objectives is the development and testing of a numerical code for accurately (let alone efficiently) representing such systems. Indeed, the difficulties associated with simulation of steady state variably saturated flow explain why the testing and verification portions of this research have been quite lengthy, and why an appendix (Appendix A) is devoted to this subject.

The problems examined under the steady state category cover a range of possible situations. Heterogeneous, multiple layer aquifers are considered in addition to the homogeneous cases. Clogging layers

exhibiting a variety of properties, as well as the case in which streambed clogging is nonexistent, are examined. Dimensions of the stream-aquifer systems are also varied. In short, the steady state simulations amount to an analysis of the response of stream-aquifer processes to various influential parameters, considering situations where unsaturated flow has a strong effect, and in which water storage in soils is not a factor.

Many of the steady state runs reported on in this chapter have been made using a stream stage of 1 foot. Thus, when this stage is used with the domain of Figure 8, the height of the stream water surface with respect to the designated origin of the simulation domain is 65 feet.

Simulation Procedure

As discussed earlier, steady state simulations are conducted with the variably saturated flow code called SATURN (Huyakorn et al., 1984). The Newton-Raphson equation solution scheme in this code is virtually indispensable to the stream-aquifer analyses. Without an algorithm of this nature, simulation of steady state flow under the condition of disconnection, combined with a deep water table, is extremely difficult (if not impossible) to attain.

Despite its virtual necessity in achieving efficient and accurate simulations, the Newton-Raphson scheme does have a slight drawback in the sense that starting head conditions placed into the model must be feasibly close to what the final computed steady state head configurations will be. Otherwise, iterative solutions of the numerical equations produced by the model may diverge, and plausible answers are never attained. To overcome this, solutions for deep water

table conditions are arrived at through a series of simulations, starting with the least nonlinear situations (i.e., connected stream) first and gradually progressing to the more nonlinear cases where disconnection and maximum infiltration rates prevail.

The actual procedure is quite simple, though somewhat laborious. First, a simulation is conducted for hydrostatic conditions, in which the uniform hydraulic head imposed in the underlying aquifer (underlying head) is identical to the elevation of the stream. This is done primarily to test the model for incorrect data input, i.e., improper nodal locations or illogical element information. If a uniform field of hydraulic head and zero flow conditions are produced by this initial run, the output heads are then used as a starting condition in a succeeding simulation in which the head below the aquitard is uniformly lowered a small amount (usually somewhere between 1 to 2.5 feet). The head configuration from this second run is in turn used as a starting condition in the next simulation, in which the underlying head is perturbed even further. By using this system of successive restarts, the starting head values fed into the model during each run provide a consistent initial configuration from which the Newton-Raphson algorithm can converge to a solution. Moreover, in addition to ultimately determining system results for deep water table situations, this approach allows system behavior (e.g., steady state flow rates, water table levels) to be ascertained as the gradual transition from connected/hydrostatic-flow to disconnected/maximum infiltration conditions takes place. In simulations with the domain of Figure 8, hydraulic heads in the underlying aquifer (underlying head) range from a high value of 65 feet to a low of 20 feet.

All of the steady state simulations have been performed on a 16 megabyte MicroVAX II VMS computer. Utilizing the above-described method of successive restarts, and a point convergence criterion of 0.005 feet, a series of steady state runs with a discretized domain like that in Figure 9 typically consumes somewhere between 2 to 5 hours of CPU time. The number of runs needed to cover the full range of heads in the underlying aquifer (underlying head) usually ranges between 19 and 40. A steady state run typically requires 3 to 7 Newton-Raphson iterations to achieve convergence.

Methods of Presenting Results

Steady state results include both scalar (zero order) measures of system behavior, as well as spatial (one-dimensional and two-dimensional) plots of head and moisture content. In order that two-dimensional plots can be presented at a level that is readable, the vertical scale is distorted (vertical exaggeration = 5:1), as is the case for the finite element mesh shown in Figure 9.

Scalar measures include system fluxes and descriptors of water table elevation. Steady state system flux is equal to the stream infiltration rate as well as the leakage rate across the aquitard, since, in a losing stream situation, the stream is the only source of water and aquitard leakage its sole means of leaving the domain. The behavior of the scalar measures is in most cases analyzed with reference to changes in head in the aquifer underlying the aquitard. That is, graphs are prepared of the increase in flux and general decline in water table as hydraulic head in the underlying aquifer (underlying head) is reduced.

Graphs of system flux and water table elevation versus hydraulic head in the underlying aquifer have obviously been developed using data from several successive steady state simulations. In order to give the reader some idea of the effort that has gone into the preparation of these plots, the number of runs comprising each series of steady state runs is indicated by the symbol NP, which also represents the number of points used to develop each graph. This also helps to provide a rough indication as to which media properties require the greatest number of runs.

In presenting two-dimensional contour plots of head and moisture content, values for these parameters in the clogging layer and aquitard are omitted; i.e., only heads and moisture contents within the aquifer material are plotted. Head profiles across the low permeability units is not of interest to the problems being examined. Additional justification for neglecting the aquitard zone, however, stems from the fact that hydraulic head contours within it will be limited to simple, relatively straight lines, as a result of steady state leakage. This is also the case in subsequently analyzed transient simulations because of the discretization scheme used for this area (see discussion in Chapter VII on model discretization). Furthermore, the potential for steep gradients existing across the small vertical extent of the aquitard, not to mention proportionately large head differentials across the even smaller clogging layer thickness, makes the contouring of hydraulic parameters in these semipermeable zones somewhat impractical.

Head and Moisture Distribution

Cross-sectional plots of total head and moisture content contours have been prepared for several steady state runs with the reference simulation case. The simulations differ with respect to the value of head imposed uniformly in the underlying aquifer. Stream depth (i.e., stage) in each of these steady state simulations is 1 foot. Three separate stream-aquifer relationships, out of the four possible (see Figure 1, Chapter II) are examined. The example of a connected gaining stream is not included as this study is mostly concerned with losing streams. A list of figure numbers, type of contour plot (total head or moisture content), and the category of stream-aquifer relationship depicted for each of the illustrated reference simulation runs is as follows:

Figure 12 - Hydraulic Head, Connected Losing Stream

Figure 13 - Moisture Content, Connected Losing Stream

Figure 14 - Hydraulic Head, Disconnected Stream with a Shallow Water Table

Figure 15 - Moisture Content, Disconnected Stream with a Shallow Water Table

Figure 16 - Hydraulic Head, Disconnected Stream with a Deep Water Table

Figure 17 - Moisture Content, Disconnected Stream with a Deep Water Table

It should be remembered that total heads are plotted in reference to the domain origin, which is located in the lower left corner of the aquitard. Hydraulic head along the streambed is 65 feet. Hydraulic heads in the underlying aquifer (underlying head) used to produce the simulations from which each of the contour plots is taken are identified in the figures. The free surface (water table) is also delineated. When viewing the moisture content plots for these

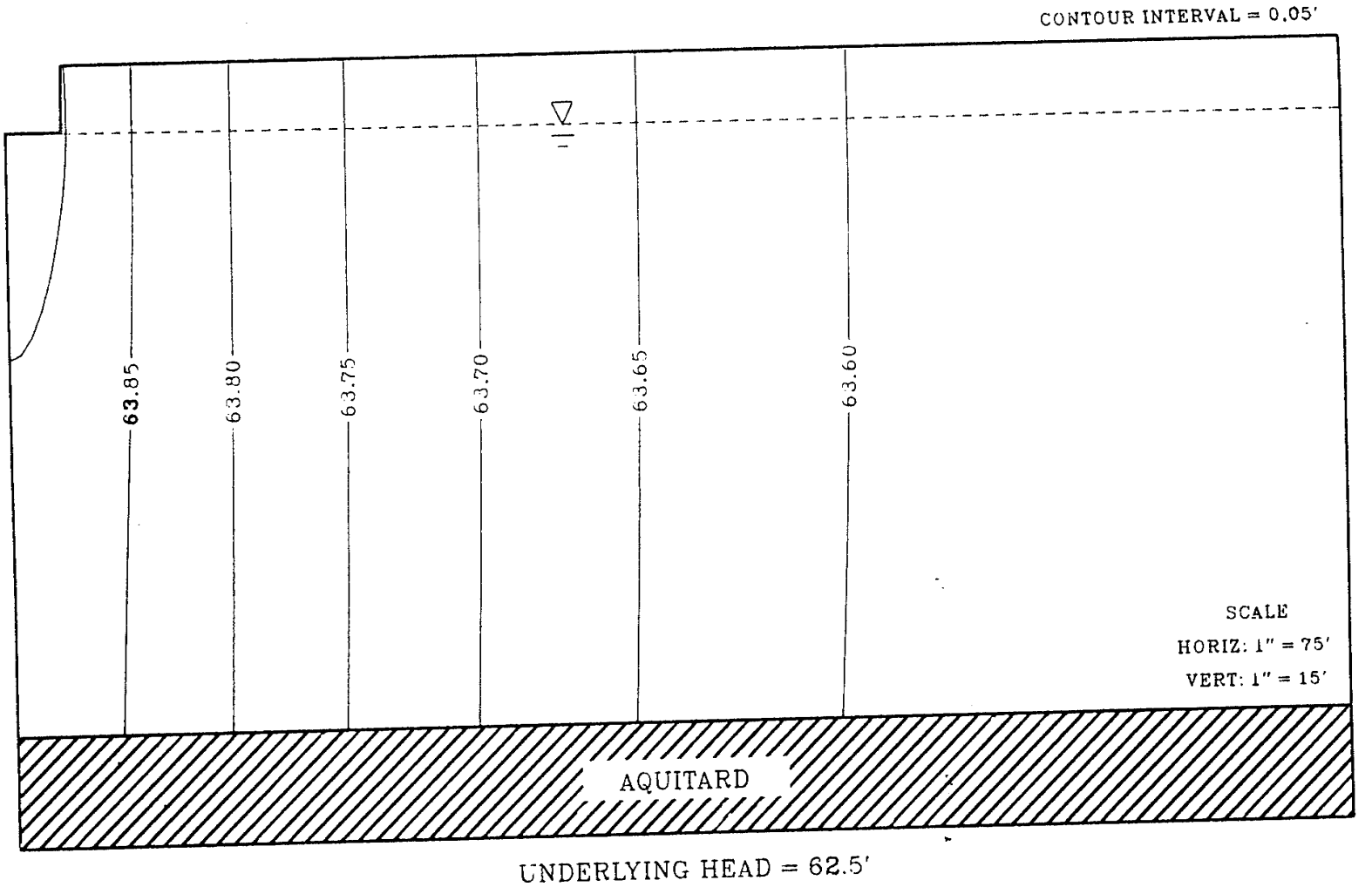

Fig. 12. Steady state hydraulic heads (in feet) in the reference simulation domain for a connected losing stream.

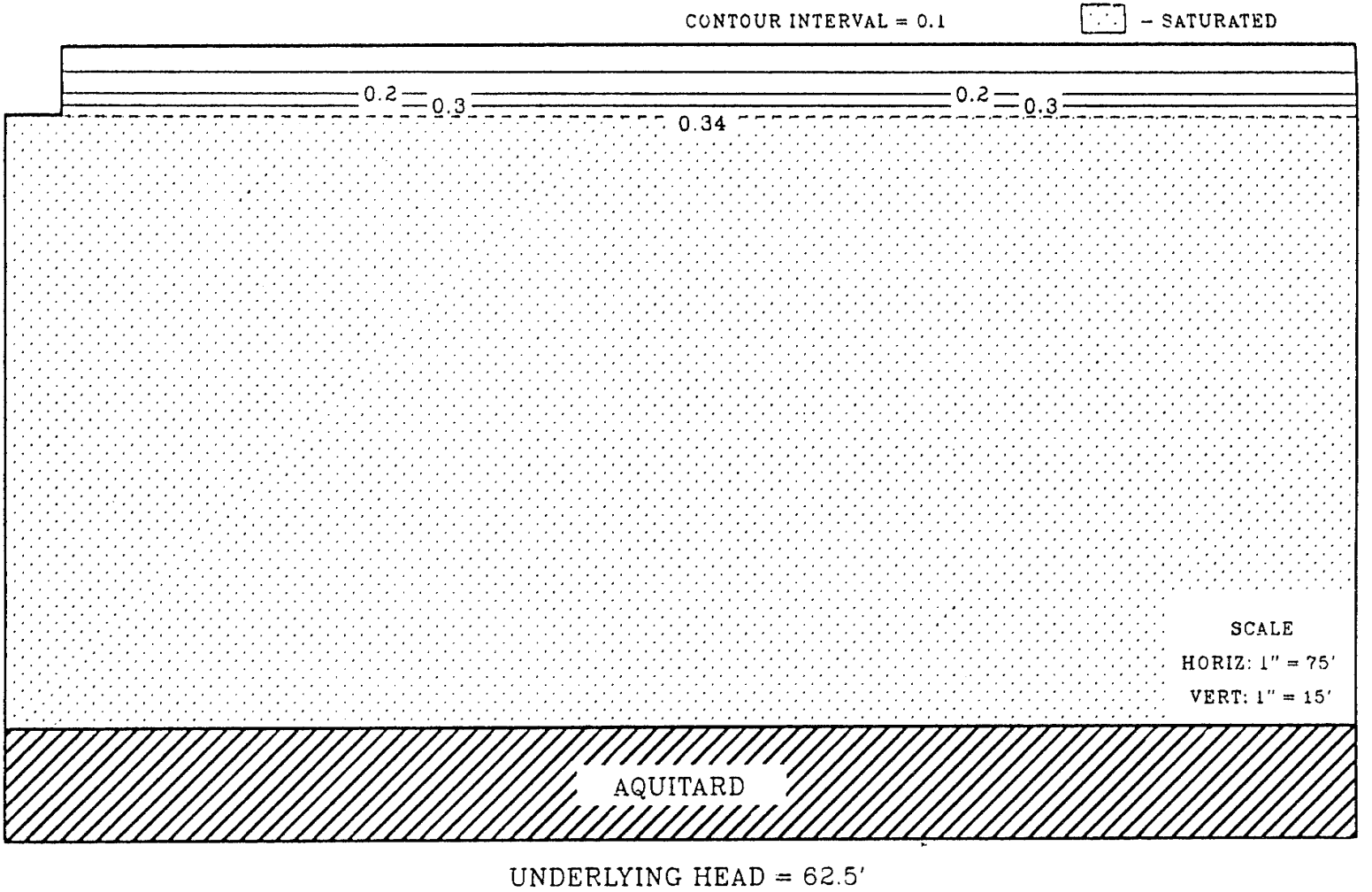

Fig. 13. Steady state moisture contents (dimensionless) in the reference simulation domain for a connected losing stream.

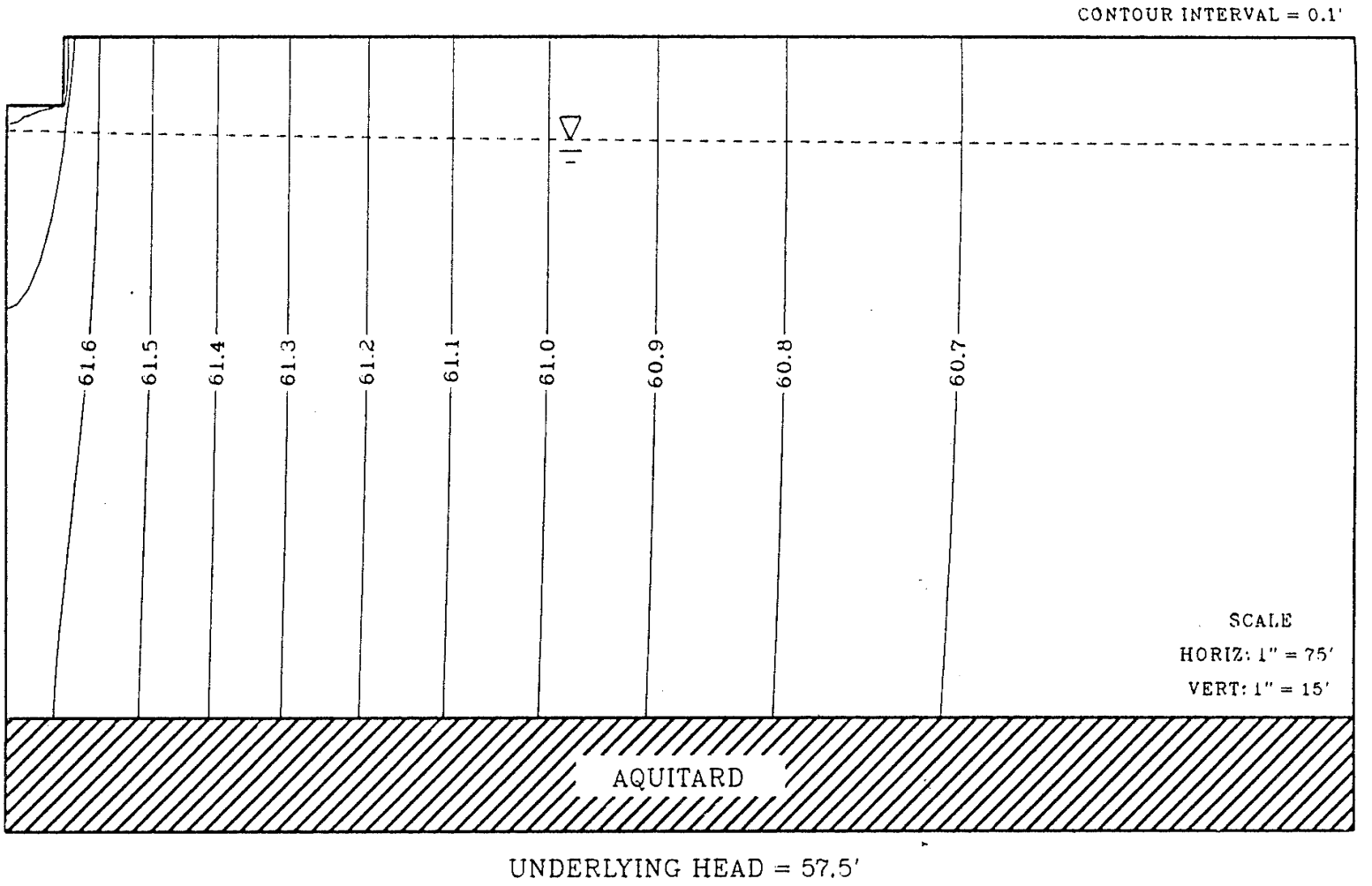

Fig. 14. Steady state hydraulic heads (in feet) in the reference simulation domain for a disconnected stream with a shallow water table.

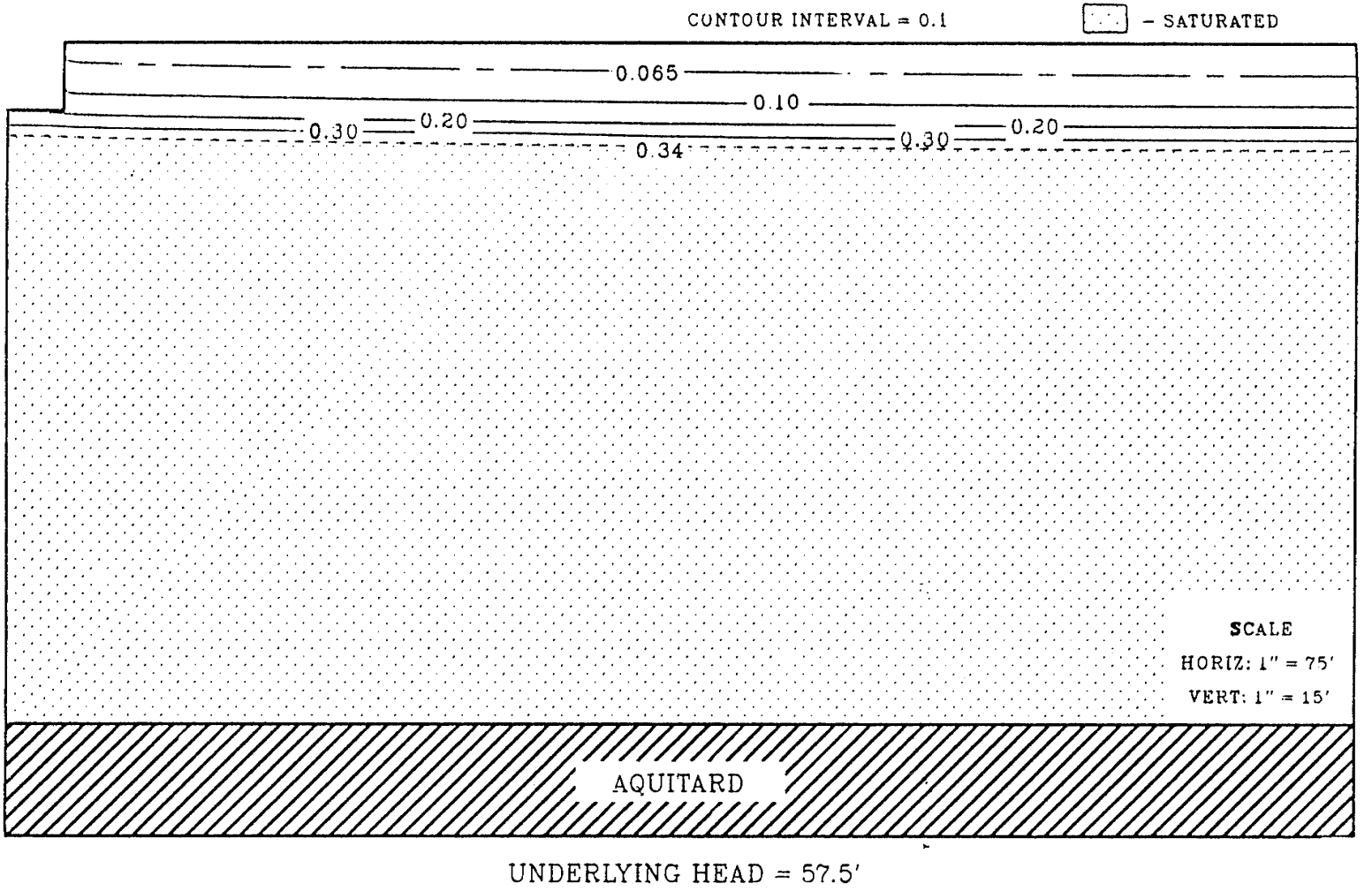

Fig. 15. Steady state moisture contents (dimensionless) in the reference simulation domain for a disconnected stream with a shallow water table.

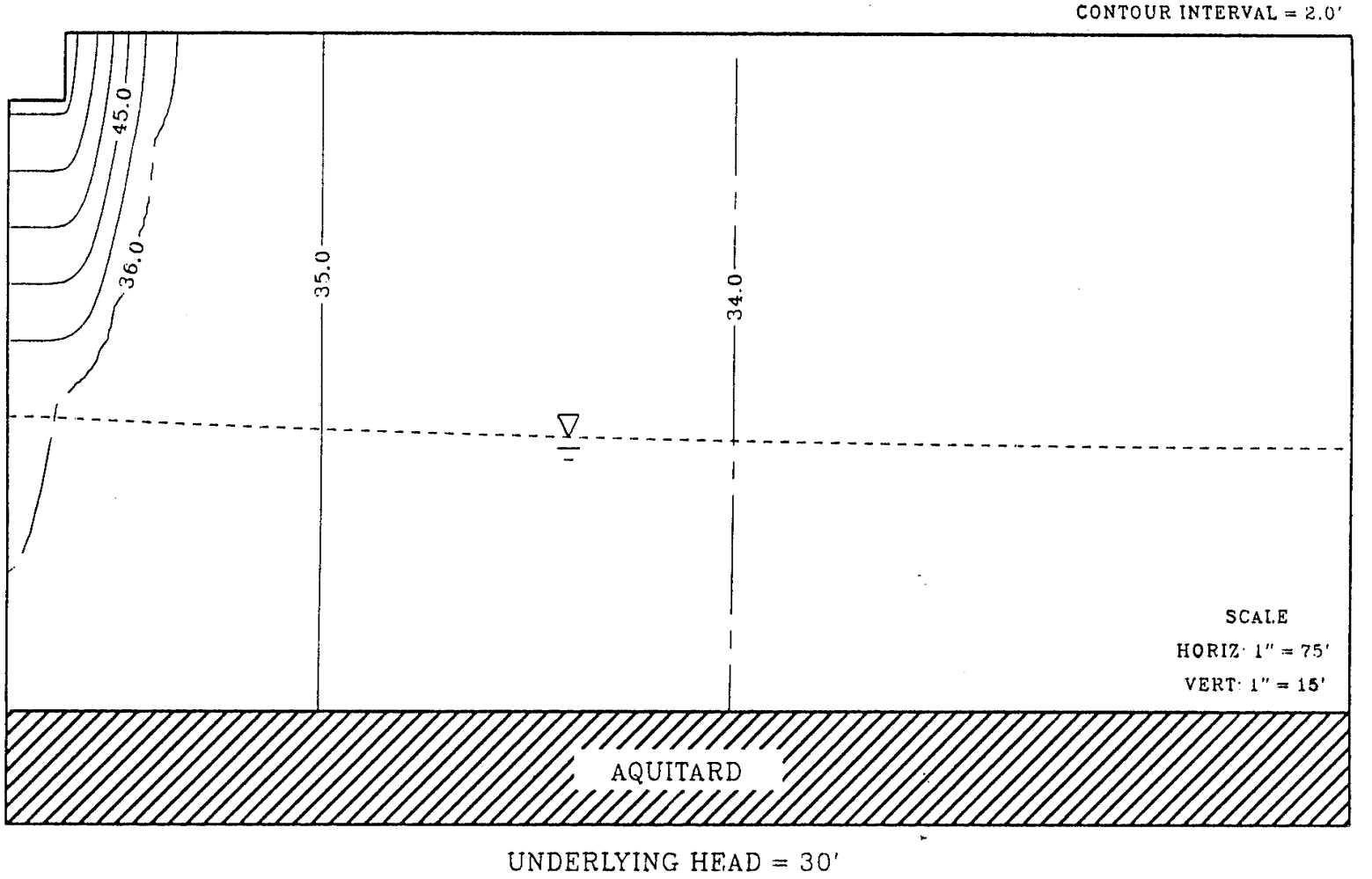

Fig. 16. Steady state hydraulic heads (in feet) in the reference simulation domain for a disconnected stream with a deep water table.

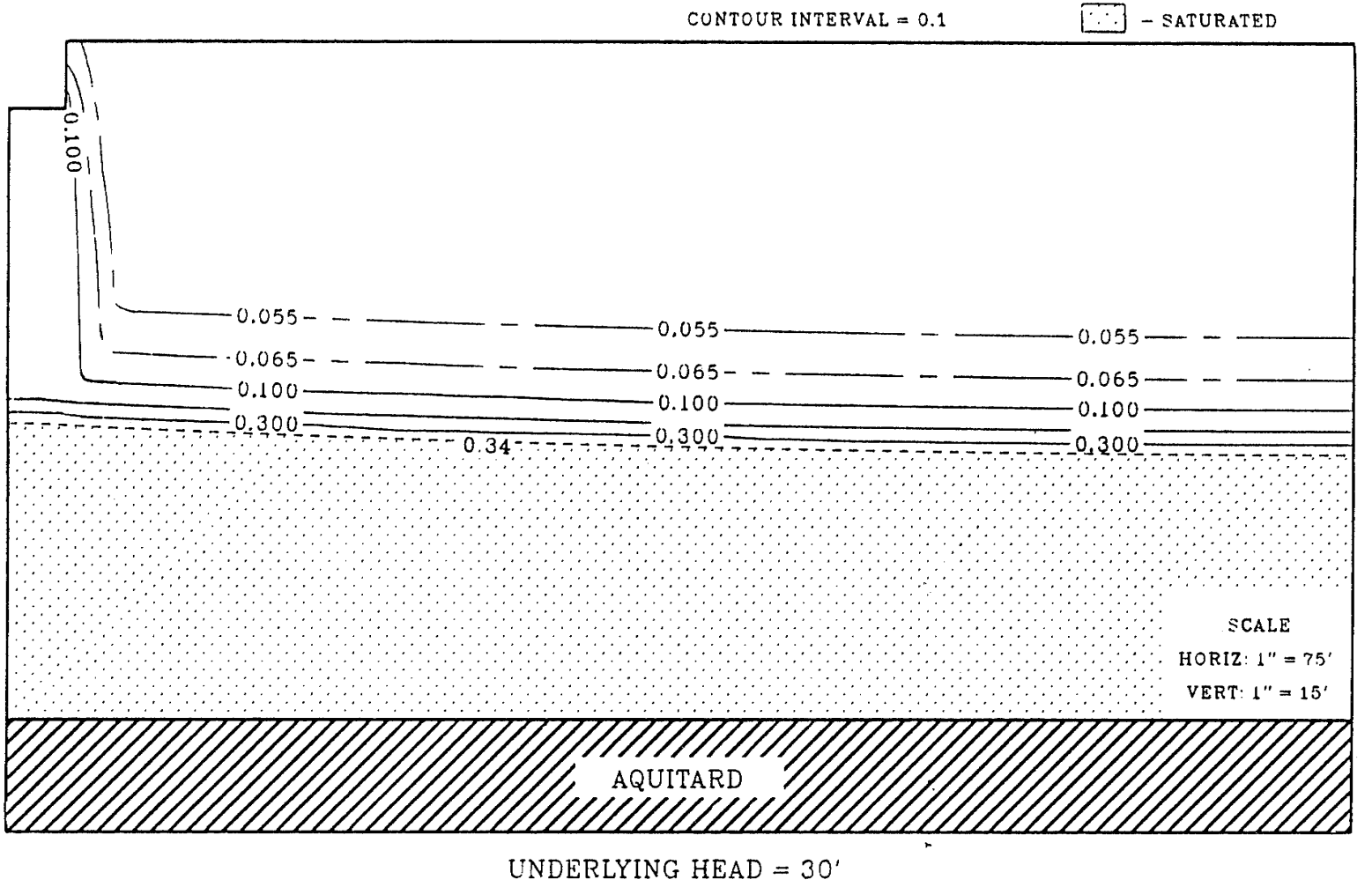

Fig. 17. Steady state moisture contents (dimensionless) in the reference simulation domain for a disconnected stream with a deep water table.

reference simulation cases, the reader should also keep in mind that the aquifer is comprised of medium sand (porosity $\phi = 0.34$); therefore, on a free surface, and in all saturated areas, moisture content $\theta = 0.34$.

Total head distribution in the case of a connected losing stream (Figure 12) appears rather simple. Vertical flow of water is shown to be significant only in an area close to the stream. To the right of the stream, the total head contours are nearly vertical, indicating that flow in this region is predominantly horizontal. As expected, the total head gradient becomes less the greater the distance from the stream. Because the right boundary of the domain is designated as a zero flow boundary, flow along this boundary is necessarily vertically downward (for a losing stream), and total head contours should be orthogonal to it. However, because total head gradients are so minor near the right side of the domain, head contours in this region are not included.

The total head contours of Figure 12 suggest that most flow moving through the system does so strictly via saturated media. The presence of a head gradient in the unsaturated zone indicates that at least some movement of water away from the stream does take place in unsaturated aquifer material. Most of the water in the unsaturated portion of the aquifer enters this zone directly by way of seepage across the clogging layer on the stream's right bank. However, a very small percentage of the water that finds its way into the unsaturated zone actually first enters the saturated portion of the aquifer along the stream channel bed, from whence it then moves laterally and up, across the free surface, just to the right of the stream channel's lower right corner.

Regardless of the means by which water enters unsaturated media, any water that does move within the unsaturated portion of the aquifer must ultimately enter the saturated area under the water table. This is necessary, of course, because aquitard leakage provides the only avenue by which water can leave the stream-aquifer system. Although flow above the water table in Figure 12 is essentially horizontal, there is a slight downward component of flow as well. This vertical flow is reflective of the movement of water from the unsaturated zone to saturated areas, which takes place incrementally with distance from the stream.

Figure 13 indicates that the moisture content distribution for the connected losing stream case is also quite simple. Vertical distribution of moisture content above the water table reflects the very small component of vertical flow existing to the right of the stream. The decrease in moisture content with height above the water table is very close to the type of vertical profile that would be observed above a free surface in the aquifer material (medium sand) under completely hydrostatic conditions.

Total head gradients in the case of the disconnected stream with a shallow water table (Figure 14) are noticeably larger than those observed in the connected losing stream simulation (Figure 12). This is due to the larger quantity of water moving through the system in this instance. As in the connected case, most vertical flow takes place close to the stream, particularly below the streambed. Mostly horizontal flow predominates in the rest of the domain located to the right of the stream. The steepest hydraulic gradients are observed in the unsaturated zone close to the stream's right bank.

Most water moving through unsaturated aquifer material in the disconnected stream/shallow water table case (Figure 14) enters the unsaturated zone by way of infiltration across the stream channel bed, rather than across the stream's right bank. Accordingly, a majority of the steady state system flux enters the saturated zone in an area located directly below the stream. As in the example of connection, the small amount of water moving laterally with the unsaturated zone situated to the right of the stream gradually passes into the saturated zone with distance from the stream. The large component of flow moving downward in the unsaturated area underlying the stream channel raises moisture contents in this area above those observed to the right of the stream where downward flow is relatively insignificant. This effect is subtly illustrated in Figure 15 in that the $\theta = 0.20$ contour does not extend below the streambed, and, instead, intersects the lower right corner of the stream channel. As in the connected stream example, moisture content profiles in the unsaturated zone located to the right of the stream are indicative of the small quantity of downward flow taking place in these outlying areas.

System flux in the simulation of disconnected stream/deep water table conditions shown in Figure 16 is a maximum flux (under steady state conditions) for the given stream width, stream stage, aquifer material and clogging layer properties. The steep hydraulic gradients shown in the figure indicate that flow in this case is indeed greater than in either of the previously described base simulation cases. More than half of the aquifer is unsaturated in the deep water table simulation.

It is deduced from the head contours in Figure 16 that seepage immediately beneath the stream and in the unsaturated zone is

predominantly vertical and moving down. Flow directions are skewed to the system axes (x,z) mostly within a zone lying in the first several feet to the right of a vertical line passing through the stream's right bank (x = 25.0 feet), and in the shallowest levels below water table level and directly beneath the stream. In the remaining portions of the aquifer, i.e., those lying beyond 50 feet of the stream's right bank, flow is again predominantly horizontal. As in the disconnected stream/shallow water table case, head gradients are steepest in the unsaturated zone located right of the stream's right bank.

Moisture content distribution for the disconnected stream/deep water table run (Figure 17) is noticeably different from comparable plots (Figures 13 and 15) involving shallower water tables. To begin with, moisture content appears to be constant over most of the unsaturated zone lying beneath the stream. This result is expected inasmuch as previous analyses of one-dimensional steady state seepage across a clogging layer (see Chapter II) indicate that constant pressure (and, therefore, constant moisture content) exists below a clogging layer in the case of a deep water table. To the right of this zone directly below the stream, moisture content decreases, and a significant horizontal component of moisture content gradient is observed. Elsewhere in unsaturated portions of the domain, moisture content profiles again resemble those found in areas of little to no vertical flow.

As an illustration of the distribution of water pressures existing near the stream, vertical profiles of pressure head have been plotted for a few steady state runs made with the reference simulation domain. Pressure heads are plotted along two vertical lines, located, respectively, at x = 0.0 feet (Figure 18a) and x = 30.0 feet (Figure

18b). Thus, the first of the graphs portrays steady state pressure behavior at the stream's centerline, while the second depicts profiles found 5 feet outside of the stream's right bank. Two separate runs are represented in both Figures 18a and 18b: one in which hydraulic head in the underlying aquifer (underlying head) is set at 57.5 feet, and another wherein the underlying head is maintained at a value of 50.0 feet. Both cases portray hydraulic disconnection. However, the first situation (underlying head = 57.5 feet) corresponds to the shallow water table case depicted in Figures 14 and 15. The second (underlying head = 50.0 feet) portrays a disconnected stream with a deep water table occurrence. The underlying head in this case is considerably greater than that utilized in Figures 16 and 17 to depict hydraulic head and moisture content, respectively, for this category of stream-aquifer relationships.

The pressure head profiles of Figure 18a are quite similar to those illustrated earlier in Figure 2 for one-dimensional steady flow. As expected in the shallow water table case, pressure heads beneath the base of the clogging layer ($z = 63.8$ feet) increase with depth from a value of $\psi = -1.96$ feet until the water table ($\psi = 0.0$) is reached. In contrast, pressures associated with the deeper water table are constant ($\psi = -2.79$ feet) for the initial 5 feet below the clogging layer, whereupon a gradual transition to the zero pressure line takes place. A profile of this nature also occurs in the runs associated with Figures 16 and 17; however, the transition to the phreatic surface takes place at a much lower elevation than shown in Figure 18a.

Note that the straight line profiles for each case between the 63.8 foot and 64.0 foot elevations are indicative of steady state flow across the clogging layer. The top surface of the clogging layer is

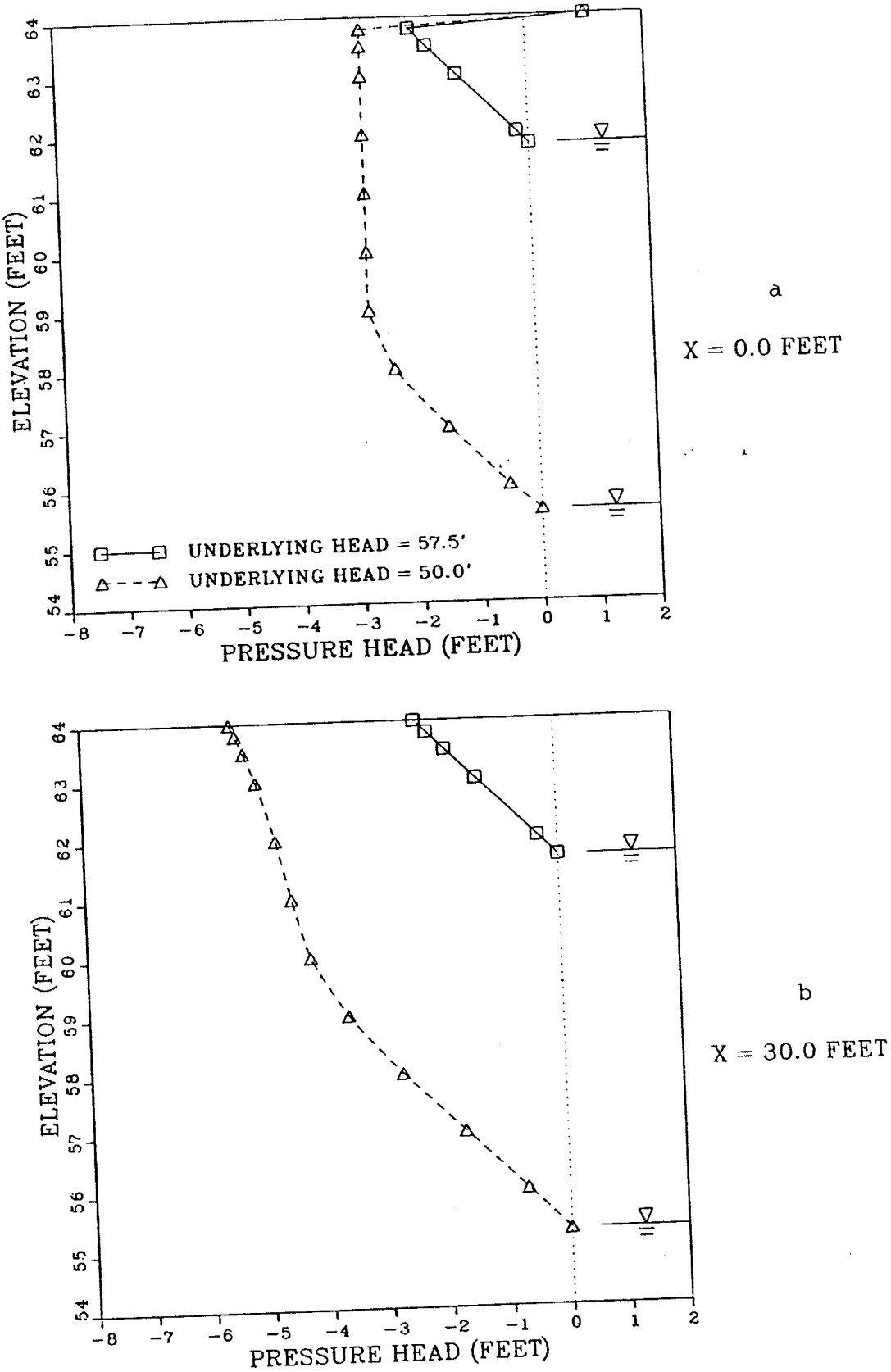

Fig. 18. Steady state vertical pressure head profiles in the reference simulation domain for underlying heads of 50.0 and 57.5 feet, at (a) x = 0.0 feet and (b) x = 30.0 feet.

exposed to a positive pressure head of 1 foot, due to a stream depth of the same magnitude.

At x = 30.0 feet, the pressure profile from the shallow water table run (Figure 18b) looks much the same as its equivalent located at x = 0.0 feet. However, differences do exist. Obviously, there is no transition from positive to negative pressures in this zone situated right of the stream, as the clogging layer is not present here. Furthermore, pressures at a given elevation are slightly less negative at x = 30.0 feet than beneath the stream channel (x = 0.0 feet). Accordingly, the water table is also slightly deeper in the situation depicted in Figure 18b.

The pressure profile for the deeper water table case of Figure 18b is also of interest. Note that near a depth of 60.0 feet, a change in slope of the profile occurs. Below this transition zone pressures appear to increase with depth at a similar rate to those shown for the deeper water table in Figure 18a. Above this zone, pressures show an inclination to approach a constant value, much in the manner that a constant pressure is observed beneath the stream. Yet this state of constant pressure with depth never results at x = 30.0 feet, nor at any other location situated just to the right of the stream bank. The reason, of course, is that lateral flow is quite strong in the zone, partly due to the significant infiltration passing through the stream banks. Pressure configurations in zones affected by this lateral seepage component, such as that illustrated in Figure 18b, are thus noticeably different than those in the unsaturated zone immediately below the stream where flow is mostly downward.

System Flux Behavior

An example of a graph of steady state system flux versus underlying head is presented in Figure 19. The fluxes shown in this figure are from the series of runs using the reference simulation domain. A total of 31 separate simulations were used to make this plot. The solid curve in Figure 19 was prepared by connecting all 31 data points (NP = 31) with straight line segments. All subsequent graphs of this nature are developed in an identical manner. System flux increases gradually with decreasing underlying head until such point that maximum flux conditions exist. To assist in analyzing this graph, a few important points are denoted, including the point at which hydrostatic conditions exist, the level at which incipient disconnection occurs, and the point of incipient maximum flux (recall definitions of these points in Table 1 and Chapter II). Naturally, the previously described case of a connected losing stream lies between the hydrostatic condition (underlying head = 65.0 feet) and the point of incipient disconnection. Similarly, fluxes observed between the point of incipient disconnection and incipient maximum flux are reflective of the disconnected stream with shallow water table conditions.

It is interesting to note that steady state flux essentially responds linearly to changes in underlying head during the connected losing stream phase and over most of the disconnected stream/shallow water table phase. Moreover, the rate of change in flux with declining head in the underlying aquifer appears to be much the same over most of each phase. Only just prior to the point of incipient maximum flux does the flux show signs of leveling off to a constant value. This is not surprising for the range of heads during which stream and aquifer remain connected, for some amount of water continues to infiltrate from

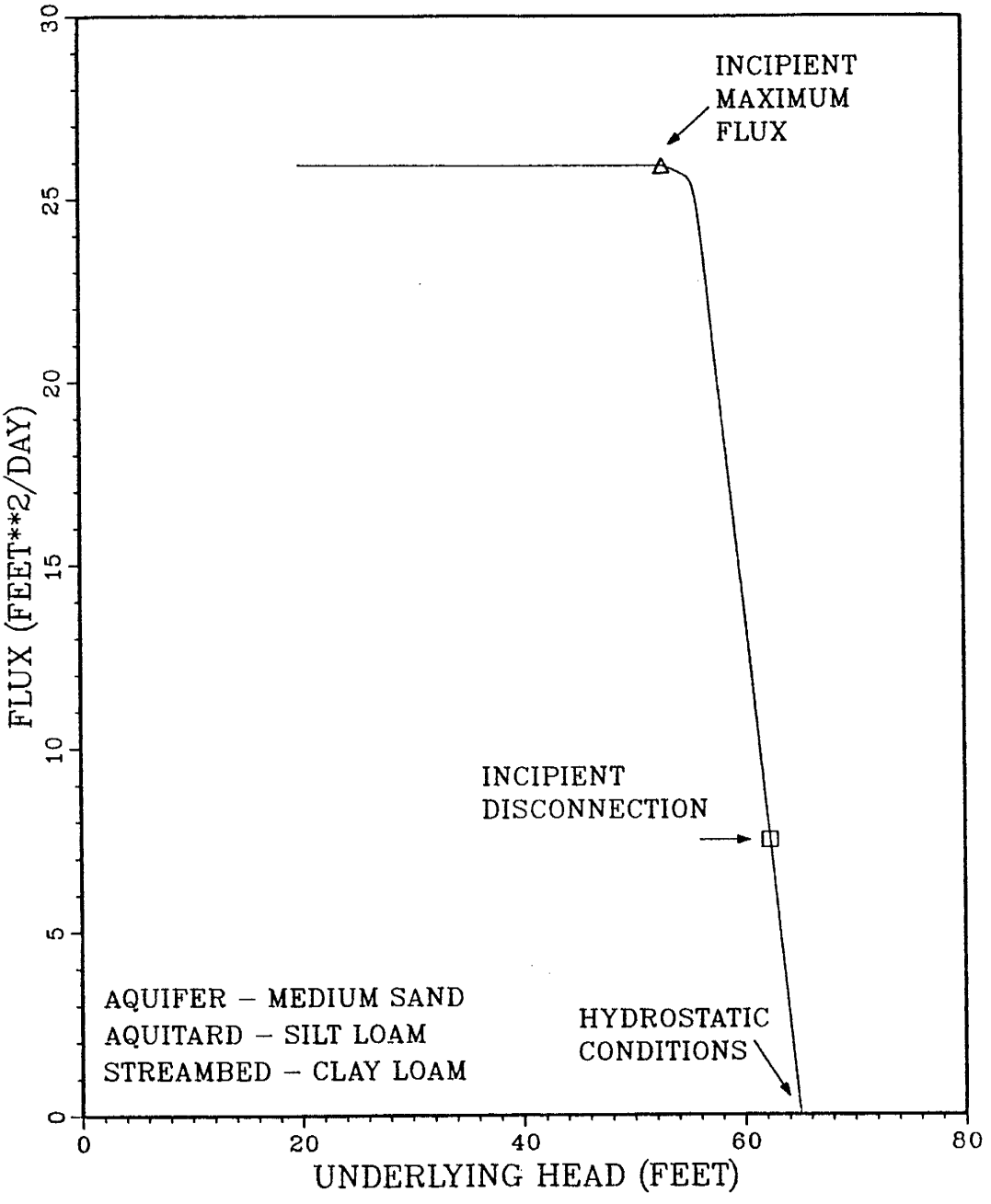

Fig. 19. Steady state system fluxes versus hydraulic head in the underlying aquifer (underlying head) for the reference simulation domain.

the stream into the aquifer via strictly saturated materials. However, the fact that a linear response is also observed over most of the disconnected stream/shallow water table phase is of some interest since all water entering the aquifer in this case must at some point or another enter the unsaturated zone.

Maximum flux under the reference simulation case is approximately 26 square feet per day (ft^2/day). Figure 18 indicates that the maximum flux is first observed (i.e., point of incipient maximum flux) when hydraulic head in the underlying aquifer (underlying head) is 53.8 feet. Incipient disconnection occurs at an underlying head of 62.1 feet, while hydrostatic conditions exist when underlying head equals 65 feet. Thus, the water table affects stream loss rates over a full range of underlying heads of about 11.2 feet, approximately 8.3 of which the stream and aquifer are disconnected.

Water Table Behavior

Figure 20 depicts steady state behavior of the water table in the reference simulation domain as hydraulic head in the underlying aquifer (underlying head) is reduced. Three separate measures of water table behavior in the aquifer material are given in Figure 20, including (1) the spatial maximum water table elevation, which under disconnection occurs at the stream centerline, (2) the spatial minimum water table elevation, observed at the right lateral boundary, and (3) a spatially averaged mean value of water table elevation. As in the graph of system flux behavior, the points of incipient disconnection and incipient maximum infiltration have been denoted. Markers are placed on the maximum water table level curve since it is this curve that provides the greatest expression of flow activity near the stream.

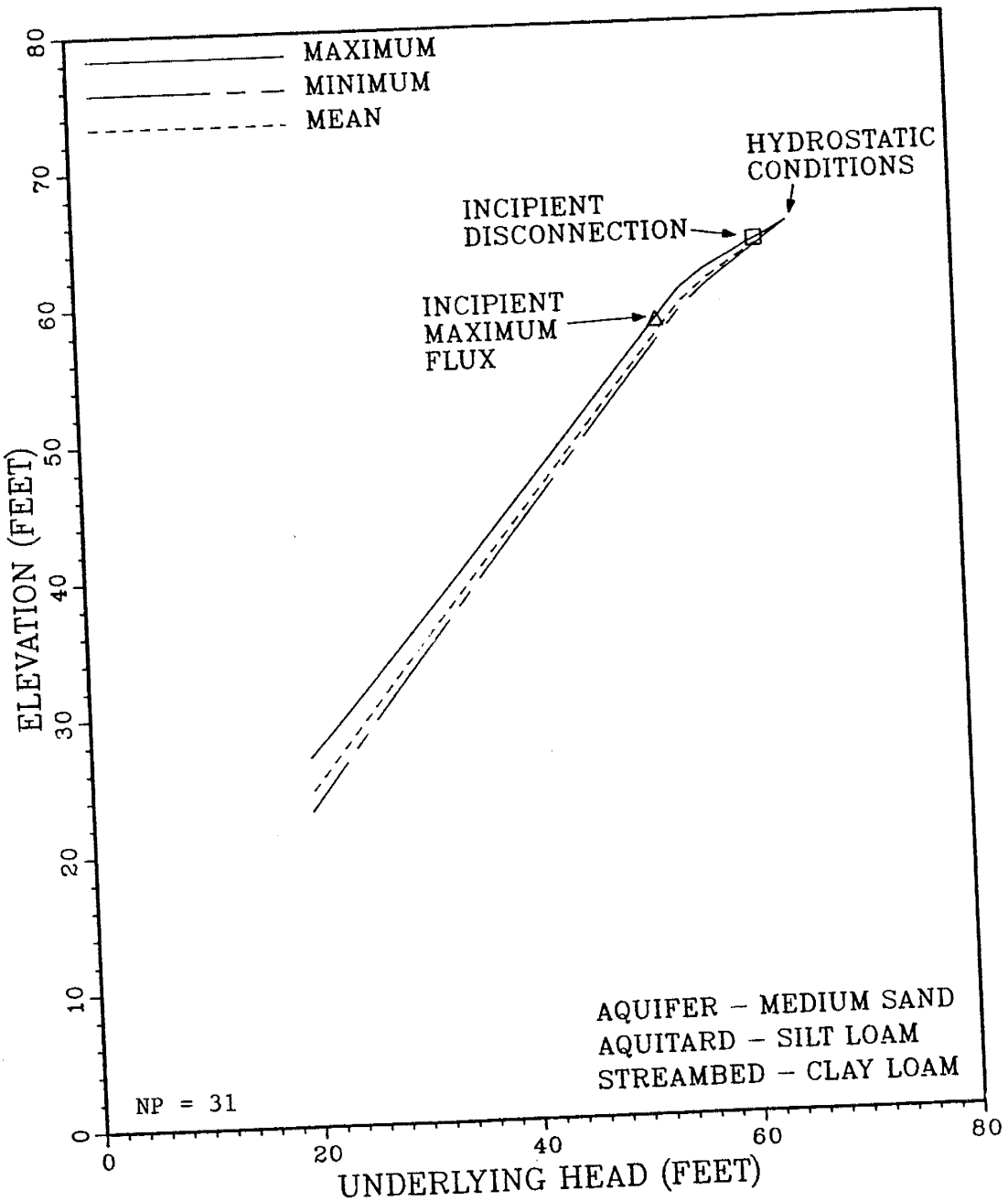

Fig. 20. Steady state, spatial maximum, minimum and mean water table elevations versus hydraulic head in the underlying aquifer (underlying head) for the reference simulation domain.

Two distinctive slopes are observed for each of the water table measures plotted in Figure 20. The break in slope of each measure takes place gradually just prior to the slope at which incipient maximum flux occurs. The water table is more sensitive to underlying heads once maximum flux conditions are reached. This occurs because stream seepage continues to increase as water table levels drop during the connected losing stream and disconnected/shallow water table phases. But after maximum flux conditions (i.e., disconnected stream with a deep water table) have come about, recharge from the stream is limited and water table levels must drop proportionately to reflect equally limited leakage across the basal aquitard. On either side of the transition that occurs at the point of incipient maximum flux, all water table measures appear to respond in a largely linear fashion to changes in underlying head.

Figure 20 is not necessarily indicative of the water table response in all simulations. To illustrate this point, an additional graph of water table behavior from a different series of simulations is presented in Figure 21. Domain dimensions in this instance are the same as those used in the reference simulation case, but different materials are now used for the aquifer and clogging layer (see Figure 21). One reason for selecting this example is that the ranges of underlying head over which the various stream-aquifer relationships are observed are much larger than in the reference simulation runs. This happens mostly because the aquifer is now comprised of the less texturally uniform sandy loam (Material 3). A larger degree of groundwater mounding results in this less permeable material as steeper hydraulic head gradients are required to drive the incoming stream water both vertically and horizontally against greater flow resistance.

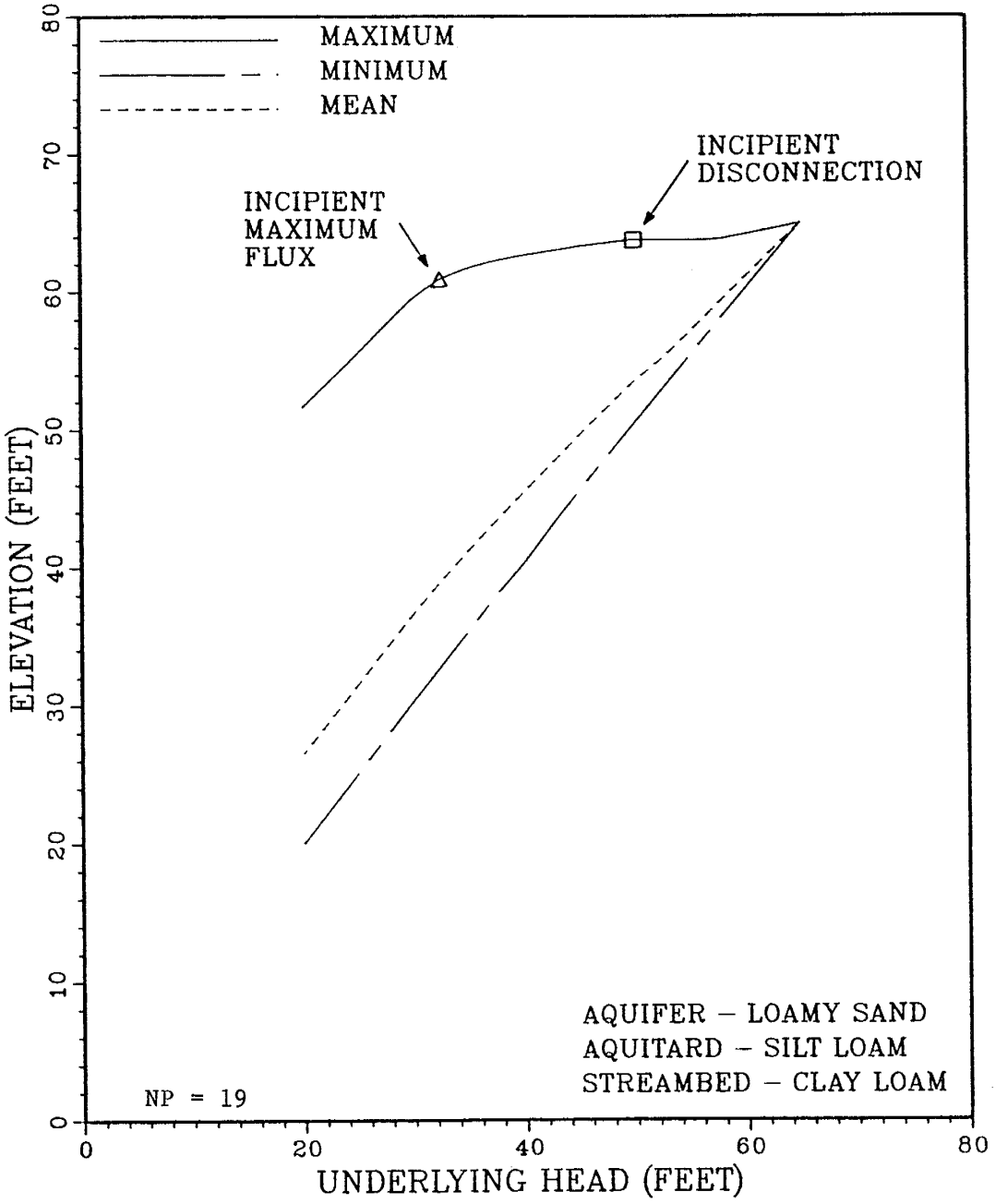

Fig. 21. Steady state, spatial maximum, minimum and mean water table elevations versus hydraulic head in the underlying aquifer for another domain.

The net effect is that maximum water table level, close to the stream, drops less quickly with declining values of underlying head.

Figure 21 shows that difference between the various water table measures (maximum, minimum, mean) is much larger than for the reference simulation runs. In addition, the maximum water table curve indicates more complex behavior than generally linear responses to declining hydraulic head in the underlying aquifer. Of some note is the flat portion of the maximum water table curve just to the right of the point of incipient disconnection. Over this portion of the curve, which spans approximately 7 feet of underlying head, the highest point of the water table is intersecting the base of the clogging layer located at 63.8 feet elevation. The span of underlying heads over which this same phenomenon takes place in the base simulation case is so small (~0.1 feet) as to be imperceptible in the previously discussed graph of water table behavior (Figure 20) for that case. One other feature of Figure 21 worth mentioning is the fact that the break in slope for the spatial mean and minimum water table curves near the point of incipient maximum flux is not as apparent in this example as it is for the reference simulation case.

Influence of Domain Properties

Steady state simulation results are now presented to illustrate the response of various stream-aquifer processes to variations in system properties. The following cases are considered: (1) homogeneous aquifer but variable aquifer material, (2) homogeneous aquifer with variable clogging layer properties, (3) homogeneous aquifer with a clogging layer not present, (4) homogeneous aquifer with

variable aquifer width, and (5) heterogeneous layered aquifer with a clogging layer not present.

Case 1 - Homogeneous Aquifer, Variable Aquifer Material

Figure 22 illustrates the effect that the aquifer material can have on steady state system fluxes. This graph is the result of several successive simulations with the domain at Figure 8 for all three types of aquifer materials. In all runs, the aquitard material is silt loam (Material 5) and the clogging layer consists of clay loam (Material 6). The series of runs made with the medium sand aquifer material corresponds to the reference simulation case, fluxes from which have been analyzed earlier in Figure 19.

Two rather obvious yet important conclusions are reached by observing Figure 22. First it is clear that, for a given value of head in the underlying aquifer, the seepage rate depends on the aquifer properties. This holds true not only over the range of heads in which disconnection occurs, but also when stream and aquifer maintain connection. Aquifer properties are obviously exerting some control on the rate at which water flows away from the stream. Second, the maximum flux is strongly dependent on the aquifer material properties. The maximum value of suction head on the underside of the clogging layer reached in each case for this designated set of aquitard, clogging layer, and stream stage properties, is determined by the unique hydraulic conductivity-pressure head (K-ψ) relationships of the aquifer material used in the simulations. It should be noted that the maximum flux rate is not affected by possible unsaturated flow within the clogging layer, since maximum suction head beneath the clogging layer in the runs represented by Figure 22 is repeatedly less than the

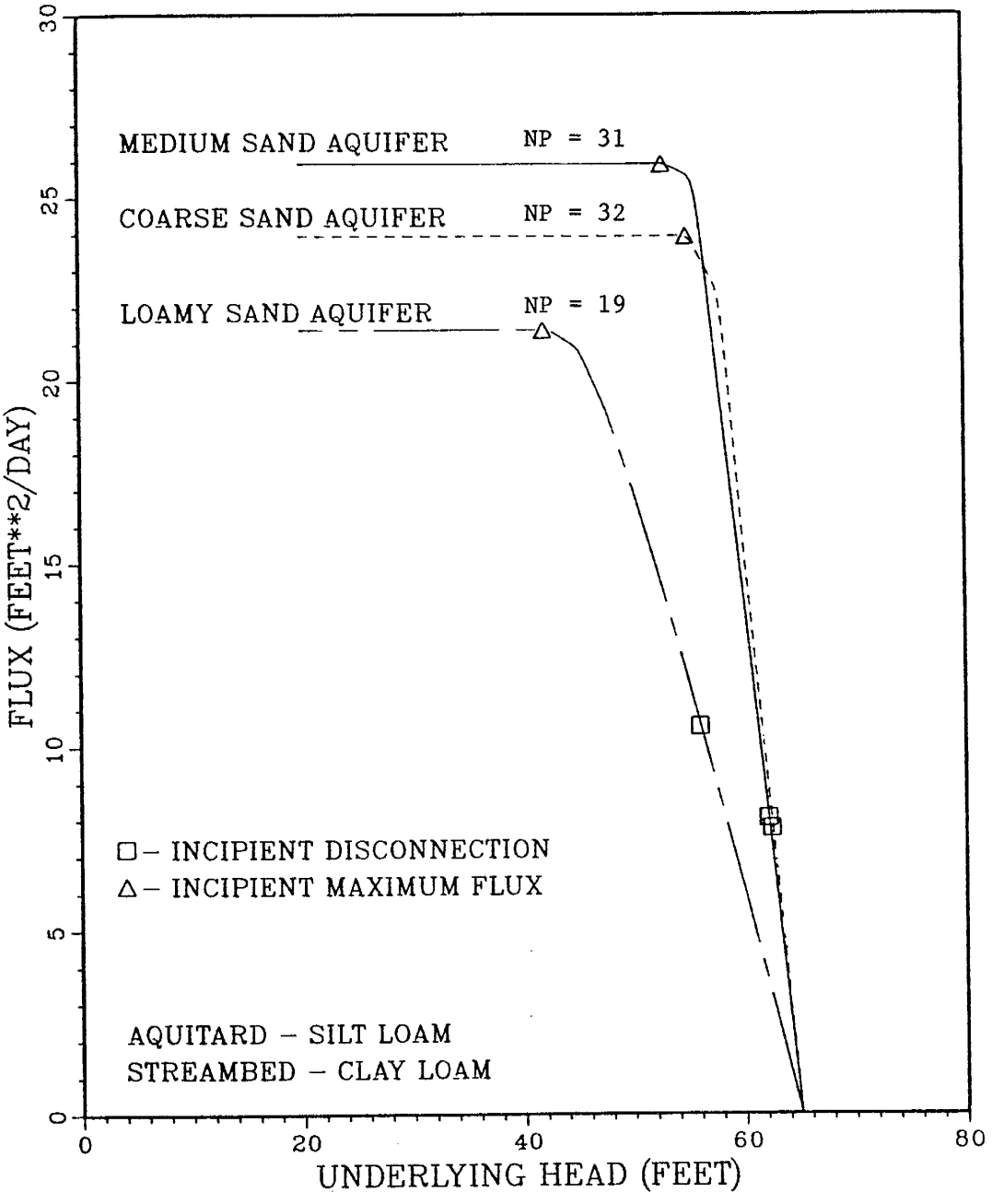

Fig. 22. Steady state system fluxes versus hydraulic head in the underlying aquifer (underlying head) for three aquifer materials.

air entry pressure head of the clogging layer material (clay loam ψ_a = 4.5 feet).

Initial inspection of Figure 22 might lead to the conclusion that aquifer materials with larger saturated hydraulic conductivities (K_s) will ultimately induce greater seepage from the stream than those with a low K_s. Although such a trend may be generally true, it would be incorrect to assume that it is always correct. For example, it is seen in Figure 22 that the maximum flux for the coarse sand (K_s = 800 ft/day) is distinctly less than that for the medium sand (K_s = 100 ft/day). Again, it is seen that the full spectrum of hydraulic conductivities of an unsaturated soil that determine the flow that takes place within it, rather than just its saturated hydraulic conductivity.

The graph in Figure 22 also illustrates how seepage into the most texturally nonuniform of the three aquifer materials, sandy loam, is affected by water table levels over a larger range of underlying heads than are the other two aquifer soils. As mentioned earlier, this result is expected, inasmuch as a greater amount of water table mounding occurs in a low permeability aquifer beneath a losing surface water body than does in a medium with high saturated hydraulic conductivity. Figure 23 provides an illustration of the sensitivity of water table measures to the aquifer material and further emphasizes the increased mounding associated with a poorly sorted aquifer soil. In this figure, the response of maximum and minimum water table levels to changes in head of the underlying aquifer have been plotted for two separate aquifer materials. Figure 23a shows water table behavior for the reference simulation domain, and is, therefore, identical to Figure 20, with the exception that the mean water table level is omitted.

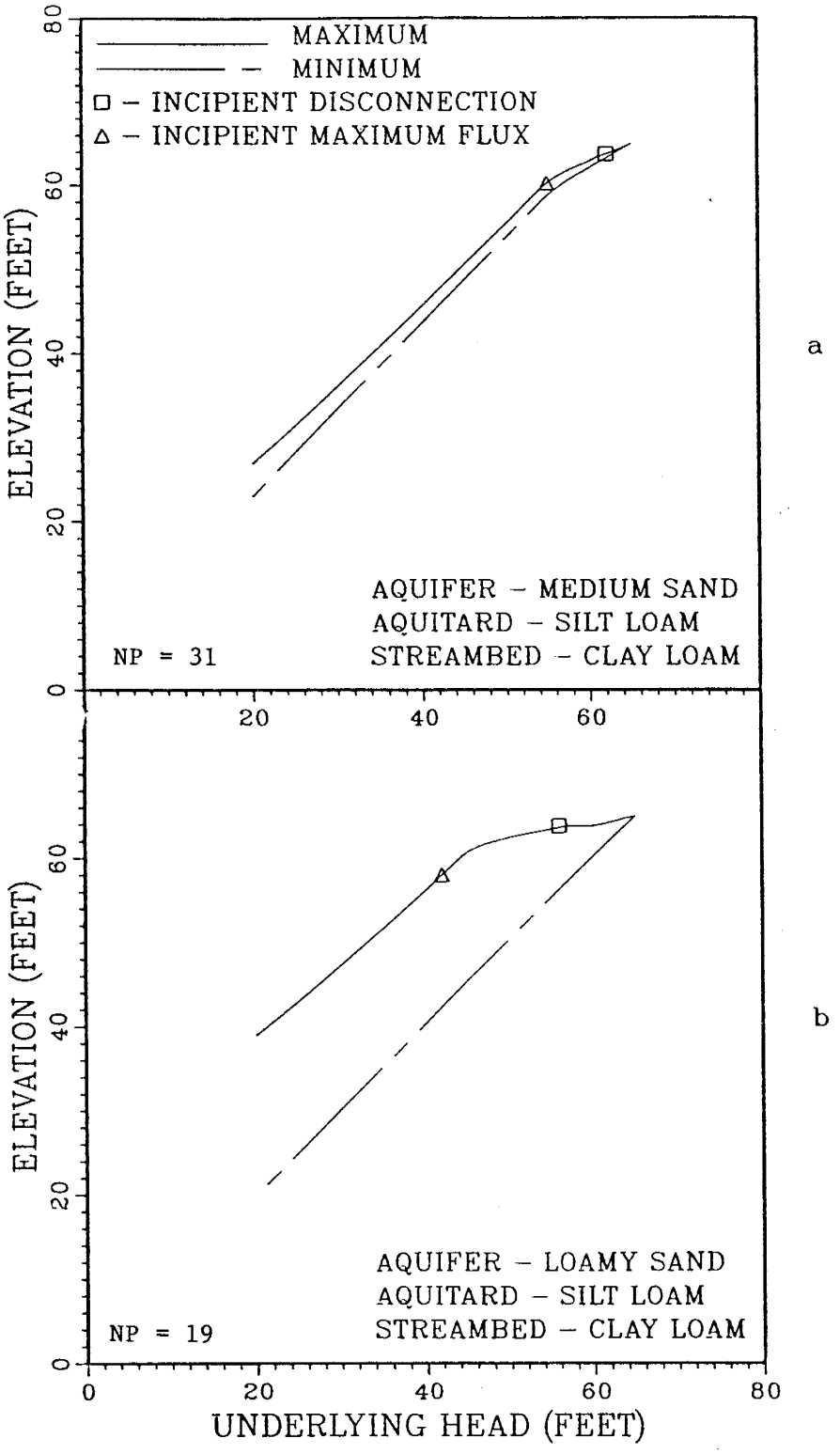

Fig. 23. Steady state, spatial maximum and minimum water table elevations versus hydraulic head in the underlying aquifer (underlying head) for (a) the reference simulation domain and (b) the same domain but with a loamy sand aquifer.

Figure 23b illustrates comparable behavior for a domain that is the same as the reference case, with the single exception that loamy sand now comprises the aquifer.

Differences between the two graphs of Figure 23 are apparent. It can be seen that the differences between the spatial maximum water table elevation (near the stream) and the spatial minimum water table level (at the domain's right boundary) is consistently larger in the case of the sandy loam aquifer material (Figure 23b). Again, this is obviously due to the additional head differential needed to transfer water laterally across this less (saturated) permeable soil. An outcome of this very basic hydraulic phenomenon is that maximum water table levels in the loamy sand case are always higher than those from the medium sand run for the same underlying aquifer head. Consistently higher water table elevations near the stream mean that hydraulic heads beneath the stream remain consistently higher, and seepage from the stream will consistently be lower in the sandy loam aquifer (see Figure 22). Unlike the spatial maximum water table elevations, minimum water table levels are consistently lower with the loamy sand aquifer.

Case 2 - Homogeneous Aquifer, Variable Clogging Layer Material

The importance of clogging layer on stream-aquifer processes is most easily and effectively demonstrated by observing steady flux behavior for the various materials that are used for this unit. Computed fluxes have been examined from simulations based on the domain dimensions of Figure 8, an aquifer comprised of medium sand, an aquitard of silt loam, and the clogging layer materials. A stream stage of 1 foot has been used in all of the steady state runs. Flux versus hydraulic head in the underlying aquifer has been graphed for

two of the clogging layer materials, namely silt loam and silty clay, as well as the case in which a clogging layer is not present. The graphs are shown in Figure 24.

A few conclusions derived from inspection of Figure 24 are predictable and easily explained. First, it is obvious that the maximum flux observed for the silt loam clogging layer (~48 ft^2/day) is considerably larger than the equivalent flux that occurs when silty clay comprises this unit (~6 ft^2/day). This is expected since the saturated hydraulic conductivity of the silt loam (K_s = 0.1 ft/day) is ten times larger than that of the silty clay, and because pressure heads beneath the clogging layer never become more negative than the respective air entry pressure heads (ψ_a) of these soils. Secondly, it is apparent that incipient maximum flux comes about at a higher value of underlying head (~56 feet) for the silty clay case than is the case with the silt loam clogging layer (underlying head ≈51 feet). This is also an expected result since fluxes are proportionately limited by the lower permeability material; hence, the rate of decline in water table height with changes in underlying head is larger for the less permeable silty clay than with the silt loam. As a natural consequence, reduction of maximum water table level, especially to the point of incipient maximum flux, takes place over a shorter range of underlying heads in the silty clay case than in the silt loam example.

Perhaps the most significant observation to be made from Figure 24 is the fact that neither disconnection nor maximum flux conditions are reached in these simulations when the clogging layer is not present. Although this specific result applies only to these particular conditions, the authors believe that it is indicative of some general findings that can be made as a consequence of this study. These

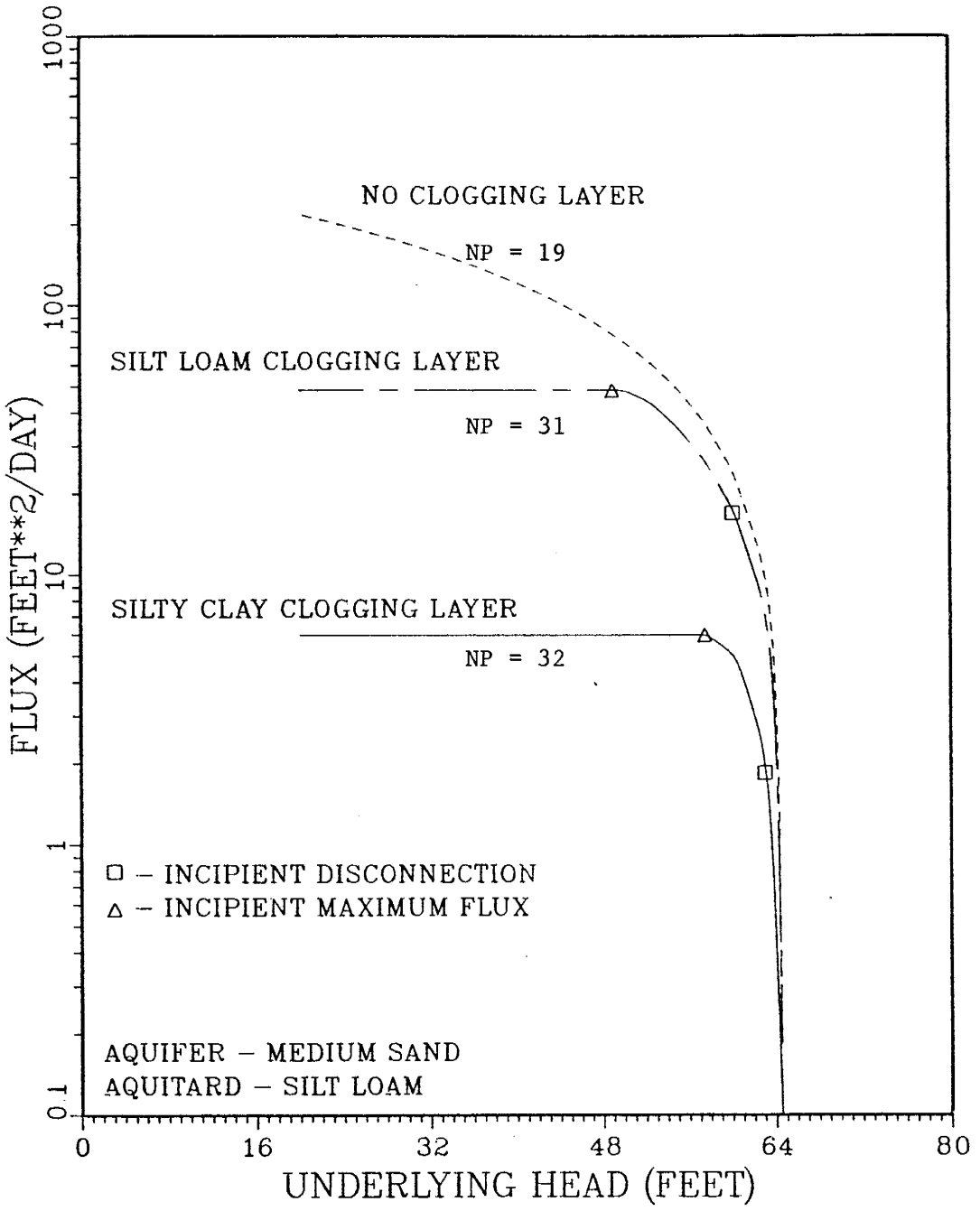

Fig. 24. Steady state systlem fluxes versus hydraulic head in the underlying aquifer (underlying head) for two clogging layer materials and the case of no clogging layer.

findings tend to support earlier speculation (see Chapter II) regarding the ability of capillary forces to be the sole mechanism by which disconnection is achieved in stream-aquifer systems where streambed clogging is not present. Further discussion of this issue is found in the next section (Case 3).

Another illustrative example of the influence of clogging layer properties on steady seepage rate is presented in Figure 25. Maximum flux rates from simulations with the domain of Figure 8 are plotted for all three aquifer materials over the full range of the saturated hydraulic conductivities exhibited by the fine-grained soils used as aquitard and clogging layer units (see Figure 11b). A sandy silt aquitard has been used in all of the simulations used to determine these maximum fluxes. The stream stage in each instance is 1 foot. Figure 25 not only demonstrates how increasing K_s of the clogging layer increases stream losses but also further emphasizes the dependence of maximum stream seepage rates on unique K-ψ properties of the aquifer medium. It is interesting to note that the maximum seepage rates for the loamy sand aquifer are diverging from those for the other two materials as clogging layer hydraulic conductivity is increased. In contrast the rates corresponding to the more coarse materials (medium and coarse sand) appear to be quite similar in magnitude over the higher range of clogging layer K_s. This occurs because the properties of the loamy sand (see Figures 10a and 10b) contrast less with those of the more permeable clogging layer materials (see Figure 11a and 11b) than do the coarse sand and medium sand aquifer materials. It might also be noted that a maximum seepage rate for the loamy sand aquifer (K_s = 5 ft/day) using a sandy silt clogging layer (K_s = 1 ft/day) is not plotted, as disconnection is not attainable for this aquifer

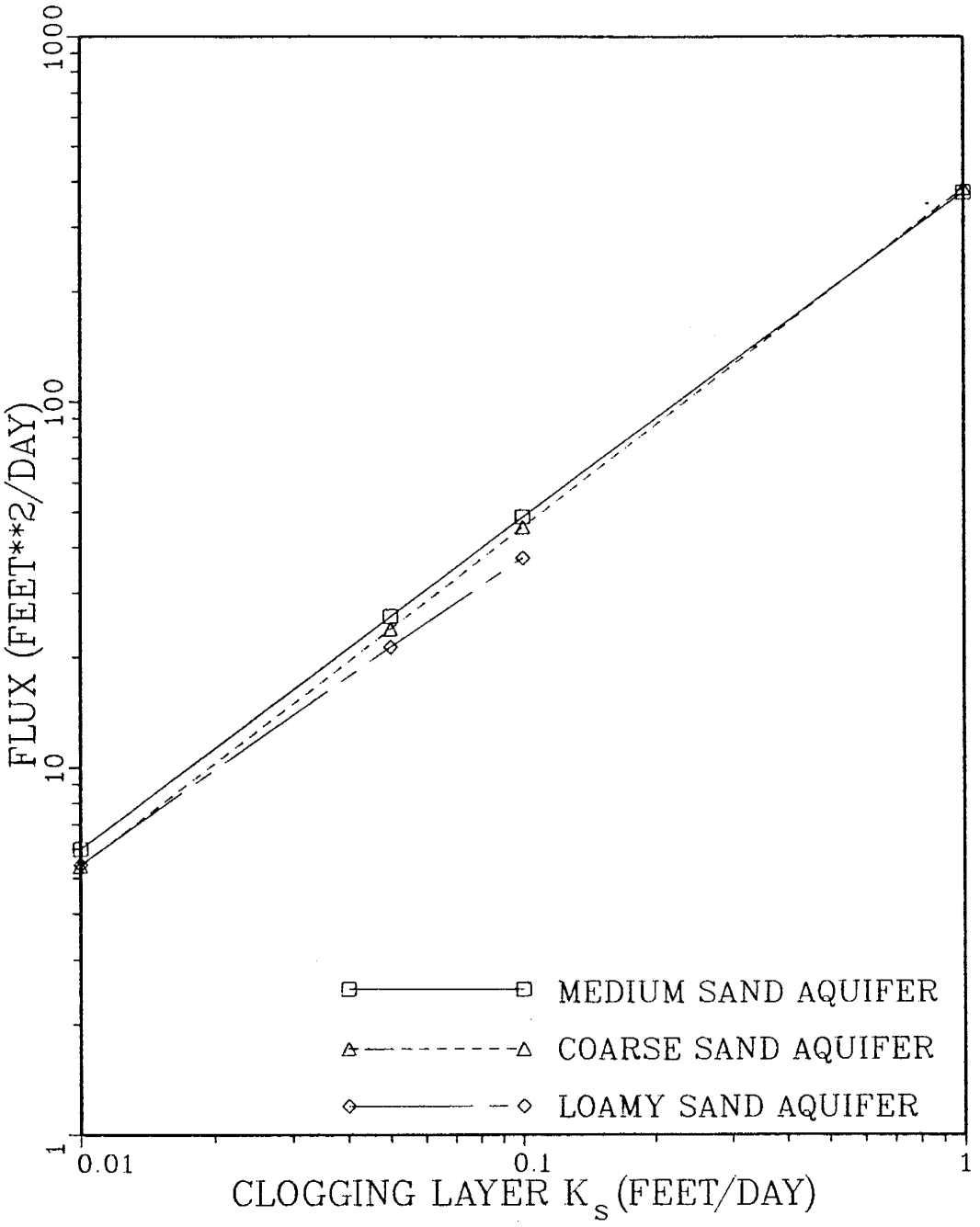

Fig. 25. Maximum steady state system fluxes versus clogging layer saturated hydraulic conductivity for three aquifer materials.

material/clogging layer combination for the assumed simulation conditions.

Case 3 - Homogeneous Aquifer, Clogging Layer Not Present

The conditions used earlier to prepare Figure 24 are such that connection is continually maintained for the series of runs in which a clogging layer is not present. This tends to suggest that, for the particular set of assumptions used to make those simulations (i.e., 25-foot stream half-width, stream stage of 1 foot, homogeneous aquifer comprised of medium sand, 10-foot thick aquitard consisting of silt loam), a streambed clogging layer is necessary if disconnection is to occur under steady state conditions. However, this should not be construed to mean that streambed clogging is always a prerequisite for disconnection. As has been stated in Chapter II, the potential for disconnection, in a situation in which streambed clogging is not present, cannot be determined until all influential factors - including stream stage, stream geometry, aquifer and aquitard properties - have been examined. With this in mind, attempts have been made in this study via several different steady state simulations to produce disconnection in homogeneous aquifers for non-clogging situations. The domains that have been considered are of the same nature as those described up to this point, with the exception that a clogging layer has not been included. By including a basal aquitard as part of the simulation domain, the location of the water table in the aquifer is determined by the variably saturated flow code. This approach differs from related variably saturated simulation studies (e.g., Reisenauer, 1963; Jeppson and Nelson, 1970) in which the location of the water

table is assumed to be known beforehand, and is, therefore, invoked as a prescribed head boundary condition on the aquifer domain.

Table 3 presents a summary of several of the steady state test runs made with the variably saturated flow code in which the clogging layer is omitted. The summary shows some of the types of conditions that have been considered and the cases in which disconnection is observed. All of these simulations have been made using a domain of the same nature as that shown in Figure 8, but dimensions of the domain have been allowed to vary. Stream half-width is reduced to be either 5 or 10 feet. Depth from the bottom of the stream to the base of the aquifer has been set at either 50 or 100 feet. Width of the domain in each series of runs has been reduced to 100 feet since stream widths are now considerably smaller than before, and the smaller domain width signifies less CPU use. Aquitard material in all cases is sandy silt (Material 4, K_s = 1 ft/day) and the aquitard thickness is 5 feet. All three aquifer materials (coarse sand, medium sand, loamy sand) are tested. Stream stage varies from 0.01 to 2 feet. The range of underlying heads (measured with respect to the base of the aquitard) employed in each series of runs is listed. The simulations in Table 3 are arranged such that the aquifer depth and stream half-width believed to be least conducive to disconnection are listed first. If disconnection is achieved for a given aquifer material and set of simulation conditions, no further simulations are made with that same material under conditions that are expected to be even more conducive to disconnection.

Table 3 shows that disconnection is never achieved in any of the runs that employ the coarse sand (Material 1) aquifer material. Connection is continually maintained for this aquifer medium despite

TABLE 3

Summary of Several Steady State Simulations for Studying Likelihood of Disconnection in Homogeneous Aquifers Overlain by Streams Unaffected by Clogging

Aquifer Depth Below Streambed (feet)	Stream Half-Width (feet)	Aquifer Material	Stream Stage (feet)	Range of Underlying Heads (feet)	Disconnection
50	10	coarse sand	2	57-5	no
50	10	medium sand	2	57-5	no
50	10	loamy sand	2	57-5	no
50	10	coarse sand	1	56-5	no
50	10	medium sand	1	56-5	no
50	10	loamy sand	1	56-5	yes
50	10	coarse sand	0.01	55.01-5	no
50	10	medium sand	0.01	55.01-5	no
50	5	coarse sand	2	57-5	no
50	5	medium sand	2	57-5	no
50	5	loamy sand	2	57-5	yes
50	5	coarse sand	1	56-5	no
50	5	medium sand	1	56-5	no
50	5	coarse sand	0.01	55.01-5	no
50	5	medium sand	0.01	55.01-5	no
100	10	coarse sand	2	57-5	no
100	10	medium sand	2	57-5	no
100	10	loamy sand	2	57-5	yes
100	10	coarse sand	1	56-5	no
100	10	medium sand	1	56-5	no
100	10	coarse sand	0.01	55.01-5	no
100	10	medium sand	0.01	55.01-5	no

TABLE 3 (continued)

Summary of Several Steady State Simulations for Studying Likelihood of Disconnection in Homogeneous Aquifers Overlain by Streams Unaffected by Clogging

Aquifer Depth Below Streambed (feet)	Stream Half-Width (feet)	Aquifer Material	Stream Stage (feet)	Range of Underlying Heads (feet)	Disconnection
100	5	coarse sand	2	57-5	no
100	5	medium sand	2	57-5	yes
100	5	coarse sand	1	56-5	no
100	5	coarse sand	0.01	55.01-5	no

the fact that the depth of aquifer below the streambed is increased to 100 feet, stream half-width is reduced to 5 feet, and stream stage is set as low as 0.01 feet. Failure to achieve disconnection is attributed to the relatively large saturated hydraulic conductivity of the coarse sand (K_s = 800 ft/day). When saturated, this material is easily capable of conveying water from the stream at the same increasing rate that water leaves the system by aquitard leakage as underlying heads are reduced.

In those simulations involving a medium sand aquifer (K_s = 100 ft/day), disconnection is also quite difficult to accomplish. Connection is continually maintained in a 50-foot deep system comprised of the medium sand even when the stream half-width is 5 feet and stream stage is set as low as 0.01 feet. Similarly, connection persists when using this material in a 100-foot deep aquifer overlain by a stream with a half-width of 10 feet, regardless of stream stage. Disconnection is observed in a medium sand aquifer when a stream with a half-width of 5 feet is used in conjunction with a 100-foot aquifer depth.

As Table 3 indicates, disconnection is most readily achieved in simulations with an aquifer of loamy sand (Material 3), the least permeable of the aquifer materials (K_s = 5 ft/day). When saturated, this material is apparently incapable of supplying water from the stream at an increasing rate equal to that of aquitard leakage as underlying heads decline. Factors other than the aquifer's relatively low saturated hydraulic conductivity appear to influence the potential for disconnection. For instance, Table 3 shows that connection is maintained in the loamy sand aquifer when depth of the aquifer (below streambed level) is 50 feet, stream half-width is 10 feet, and stream

stage is 2 feet. Yet, disconnection comes about for the same aquifer and stream geometry when the stage is reduced to 1 foot. Similarly, disconnection is also achieved by reducing the stream half-width to 5 feet, while maintaining aquifer depth at 50 feet and stream stage at 2 feet.

The test simulations of Table 3 help support earlier reasoning regarding the effect of properties such as stream width and stage on disconnection, and also shed light on other influences such as aquifer permeability and depth. From the steady state analyses presented in this section, it appears that the potential for disconnection in homogeneous aquifers unaffected by streambed clogging increases as (a) the width of the stream decreases, (b) stream stage is reduced, (c) saturated hydraulic conductivity (K_s) of the aquifer becomes lower, and (d) the depth over which homogeneity is maintained in the aquifer increases.

Although disconnection does take place in a 50-foot deep loamy sand aquifer and a 100-foot deep medium sand aquifer, it probably occurs less frequently than these simulation results would suggest. Homogeneous alluvial media, composed of these or any other aquifer materials, are seldom observed to extend to depths as great as 50 to 100 feet in real stream-aquifer systems. Rather, it is more likely that aquifer heterogeneity, especially aquifer stratification is found within short depths below most streams. When shallow stratification consists of interbedded fine and coarse grained materials, it becomes a major cause of increased lateral movement (and decreased vertical movement) of water infiltrating from the stream. Consequently, it is possible that media stratification is often as important as (if not

more important than) capillarity in leading to disconnection of stream and aquifer.

The propensity for flow spreading beneath an unclogged stream by capillary forces, to the extent that disconnection occurs, is, of course, going to vary with every combination of stream-aquifer conditions that might be considered. Naturally, it is impossible to examine all possible cases as part of this research. Nevertheless, based on the model runs made in this study and the fact that vertical heterogeneity is common in alluvial aquifers, the author feels that disconnection is not always attributable to capillary forces alone in stream-aquifer systems in which streambed clogging is not a factor. The mechanisms by which a clogging layer brings about disconnection has already been illustrated. In a subsequent section (Case 5), a means which layering of aquifer materials brings about disconnection is demonstrated.

Case 4 - Homogeneous Aquifer, Variable Aquifer Width

To evaluate domain response to variations in aquifer width, another series of simulations has been conducted using a domain like that shown in Figure 8, but with a width of 1200 feet. Aquifer, aquitard and clogging layer materials are the same as those used in the reference simulation case and stream stage is set at 1 foot. The discretization scheme employed in the reference domain (i.e., Figure 9) is also used for the first 600 lateral feet of the 1200 foot long domain. Discretization of the remaining 600 feet of length is essentially an extension of this original scheme, with 12 columns of 50 foot long rectangular elements being employed. Vertical dimensions of

the additional elements are the same as those shown in Figure 9. Hydraulic heads in the underlying aquifer range from 65 to 20 feet.

Differences between the reference case simulations and those with the 1200-foot wide domain are minor. Comparison of fluxes from the two runs, both of which are presented in Figure 26, shows that maximum fluxes in the two domains are essentially equal. In other words, the width of the domain has little, if any, effect on the pressures that are observed beneath the stream when the water table is deep. Since pressures in this zone determine seepage rates from the stream, equal maximum fluxes from the two cases is expected.

Slight differences in steady state seepage rate do occur over the range of underlying heads at which maximum flux has not been achieved. Within this short range, fluxes are consistently higher in the wider domain for the same underlying head. This is readily understood if one also examines water table behavior for each case. A graph of the spatial mean water table elevations versus head in the underlying aquifer is provided in Figure 27. As might be anticipated, the water table in the larger of the two domains is always at a lower elevation than that in the smaller system. This occurs because the larger lateral extent of the 1200 foot wide domain provides a greater length of aquitard surface across which leakage to the underlying aquifer can take place. Given the longer aquitard surface, a smaller head difference is needed across the aquitard thickness in order to produce the same leakage rate. The resulting lower water table elevations in the larger system also signify larger suction heads on the underside of the clogging layer than occurs in the 600 foot long system for the same underlying head. As a consequence, head differences across the clogging layer are larger in the case of the 1200 foot wide domain, and

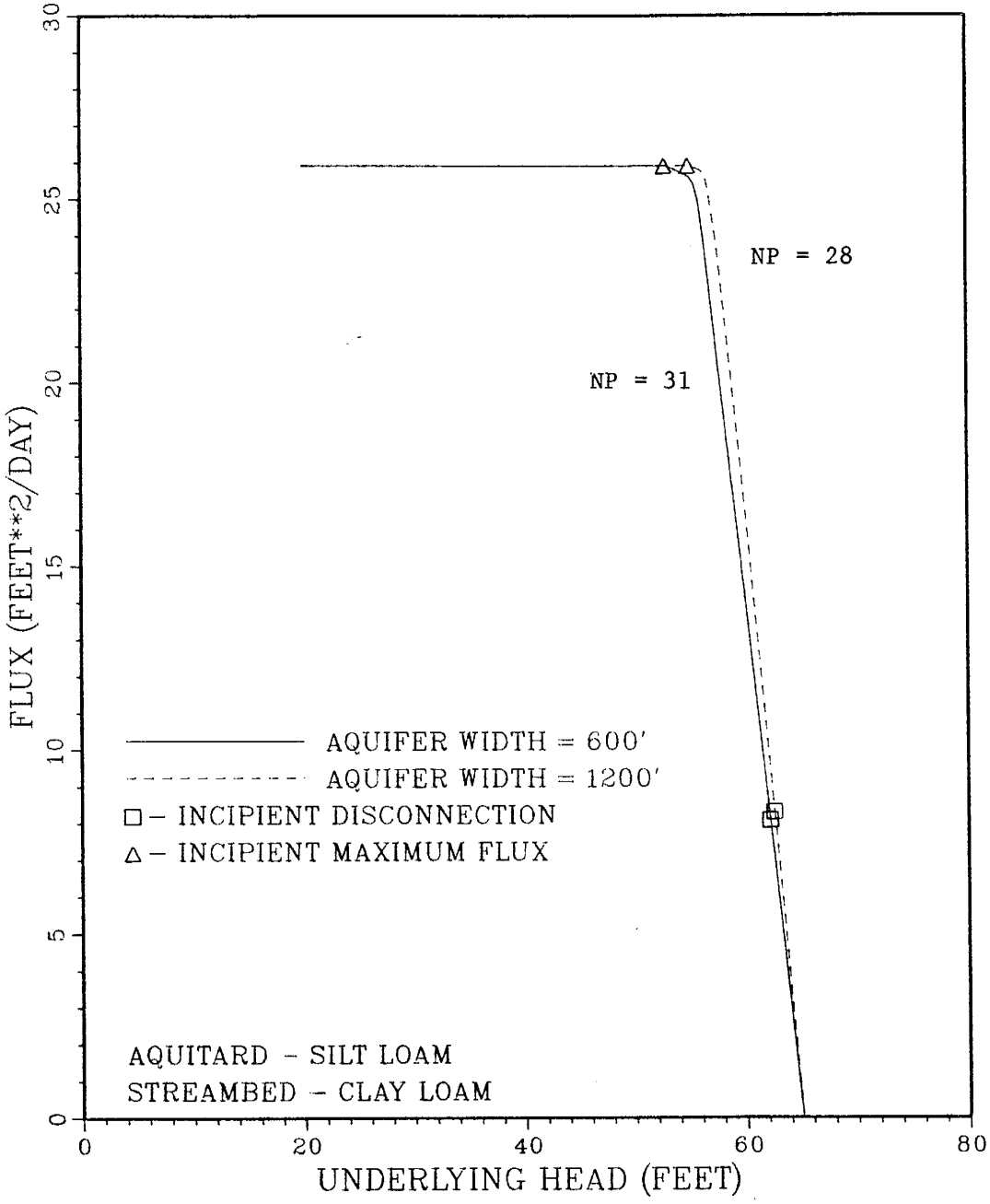

Fig. 26. Steady state system fluxes versus hydraulic head in the underlying aquifer (underlying head) for two aquifer widths.

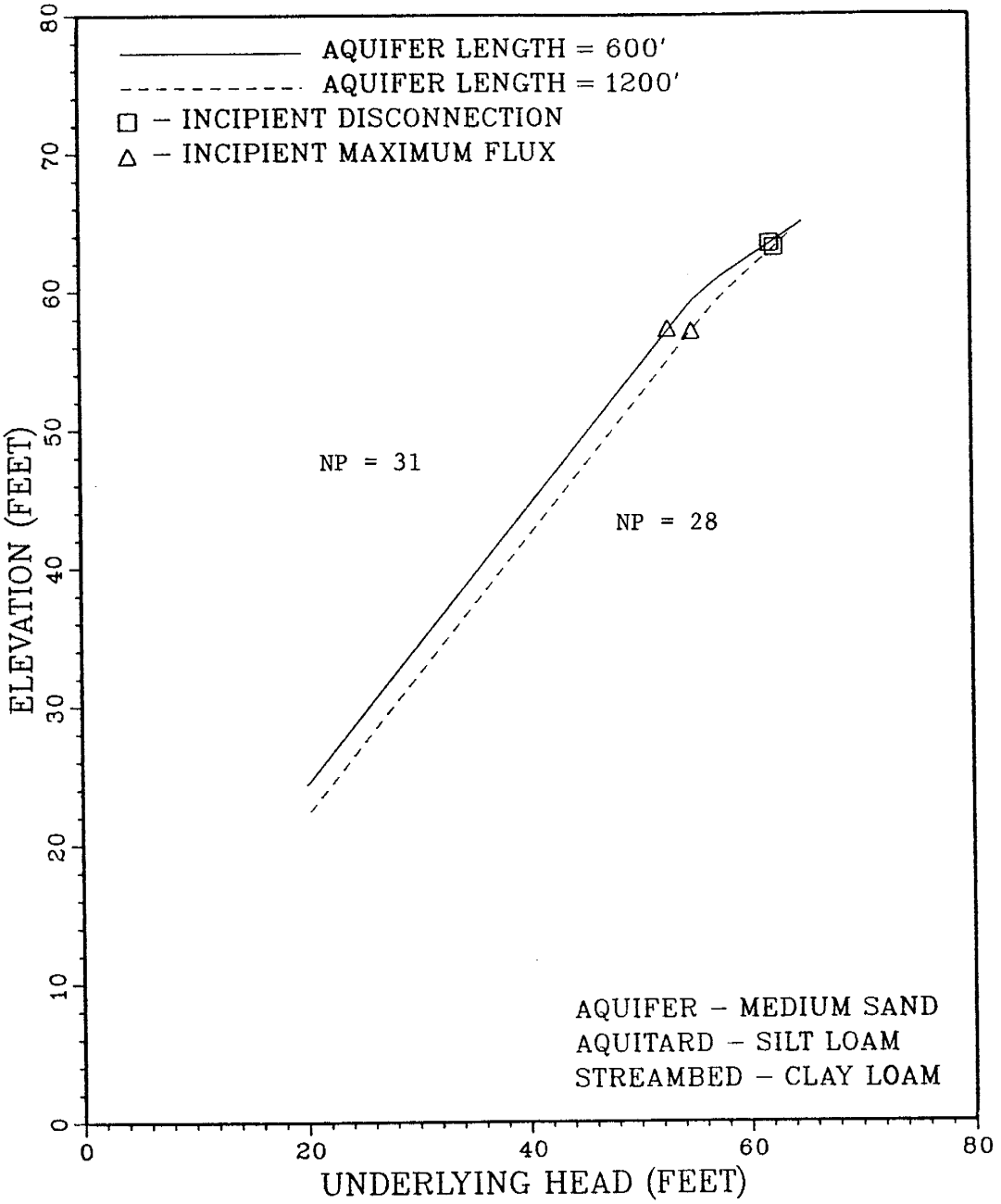

Fig. 27. Steady state, spatial mean water table elevation for two aquifer widths.

steady state stream loss rates are higher. Due to the consistently larger fluxes in the larger domain during the connected losing stream and disconnected/shallow water table phases, incipient maximum flux is reached in the 1200 foot domain at a higher value of the underlying head than is observed for the reference domain.

Case 5 - Layered Aquifer, Clogging Layer Not Present

A very simple two-layered system has been selected to analyze the effects that a layered aquifer domain has on stream infiltration. In this analysis, there is no streambed clogging. A pictorial representation of the type of two-tiered system used in the variably saturated flow simulations is presented in Figure 28. It can be seen in this schematic that the less texturally uniform loamy sand (Material 3) is assumed to overly a unit of coarse sand (Material 1). The basal aquitard is comprised of sandy silt (Material 4). With the exception of an absent clogging layer, dimensions and boundary conditions of this system are identical to those of the reference simulation domain (Figure 8).

Three separate series of steady state runs are made with the domain shown in Figure 28. The three differ with respect to the height of the interface separating the loamy sand from the coarse sand. Using the lower left corner of the aquitard as the system origin, the interface height for the three series of simulations are 60 feet, 50 feet and 40 feet, respectively. Hence, depths to the interface below streambed elevation (64 feet) are 4, 14 and 24 feet, respectively. As before, each set of steady state runs is performed using a stream stage of 1 foot and by allowing heads in the underlying aquifer to be lowered from a uniform high value of 65 feet to a low of 20 feet.

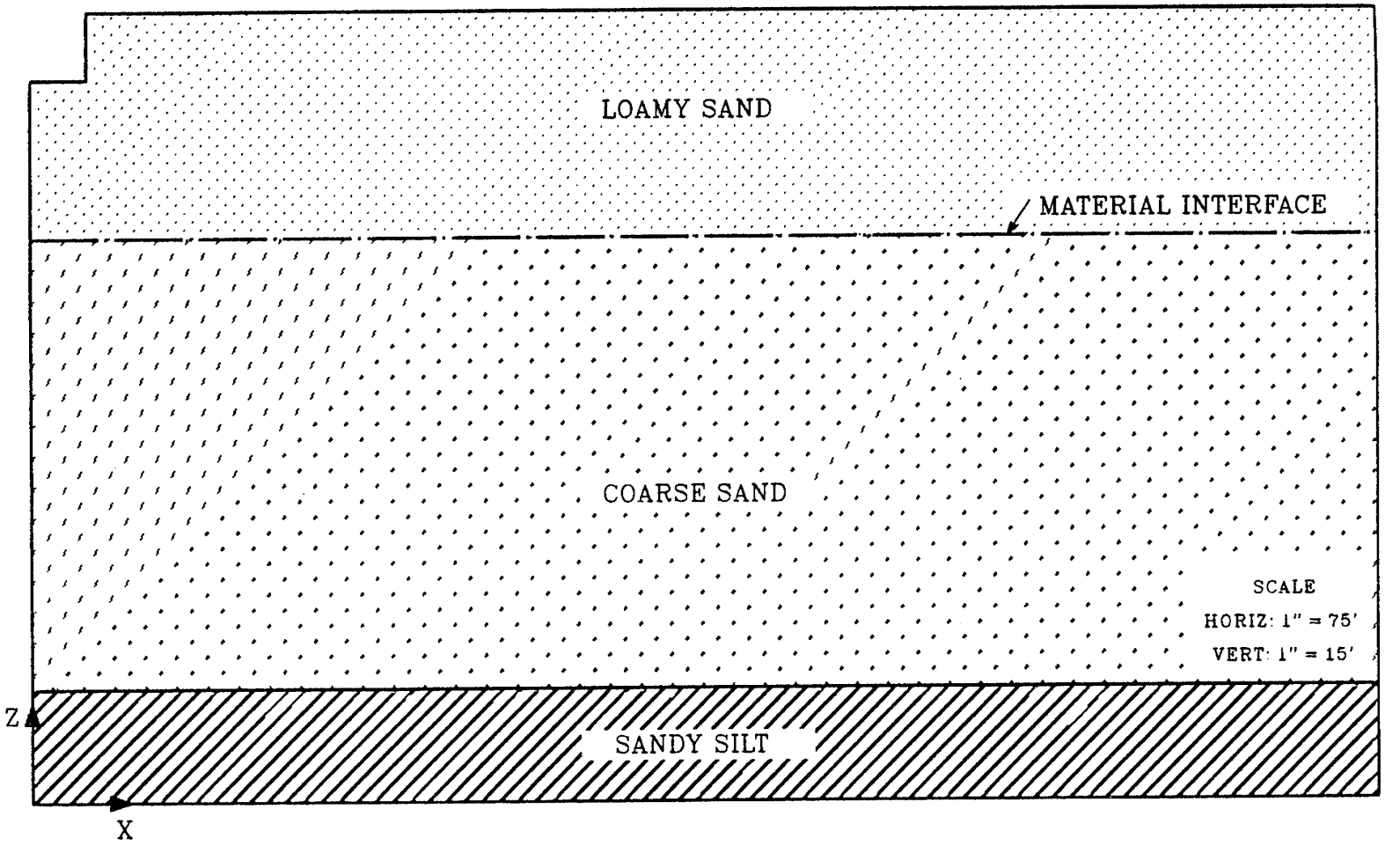

Fig. 28. General two-layered aquifer system overlain by a stream unaffected by streambed clogging.

As has been the case throughout this study, the motivation for conducting the variably saturated flow simulations is to ascertain, in a general sense, how hydraulic processes observed in simple systems might translate into phenomena recorded in actual stream-aquifer systems. The two-tiered domain, consisting of non-uniform less permeable materials overlying relatively uniform and coarse sand, is selected as being representative of an alluvial aquifer associated with an underfit stream. Depth of the aquifer and respective heights of the two aquifer units are thought to be somewhat characteristic of vertical material distributions in the Mesilla Valley flood-plain alluvium. Changing the elevation of the interface separating the two units, is done, therefore, in the interest of assessing how the height of the transition between the two types of alluvial sediments generally affects flow processes in such stream-aquifer systems.

The three series of steady state runs with the layered domain are all of interest because disconnection of stream and aquifer is observed during each despite the absence of a clogging layer. Plots of head, moisture content and water table elevation, taken from the series of simulations based on a material interface height of 50 feet, are used to illustrate general phenomena associated with the disconnection process. Comparison of results from runs made with the three different material interface heights is done through analyses of system flux behavior with declining underlying head.

Figure 29 provides one example of hydraulic head distribution in the two-layered domain in which the interface height is set at 50 feet. In this instance, total head in the underlying aquifer is also 50 feet. Stream and aquifer remain connected, and all unsaturated flow takes place entirely within the upper layer. Head distribution for this

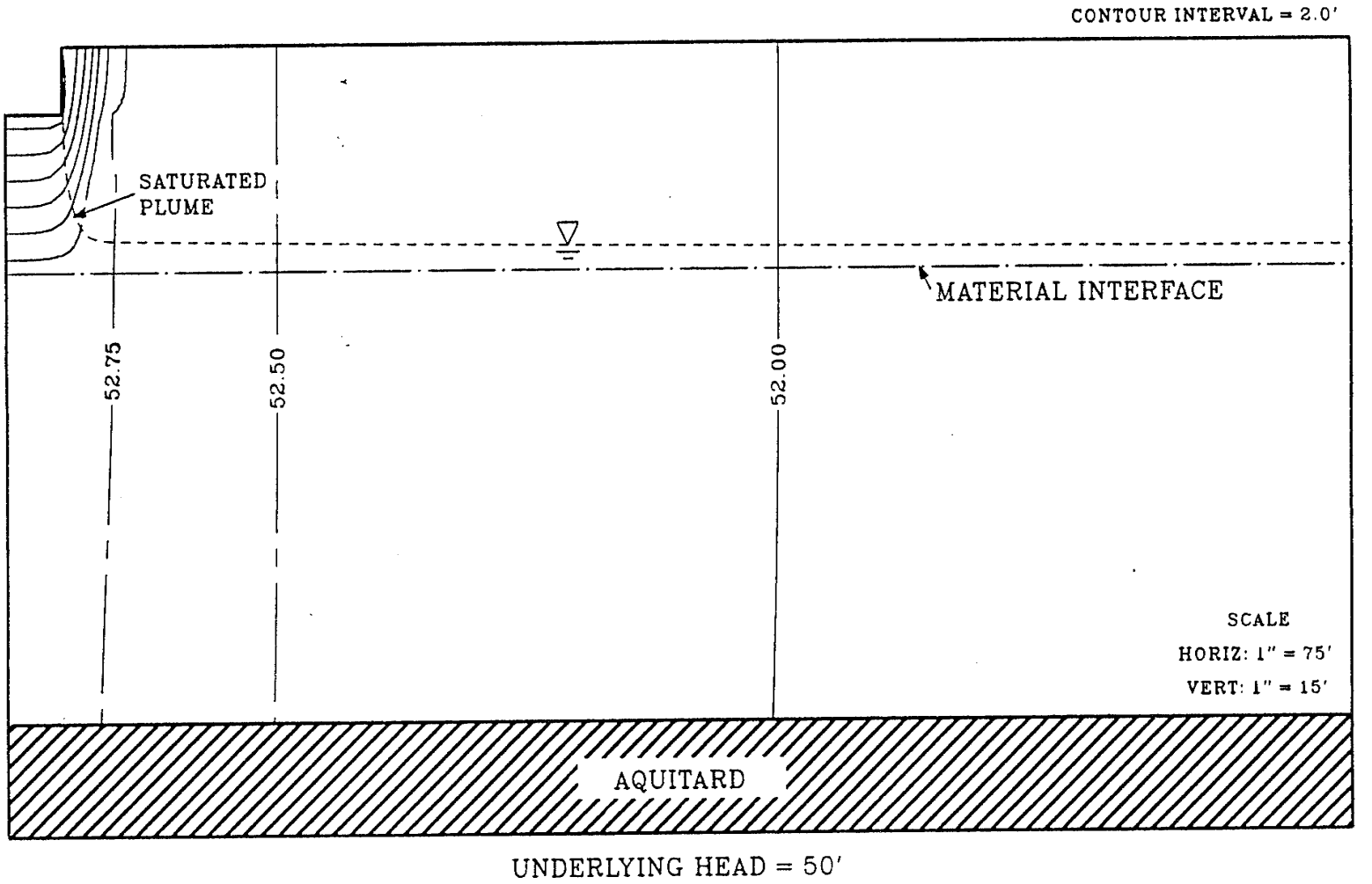

Fig. 29. Steady state hydraulic heads (in feet) in the two-layered domain under connected losing stream conditions.

connected losing stream case is in many ways similar to previously analyzed head configurations for the reference simulation domain. Hydraulic gradients are largest near the stream and decrease quickly with distance from the stream. However, the distribution in Figure 29 is distinctive in that the total head contours indicate a significant quantity of water moving from saturated aquifer material into the unsaturated zone. This takes place along the right edge of a saturated plume found mostly below the stream channel. The majority of this water originates as infiltration across the streambed, while a small portion comes from seepage through the stream bank. Although flow in the unsaturated zone is substantial in this instance, most of the water moving through the system does so within saturated media. As in the reference case simulations, water in the unsaturated zone gradually reenters the saturated zone with distance from the stream.

Moisture content profiles corresponding to the hydraulic head plot of Figure 29 are presented in Figure 30. The steepest gradients of moisture content are found just to the right of the saturated plume underlying the stream and just to the right of the stream's right bank. In the remaining portions of the unsaturated zone, moisture content increases gradually with height above the water table (θ = 0.38), reflecting flow conditions that are close to hydrostatic. The vertical moisture content gradient in these outlying areas is much smaller than observed in comparable areas in the reference simulation runs. This is attributed to the presence of loamy sand (Material 3) in the upper aquifer layer. The moisture characteristic for this texturally nonuniform material (see Figure 10a) shows that its moisture content decreases less rapidly with increasing suction head (and, therefore,

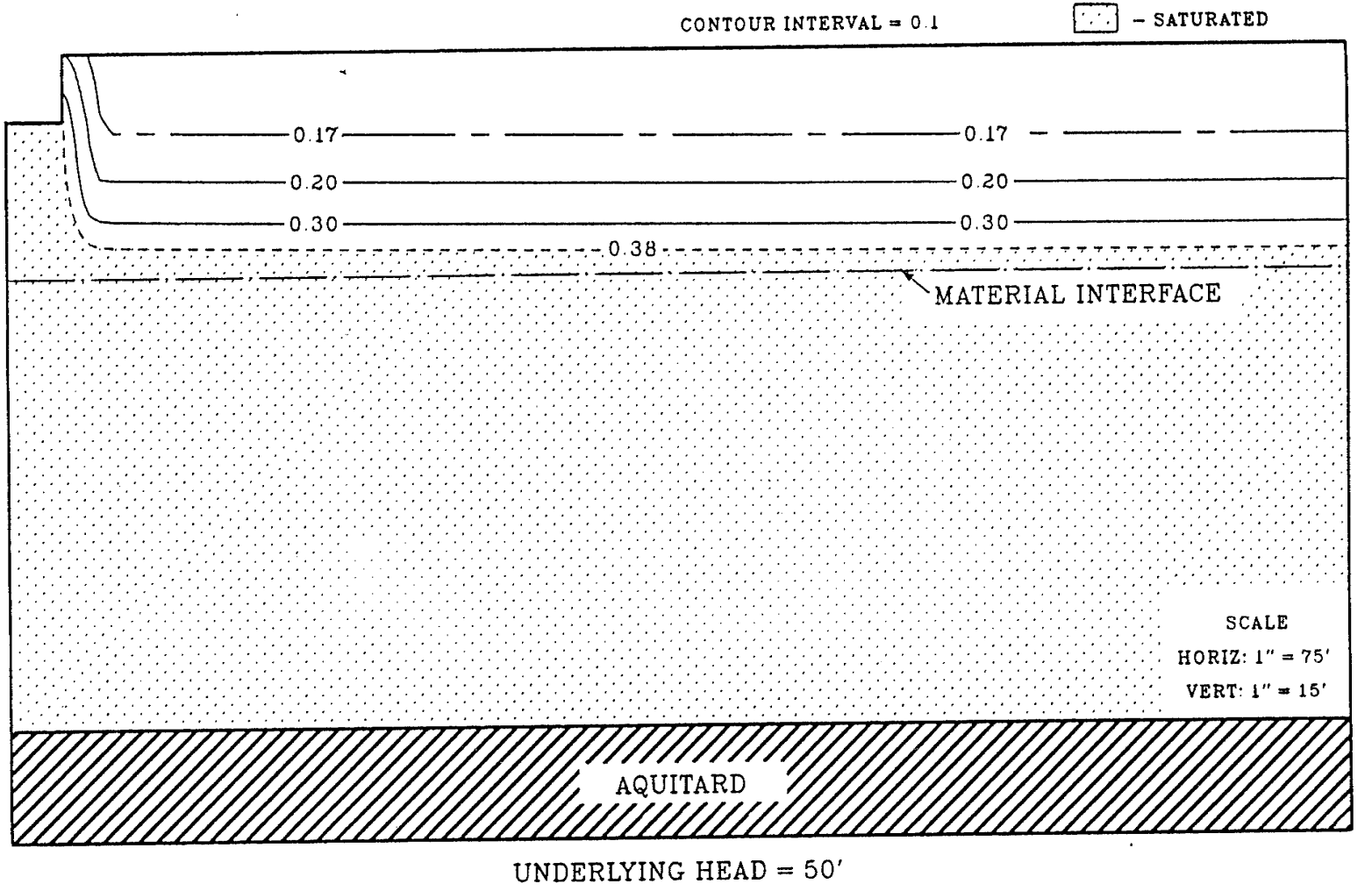

Fig. 30. Steady state moisture contents (dimensionless) in the two-layered domain under connected losing stream conditions.

with elevation above the water table) than does the medium sand used as aquifer material in the reference simulation runs.

Figure 31 illustrates the steady state hydraulic head distribution in the two-layered domain from a simulation in which underlying head is set at 46.51 feet. In this example, water table levels have been lowered to the extent that most of the free surface is now located in the lower layer of coarse sand, just below the material interface. Moreover, the base of the saturated plume, found below the stream in Figures 29 and 30, has now contracted considerably just above the material interface. Thus, the beginnings of a saturated bulb have become apparent (see e.g., Figure 3). A slight decline in underlying head (to 46.5 feet) is all that is required to bring disconnection and complete the formation of a saturated bulb.

By definition, the stream and aquifer are still considered to be hydraulically connected in Figure 31. Yet a very large portion of water moving through the system at some point or another passes through unsaturated media. Again, water entering the unsaturated zone is coming from the saturated plume located below the stream. A great deal of the transfer of water from saturated to unsaturated media takes place near the base of the saturated plume, in the area of greatest plume contraction, and just above the material interface. As the total head contours in Figure 31 suggest, most of the water reentering the saturated zone in the lower layer does so in an area located either below or within a very short distance (25-50 feet) to the right of a vertical line coinciding with the stream's right bank.

Figure 32 illustrates the moisture content configuration corresponding to the hydraulic heads plotted in Figure 31. Moisture distributions in this instance are quite similar to those presented in

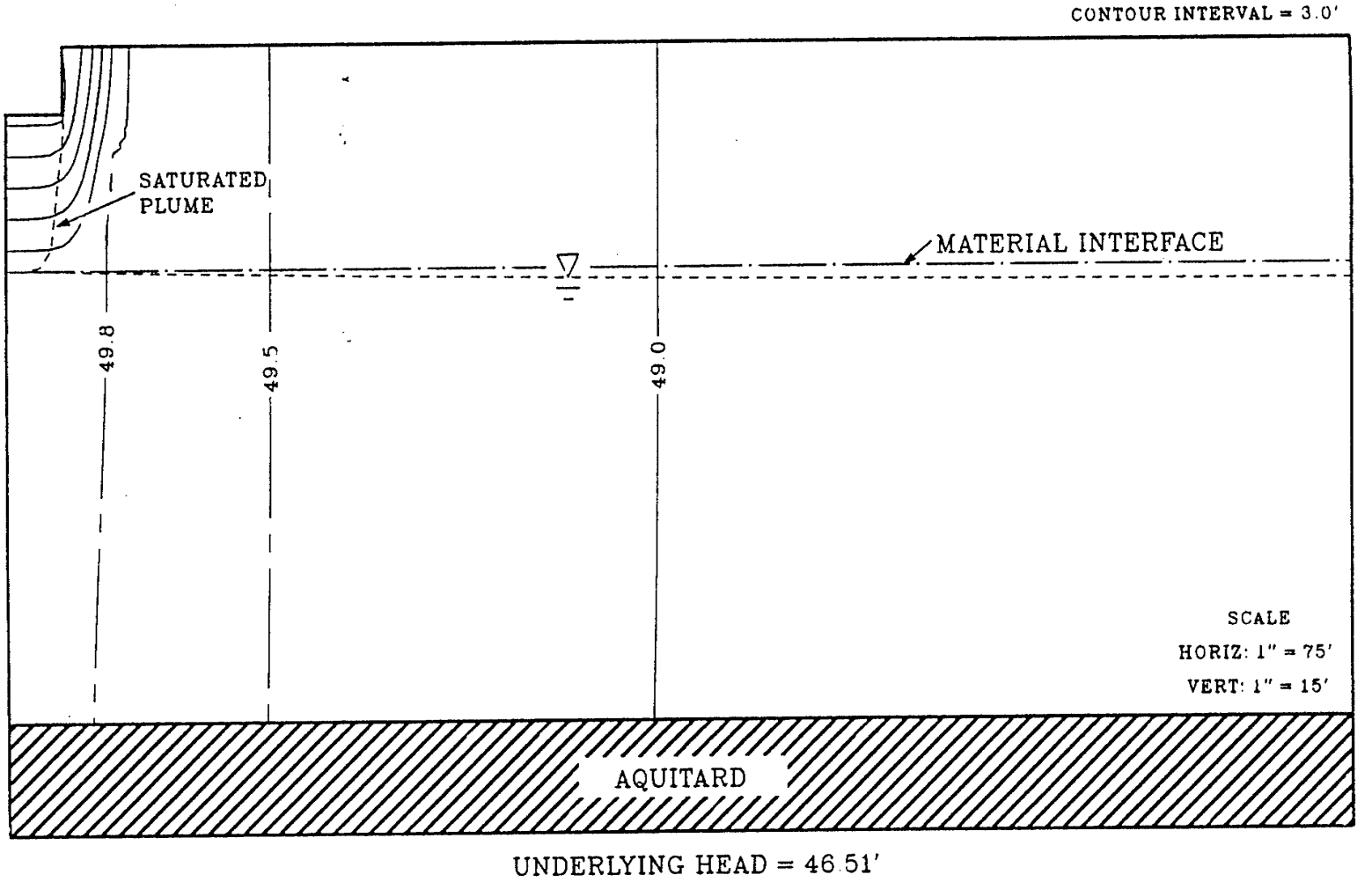

Fig. 31. Steady state hydraulic heads (in feet) in the two-layered domain just prior to disconnection.

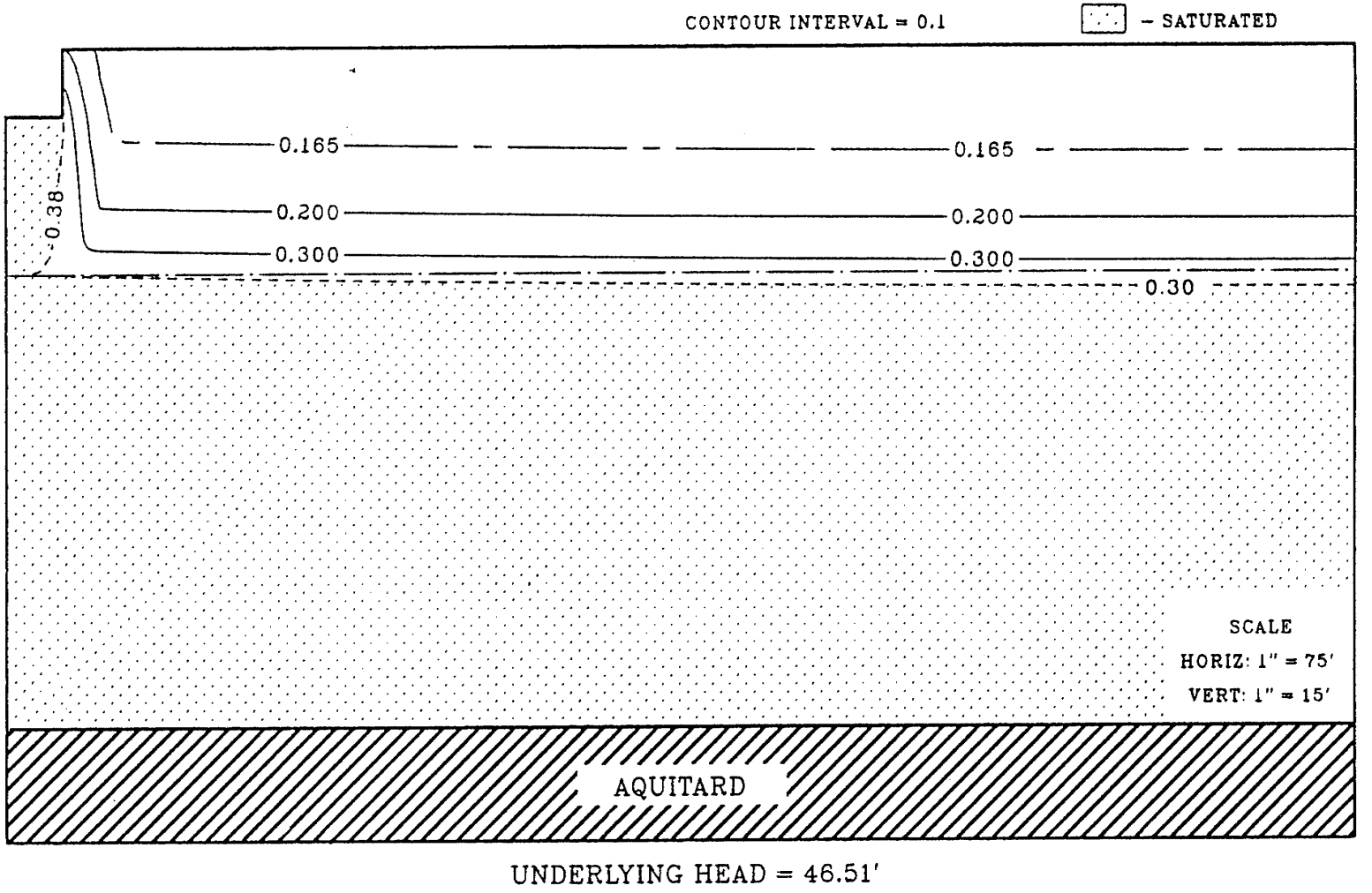

Fig. 32. Steady state moisture contents (dimensionless) in the two-layered domain just prior to disconnection.

the previously discussed simulation based on an underlying head of 50 feet. The greatest moisture content gradients are found just to the right of the stream and along the right side of the saturated plume beneath the stream. Because the water table within the lower aquifer layer is situated just below the material interface, no contours are plotted in the coarse sand material, other than at the free surface itself. Note that the moisture content at the free surface in the lower layer ($\theta = 0.30$) is less than that along the saturated plume in the upper layer ($\theta = 0.38$), reflecting the lower porosity of the coarse sand (see Figure 10a, Chapter VII).

An example of total head distribution in the layered domain after disconnection has taken place is presented in Figure 33. Total head in the underlying aquifer has been lowered further to a uniform value of 30 feet in this run. A distinct saturated bulb, situated entirely within the loamy sand, is now evident. More than 20 vertical feet of unsaturated media (in both layers) separate the deepest point of the saturated bulb from the highest point of the water table (at the stream centerline). The stream-aquifer relationship exhibited here corresponds to the case of a disconnected stream with a deep water table. Steady state flux in this example is a maximum for the given aquifer layering scheme, aquifer materials, stream width and stream stage.

Two distinctive features are observed in the hydraulic head distribution of Figure 33. First it can be seen that head gradients in the area located directly below the stream are noticeably steeper in the sandy loam than in the coarse sand above water table level. This suggests, for the steady state flux occurring in this example, that hydraulic conductivity (both saturated and unsaturated) in the loamy

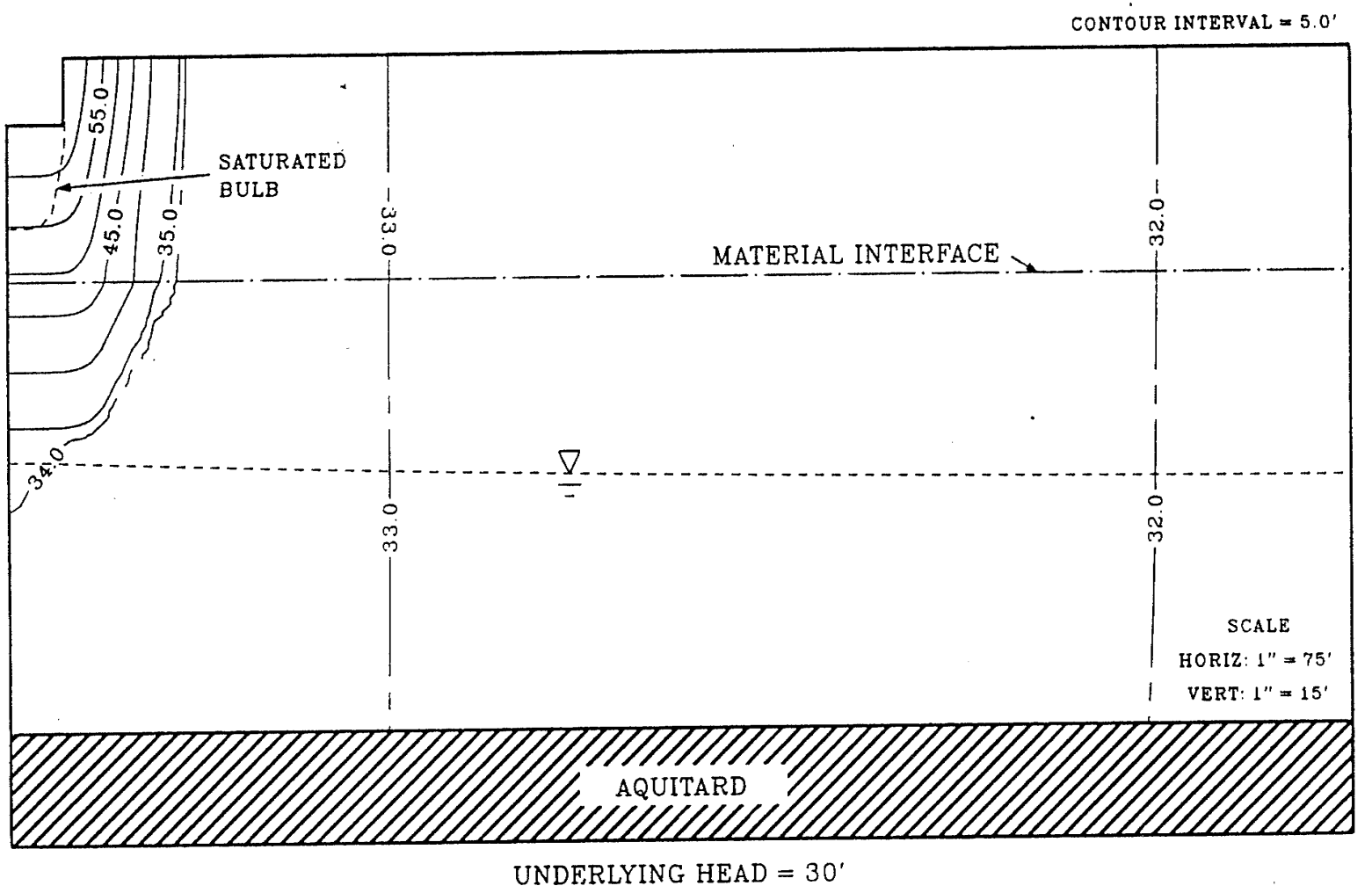

Fig. 33. Steady state hydraulic heads (in feet) in the two-layered domain for a disconnected stream with a deep water table.

sand below the stream is less than the underlying unsaturated hydraulic conductivity in the coarse sand. Secondly, head contours show a tendency to bend at the material interface in the unsaturated zone located 10 to 50 feet right of a vertical line passing through the stream's right bank. Flow in the upper material in this general area is oriented more in a horizontal direction than in the deeper material. Pressure heads in this area are so small (-3.0 to -15.0 feet) that hydraulic conductivity in the loamy sand is less than in the coarse sand. The concomitant strong component of horizontal flow in the loamy sand relative to that in the coarse sand is similar to the increased lateral flow effects described earlier (Chapter II) for unsaturated flow in layered soils (e.g., Figure 4c).

Figure 34 show steady state moisture contents in the layered domain from the simulation based on an underlying head of 30 feet. Discontinuity of moisture content at the material interface is apparent here. For example, the $\theta = 0.05$ contour in the coarse sand meets the $\theta = 0.30$ contour in the loamy sand. Also apparent is a pocket of essentially constant moisture content, located beneath the stream and in the unsaturated zone below the material interface. This region is similar in nature to the zone of constant moisture content found underneath a streambed clogging layer (see Figure 17) under disconnected stream/deep water table conditions.

The presence of constant moisture content (and, therefore, constant pressure) directly below the stream and under the material interface in Figure 34 suggests that the upper layer of loamy sand acts much like a clogging layer in bringing about disconnection. To further illustrate this phenomenon, the pressure head profile along the stream centerline (x = 0.0 feet) for this case has been plotted in Figure 35.

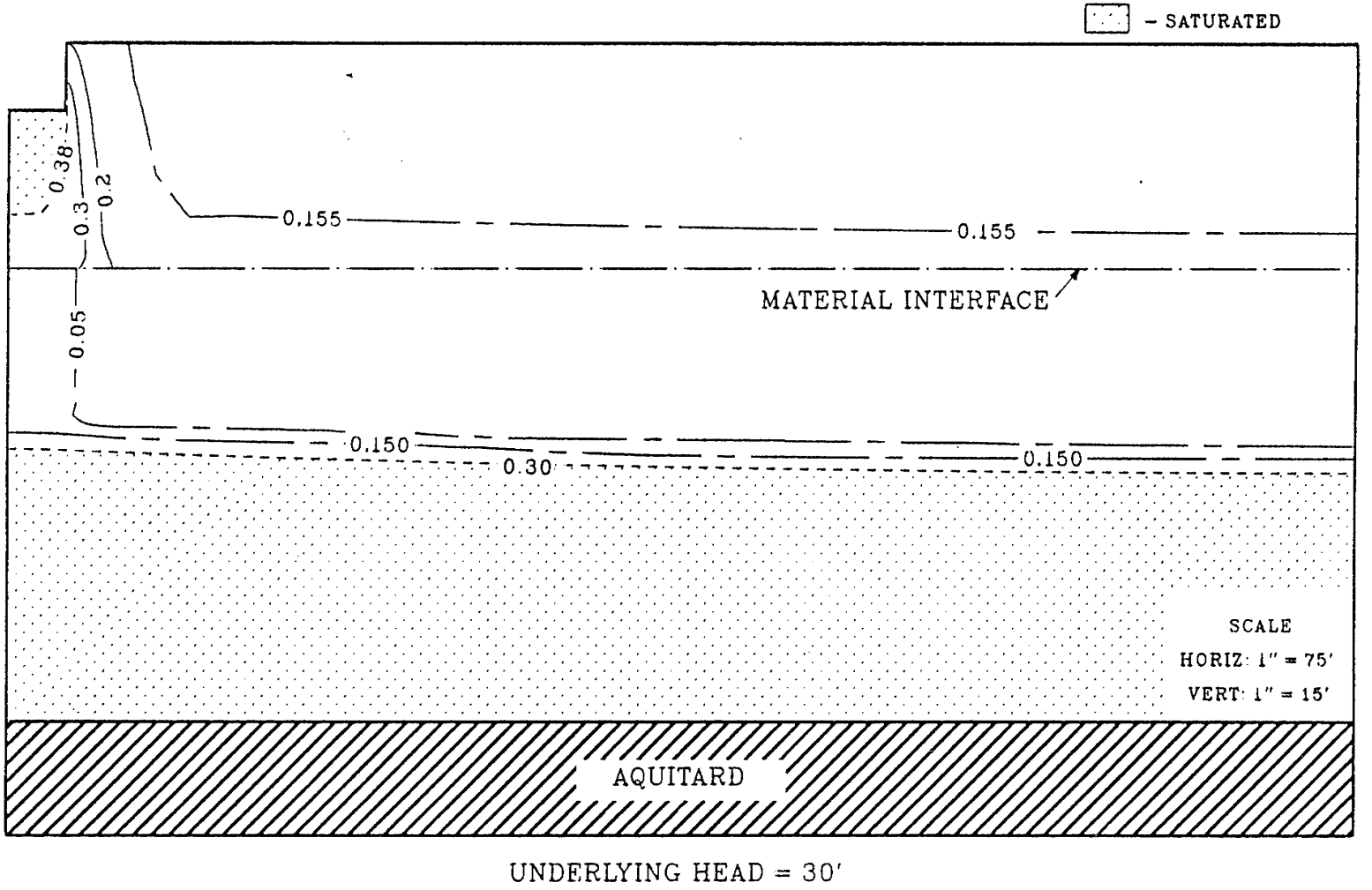

Fig. 34. Steady state moisture contents (dimensionless) in the two-layered domain for a disconnected stream with a deep water table.

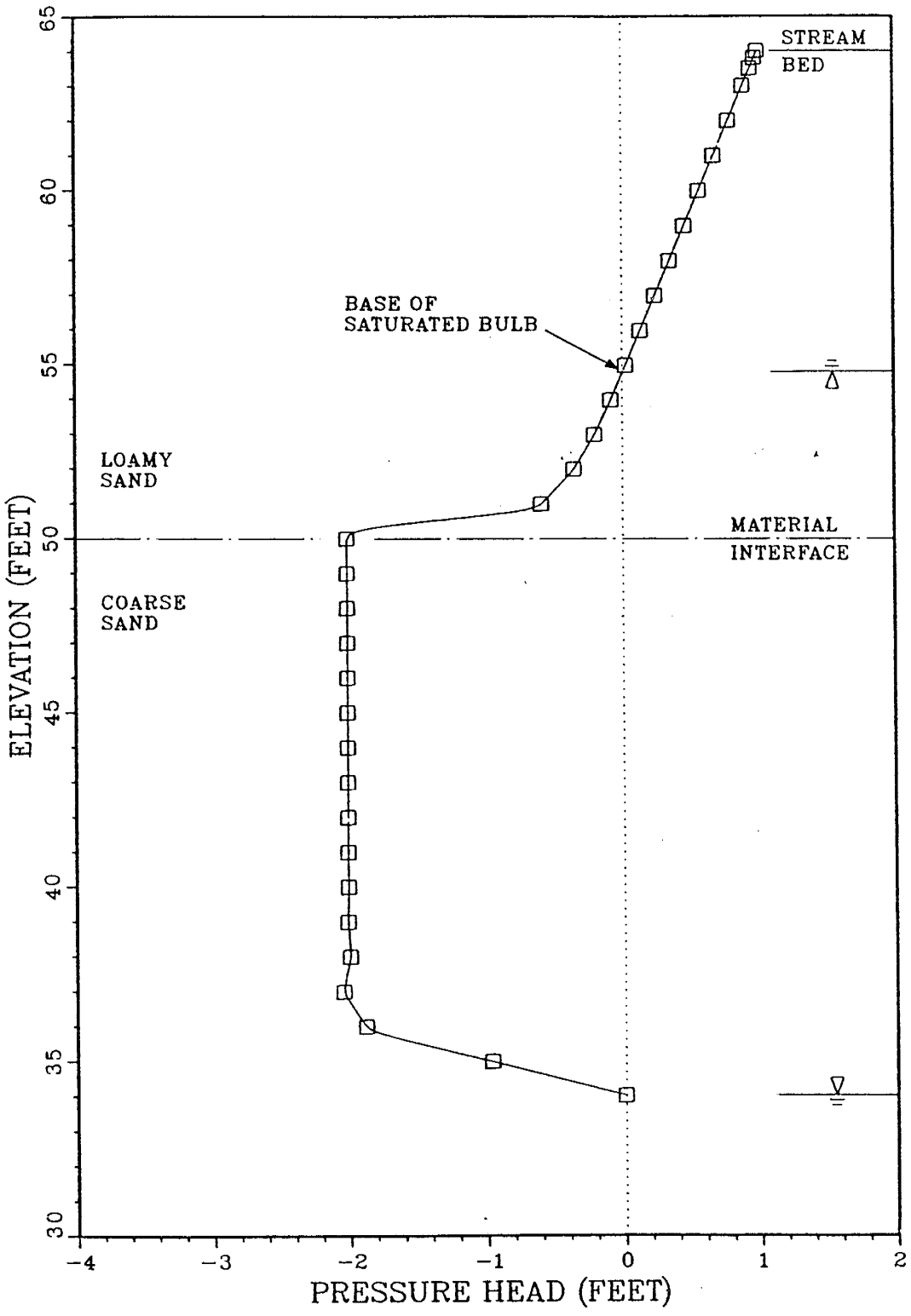

Fig. 35. Steady state, vertical pressure head profiles at x = 0.0 feet in the two-layered domain for a disconnected stream with a deep water table.

This graph looks very similar to the pressure head profile resulting from steady state, one-dimensional flow across a clogging layer under deep water table conditions (Figure 2, Chapter II). Constant pressure does exist over much of the profile below the material interface. The slight fluctuations in pressure head near an elevation of 36 to 38 feet reflect minor numerical error due to the finite element discretization scheme for this region, and do not signify any unusual physical phenomena taking place near the water table. Above the material interface and in the zone of positive pressure (i.e., saturated bulb), pressure heads decrease linearly with depth below the streambed. In the zone of negative pressures above the interface, the vertical pressure gradient is not linear, particularly within the first two feet above the interface. Unsaturated flow exists over the entire elevation range of negative pressures, since both the loamy sand and coarse sand materials exhibit zero air entry pressures (see Figure 10a).

Water table measures determined from steady state simulations with the two-layered domain provide an additional way of portraying the disconnection process as underlying heads are decreased. Figure 36 shows spatial maximum and spatial minimum water table response to declining underlying heads in the series of simulations in which interface height is 50 feet. Also plotted is the deepest point (base) of the saturated bulb, which is only observed once disconnection comes about. Note that between underlying heads of 65 and 46.5 feet, maximum water table elevation is maintained at a level of 65 feet. This happens because stream and aquifer remain connected over this range, in which case the maximum water table level is necessarily the same as the stream surface elevation. In other words, even as the beginnings of the saturated bulb are observed in the upper layer as underlying head

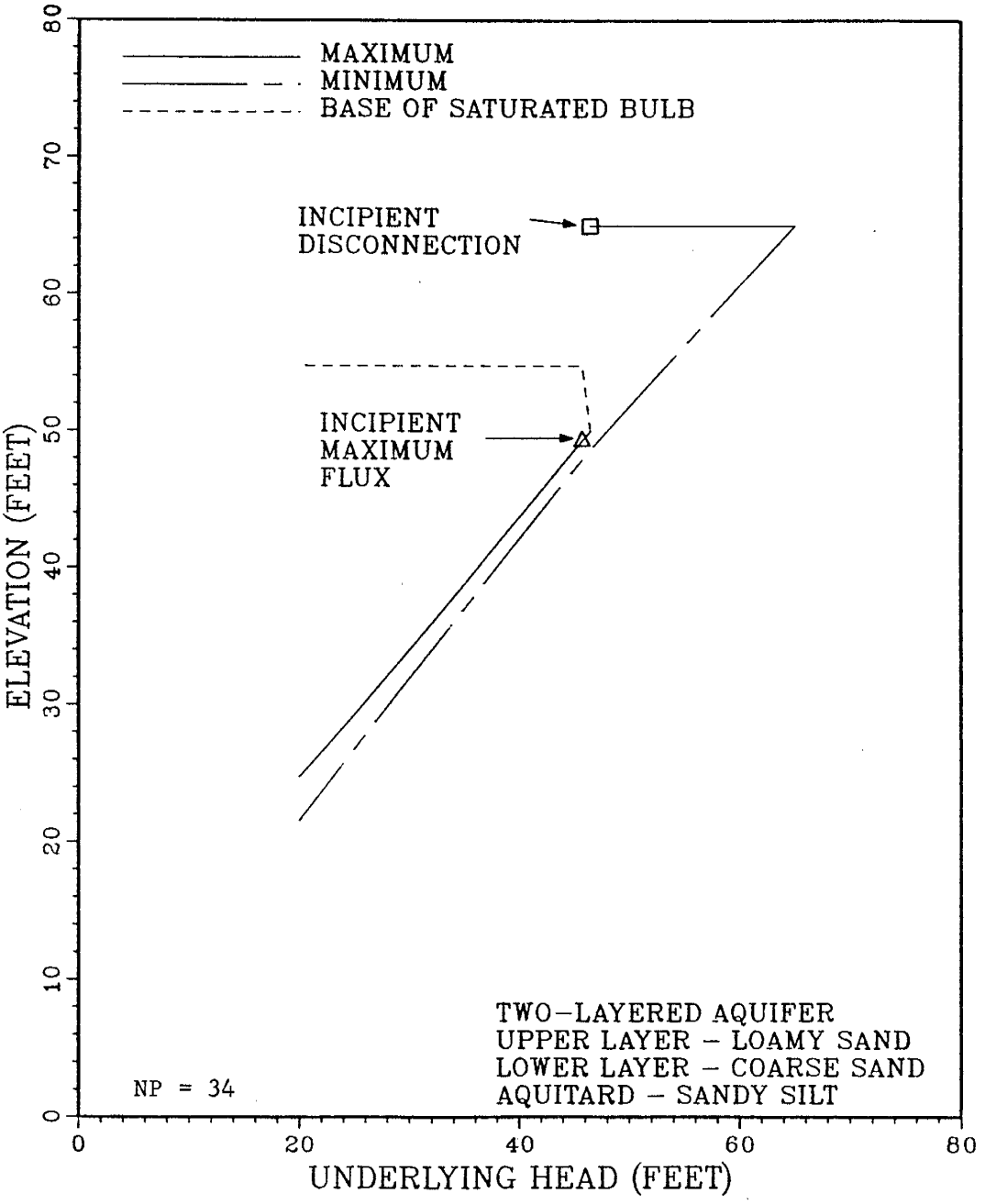

Fig. 36. Steady state, spatial maximum and minimum water table elevations, and base of saturated bulb, versus hydraulic head in the underlying aquifer (underlying head) for two-layered domain.

nears 46.5 feet (see Figure 31), the free surface (i.e., water table) consists of one continuous line. The highest point of that free surface is situated at stream surface elevation on the stream's right bank. However, at an underlying head of 46.5 feet, steady state connection can no longer be maintained and incipient disconnection takes place. The conversion from connected to disconnected conditions is abrupt (as it is in all previous analyses), and occurs at a single value of underlying head. This explains the break in the maximum water table curve near an underlying head of 46.5 feet, since, upon disconnection, the deeper free surface, and not the saturated bulb, is now considered to be the water table. Note also that the base of the saturated bulb rises rather quickly once disconnection is achieved, and is maintained at a constant elevation (~54.8 feet) after the point of incipient maximum flux.

A graph of system flux compared with underlying aquifer head for the three interface heights is given in Figure 37. As might be anticipated, the shallowest interface depth (interface height = 60 feet) causes maximum flux conditions to come about at a higher underlying head than do the deeper interface depths. Naturally, the water table drops below the material interface in the shallowest case at a higher value of underlying head than occurs with the two deeper interfaces. Accordingly, disconnection and eventual limited stream seepage, both of which appear to be caused by the interface, are brought about at a higher value of underlying head.

Figure 37 also clearly shows that the maximum flux associated with the shallowest interface is larger than the maximum fluxes occurring in the remaining two situations. This can be explained hydraulically by again viewing the upper aquifer unit (loamy sand) as acting much like a

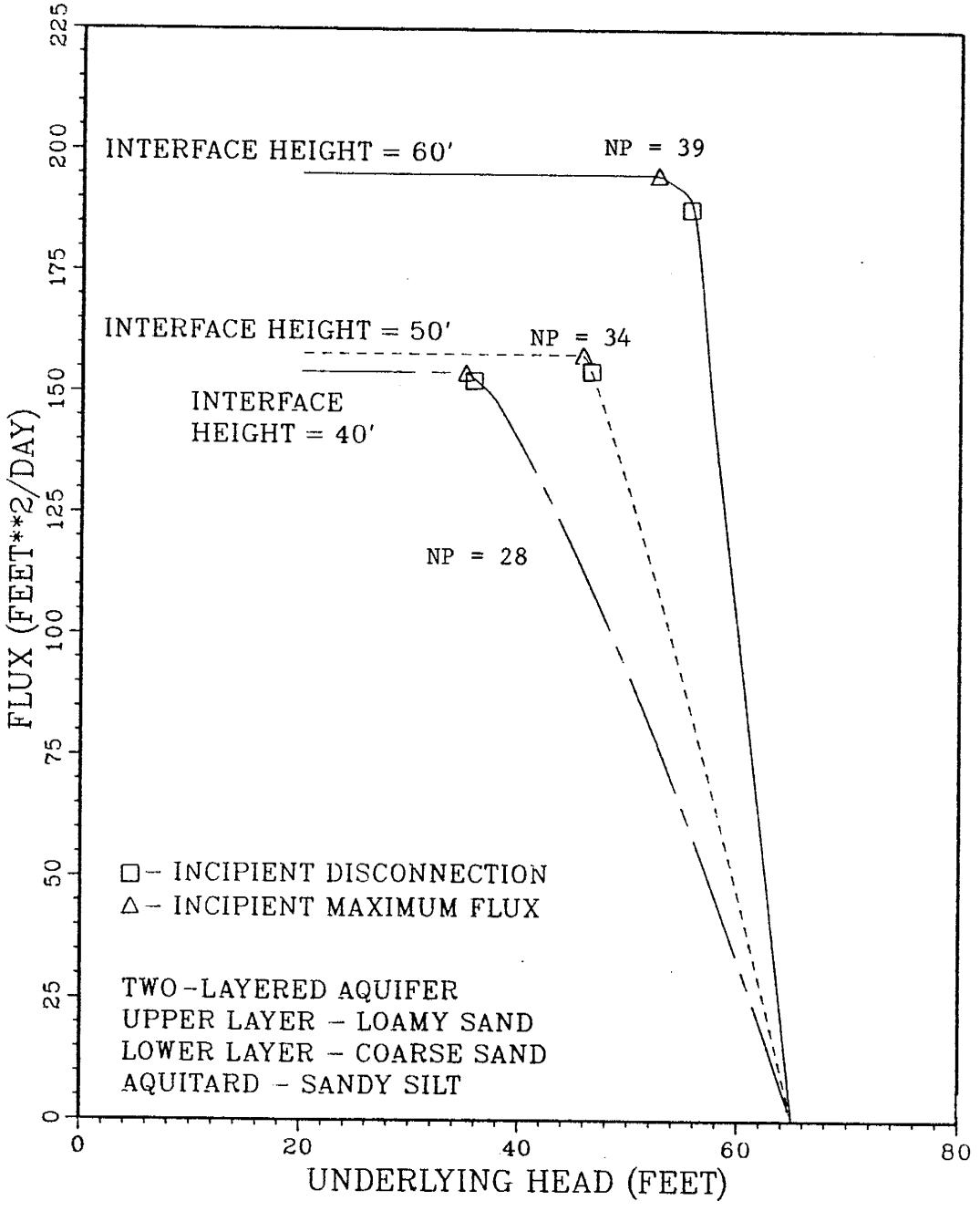

Fig. 37. Steady state system fluxes versus hydraulic head in the underlying aquifer (underlying head) in two-layered domains for three different material interface heights.

large clogging layer. As this flow retarding unit becomes thinner, the flow that moves across it becomes greater. The degree to which that flow is affected by upper unit thickness is illustrated in Figure 38, in which the maximum flux for each of the three sets of runs is plotted against depth of interface below streambed elevation. From this plot, it can be deduced that the rate of decrease of maximum flux with increasing interface depth becomes less as larger thicknesses of the upper loamy sand unit are approached. This in turn suggests that thicknesses of the upper aquifer layer might eventually become thick enough such that any additional increases in thickness would do little to further decrease maximum system flux.

The above-given results strongly infer that it is the juxtaposition of two different aquifer materials that is most influential in bringing about disconnection. Yet the question remains as to whether disconnection would have been observed anyway even if the aquifer was not layered, but consisted solely of either loamy sand or coarse sand. To answer this concern, two separate sets of steady state runs have been made using homogeneous aquifers of each of these materials while maintaining all other conditions used in the layered simulations. In neither case is disconnection achieved for the same range of underlying heads applied in the layered cases. Indeed, therefore, aquifer heterogeneity is the primary cause of disconnection in this set of analyses. Disconnection is brought about because the less uniform material comprising the upper layer is incapable of providing water at the same rate at which the deeper, more uniform material is draining water from the system.

The analyses described thus far regarding behavior in a layered stream-aquifer domain are for a specific set of domain properties.

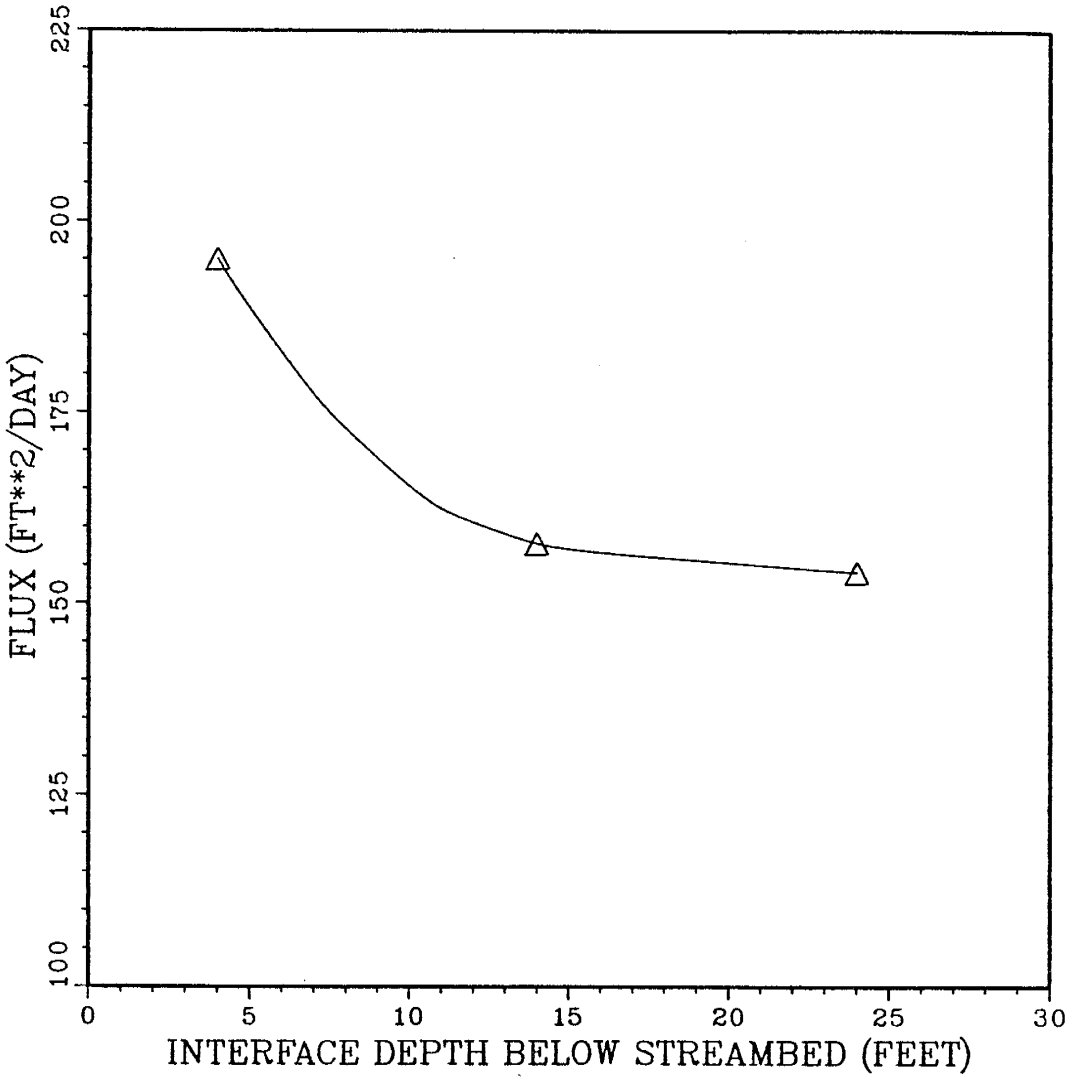

Fig. 38. Steady state system flux versus material interface depth below the streambed for two-layered domains.

However, some of the findings presented here can be used to summarize what might be generally expected of two-layered aquifer systems of the type studied here. Clearly, such systems are capable of inducing disconnection even when streambed clogging is nonexistent, or when comparable homogeneous systems are unable to exhibit disconnection. Disconnection under steady state conditions appears likely when the ambient water table drops to levels below the so-called interface that separates a shallow, texturally nonuniform soil, from a deeper, more texturally uniform aquifer material. The upper layer material, with a saturated hydraulic conductivity far less than that in the lower layer, apparently behaves something like a streambed clogging layer, by impeding flow from the stream to the deeper aquifer material. Since disconnection results when the ambient water table drops below the material interface, a system with a shallow interface undergoes disconnection at shallower water table levels than is needed in cases where the interface is deep. When the water table lies at a substantial distance below the material interface, steady state flux from the stream is limited to a maximum value. A layered aquifer system with a shallow interface exhibits maximum flux conditions at shallower water table levels than occurs in a system where the interface is deep. Furthermore, steady state maximum flux through a two-layered aquifer decreases with increasing depth of the nonuniform material comprising the upper layer.

The above general observations may have implications for general system-wide behavior of stream-aquifer domains associated with underfit streams. In actual systems, however, it is improbable that two largely homogeneous aquifer units, separated by a distinct interface, will exist. Rather, it is more feasible to divide a porous medium up into

two or more general material zones, much in the manner of Sharp (1977). Correspond- ingly, gradual "transitions" from one general material group to another, instead of a sharp interface boundary between them, will likely be observed.

Translation of findings from simple two-layered simulations to situations involving real systems that are very heterogeneous and complex is certainly questionable. However, it should be kept in mind that the overall effect of the two-tiered systems examined here has been the retardation of downward moving water that has infiltrated from a stream. Highly stratified and nonuniform materials typically found at shallow depths in aquifers associated with underfit streams also produce the same effect (recall discussion of effects of stratification, Chapter II). Therefore, there exists some rationale for using the findings from the generic, two-layered aquifer simulations to interpret, and possibly predict, processes occurring in actual aquifer systems that are roughly similar in nature.

Summary of Steady State Findings

Results from the steady state simulations discussed in this chapter have helped focus on the importance of unsaturated media on stream-aquifer processes in general. Although this work has centered around very basic situations, such as homogeneous or simple two-layered domains, and assumed symmetric flow, the findings from the the generic cases considered are pertinent to the more complex conditions found in actual systems. A summary of the analyses made in this chapter along with findings from the steady state simulations is a follows:

(1) Two-dimensional steady state simulations have been performed with a variably saturated flow code for a variety of domains, all of which consist of a stream, an aquifer and a basal aquitard. Some of the simulations take into account the

presence of a streambed clogging layer, while others are based on the assumption that this unit is absent.

(2) The steady state runs for a given domain consist of a series of sequential simulations in which hydraulic head in the aquifer underlying the basal aquitard (underlying head) is incrementally reduced. Computed heads from each simulation are used as initial input (i.e. starting conditions) in subsequent simulation based on a lower underlying head.

(3) Contour plots of total head and moisture content distribution have been prepared from a few of the simulations conducted with a "reference" simulation domain. Three stream-aquifer relationships are represented in the plots: (a) connected losing stream, (b) disconnected stream with a shallow water table, and (c) disconnected stream with a deep water table.

(4) Total head and moisture content distributions in the connected losing stream example with the reference simulation domain are relatively simple. The largest hydraulic gradients are observed near the stream, while flow conditions become closer to hydrostatic with distance from the stream. Unsaturated flow comprises a small portion of the total system flux in this case. Water in the unsaturated zone enters the saturated zone incrementally with distance from the stream.

(5) Total head distribution in the disconnected/shallow water table example with the reference simulation domain reflects larger system fluxes moving through the system than occurs in the connected stream case. The largest quantity of flow in the unsaturated zone is found in the area immediately below the stream; larger moisture content due to the large flow concentration in this area is subtly illustrated in the moisture content plot for this example.

(6) The example of a disconnected stream with a deep water table exhibits some of the hydraulic properties associated with this stream-aquifer relationship discussed in Chapter II. The presence of a constant moisture content (and, therefore, a constant pressure head) for some distance below the streambed clogging layer is apparent in a plot of moisture contents. Constant pressure with depth is also evident in a vertical profile of pressure head for this case.

(7) Graphs of steady state flux versus hydraulic head in the underlying aquifer (underlying head) have been used to help illustrate the transition of stream-aquifer systems from hydrostatic flow conditions to disconnected stream/deep water table conditions as water table levels decline. Similar graphs of spatial water table (maximum, minimum, mean) behavior are also helpful. The point demarcating the transition from a connected losing stream to a disconnected stream with a shallow water table (i.e., incipient disconnection), and the point at which disconnected stream/deep water table conditions are first observed (i.e., incipient maximum flux), have been included in the graphs.

(8) The response of system flux to decreasing underlying head in the base case simulations is essentially linear over most of the range of a connected losing stream and a disconnected stream with a shallow water table. Steady state flux shows signs of leveling off to a constant maximum value only just prior to the point of incipient maximum flux.

(9) Two separate, largely linear slopes are observed in the water table response of the reference simulation domain to declining underlying heads. The transition between the two slopes occurs just prior to incipient maximum flux, with the slope being steeper once maximum flux conditions are reached.

(10) The reference case simulations do not appropriately exhibit all facets of water table behavior that take place as underlying heads are reduced. Water table behavior from a series of simulations based on a less permeable aquifer material illustrates how spatial maximum water table response to declining underlying heads can be more complex, and how the range of underlying heads over which the various stream-aquifer relationships exists is enlarged.

(11) A graph of steady state system flux versus hydraulic head in the underlying aquifer (underlying head) from simulations involving the three aquifer materials demonstrates how aquifer material properties strongly affects system flux, both prior to the onset of maximum flux/deep water table conditions and after. Flux from a disconnected stream whose streambed is clogged cannot be determined until all properties of the stream-aquifer system have been considered, including the interrelated hydraulic conductivity-pressure head (K-ψ) characteristics of the aquifer material, and clogging layer and stream properties.

(12) A comparison of water table response of two aquifer materials to decreasing underlying heads indicates that the aquifer domain containing the less permeable material causes a larger water table level gradient than when the aquifer is more permeable.

(13) Steady state simulations with various clogging layer materials show, as expected, that increasing saturated hydraulic conductivity of the clogging layer clearly leads to larger system flux, including maximum flux.

(14) Difficulty in achieving disconnected stream/maximum flux conditions in several test simulations in homogeneous aquifers overlain by unclogged streams suggests that flow spreading by capillary forces is not always the sole cause of disconnection in actual stream-aquifer systems. Rather reduced vertical flow due to aquifer stratification appears to be an equal, if not more probable, cause of disconnection in situations where the streambed is unclogged.

(15) In homogeneous aquifers overlain by unclogged streams, the potential for disconnection, induced by capillarity alone, appears to increase as (a) the width of the stream decreases,

(b) stream stage is reduced, (c) saturated hydraulic conductivity (K_s) of the aquifer becomes lower, and (d) the depth over which homogeneity is maintained in the aquifer increases.

(16) A steady state simulation with a stream-aquifer system twice as wide as the reference simulation domain indicates that, for sufficiently wide aquifers, the maximum system flux is independent of width. Fluxes are slightly, yet consistently, larger in the wider domain during connected losing stream and disconnected stream/shallow water table phases. This happens because the additional aquitard surface provides more area across which leakage to the underlying aquifer can take place; consequently, heads on the topside of the aquitard, and water table levels, become less, thereby lowering pressure head on the underside of the clogging layer and increasing the stream loss rate.

(17) Generic simulations have been performed on a two-layered aquifer domain, in which streambed clogging is absent. The upper layer consists of a relatively nonuniform soil (loamy sand), while the lower layer is comprised of a uniform, highly permeable material (coarse sand). This layering scheme is analyzed as it is felt to be somewhat similar to the material makeup of aquifers associated with underfit streams.

(18) Contour plots of total head and moisture content taken from a few of the simulations with the layered system illustrate the process by which disconnection comes about in such systems. The early beginnings and final form of a saturated bulb found beneath the disconnected (and unclogged) stream are depicted. In all of the simulations included in the contour plots, unsaturated flow in the upper layer is observed to be quite significant, even during the connected losing stream phase.

(19) Disconnection in a two-layered domain, with a less permeable (saturated) material overlying a more permeable one, seems to take place because the upper layer acts much like a large clogging layer. Moisture content and pressure head plots for disconnected stream/maximum flux conditions illustrate that a zone of constant pressure exists directly beneath the stream and under the material interface between the two layers. The effect is similar to pressure head profiles displayed for one-dimensional, steady state flow across a clogging layer under deep water table conditions (see Figure 2, Chapter II).

(20) In a two-layered system, the conversion from connected losing stream conditions to a disconnected stream as heads in the underlying aquifer are reduced is an abrupt process. As in the simulations with homogeneous aquifer domains, the conversion to disconnection takes place at a single value of underlying head. Water table measures manifest the abruptness in that (a) spatial maximum water table level equals the stream surface elevation during the entire connected losing stream phase, up to and including the point of incipient disconnection; after which, (b) the new maximum

water table level exists entirely in the lower layer, and is considered separate of the saturated bulb in the upper layer.

(21) The effect of material interface location (and, therefore of variable upper layer thickness) on fluxes in a two-layered system has also been examined. Results from runs based on three different heights of the material interface indicate that (a) for a given underlying head, steady state flux decreases with increasing thickness of the upper layer, (b) a system with a shallow interface undergoes disconnection at shallower water table levels than is needed in cases where the interface is deep, and (c) a system with a shallow interface exhibits maximum flux conditions at shallower water table levels than occurs in a system where the interface is deep.

(22) Disconnection in the layered domain simulations is most directly attributable to the presence of a texturally nonuniform aquifer material overlying a much more texturally uniform material, and is effectively independent of any other influential parameters. Additional simulations with homogeneous aquifers comprised of either of the aquifer materials used in the layered domains, and with all other simulation conditions remaining the same, fails to result in disconnection.

IX. TRANSIENT ANALYSES

Transient simulations are performed mostly in the interest of analyzing temporal changes in subsurface flow during seasonal changes of stream flow. Stream stage is the only boundary condition changed with time during each transient simulation, while the uniform underlying aquifer head assigned to the base of the aquitard is maintained at a constant value. Subsequent to the transient simulations, an approximate analysis is made of the long-term effects of declining regional groundwater levels on local stream-aquifer systems.

A total of three separate transient simulations have been performed. Two of these are conducted with the reference simulation domain illustrated in Figure 8. The third has been made with the two-layer stratified domain shown in Figure 28 (material interface height = 50'). The third case is, therefore, more representative of aquifer material trends in fluvial systems associated with underfit streams. The two transient runs with the base simulation domain are made, respectively, for a shallow water table case and for a situation involving a deep water table. The transient simulation made with the layered domain is based on deep water table conditions. All of the runs have been selected on the basis that unsaturated flow is expected to show significant influence in each. Parameters describing the three simulations are listed in Table 4.

Stream stages are changed over the course of a year such that the mean annual stage is 1 foot; i.e., mean annual stage is equal to the stage used in the steady state simulations with the reference and layered domains. Accordingly, results from the corresponding steady

TABLE 4

Transient Simulation Descriptors

Simulation Number	Domain Dimensions	Domain Materials	Hydraulic Head in Underlying Aquifer
1	See Figure 8	Aquifer - medium sand Aquitard - silt loam Clogging layer - clay loam	60 feet
2	See Figure 8	Aquifer - medium sand Aquitard - silt loam Clogging layer - clay loam	20 feet
3	See Figure 8 and Figure 28	Two layered aquifer Upper layer - loamy sand Lower layer - coarse sand Material interface height = 50 feet Aquitard - sandy silt No clogging layer	20 feet

state simulation for a given set of system properties and underlying head are always used as starting conditions in a transient run.

In keeping with the intent to base the simulations on Mesilla Valley conditions, seasonal fluctuations in stream flow (and, consequently, stream stage) are loosely patterned after generally observed flow conditions on the surface waterways found in this region. In generating the stream flows, the 50-foot wide channel (25-foot half-width) of Figure 8 (and Figure 28) is assumed to have a bed slope of 4.5 feet per mile. Assuming uniform channel flow and a streambed roughness coefficient of 0.030, Manning's equation (e.g., Chow, 1959) is used to determine flows during each month of the year. The resulting monthly breakdown of stream discharges (in cubic feet per second) and associated stages is presented in Table 5.

The flows given in Table 5 tend to reflect typical flows observed on some of the major irrigation canals in the Mesilla Valley. The listed stages, however, probably differ from those observed on some reaches of the canals. Actual stream stages on these waterways are often affected by backwater profiles created by damming of flow at diversion structures. Consequently, depths of flow in these areas are usually larger, and fluctuate less, than occurs under uniform flow conditions. It follows, therefore, that the transient simulations are probably more representative of stream reaches located upstream of zones heavily affected by backwater conditions.

The flow distribution given in Table 5 is somewhat representative of a surface water system that is regulated for irrigation purposes. Natural, non-regulated stream systems will show significantly different patterns than those assumed here. Average monthly distributions of stream flow will also vary, depending on climate, geographical

TABLE 5

Mean Monthly Discharges and Stages,
50-Foot Wide Rectangular Channel

Month	Mean Flow (cfs)	Stage (feet)
October	14.09	0.376
November	8.45	0.277
December	8.45	0.277
January	8.45	0.277
February	8.45	0.277
March	63.24	1.673
April	101.41	1.250
May	101.41	1.250
June	163.24	1.673
July	191.67	1.847
August	191.67	1.847
September	70.43	1.000

location, regional hydrology, and other factors.

In the transient simulations, each change in stream stage is assumed to be instantaneous. In other words, no mechanism is utilized such that the change takes place gradually with time. This approach, although somewhat unrealistic, is taken primarily because it is simple to implement in the variably saturated flow code. It is recommended in future transient analyses that stream stages be changed gradually.

Total simulation time for each transient run is two years. Stream stages listed in Table 5 are employed during both years. As will be demonstrated later, response times of the domains used in the three transient simulations are relatively quick. Indeed, all of the simulations have shown that transient results at the end of the first and second years are virtually identical. Therefore, any effects of the assumed starting conditions at the beginning of the first year are erased by the time the second year of simulation begins. This not only indicates that each stream-aquifer system exists in a state of dynamic equilibrium, but also provides some justification for assuming steady state results to be representative of average flow conditions during a year. Only second year results are utilized to analyze seasonal stream-aquifer behavior.

Simulation years coincide with water years, which begin at the start of October and extend through the following September. This approach is felt to be appropriate in two ways:

(1) stream discharge is commonly reported by water year; thus, it is often convenient for hydrologists and irrigation specialists to think in terms of water years, and

(2) stream stage during September is 1 foot, which is identical to the mean annual stage used in the corresponding steady state simulations. Consequently, the assumed initial conditions for a transient run, taken from a corresponding steady state simulation, are expected to be similar to those that would have normally been seen at the beginning of October during the first simulation year. It is hoped,

therefore, that any bias imposed on the transient simulations by the assumed initial conditions is minimized.

Numerical Observations

In the course of conducting the transient runs, it has been found that SATURN'S ability to handle the variety of conditions encountered is strongly affected by the equation solving scheme being implemented. Observations of this regard are similar to those made during the steady state analyses.

Although the transient simulations have generally not been hampered by as many obstacles as experienced with the steady state runs, the Newton-Raphson iteration scheme has been found to be an essential tool for obtaining accurate temporal solutions in a reasonable fashion. As in steady state cases, this algorithm is particularly beneficial in situations in which the water table is located several feet below streambed level (e.g., Transient Simulations 2 and 3). In these instances, the Picard iteration scheme converges to a solution; however, continuous use of extremely small time steps (5 minutes and less) is often required to achieve model convergence. Using such short time steps over numerous portions of a two-year simulation leads to unacceptable consumption of CPU time. With the Newton-Raphson solver, however, model convergence is achieved using time steps that are continually increased during each period associated with a single stream stage. Individual time intervals exceeding ten days are common.

This result further illustrates the importance that needs to be placed on nonlinear solution algorithms in variably saturated flow codes. Unlike the steady state simulations, temporal solutions for domains with deep water tables are at least physically possible in

SATURN using Picard iteration. However, the exorbitant computer times required for solving long-duration problems with a Picard scheme appears to make this procedure very unattractive. Despite the fact that Newton-Raphson iteration requires more computer memory than the Picard scheme, utilization of large time steps clearly affords an obvious reduction in computer expense.

Temporal Response of the Reference Simulation Domain

Much like the steady state analyses, influence of unsaturated media on transient phenomena in a stream-aquifer system can be assessed via general system measures, such as fluxes and water table levels. In addition to further emphasizing many of the findings derived from the steady state simulations, transient model runs have allowed the author to evaluate the effect of variable stream stage on these system measures.

A graph of second year system inflow (stream seepage) and outflow (aquitard leakage) from Transient Simulation 1 is presented in Figure 39a. A plot of corresponding water table measures is shown in Figure 39b. Both of these plots depict response of a shallow water table system. The deep water table equivalents to these graphs (i.e., from Transient Simulation 2) are given in Figures 40a and 40b, respectively. To assist in the interpretation of the graphs, a plot of monthly stream stages is included in each set of figures. All of the curves in these figures have been prepared by connecting data points at all simulation times with straight line segments. The data points in these graphs, as well as in all remaining figures in this chapter are too numerous to illustrate. Similarities and differences between the Transient Simulations 1 and 2 are mentioned in the following paragraphs.

SATURN using Picard iteration. However, the exorbitant computer times required for solving long-duration problems with a Picard scheme appears to make this procedure very unattractive. Despite the fact that Newton-Raphson iteration requires more computer memory than the Picard scheme, utilization of large time steps clearly affords an obvious reduction in computer expense.

Temporal Response of the Reference Simulation Domain

Much like the steady state analyses, influence of unsaturated media on transient phenomena in a stream-aquifer system can be assessed via general system measures, such as fluxes and water table levels. In addition to further emphasizing many of the findings derived from the steady state simulations, transient model runs have allowed the author to evaluate the effect of variable stream stage on these system measures.

A graph of second year system inflow (stream seepage) and outflow (aquitard leakage) from Transient Simulation 1 is presented in Figure 39a. A plot of corresponding water table measures is shown in Figure 39b. Both of these plots depict response of a shallow water table system. The deep water table equivalents to these graphs (i.e., from Transient Simulation 2) are given in Figures 40a and 40b, respectively. To assist in the interpretation of the graphs, a plot of monthly stream stages is included in each set of figures. All of the curves in these figures have been prepared by connecting data points at all simulation times with straight line segments. The data points in these graphs, as well as in all remaining figures in this chapter are too numerous to illustrate. Similarities and differences between the Transient Simulations 1 and 2 are mentioned in the following paragraphs.

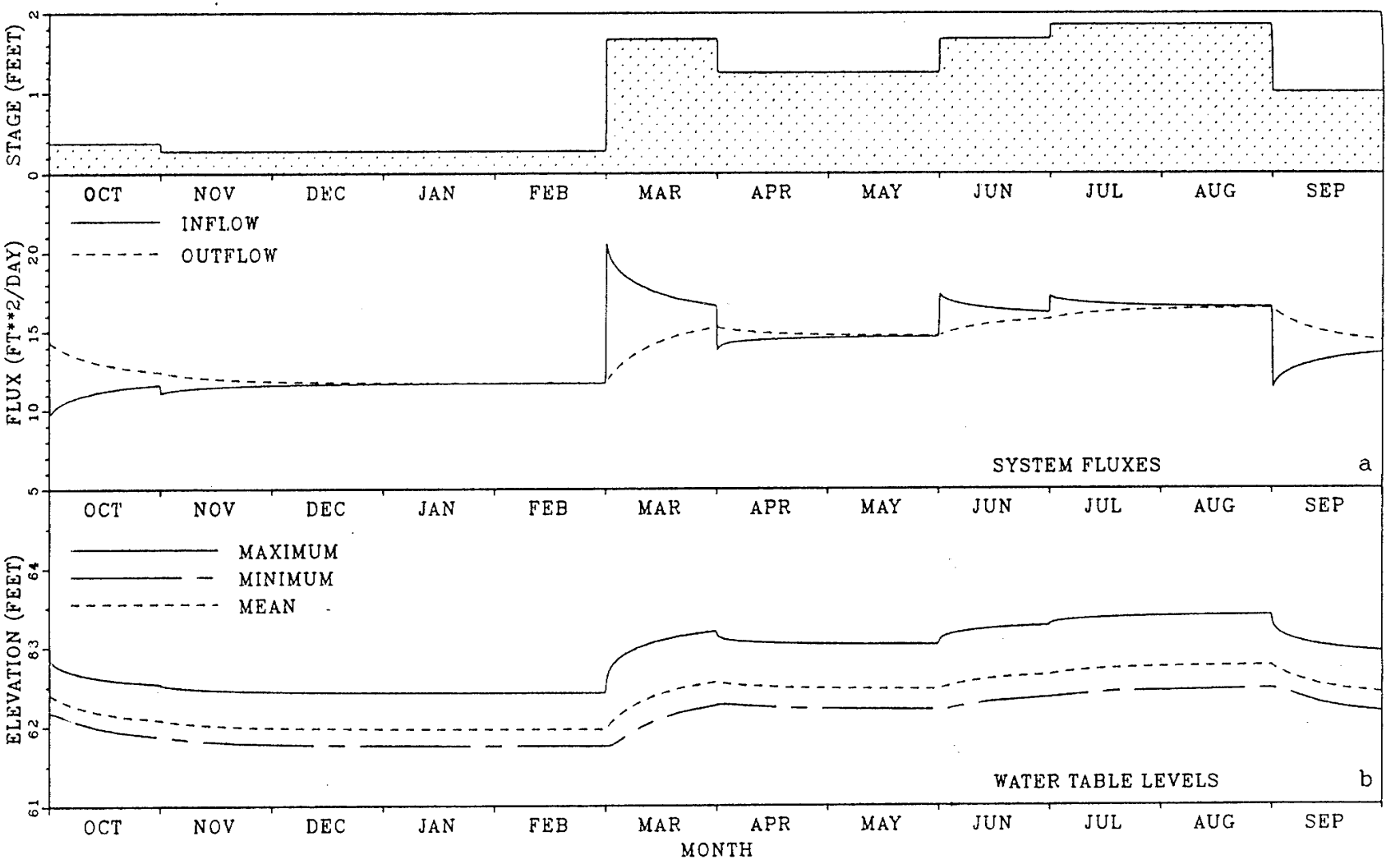

Fig. 39. Transient system response of the reference simulation domain to seasonal changes in stream stage for a disconnected stream wtih a shallow water table: (a) system fluxes and (b) water table levels.

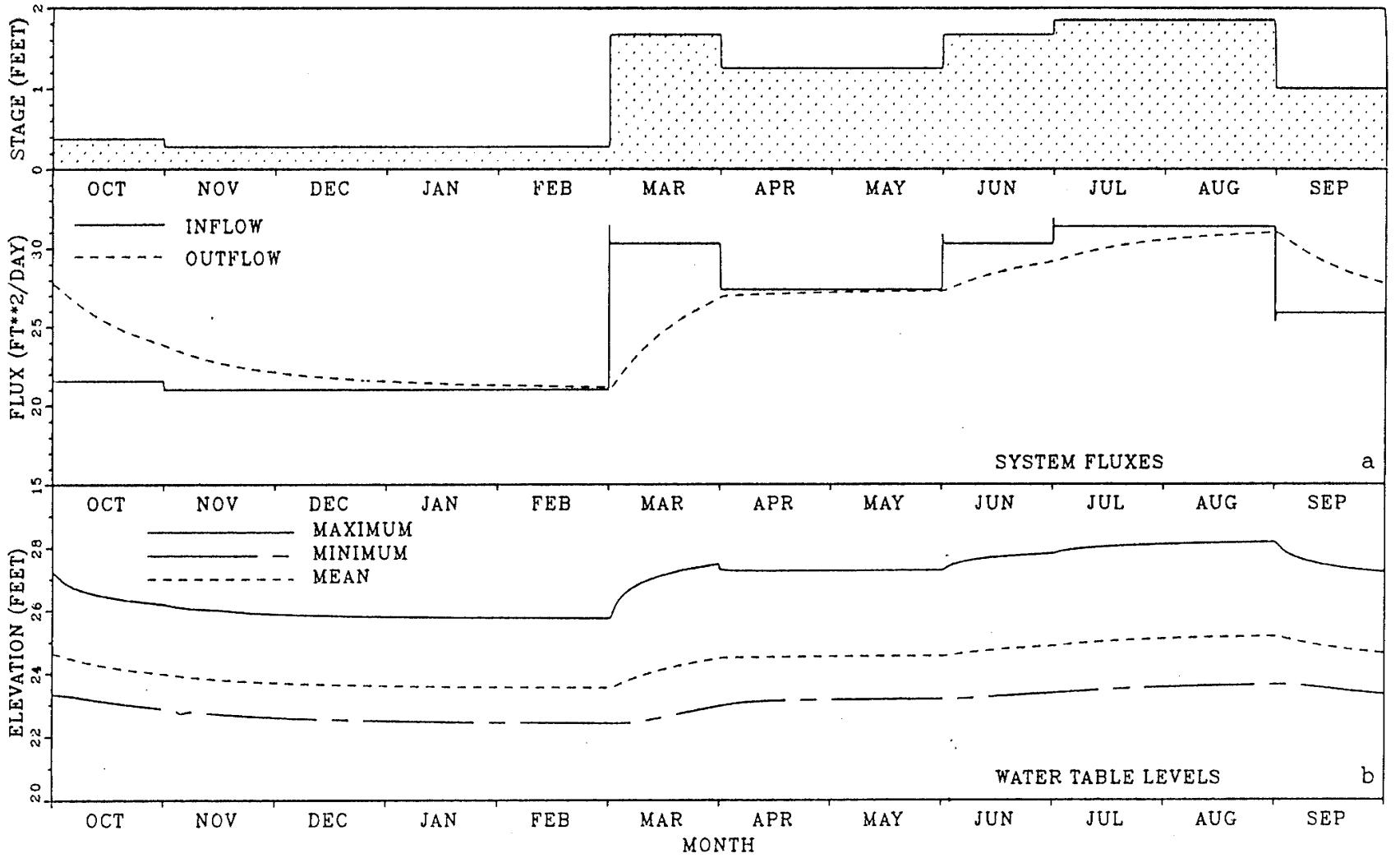

Fig. 40. Transient system response of the reference simulation domain to seasonal changes in stream stage for a disconnected stream with a deep water table: (a) system fluxes and (b) water table levels.

One of the most apparent features of the time sequences presented in Figures 39a and 39b, and Figures 40a and 40b, is the relatively quick response of the stream-aquifer domain to changes in stream stage. This rapid response is partly evidenced by the ability of inflow and outflow rates to reach common equilibrium values within relatively short times after a change in stage has taken place. Although equilibrium is not reached within a month of any of the stage variations, conditions closely approximating steady state do appear to occur when the system is given at least two months (i.e., April-May, July-August) to respond. This is generally the case for both simulations using the reference domain. However, time needed to reach steady state in the deep water table simulation (Transient Simulation 2) is somewhat longer. This is partly due to the fact that differences between inflow and outflow at the beginning of a new stage interval are commonly larger for this case than in the shallow water table sequence (Transient Simulation 1). In other words, it takes longer for such widely varying fluxes to approach a common equilibrium value. However, a more likely cause of the less rapid response in the deep water table example is the presence of a much larger unsaturated zone. Lower hydraulic conductivities and moisture contents associated with unsaturated media signify larger time constants for this case. Both runs appear to exhibit steady state conditions at the end of the four-month low flow period extending from the beginning of November to the end of February. The relatively short time constants indicated by both Transient Simulation 1 and Transient Simulation 2 are not surprising, given the somewhat small dimensions (aquifer depth = 60 feet, width = 600 feet) of the flow domain.

As shown in Figure 39b, the spatial maximum water table level during the shallow water table run often approaches the elevation of the base of the clogging layer (63.8 feet), yet always falls short of this mark. In addition, the lowest elevation of the maximum water table level, which occurs at the end of February, is only 1.4 feet below the clogging layer's underside. Clearly, disconnection prevails throughout the year, but water table levels are always shallow. Such conditions are identical to what has previously been described as a disconnected stream with a shallow water table. In this instance, water table level is expected to influence stream infiltration rates.

Figure 39a suggests that increases in stream seepage induced by a raise in stream stage are immediately followed by a decrease in the stream loss rate. Likewise, system inflows that are immediately reduced by stage reductions are quickly followed by an increase in the inflow rate. Such observations are explained by hydraulic processes occurring in the unsaturated soils located immediately below the clogging layer. These phenomena can be described by analyzing, for example, pressure heads below the clogging layer as stream stage undergoes a large increase in the beginning of March. Just prior to this time, the system exists in a virtual steady state, with pressures below the clogging layer, and, consequently, the inflow rate being controlled by an equilibrium water table profile. Upon raising depth of flow in the stream, the concomitant increase of flow across the thin clogging layer almost immediately begins to contribute additional water to the unsaturated materials found beneath it. As moisture contents increase, pressure heads in the unsaturated zone become less negative. As a result, the head differential across the clogging layer is quickly reduced. Accordingly, stream loss rates begin dropping from the

initial high value. Furthermore, after the pressure front created by the increased inflow has reached the water table (usually within seconds to a few minutes), the rising phreatic surface then begins to affect pressures in the unsaturated zone above it. The effect is that pressure heads and moisture contents on the underside of the clogging layer begin to increase. A natural consequence of the gradually rising water table, therefore, is that inflow rates also continue to gradually decline.

The opposite effect occurs after a decrease in stream stage. In other words, at the moment the stage is first lowered, the stream infiltration rate drops instantaneously. But this reduced rate of infiltration causes pressure heads on the underside of the clogging layer to drop. Conse- quently, the stream seepage rate then begins to increase. And, as in the example when stream stage is increased, the pressure pulse stemming from the reduction in stage soon reaches the water table. The water table begins to drop due to the decreased inflow rate, which further causes reduction of pressure beneath the clogging layer. Accordingly, as the water table gradually drops, the stream loss rate gradually increases.

In contrast to the gradual response of stream seepage in shallow water table instances, the deep water table run (Transient Simulation 2) shows that initially enlarged infiltration rates caused by a stage increase drop very rapidly to a constant steady value (Figure 40a). The steady infiltration rate results from the aquifer material's ability to quickly establish a zone of constant pressure (and moisture content) just below the clogging layer. In this instance, water table levels are not rapidly affected by the incoming additional water. In fact, there is some delay between the time at which stage is initially

raised and the time at which the pressure pulse created by the increased seepage first reaches the phreatic surface. Even after the water table begins to rise in response to the incoming water (Figure 40b), it has no effect on stream seepage, as it is still too deep to influence pressure heads near streambed level. This situation is akin to, what was described in terms of steady state flow in Chapter II, a disconnected stream with a deep water table.

Some of the above-described temporal phenomena in the deep water table simulation are not clearly depicted in the time sequence of Figures 40a and 40b. Constant inflow over most of the duration of a period of constant stage is apparent, yet the initial changes in inflow after a stage change usually show up as small spikes in the inflow curve. Moreover, the large time scale of Figures 40a and 40b makes it difficult to discern the time lag that occurs between initial changes in stream loss rate and concomitant effects on water table elevation. In the interest of providing a better illustration of these phenomena, system fluxes and water table levels have been plotted over the first two days of March, the same period used in a previous example for the purpose of describing system response to a large increase in stream stage. The resulting graphs are shown in Figure 41a and 41b.

As can be seen in Figure 41a, time needed for the stream seepage to be reduced from its initially high value to a relatively constant rate is on the order of 0.2 days ($\approx$288 minutes). The response of system outlfow via aquitard leakage is considerably slower, with nearly a full day passing before any significant increase in outflow is observed. This effect can be largely explained by the corresponding water table time sequence, since water table elevations are an approximate indicator of the heads occurring just above the aquitard.

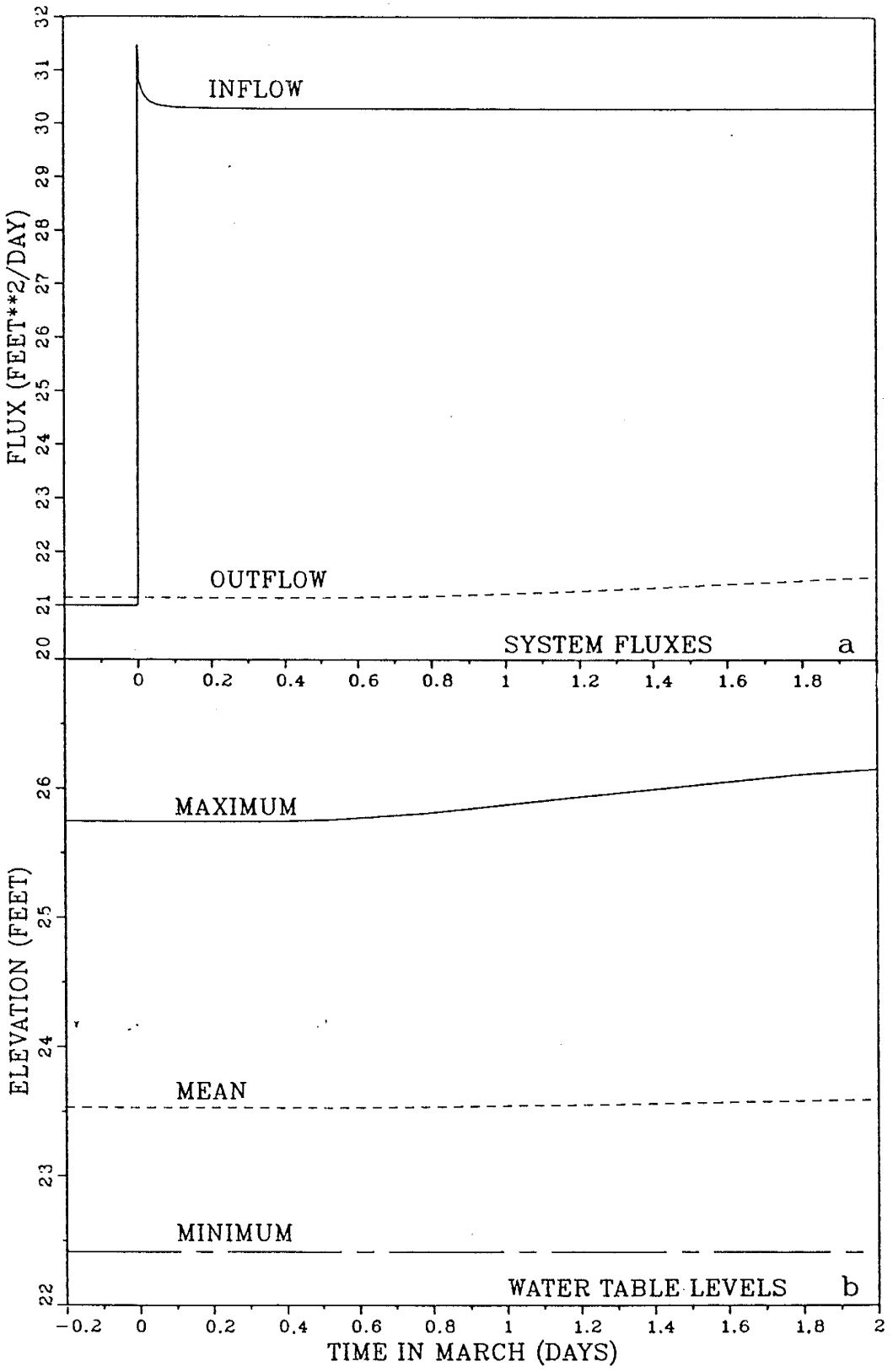

Fig. 41. System response of the reference simulation domain during the first two days in March for a disconnected stream with a deep water table: (a) system fluxes and (b) water table levels.

Inspection of Figure 41b indicates that about 0.5 day (720 minutes) elapses before the maximum water table level begins to rise. This, therefore, is the time it takes for the effect of increased seepage to first show its effects on the deeper saturated zones. Even after the incipient water table rise takes place, an additional 0.6 day (~860 minutes) to 0.8 day (~1150 minutes) of continued infiltration is necessary before the mean water table elevation shows signs of significant increase (at about 1.1 to 1.3 days total time). Of even greater interest is the fact that the minimum water table level on the right domain boundary is not affected at all within two days of the increase in stage. Assuming that water table heights are somewhat representative of hydraulic heads on the topside of the aquitard, it is easy to understand why aquitard leakage responds more slowly than stream seepage to stream stage variations. Such disparate response times of the system fluxes is generally expected since stream stage is the only boundary condition that is varied over the course of the transient simulations.

The time delay of approximately 0.5 days between initially increased infiltration and subsequent recharge of the water table in the foregoing example is certainly a matter of concern when modeling transient systems in which system stresses change within hours to a few days. However, this time span can be considered relatively short when simulating domains wherein the stresses change less frequently. In the simulations described in this chapter, in which stream stage is assumed constant for durations of a month or more, it is likely that the times associated with transmission of pressure pulses across the unsaturated zone below the stream have little influence on the seasonal response of a stream-aquifer system.

Response of Layered Domain

Time sequences of system flow and water table elevations for Transient Simulation 3 are presented, respectively, in Figures 42a and 42b. These graphs exemplify system behavior for a domain that has been drained to a great extent by leakage to an underlying aquifer (hydraulic head in underlying aquifer = 20 feet) that is undergoing heavy pumpage. Ambient water table levels are quite deep in this case, and are located significant distances below the material interface between the two layers of material comprising the aquifer. As there is no streambed clogging layer in the layered domain, there exists a second zone of saturation, other than that located beneath the water table. This zone, described earlier as a saturated bulb, exists mostly beneath the stream and entirely within the upper aquifer layer. Distances separating the water table from the saturated bulb are of sufficient magnitude such that fluctuations in the water table have no effect on stream loss rates.

Of some interest is the fact that system response in Transient Simulation 3 is much faster than in either of the two previous model runs using the reference simulation domain. In other words, equilibrium appears to be reached at the end of each period associated with a single stream stage (see Figures 42a and 42b). This occurs even in those periods with one-month durations after major changes in stage (i.e., March, September) have taken place. It is not immediately obvious why equilibrium comes about so quickly in this instance, since a great portion of the domain and flow within it in this instance is unsaturated. It is likely that the short response times are partly due to saturated flow within the coarse sand (K_s = 800 feet/day). Yet, it is also probable that the overall quick system response is partly

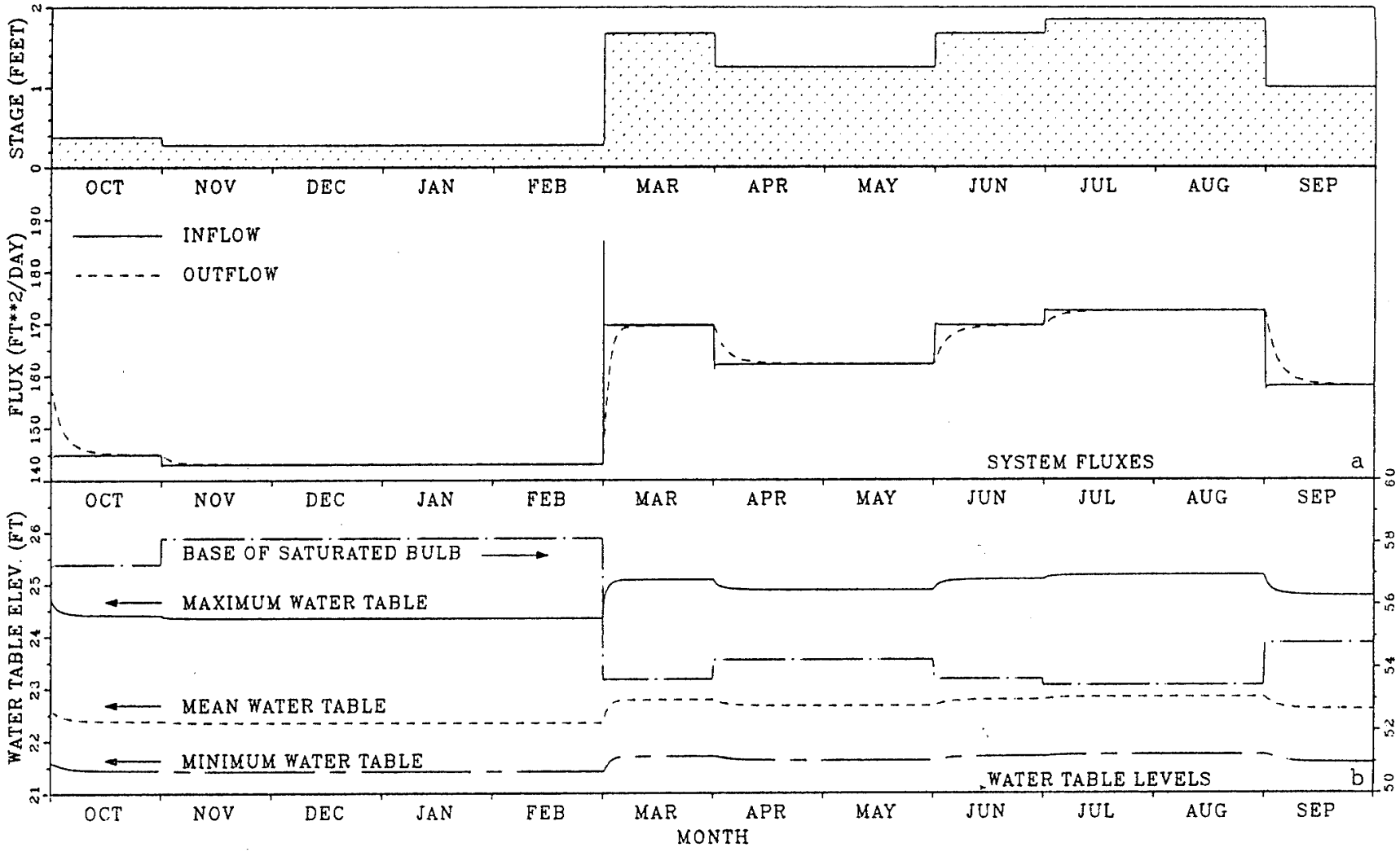

Fig. 42. Transient system response of the two-layered domain to seasonal changes in stream stage for a disconnected stream with a deep water table: (a) system fluxes and (b) water table levels.

attributable to the relatively large flows moving through the stream-aquifer system in this case. As Figure 42a indicates, both inflow and outflow are several times larger than comparable fluxes observed during the transient runs with the reference simulation domain (see Figures 39a and 39b). Such high flows help to speed up the transmission of stresses brought on by stream fluctuations in two ways:

(1) Larger stream loss rates cause the saturated bulb beneath the stream to penetrate deeper into the upper aquifer layer. A saturated bulb of significant vertical extent provides a longer saturated flow path in the upper layer, which in turn means that downward transmission of a pressure pulse through the upper system is generally more rapid. This phenomenon might perhaps be better understood by comparing the saturated hydraulic conductivity of the upper layer material (loamy sand) in Transient Simulation 3 with the comparable unsaturated hydraulic conductivities of the medium sand beneath the stream during Transient Simulation 2. Indeed, negative pressure heads on the underside of the clogging layer at several times during Transient Simulation 2 indicate that the hydraulic conductivity of the unsaturated medium sand hovers near a value of 1 foot per day. On the other hand, the saturated hydraulic conductivity of the loamy sand in Transient Simulation 3 is 5 feet per day. Moreover, since system response usually speeds up with increasing moisture content, loamy sand materials within the saturated bulb of Transient Simulation 3 are expected to transmit pressure pulses quicker (see moisture characteristic curves, Figure 10a).

(2) Larger flows also help to keep suction heads in the unsaturated zone between the saturated bulb and the underlying water table to relatively low values. Consequently, hydraulic conductivities in these unsaturated areas, especially within the coarse sand layer, tend to remain high (6-8 ft/day in the coarse sand) relative to those in the medium sand (~1 ft/day) of Transient Simulation 2.

Flow behavior in the deep water table simulation using the layered domain (Transient Simulation 3) is in some ways similar to its counterpart for the reference domain (Transient Simulation 2). As in the non-layered case, system inflow stabilizes soon after stream change undergoes a change (Figure 42a). In other words, flow conditions in the zone below the stream are such that a local equilibrium is quickly

reached. And, much in manner of Transient Simulation 2, the response of system outflow is much more gradual.

As mentioned before, the vertical extent of the saturated bulb in Transient Simulation 3 fluctuates with changes in system flux. To better illustrate this, the elevation of the deepest point of the saturated bulb over time has been included in the graph of water table behavior in Figure 42b. As expected, the bulb expands to greater depths during periods of high flow and contracts to shallower depths when the flow has decreased. Figure 42b suggests that the saturated bulb's vertical extent stabilizes soon after a change in stage has taken place. This behavior is similar to that of the stream seepage rate, and is an additional indicator of the speed with which flow conditions in shallower depths near the stream channel become relatively constant.

Water table measures behave quite differently from the base of the saturated bulb. During large inflow periods, water table elevations increase; accordingly, as flows decline, so does the water table. Figure 42b shows that water table levels, especially the minimum level, respond much more gradually to changes in stream stage than does the saturated bulb.

Long-Term Response

The fact that each stream-aquifer system analyzed in this chapter exists in a state of dynamic equilibrium suggests that the long-term behavior of the systems can be roughly ascertained through examination of a series of "quasi-equilibrium" states. In particular, the temporal response of the stream-aquifer domains can be studied as heads in the aquifer underlying each domain are gradually lowered. Such reductions

in underlying head would be analogous to the gradual decline in regional groundwater levels expected to occur in the Mesilla Valley (e.g., Peterson et al., 1984) in the event proposed pumping schemes for the Mesilla Bolson are implemented. Since the time constants of the local stream-aquifer systems are quite short, such long-term analyses can be approximately made by simply piecing together steady state simulation results for various values of underlying head. Consequently, expensive transient simulations spanning several years are not necessary. As has been the case in all previous transient analyses, stream stage in each of the steady state simulations used to make these long-term analyses is set equal to the mean annual stage of the respective stream-aquifer system.

Applying this concept of successive "quasi-equilibrium" states, the temporal behavior of the base simulation domain and the two-layered domain (material interface height = 50 feet) has been examined for a 100-year period of progressively declining regional groundwater levels. As before, mean annual stream stage is assumed to always be 1 foot. Underlying heads are decreased linearly from 65 feet to 20 feet during the 100-year period. This drop of 45 feet is similar to regional groundwater level declines predicted by Peterson et al. (1984) for some areas of the Mesilla Valley based on proposed future pumping schemes.

Long-term response of mean annual system flux and the spatial mean water table elevation in the reference simulation domain is presented in Figure 43, along with the assumed gradual decline in heads in the underlying aquifer. Hydrostatic conditions are assumed to exist at the start of the analysis. Incipient disconnection takes place at an elapsed time of about 6 years. Incipient maximum flux conditions are not observed until several years later (total time ~27 years),

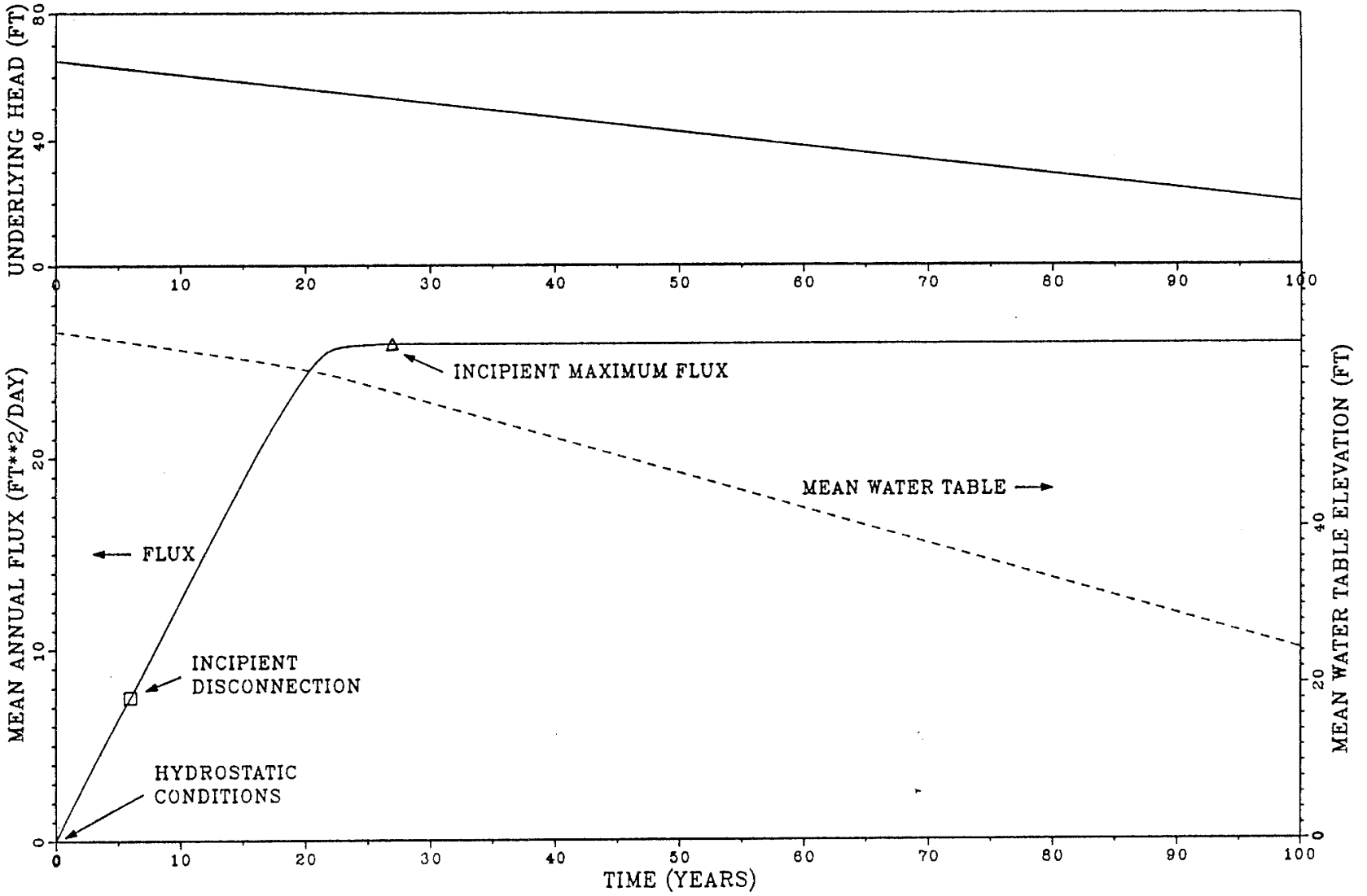

Fig. 43. Long term response of the reference simulation domain to progressively declining hydraulic heads in the underlying aquifer (underlying head).

indicating that disconnected stream/shallow water table conditions would exist in this system over a significant time span (~21 years). As in steady state analyses of water table behavior (e.g., Figure 20), the spatial mean water table level generally responds in a linear fashion to the drop in underlying head both prior to and after the onset of maximum flux conditions. Similarly, the rate of water table decline is greater once maximum flux conditions exist.

Figure 44 illustrates the response of the two-layered domain during the 100-year analysis period. In this example, the time of incipient disconnection (~41 years) takes place considerably later than in the reference case simulation. In other words, more than 40 years elapses before local water table levels drop below the material interface separating the two aquifers. Incipient maximum flux takes place near a total time of about 43 years, thus, limiting the duration of disconnected stream/shallow water table conditions to a period of about 2 years. As before, the rate of water table decline is essentially linear both prior to and after incipient maximum flux, with the more rapid decline occurring once maximum flux conditions exist. However, the difference in rate of water table drop between the years before and after incipient maximum flux is relatively imperceptible with the layered system. This is mostly due to the fact that head differences across the sandy silt aquitard used in the layered simulations do not change greatly with substantial variations in system flux. In other words, the head difference across this aquitard material, once maximum flux conditions are reached, is not radically different from those observed during the connected losing stream and disconnected stream/shallow water table phases. As a consequence, the

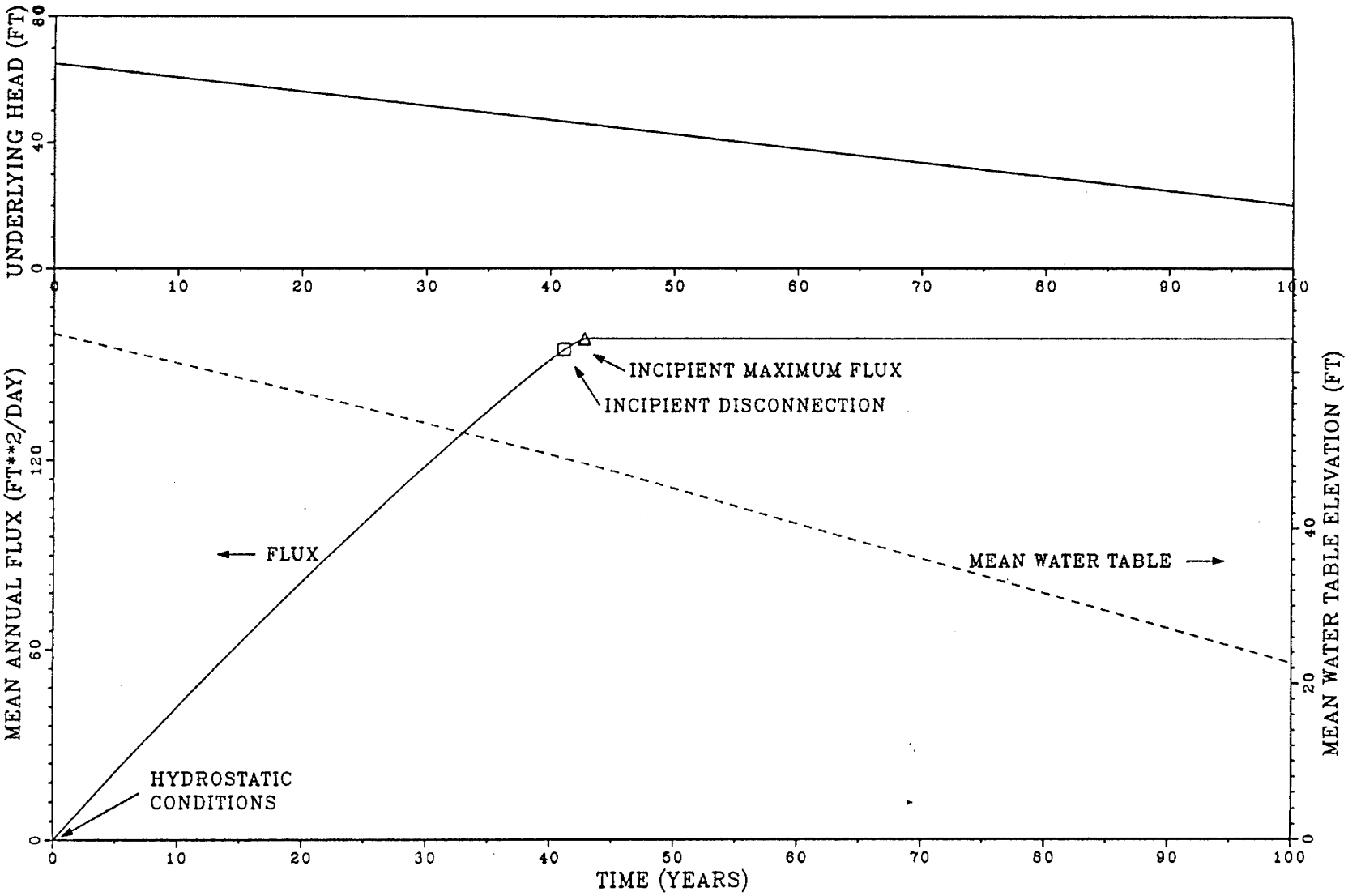

Fig. 44. Long term response of the two-layered domain to progressively declining hydraulic heads in the underlying aquifer (underlying head).

rate of water table drop stays relatively constant regardless of the stream-aquifer relationship that happens to exist at any given time.

Summary of Transient Analyses

Three transient simulations of variably saturated flow in stream-aquifer systems have been conducted. The purpose of each has been to determine temporal system response to seasonal changes of stream stage in situations wherein unsaturated flow has a significant influence on stream-aquifer interaction.

Transient Simulation 1 is representative of system response of the reference simulation domain under disconnected stream/shallow water table conditions. Transient Simulation 2 is an example of temporal behavior of the reference simulation domain for deep water table conditions. The third run, Transient Simulation 3, reflects the response of a two-layered domain used earlier in the steady state analyses (Figure 28), and is also based on deep water table conditions.

In each of the transient runs, system response to changes in stream stage is found to be relatively rapid. System fluxes and water table measures are repeated each year, indicating that a state of dynamic equilibrium exists in each case. The shallow water table regime of Transient Simulation 1 approaches steady state after a change in stage more quickly than in the deep water table equivalent (Transient Simulation 2). This happens partly because the difference between system inflow (stream infiltration) and outflow (aquitard leakage) is much larger in the deep water table example at the beginning of a new stage period; consequently, more time is needed for inflow and outflow to reach a common equilibrium value. Quicker response time in the shallow water table example is also attributed to

the larger amount of saturated aquifer material in this example. The saturated hydraulic conductivity and moisture content in the predominantly saturated medium of Transient Simulation 1 are obviously larger than the unsaturated equivalents existing within the mostly unsaturated domain in Transient Simulation 2. Accordingly, system time constants are noticeably smaller in Transient Simulation 1.

The response of the layered domain (Transient Simulation 3) is even faster than in either of the runs with the reference simulation domain. Large flows in Transient Simulation 3, due to the absence of a clogging layer in the layered domain, help to bring about the rapid response. High values of stream seepage in this example cause the saturated bulb located beneath the stream to penetrate relatively deep into the upper layer. Saturated hydraulic conductivities of the upper layer material (loamy sand) are consistently larger than unsaturated hydraulic conductivities of unsaturated media (medium sand) found beneath the stream in Transient Simulation 2. Furthermore, moisture content of the saturated loamy sand is consistently larger than moisture content of the medium sand aquifer (see moisture characteristic curves, Figure 10a) in Transient Simulation 2. Similarly, the sizable stream loss rates observed in Transient Simulation 3 help to maintain relatively large hydraulic conductivities in unsaturated portions of the lower aquifer layer (coarse sand) situated directly beneath the stream. The combination of relatively large hydraulic conductivities in both layers and high moisture contents in the saturated portion of the upper layer signify that the time constant of the layered system will be quite short, despite the fact that most of the domain is unsaturated.

The shallow water table in Transient Simulation 1 strongly affects stream infiltration rates. When stream stage is raised, the stream seepage rate initially increases. Effects of the increased inflow, however, are usually felt at the water table within seconds to a few minutes, whereupon water table levels begin climbing. The rising water table then leads to reduced pressure heads on the underside of the clogging layer, which in turn causes the stream infiltration rate to decrease. A gradually rising water table, therefore, results in a gradually declining system inflow rate. An opposite effect is observed when stream stage is lowered. In this case, the stream loss rate gradually increases from an initial low value in response to a steadily declining water table.

Under the deep water table conditions of Transient Simulation 2, water table level has no effect on the stream seepage rate, regardless of the stream stage. Therefore, the stream loss rate is determined entirely by stream properties (width, stage), clogging layer characteristics, and the aquifer material lying underneath the clogging layer. In this example, pressure heads on the underside of the clogging layer stabilize relatively quickly (in less than a day) after a change in stream stage. As a consequence, the rate of stream loss also quickly reaches a constant value.

A graph has been prepared of system fluxes and water table levels from Transient Simulation 2 over the first two days of a month in which a large increase in stream stage is observed. System inflow (i.e., the stream infiltration rate) is seen to decrease to a relatively constant value from an initially high rate within 0.2 days of the stage increase. Effects of the pressure pulse stemming from the stage increase are not felt at the water table until 0.5 days has elapsed,

after which that part of the water table lying directly beneath the stream begins rising. However, the spatial mean water table elevation does not show a significant rise until about 1 day after the stage increase. Accordingly, heads on the upperside of the aquitard and leakage from the system is similarly delayed. The spatial minimum water table level on the right side of the domain shows no signs of being affected at any time during the two days of analysis.

The stream seepage rate in the layered domain of Transient Simulation 3 stabilizes very quickly (in less than 0.5 days) in response to a change in stream stage. As in the deep water table example of Transient Simulation 2, this happens because pressure heads on the stream channel bed and banks quickly reach a constant value. The vertical extent of the saturated bulb in the upper aquifer layer also stabilizes quite rapidly, reflecting the speed with which relatively steady head distributions are reached below the stream. The base of the saturated bulb extends deeper into the upper aquifer layer with increasing stream loss rate, and retreats to shallower depths as stream flux decreases. Spatial water table measures (maximum, minimum and mean) respond in an opposite manner, increasing in elevation as the stream infiltration rate becomes larger. Consequently, the vertical distance separating the saturated bulb from the highest point of the water table becomes less when stream infiltration rate increases, and increases with reduced stream loss rate.

Approximate analyses have also been made of long-term system response of the reference simulation domain and the two-layered domain to decline in regional groundwater levels. Mean annual system fluxes and spatial mean water table levels are examined over a 100-year period in which hydraulic heads in the aquifer underlying each domain are

progressively lowered a total of 45 feet. Essentially hydrostatic conditions are assumed to exist in each system prior to the gradual decline in underlying head. In the reference domain, incipient disconnection takes place at a total time of about 6 years, while incipient maximum flux does not occur until some 21 years later (~27 years total time). In the layered system analysis, incipient disconnection is observed at a total time of about 41 years, which is the time needed for water table levels to drop below the material interface separating the two aquifer layers. Incipient maximum flux takes place at a total time of about 43 years, thus limiting the disconnected stream/shallow water table phase to about 2 years. In both the reference case and layered systems, the mean water table level declines in an essentially linear fashion both prior to and after the onset of maximum flux conditions. The rate of drop in the water table is larger after maximum flux conditions have come about.

X. COMPARISONS WITH SATURATED FLOW MODELS

Few saturated flow models make allowances for the negative pressure heads that may exist beneath a stream when disconnection occurs. As a consequence, results from those models may diverge greatly from those based on variably saturated flow theory. Comparison of fully saturated and variably saturated simulations is, therefore, yet another means of illustrating the effect of the unsaturated zone on stream-aquifer processes. In this chapter, some of the fundamental differences between the two approaches are examined, and example simulations are used to show how disparate their results can be.

Equations of Flow and Stream Seepage

The governing equation of variably saturated subsurface seepage, an example of which was presented earlier in equation (1), is usually formulated in terms of both pressure (positive and negative) and elevation components of hydraulic head. In contrast, saturated flow theory does not provide a means of taking into account the negative pressure heads (and, consequently, the moisture content) of unsaturated zones. Furthermore, the Dupuit flow assumptions are frequently invoked in the mathematical development of a saturated flow model. As a consequence, vertical variations in total head, even within saturated portions of an aquifer, are commonly overlooked. The resulting formulation brings about a decrease in dimensionality of the flow problem, with what may have originally been a a three-dimensional, or two-dimensional vertical slice simulation in a variably saturated regime now being represented by, respectively, two-dimensional or one-dimensional vertically averaged flow solely below the water table.

Assuming Dupuit flow conditions and a horizontal aquifer bottom , the equation of transient one-dimensional saturated flow in an unconfined aquifer is

$$\frac{\partial}{\partial x}\left[K_x H\frac{\partial H}{\partial x}\right] = S_y \frac{\partial H}{\partial t} - R(x,t) \qquad (14)$$

where:

H = total head in the saturated zone (L)

x = horizontal distance (L)

K_x = saturated hydraulic conductivity in the x-direction (L/T)

S_y = specific yield (dimensionless)

R = source/sink rate per unit area of medium, including head-dependent leakage (L/T)

It should be noted that only the effects of gravity drainage have been included in the storage term on the right-hand-side of (14), i.e., matrix and aquifer compressibilities have been disregarded.

In a saturated flow model based on (14), aquifer seepage either from or to a stream is usually handled through the source/sink term R. The seepage rate can be taken into account by either of two ways: (1) the rate can be specified by the model user, or (2) it can be allowed to vary as a head-dependent (Cauchy boundary) flux across a flow retarding material, such as a clogging layer. An altogether different technique of treating a stream in a saturated model is to establish Dirichlet (prescribed head) boundaries along its course. This third approach, however, is normally only justified if the stream fully penetrates its adjoining aquifer. In cases where it is justified, the stream thus constitutes a boundary, and does not involve the R term in (14).

Since this study attempts to assess the effect of suction pressures on stream seepage, only the head-dependent boundary method of estimating stream losses in a saturated model is considered, i.e., the second of the three techniques mentioned above. In other words, it serves little purpose to assume that the flux is already known and can be specified a priori. Such an assumption implies foreknowledge of pressure conditions in the aquifer, and, consequently, of hydraulic heads within the saturated zone.

An example of one-dimensional equations that are typically used to calculate flux across a clogging layer (see, e.g., Prickett and Lonnquist, 1971; Townley and Wilson, 1980; McDonald and Harbaugh, 1984) is as follows:

$$Q_s = \begin{cases} \frac{K''}{B} A (H_s - H) & \text{if } H > H_b \\ \frac{K''}{B} A (H_s - H_b) & \text{if } H \leq H_b \end{cases} \qquad (15)$$

where

Q_s = stream seepage (L^3/T)

K'' = saturated vertical hydraulic conductivity of the clogging layer (L/T)

B = thickness of the clogging layer (L)

A = surface area of the streambed (L^2)

H_s = stream surface elevation (L)

H_b = elevation at base of clogging layer (L)

Figure 45a shows the spatial relationship of the parameters used in equation (15). General behavior of net stream seepage into the aquifer with changing head is illustrated in Figure 45b. Positive values of Q_s signify seepage from the stream to the aquifer, whereas negative values

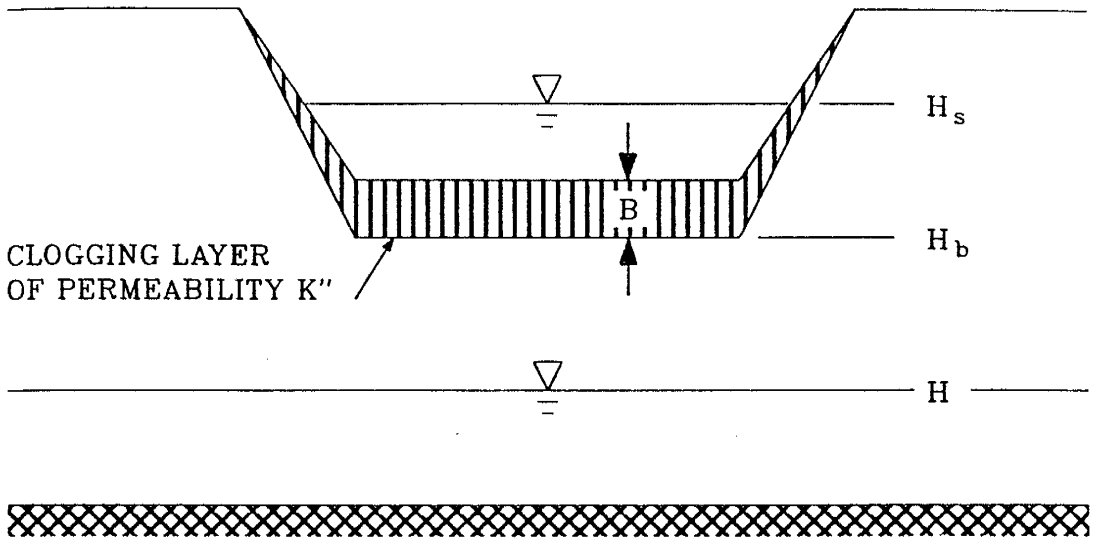

a

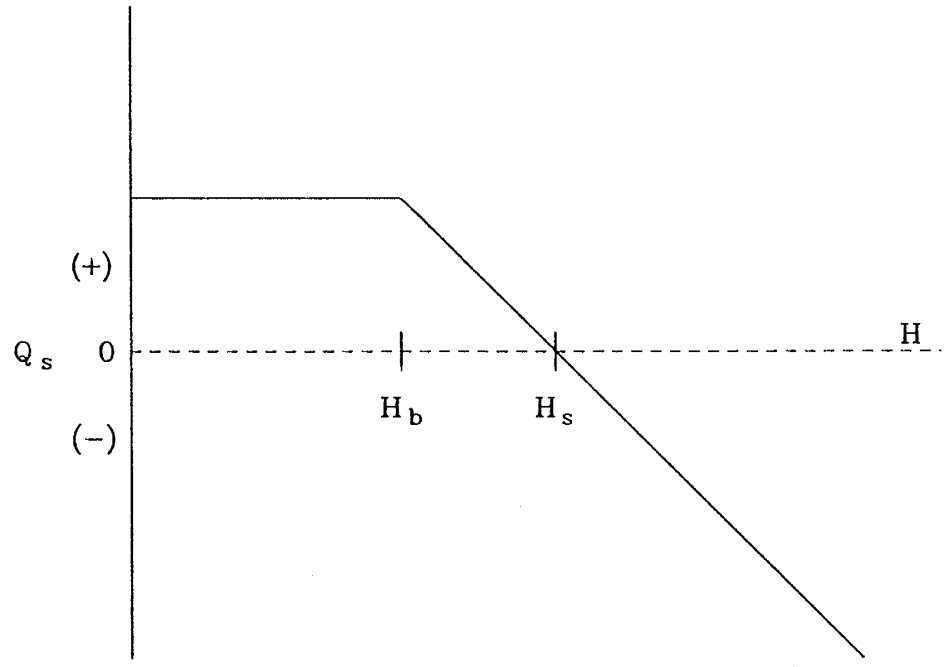

b

Fig. 45. Stream seepage algorithm in most saturated flow models: (a) spatial relationship of stream-seepage parameters and (b) stream seepage rate versus saturated hydraulic head.

are representative of aquifer discharges to the stream. It is the per unit area equivalent of Q_s that is normally incorporated into the source/sink term R of equation (14).

Equation (15) is formulated on the assumption that the vertical head gradient across the clogging layer is linear, and, therefore, that flow across the clogging layer is steady state. Since the value of K" is a constant, the clogging layer is assumed at all times to be saturated; i.e., negative pressure heads, either within the clogging layer or in the aquifer beneath it, are assumed to never exceed the air entry pressure head of the clogging layer material. Although this condition may be adhered to in many cases, there is certainly no guarantee that it will always be met (recall Figure 2, Chapter II) if hydraulic disconnection takes place.

The most notable feature of equation (15) with respect to the estimation of stream loss rate, is that nothing is included regarding negative pressure heads on the underside of the clogging layer that may come about should disconnection occur. In other words it is implied that, once water table levels drop below the base of the clogging layer (H_b), matric potential immediately below the clogging layer is equal to atmospheric (zero) pressure. This condition is assumed over the full range of disconnection, regardless of water table level. An intrinsic feature of this scheme is that maximum flux conditions come about the moment disconnection is reached. Consequently, the points of incipient disconnection and incipient maximum flux are the same when using (15).

In contrast to the saturated flow approach, it is not necessary in variably saturated models to treat stream seepage as a source/sink parameter. Instead, owing to the fact that both elevation and pressure components of head are incorporated into unsaturated flow theory, the

effect of stream water on the porous medium connected to the stream can be simulated by establishing prescribed (Dirichlet) pressure heads along the wetted portions of a streambed. Fluxes across the streambed at these prescribed head boundary nodes must then be determined via the numerical technique in a given model that has been designed to calculate fluxes at such boundaries. In the stream-aquifer simulations with SATURN, stream stages have indeed been represented by prescribed boundary heads, and fluxes at the prescribed head nodes have been determined by equation back-substitution (see, e.g., Huyakorn and Pinder, 1983).

Even after the infiltration flux from a disconnected stream has been computed in a saturated flow model, there is generally no scheme available in this type of model for determining the delay time it takes for the water infiltrating through the streambed to have on effect on the underlying saturated zone. It is usually assumed that the transfer of a pressure pulse at the stream to the water table is instantaneous (see e.g., Vauclin et al., 1979). Such assumptions could be quite inappropriate for transient simulations involving deep water tables (see, e.g., Figure 41). Variably saturated flow models are not hampered, at least theoretically, by this difficulty as they are able to represent flow and storage across the unsaturated zone.

Improved Stream Seepage Estimation in Saturated Flow Models

Not all attempts at modeling of disconnected stream-aquifer systems totally ignore negative pressure heads at the base of the clogging layer. But most of the codes included in this latter category, a few of which are briefly mentioned hereafter, assume that

the suction head beneath the stream maintains a constant value, regardless of the depth to the underlying water table.

For example, Rovey (1975), in her model of three-dimensional flow, used a single Darcy's Law expression for calculating stream losses in the case of a disconnected stream. That expression, written partially in terms of some previously defined parameters, is

$$q_s = \frac{K''}{B} (H_s - H_b - \psi_a) \tag{16}$$

where

q_s = seepage rate per unit area of the streambed (L/T)

ψ_a = air entry (bubbling pressure) head of the clogging layer (L)

The flux q_s in (16) is described by Rovey (1975) as a "maximum seepage velocity", which, for a given stream depth, cannot be exceeded, even if pressure heads at the base of the clogging layer become more negative than the clogging layer air entry pressure head ψ_a. This latter condition seems to contradict the one-dimensional infiltration theory of Zaslavsky (1963), who presents hydraulic arguments for the existence of the steady state pressure profile presented in the deep water table case shown in Figure 2. In other words, Zaslavsky's (1963) analyses suggest that the maximum infiltration rate for a given stream stage is dependent on the soil properties of both the clogging layer and the aquifer, and not just on the air entry pressure head of the clogging layer.

Rovey (1975) uses (16) to compute influx to the groundwater domain from streams for all cases in which disconnection exists. Thus, she makes no attempt to account for possible variations in the stream

seepage rate such as may occur when the water table still lies at a shallow depth below the streambed.

Bouwer (1969) utilizes a formula similar to (16) to compute stream losses in the case of disconnection. However, instead of using a constant suction head on the base of the clogging layer equal to that material's air entry pressure head, a more representative, or average, value of pressure head in the underlying aquifer is assumed. The resulting formulation is

$$q_s = \frac{K''}{B} (H_s - H_b - \psi_{cr}) \tag{17}$$

Bouwer (1969) uses the expression "critical pressure head" to describe the term ψ_{cr}. It is, in effect, a measure of the thickness of a fictitious capillary fringe that would be found in a hydrostatic moisture profile above the water table in the aquifer material that one is considering. Specifically, ψ_{cr} is defined (Bouwer, 1969) as

$$\psi_{cr} = \int_0^{\psi_w} \frac{K(\psi)\,d\psi}{K_s} \tag{18}$$

where $K(\psi)$ is unsaturated hydraulic conductivity (L/T) of the aquifer material, K_s is its saturated hydraulic conductivity (L/T), and the limit of integration ψ_w is the pressure head at which moisture content (and, therefore, hydraulic conductivity) essentially becomes irreducible. Figure 46, which is adapted from Bouwer (1969), helps to define the relationships between K, ψ and ψ_{cr}.

Laboratory studies by Bouwer (1964) indicate that (17) provides a viable method for computing steady state seepage of surface water

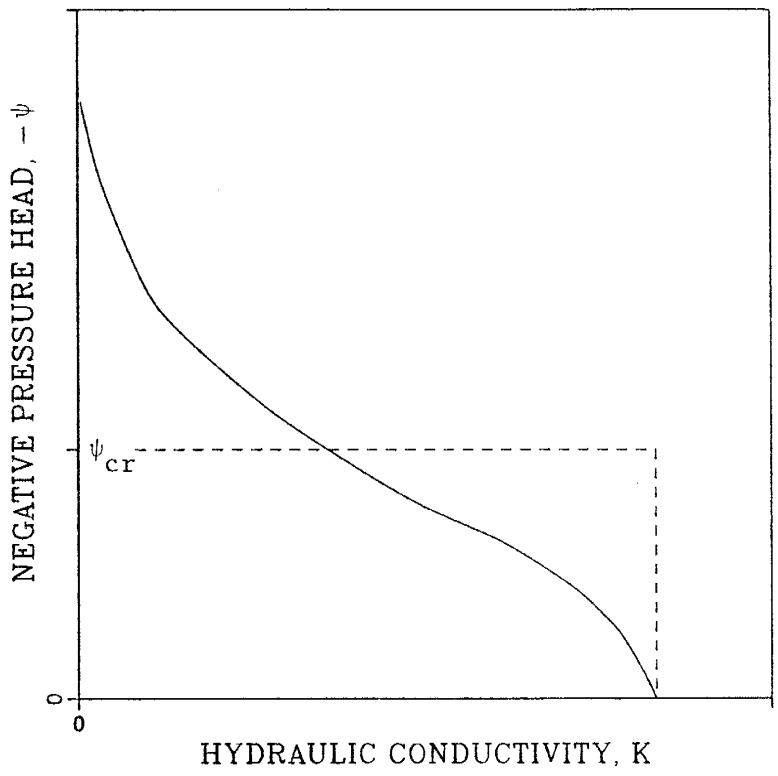

Fig. 46. Relationships between unsaturated hydraulic conductivity (K), pressure head (ψ) and Bouwer's ψ_{cr}

across a restricting layer much like the clogging layer considered in stream-aquifer studies. However, it should again be mentioned that equation (17) assumes a single fixed value of pressure head on the underside of the clogging layer in the event of disconnection. Consequently, for a given stream stage, the computed stream loss rate is constant regardless of the depth to the water table. Therefore, Bouwer's (1969) approach, like Rovey's (1975), appears to be limited in the sense that it is incapable of taking into account variable stream seepage rates under disconnected stream/shallow water table conditions. Nor can it be guaranteed that (17) will do a reasonable job of estimating maximum flux in deep water table situations.

One further example of a saturated flow code in which the suction heads beneath a disconnected stream are considered is that of Dillon and Liggett (1983). This simulator is also useful in that negative pressure heads in the aquifer are also included in a Green-Ampt (Green and Ampt, 1911) algorithm for determining delay time between incipient stream infiltration and subsequent recharge of the water table. However, as in previous cases, it appears (Dillon and Liggett, 1983) that the pressure head is assumed to be constant, and cannot be altered with fluctuations of a shallow phreatic surface.

Steady State Comparisons

Although the above given saturated flow simulators are capable of incorporating suction heads into their algorithms for determining stream loss, most public domain codes utilize formulae such as (15) to estimate stream seepage. Frequently used codes included in this latter category include Prickett and Lonnquist (1971), Trescott et al. (1976) and McDonald and Harbaugh (1984). Since an assumed atmospheric

pressure within the unsaturated zone is most commonly applied, the authors have chosen to compare variably saturated results from this study with those from a simulator that uses equation (15). The saturated flow code selected for the comparative runs is AQUIFEM (Townley and Wilson, 1980). This code utilizes triangular finite elements. Although AQUIFEM is designed to simulate two-dimensional areal groundwater flow, it has been used in this study to simulate one-dimensional Dupuit flow, the governing equation of which is described in equation (14).

In conducting the comparative simulations with SATURN and AQUIFEM, steps have been taken to insure that differences in results between the two codes is due to inherent differences between variably saturated and conventional saturated flow modeling, and not due to extraneous features such as numerical error. Lengths of the triangular elements employed in the AQUIFEM runs are identical to the horizontal (x-direction) dimensions of the rectangular elements used in the SATURN simulations. In addition, the finite element meshes employed in the AQUIFEM simulations have been designed such that any bias in the numerical solution due to elements having the same aspect (i.e., orientation) is avoided (e.g., Cooley, 1983). Steps have also been taken to minimize possible numerical errors arising from the use of triangular elements whose length to breadth ratios are large (e.g., Townley and Wilson, 1979). Aside from differences in the respective codes results stemming from the effects of unsaturated flow, some differences are also expected due to the fact that the AQUIFEM runs do not take into account two-dimensional flow in the aquifer. The importance of vertical flow is addressed in a later section.

Effect of Simulator Type on Steady State System Fluxes

A plot of steady state system fluxes, versus head in the underlying aquifer, for the base simulation case and a stream stage of 1 foot is presented in Figure 47a. Results from both simulator types are included. From this graph it can be seen that the curves for each code do not differ much from each other until such point that the saturated flow code determines that disconnection has occurred. At this juncture, the saturated flow codes assumes that atmospheric pressures exist at the base of the clogging layer, and a constant infiltration rate is computed as per (15). In stark contrast, the variably saturated model indicates that stream infiltration continues to increase with declining underlying heads. As a consequence, maximum system fluxes indicated by the two model types are significantly different. Maximum steady state flux computed by AQUIFEM for the base simulation case is 7.5 ft^2/day, whereas the variably saturated equivalent determined by SATURN is almost 26 ft^2/day. Obviously, pressure heads at the base of the clogging layer have become quite small as underlying heads and the water table have dropped. The additional difference in head that drives flow across the clogging layer is, therefore, significant. The saturated flow model falls far short of catching the effect of this additional head differential, and thus drastically underpredicts stream seepage.

An additional example of steady state system flux comparisons is given in Figure 47b. In this case the simulations are performed using the domain of Figure 8 and a medium sand aquifer, but with a less permeable aquitard material than in the reference simulation case. Clay loam once more comprises the clogging layer, and stream stage is again 1 foot. Much of what has been stated regarding Figure 47a also

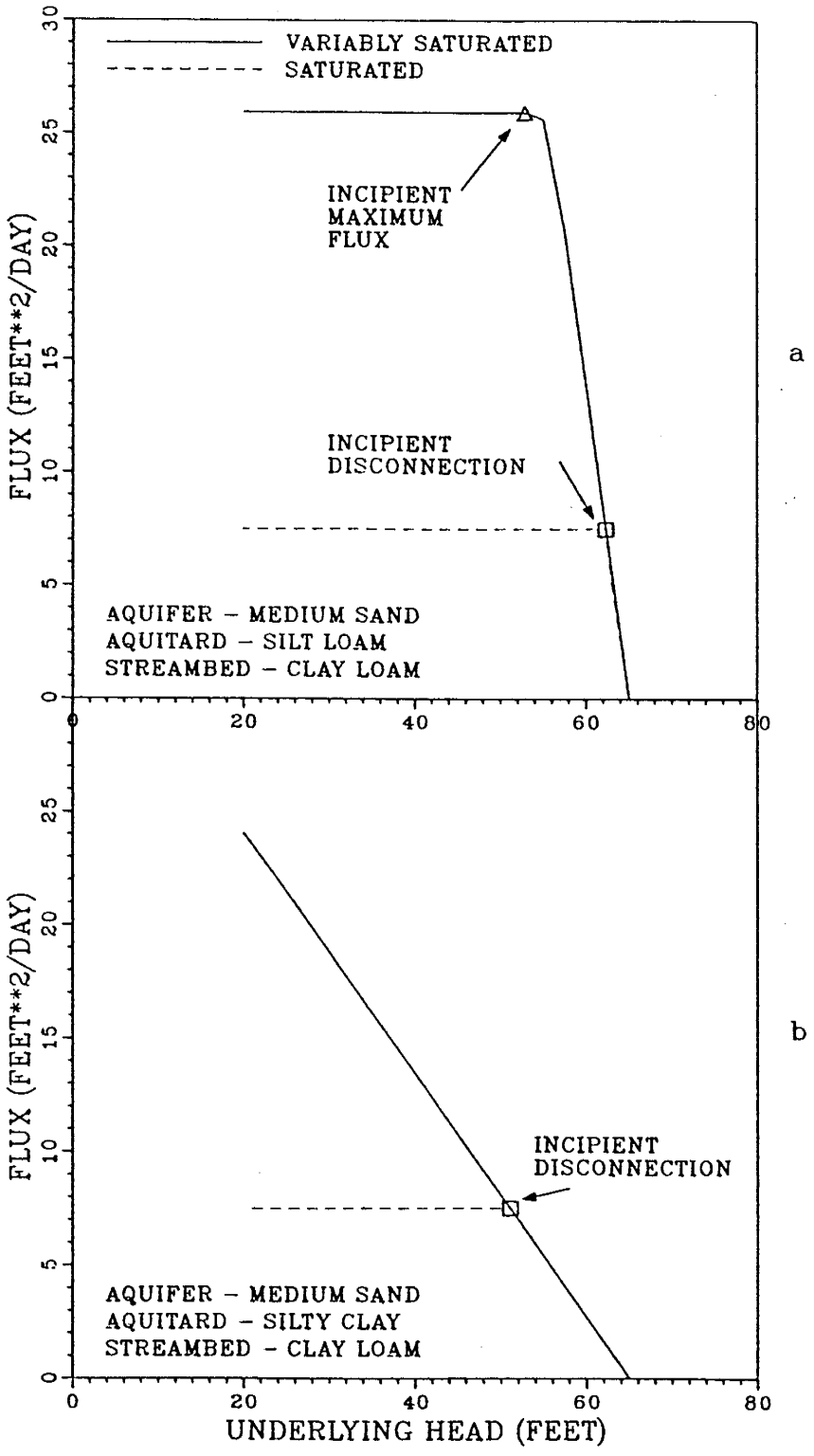

Fig. 47. Steady system fluxes versus hydraulic head in the underlying aquifer (underlying head), as determined by saturated and variably saturated flow codes for (a) the reference simulation domain and (b) the same domain but with a silty clay aquitard.

applies to Figure 47b. Again, the saturated flow model is seriously underestimating stream seepage once disconnection has taken place. But this set of runs with the silty clay aquitard tends to stand apart from the previously discussed reference simulation case in other ways. Specifically, differences in water table configuration between the simulator types is much more prevalent in this last example, an issue which is discussed further in a following section. It is noteworthy to point out that maximum flux conditions are not reached in the variably saturated curve of Figure 47b. If additional simulations were conducted for underlying heads less than 20 feet, a maximum flux situation would ultimately result.

Further graphical evidence of the large differences that sometimes exist in computed steady state flux from the two types of models is given in Figure 48. This graph represents an extension of Figure 27, in which maximum steady fluxes in all three aquifer materials are compared for the saturated hydraulic conductivities of the four clogging layer materials. Included now in Figure 48 is one additional curve representing the maximum flux computed by the saturated code AQUIFEM for the same simulation domain used to prepare Figure 27. The most striking feature of this latest comparison of model results is the radical underestimation of system flux by the saturated flow code. When sandy silt (K_s = 1 ft/day) is assumed to comprise the streambed clogging layer, the AQUIFEM computed flux is 150 ft^2/day, while fluxes determined by SATURN range from 375 to 384 ft^2/day, depending on aquifer material. Figure 48 is also instructive in the sense that it graphically demonstrates the inability of the saturated flow code to take into account the type of aquifer material into which the infiltrating stream water is being transported. In other words,

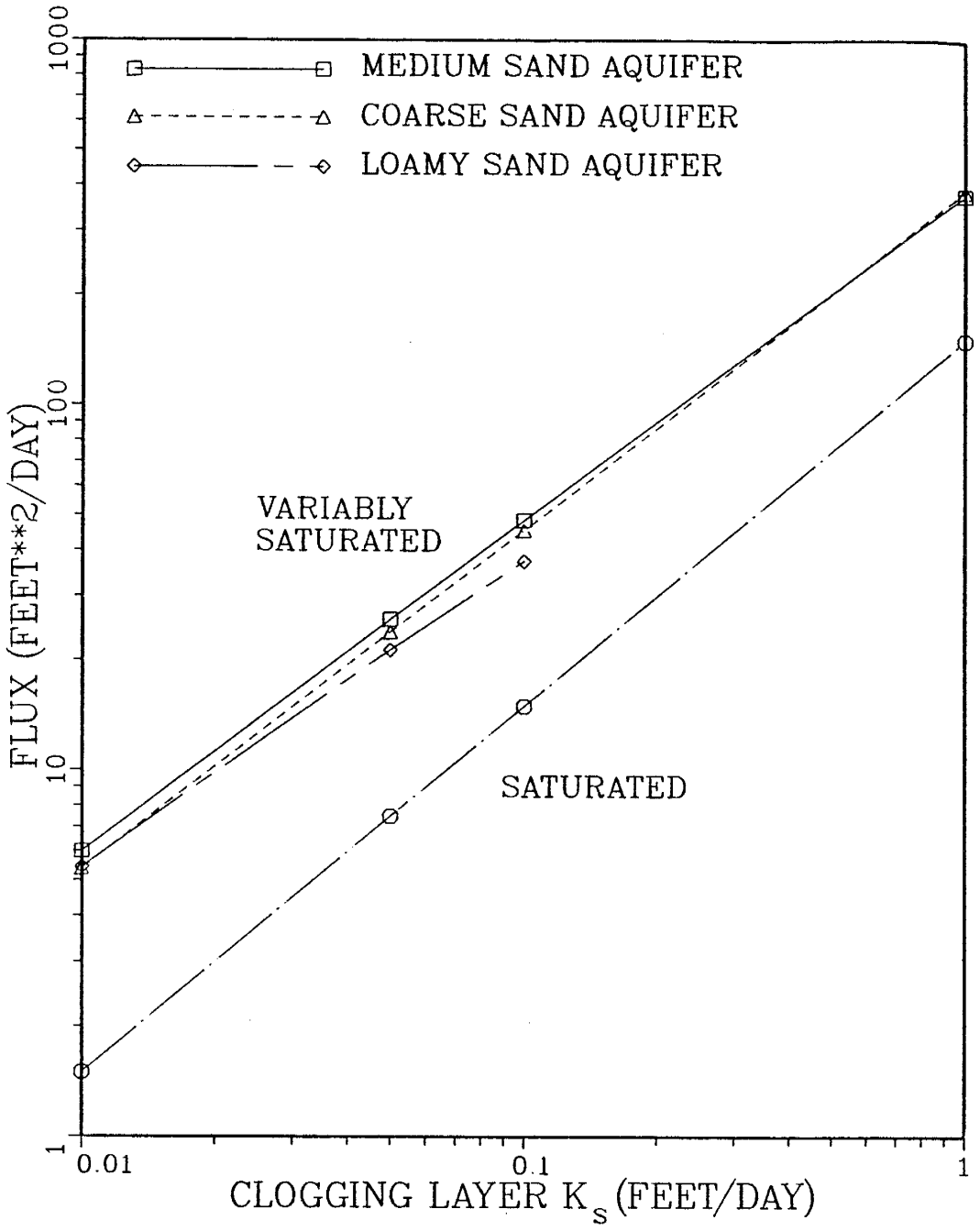

Fig. 48. Maximum steady state system fluxes versus clogging layer saturated hydraulic conductivity determined by saturated and variably saturated flow codes.

maximum fluxes computed by (15) for a given clogging layer material and stream stage are constant in value, regardless of the aquifer material below the stream; ergo, the single curve in Figure 48 of maximum flux calculated by the saturated flow code.

Effect of Simulator Type on Steady State Water Table Profiles

If, as indicated in the previous section, saturated flow codes tend to underestimate stream infiltration after disconnection is assumed, it seems likely that they will also underpredict water table mound levels below the stream during disconnection. Indeed this is shown to be the case in Figures 49a and 49b, in which water table behavior has been graphed for the two sets of model runs whose steady state fluxes were previously depicted in Figures 47a and 47b, respectively. The spatial maximum and mean water table measures from both the variably saturated and conventional saturated flow codes are provided in each graph. Prior to assumed disconnection in the saturated flow code, differences between the two simulator types are relatively nondiscernible. After this point, however, disparities in the results are quite evident.

Of some distinction is the fact that divergence of computed water table elevation for the two codes is much greater in Figure 49b than in Figure 49a. At an underlying head of 20.0 feet, AQUIFEM underestimates mean water table elevation in the example with the silt loam aquitard by some 3 feet. The comparable difference for the silty clay aquitard runs is as much as 27 feet. This can be explained by the large flow resistance provided by the less permeable (at saturation) silty clay. As underlying heads are reduced, and system flux increases, the increase in head difference across this aquitard material is quite

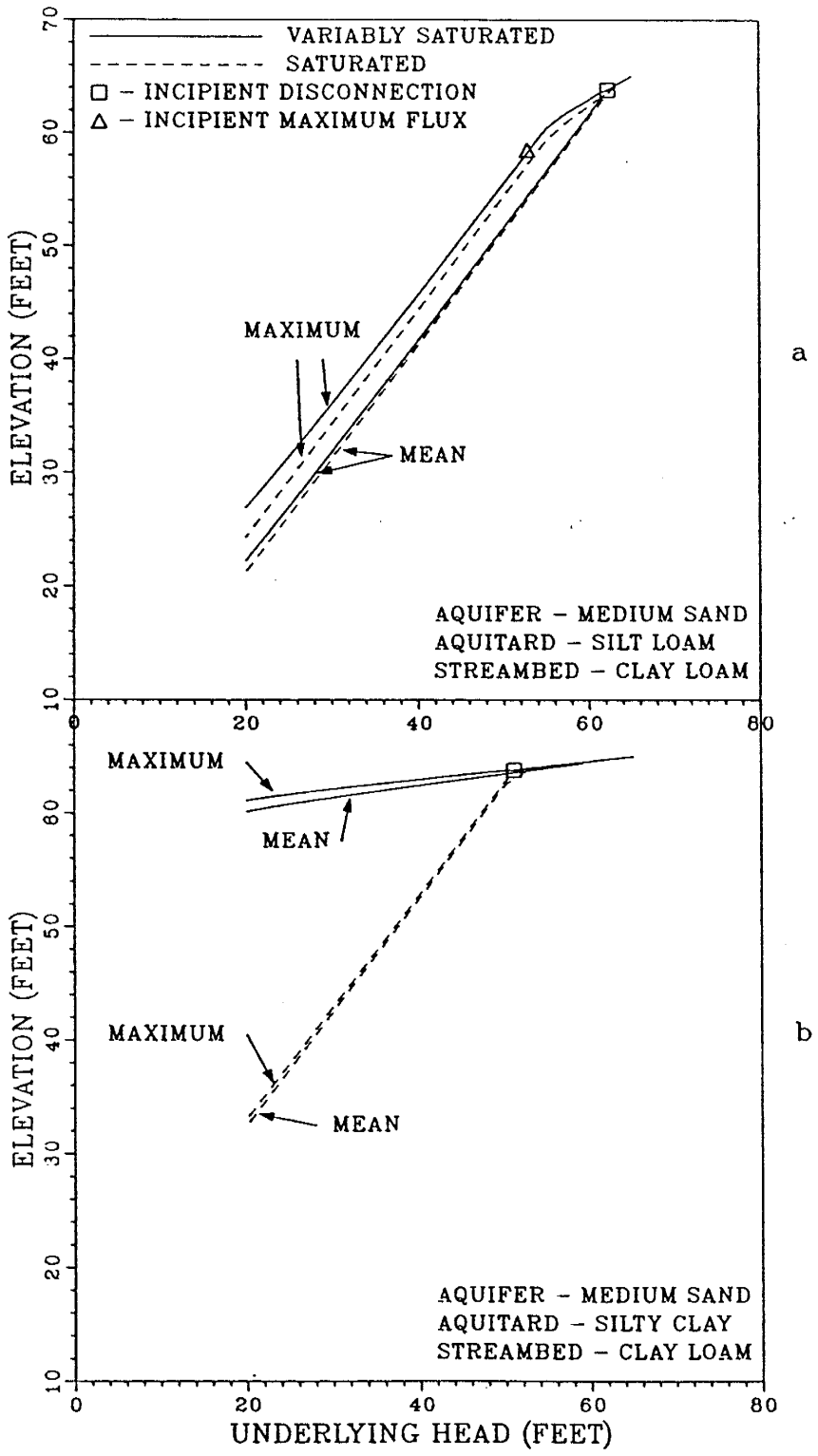

Fig. 49. Steady state water table elevations versus hydraulic head in the underlying aquifer (underlying head) as determined by saturated and variably saturated flow codes for (a) the reference simulation domain and (b) the same domain but with a silty clay aquitard.

substantial. In contrast, the more permeable silt loam requires much less of an increase in head differential as fluxes become larger. It stands to reason, then, that total heads, and, therefore, water table levels, will tend to remain higher in an aquifer situated above the silty clay aquitard than in one above the silt loam. Since the saturated flow code assumes a constant flux rate at disconnection that is considerably less than that determined by the variably saturated simulator (Figure 47b), large divergence in computed water table measures can be expected with the less permeable aquitard material. Such findings indicate the importance of accurately computing stream loss rates in groundwater models, and help demonstrate the significant effect that the aquitard unit has on the type of simulations made in this study.

Significance of Vertical Flow

It may be argued that the heretofore described disparities in results from AQUIFEM and SATURN stem from differences in the respective codes' makeup other than AQUIFEM's limited capability to compute stream infiltration. Indeed, as has been stated, heads computed by the codes will differ simply due to the fact that one is developed upon two-dimensional (horizontal and vertical) seepage whereas the other is based entirely on assumed one-dimensional (horizontal) Dupuit flow. Yet it can be shown that omission of the vertical flow component in AQUIFEM often explains only a small part of the discrepancies in model determinations. Inspection of Figures 47a and 47b, as well as Figures 49a and 49b, helps to initially demonstrate this point. As these figures suggest, system measures from the two model types, whether in the form of computed flux or water table levels, are close in value

over the range of conditions in which both models assume hydraulic connection. Thus, the effect of vertical flow, at least under connected conditions, would appear minimal.

To evaluate vertical flow influences in the case of disconnection, a different approach can be taken. Specifically, water table profiles computed by each type of simulator can be compared for the same steady state flux. An example of such a comparison is presented in Figure 50. Here, water table profiles from three separate simulations are plotted. The first (solid curve) is from a steady run with SATURN using a domain with the same dimensions shown in Figure 8, a stream stage of 1 foot and a hydraulic head of 20 feet. Sandy loam (Material 3) comprises the aquifer in this instance, while the aquitard and clogging layer each consist of silt loam (Material 5). The second (dashed curve) is the water table profile predicted by AQUIFEM for the same simulation conditions. The stream loss rate determined by AQUIFEM in this second simulation is 12.5 ft^2/day, whereas the SATURN computed flux is 37.50 ft^2/day. The third profile (chain dotted curve) is the result of a steady state run with AQUIFEM in which the clogging layer is no longer assumed present and flux from the stream is prescribed at the correct value of 37.50 ft^2/day. In this last simulation, the stream loss is distributed uniformly along the stream bottom.

Figure 50 clearly demonstrates that the original water table profile predicted by AQUIFEM (dashed curve) is far below the correct profile computed by SATURN (solid curve). Yet, the revised AQUIFEM run (chain dotted curve) produces a water table configuration that is much closer to the SATURN result. The most apparent differences between the revised AQUIFEM water table and the SATURN configuration are found in the area located directly below the stream, where vertical flow

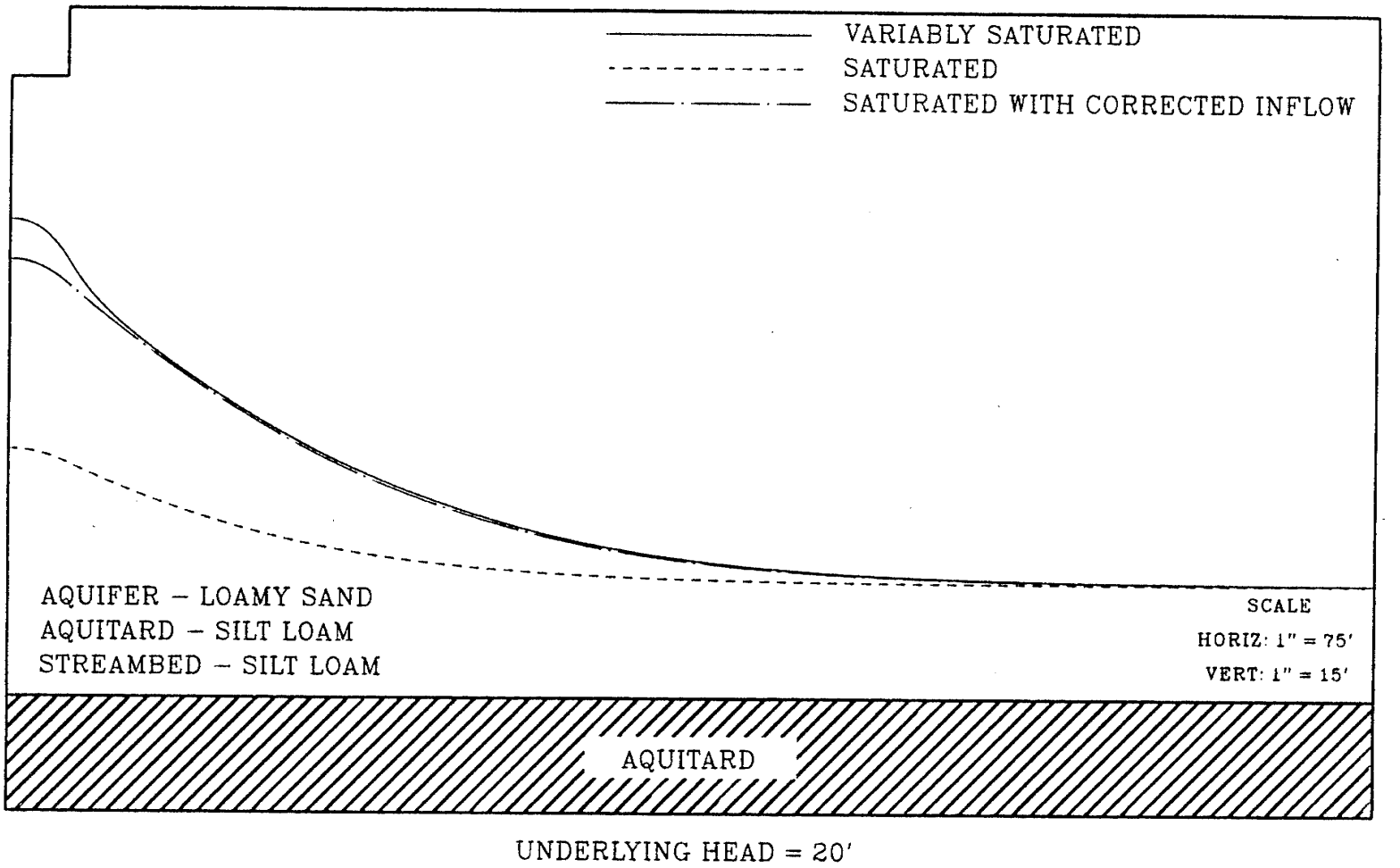

Fig. 50. Comparison of water table profiles determined by the variably saturated flow code, saturated flow code and saturated code with corrected inflow.

components in the variably saturated simulation are concentrated. However, elsewhere in the domain, the differences are relatively minor. In this example, therefore, disparities in water table elevation determined by the two modeling approaches are mostly attributed to the inability of (15) to properly compute stream loss, rather than the assumed Dupuit conditions in the saturated flow code. Additional comparisons of this nature produce similar findings.

Transient Comparisons

Comparison of transient simulation results from the saturated flow and variably saturated codes is also of interest. To illustrate the differences that can result from the two approaches, saturated flow runs have been made for the two problems comprising Transient Simulations 1 and 2, described earlier in Chapter IX. Both runs are for the reference simulation case, with the first representing shallow water table conditions, and the second portraying a deep water table situation. Only second year results are used in the comparisons. As in the steady state comparisons, AQUIFEM is used to perform the saturated flow runs, SATURN the variably saturated simulations.

Figure 51a presents a comparison of seasonal inflows computed by the two codes for the shallow water table (underlying head = 60 feet) example of Transient Simulation 1. System outflows for the same example are given in Figure 51b. Differences in spatial maximum and mean water table elevations predicted by each simulator are shown in Figures 52a and 52b, respectively. It is obvious from these sets of graphs that the saturated flow model underpredicts both flow and water table levels throughout the year. The cause of such underprediction, of course, stems from the saturated flow code's inability to adjust

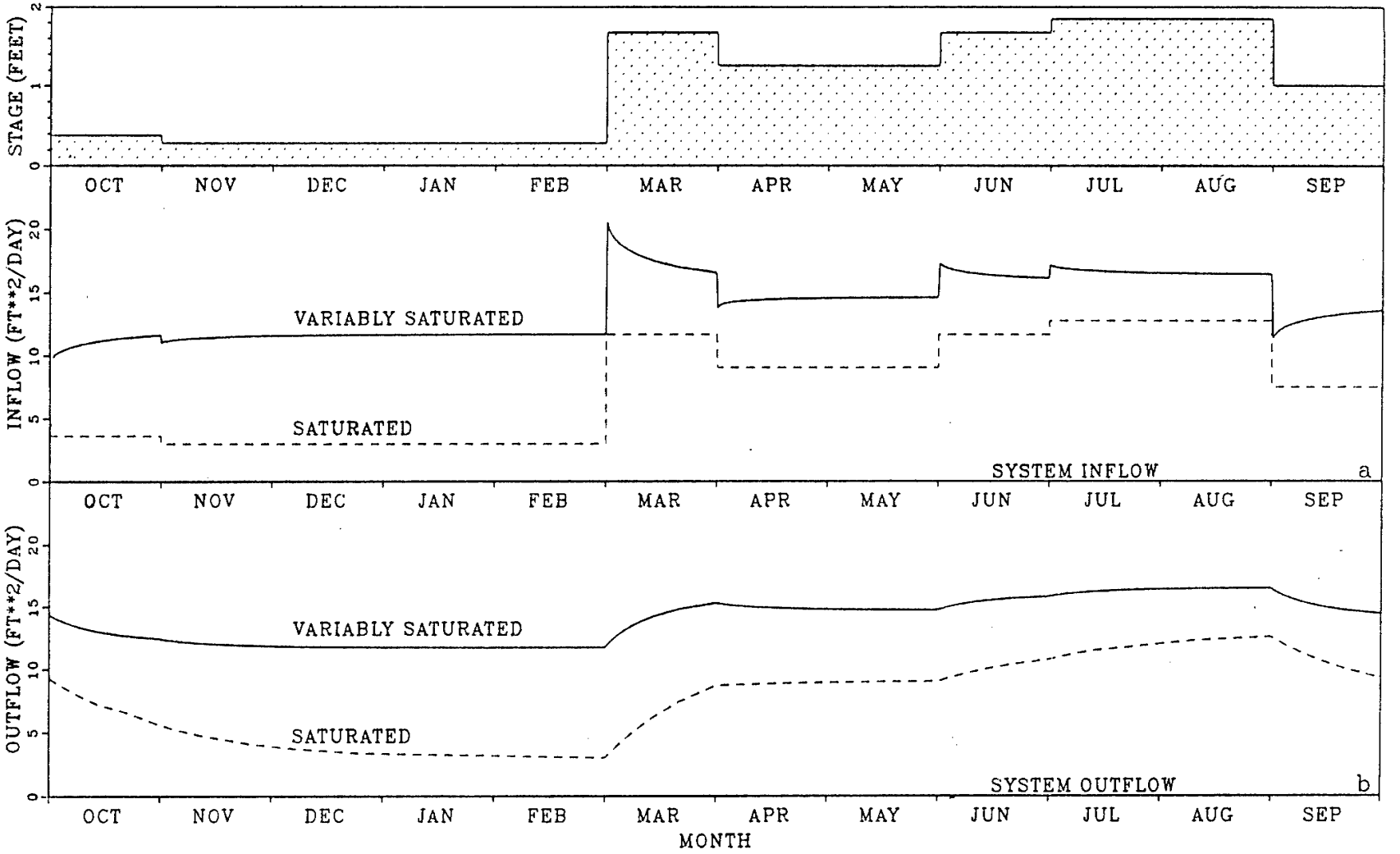

Fig. 51. Transient system (a) inflows and (b) outflows determined by the saturated and variably saturated flow codes for the reference simulation domain under disconnected stream/shallow water table conditions.

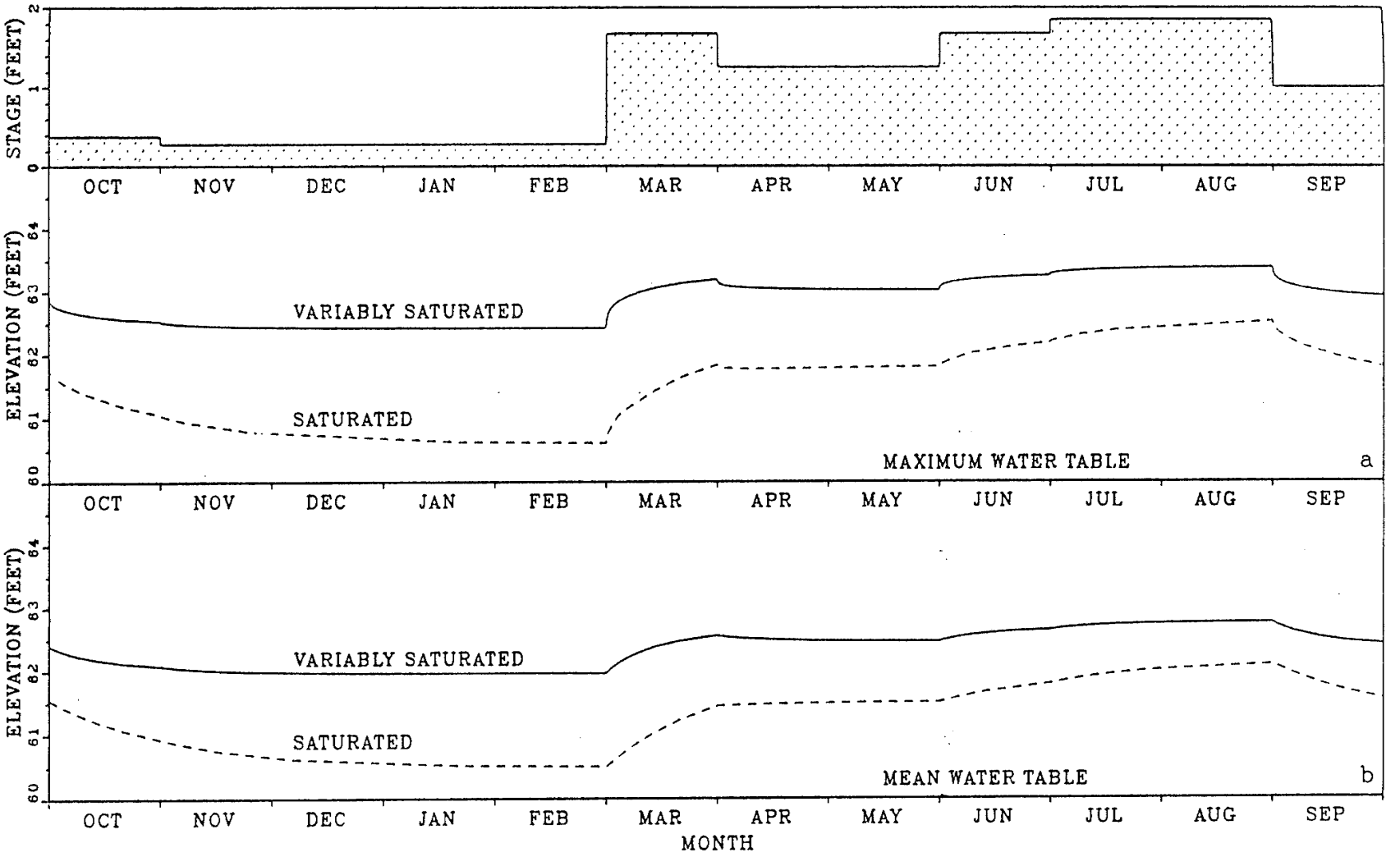

Fig. 52. Transient (a) spatial maximum and (b) spatial mean water table elevations determined by the saturated and variably saturated flow codes for the reference simulation domain under disconnected stream/shallow water table conditions.

stream loss rates for various levels of suction beneath the clogging layer in a disconnected stream/shallow water table situation. Indeed, as Figure 51a shows, inflow rates computed by the saturated code are constant for each stream stage, since hydraulic connection never comes about during the course of the year-long simulation.

It is interesting to note in the shallow water table example that the discrepancies between computed inflows from the two codes (Figure 51a) become less as the stream stage increases. This phenomenon is easily understood if one considers what is happening hydraulically on the underside of the clogging layer in the variably saturated flow code. When stream infiltration initially increases due to an increased stream stage, suction head at the base of the clogging layer immediately begins decreasing due to the higher moisture contents that are now present. Moreover, as the water table begins rising due to the increased recharge, the suction head below the stream responds by decreasing even more. Both factors, therefore, cause pressures at the base of the clogging layer to approach atmospheric (zero) pressure. The closer negative pressures come to values of zero, algorithms represented by equations such as (15) become more appropriate for estimating stream losses. Figure 52a and 52b shows that improved estimates of stream loss also allow the saturated flow code to do a better job of predicting water table elevation.

Comparisons of system flow for the deep water table conditions found in Transient Simulation 2 are presented in Figure 53a (inflow) and Figure 53b (outflow). Water table elevations predicted by the two codes for this transient run are given in Figure 54a (spatial maximum) and Figure 54b (spatial mean). Underprediction of inflow and water table levels in this case is much greater than observed earlier for the

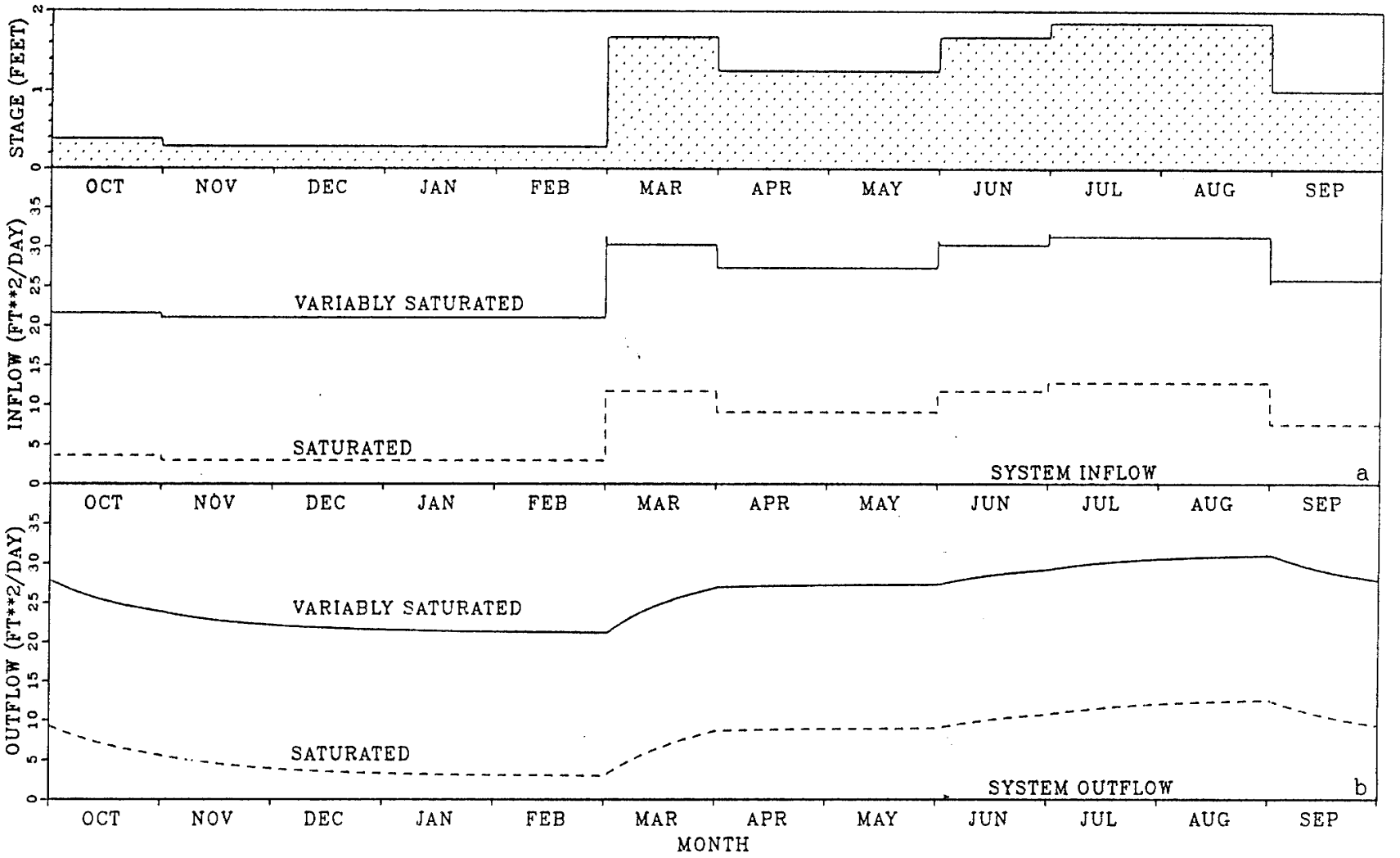

Fig. 53. Transient system (a) inflows and (b) outflows determined by the saturated and variably saturated flow codes for the reference domain under disconnected stream/deep water table conditions.

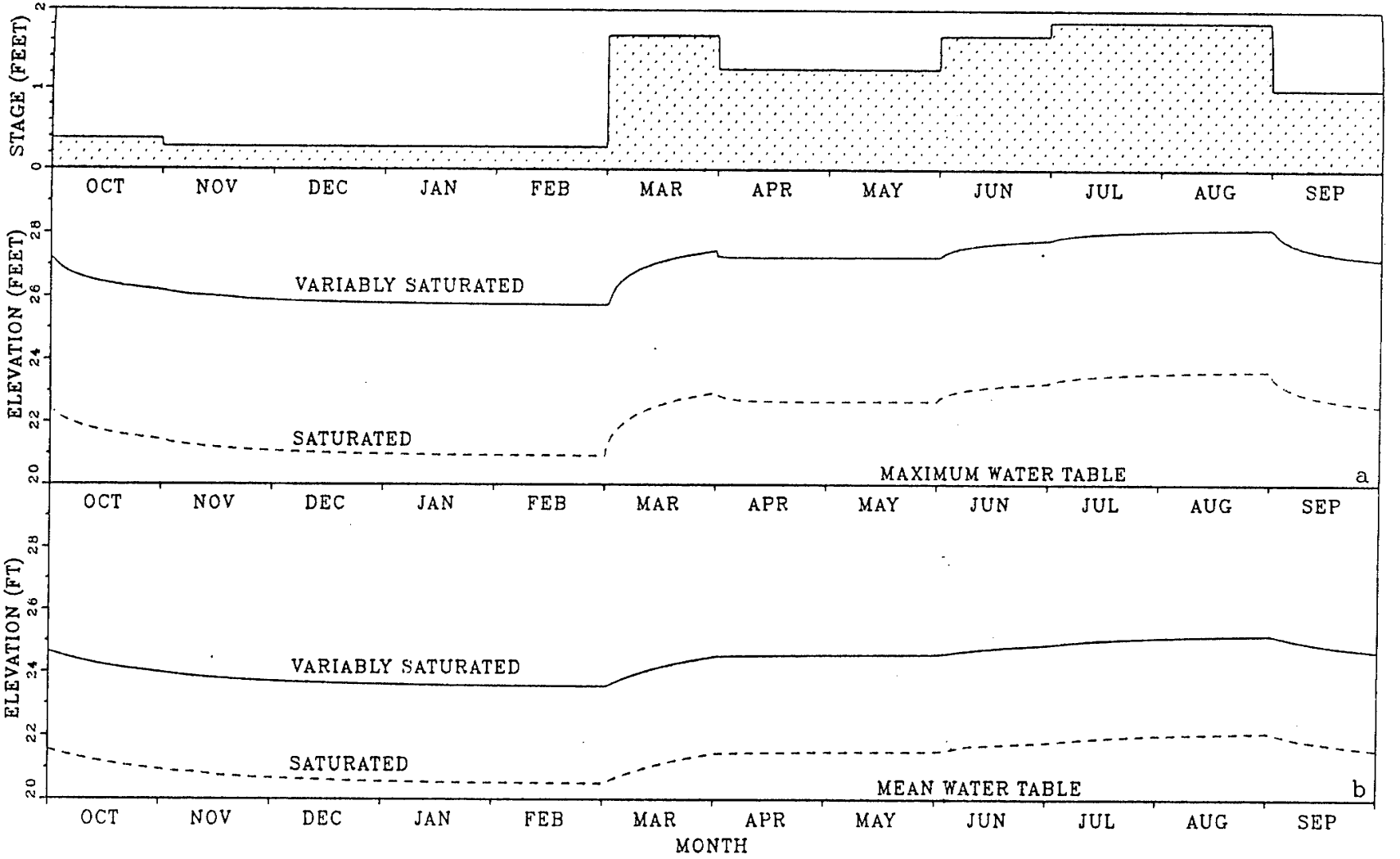

Fig. 54. Transient (a) spatial maximum and (b) spatial minimum water table elevtions determined by the saturated and variably saturated flow codes for the reference simulation domain under disconnected stream/deep water table conditions.

shallow water table example. This occurs because maximum flux conditions prevail in the variably saturated version of Transient Simulation 2, while the shallow water table in Transient Simulation 1 manages to keep SATURN computed inflows to less than maximum value. It is interesting to note that the difference in system inflow computed by the two codes for the deep water table simulation (~17 ft^2/day) is virtually constant throughout the simulation year. This results from the fact that pressure heads at the base of the clogging layer remain relatively constant in the variably saturated simulation regardless of stream stage. Apparently, moisture contents within the medium sand aquifer underlying the stream are maintained over a range of values in which the suction head varies only slightly (see Figure 10a). Hence, unlike the comparisons in the shallow water table case, disparities between results from the two codes are not significantly reduced with increasing stage. Virtually constant differences in system inflow (Figure 53a) help assure that disparities in system outflow (Figure 53b) will also remain effectively constant, as do the differences in water table measures (Figures 54a and 54b).

Comparison of inflow volumes predicted by the two codes also helps to emphasize the errors that may stem from the conventional saturated modeling approach. In the shallow water table case, total inflow volume over the course of the year-long simulation is predicted by AQUIFEM to be 2740 cubic (ft^3). The equivalent value determined by SATURN is 5100 ft^3. Inflow volumes for the deep water table example are again 2740 ft^3 with the saturated code, and 9460 ft^3 with the variably saturated code. Hence, underprediction of annual recharge with the saturated flow approach is clearly evident in these examples, and is noticeably worse in the deep water table case.

If a flow model such as AQUIFEM is calibrated for connected water table conditions, using an equation such as (15), the potential for underestimating annual recharge from stream losses in disconnected systems is significant. To demonstrate this potential problem, one final set of comparisons has been prepared for the long-term transient analyses presented earlier in Chapter IX, in which hydraulic head in the underlying aquifer (underlying head) is lowered a total of 45 feet over a 100-year period. Figure 55 shows the long-term response of system flux and the spatial mean water table elevation in the reference simulation case as determined by both SATURN and AQUIFEM. Again it becomes apparent that maximum flux conditions are assumed much earlier with the saturated simulator (at ~6 years) than is determined with the variably saturated code (~27 years). Consequently, the saturated flow code considerably underpredicts system flux (and, therefore, system recharge), for over 90 years of the full 100-year analysis period. Underprediction of the mean water table elevation by the saturated simulator is of less consequence in this case. However, it should be remembered that the differences in predicted water table elevations by the two codes could be much more sizable under different simulation conditions (e.g., recall Figure 49).

Summary of Model Comparisons

Differences between the approaches taken in variably saturated flow simulation and conventional saturated flow codes have been evaluated. It has been shown that the technique most commonly used to estimate the rate of flow from a stream in saturated flow codes tends to underpredict stream losses. This happens because few saturated models make allowances for the suction heads that exist below a

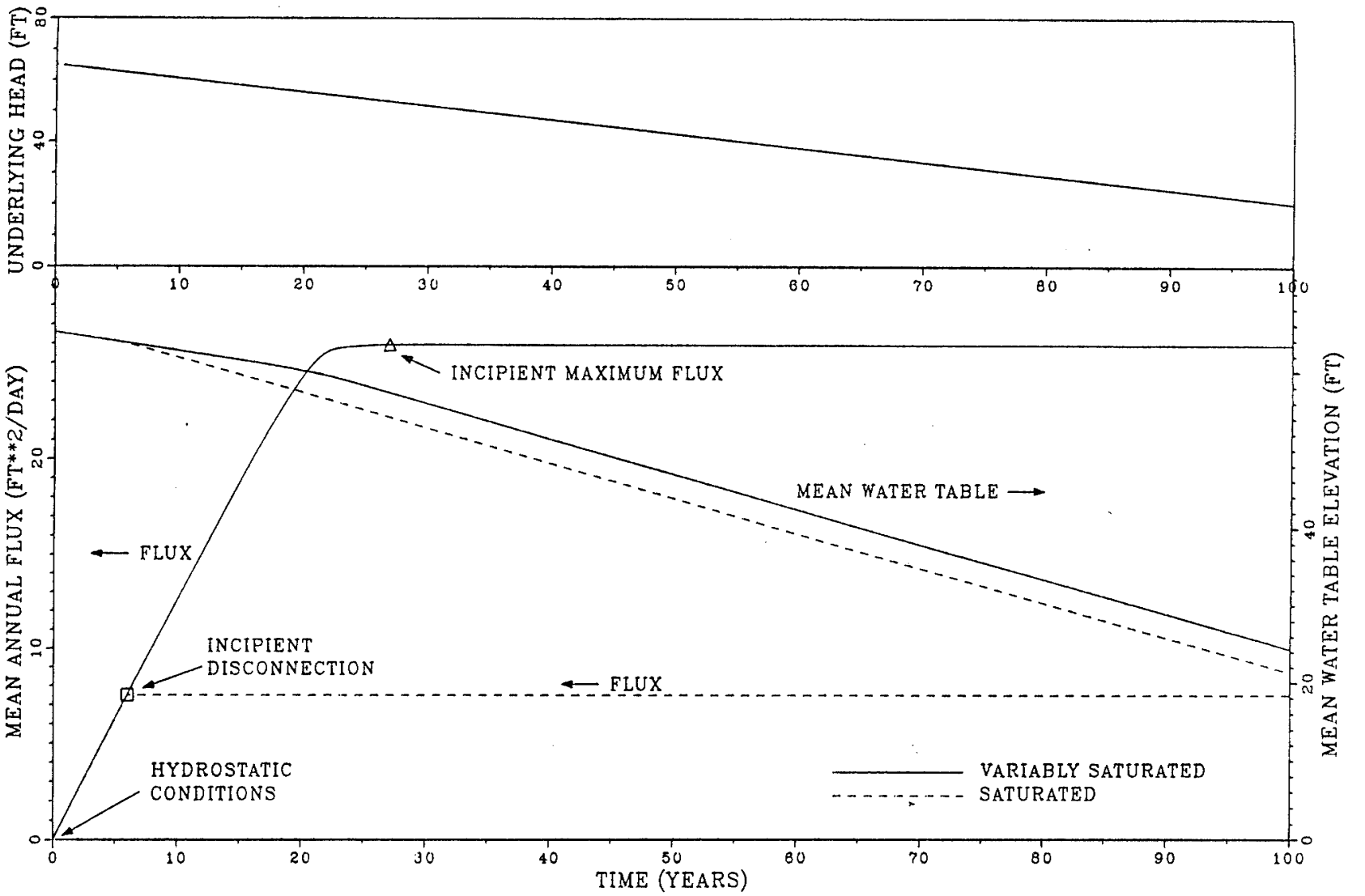

Fig. 55. Long term response of the reference simulation domain to progressively declining hydraulic heads in the underlying aquifer (underlying head) as determined by the saturated and variably saturated flow codes.

clogging layer when stream and aquifer are disconnected. It is commonly assumed in conventional modeling schemes that atmospheric pressure persists at the base of the clogging layer in any disconnected stream-aquifer system; consequently, maximum flux conditions are assumed the moment disconnection occurs. In reality, a steady state maximum stream infiltration rate is only observed when the water table lies at some distance below the stream. The few algorithms that have been designed to take into account negative pressures underneath a stream assume that those pressures remain constant regardless of depth to the water table. Hence, none of the techniques included in this latter category are capable of determining variable fluxes frequently observed under disconnected stream/shallow water table conditions.

Comparisons of system flow and water table measures predicted by the variably saturated flow code SATURN (Huyakorn et al., 1984) and the saturated flow simulator AQUIFEM (Townley and Wilson, 1980) have been made for several example simulations. Both steady state and transient cases have been included in the comparisons. Based on the selected examples, there appears to be a significant tendency for saturated flow models to seriously underestimate stream losses, hydraulic heads and water table levels for disconnection conditions. Such errors seem particularly possible if a model is calibrated for connected stream conditions and is later used to predict stream losses and head configurations in a disconnected system. The comparisons made in the example simulations tend to suggest that it is the inability of saturated flow simulators to accurately predict the stream loss rate that is the major cause of disparities between water table levels determined by SATURN and AQUIFEM. Other factors affecting the disparities, such as assumed Dupuit flow conditions in the saturated

code, appear, in some cases, to be of much less consequence. An example simulation with AQUIFEM, in which the stream loss rate was revised to a correct value, resulted in a water table profile that reasonably approximated the profile determined by SATURN for the same problem.

XI. IMPLICATIONS FOR APPLIED MODELING

Consideration of Various Modeling Approaches

When modeling stream-aquifer systems in which streambed clogging is pervasive, the propensity of most saturated flow models to underestimate stream losses and water table levels for disconnected conditions should be of concern. In many engineering projects and water resource studies, this problem should not be overlooked.

A logical conclusion reached from such concerns is that models of actual stream-aquifer systems should be based on variably saturated flow theory. Previous investigators have made similar arguments based partly on laboratory results (e.g., Vauclin, et al., 1979) and on numerical simulations performed on a larger scale (e.g., Winter, 1983). But, as has been emphasized in this study, numerical simulation of combined saturated-unsaturated flow on a regional scale is not easily accomplished.

Even if numerical obstacles to successful simulations were minor, it can be argued that modeling of unsaturated media flow for large-scale simulations is of limited utility. Part of the argument centers around the fact that it is virtually impossible to determine unsaturated soil properties for areas of considerable size. Large variations in these properties are often observed over very short distances. Accordingly, the cost of attempting to reasonably characterize unsaturated media on a regional scale, (whether it be through point sampling, field permeability tests, stochastic methods, etc.), is, for all practical purposes, prohibitive.

Why then even consider the effect of variably saturated flow in modeling studies on a scale that exceeds, say, tens of feet? The

answer to this question seems to lie in the objective of the modeling. In the case of stream-aquifer simulations, the objective would appear to be the need to grasp the effects of negative pressure heads on stream infiltration rates, subsequent movement of that infiltrated water across an unsaturated zone, and ultimately how the concomitant recharge of the water table influences heads in the saturated areas. Clearly these factors come mostly into play when disconnection phenomena are present.

With these objectives in mind, it would seem that saturated flow codes could be improved if unsaturated flow properties were to some degree included, even if exact measures of those properties were impossible to obtain. For instance, when computing infiltration flux across a clogging layer, attempts to estimate the negative pressure heads at the base of the clogging layer, such as in (16) or (17), would at least partly counteract gross underestimates of stream flux that might come about should the simpler algorithm of (15) be applied.

Some investigators might play down the importance of negative matric pressure heads on the underside of the clogging layer and instead emphasize the use of strictly saturated flow codes that simulate vertical flow as well as horizontal. The intent here would be to partly overcome some of the problems typically encountered when applying simulators based on Dupuit flow theory to unconfined aquifer simulation. For instance, the use of finite element codes in which the finite element mesh can be varied to fit a changing phreatic surface boundary (e.g., Neuman and Witherspoon, 1970; 1971) might be promoted. Such codes are obviously beneficial to investigations where analysis of vertical head distributions is an important objective. But in many studies of large-scale groundwater flow in unconfined aquifers,

determination of spatial and temporal variations in the water table is all that is required. As has been demonstrated in the previous chapter, the effects of vertical saturated flow on water table levels in some unconfined stream-aquifer systems can be relatively minor. The benefits derived from using the so-called adaptive gridding techniques in such situations would, consequently, appear to be limited. Furthermore, the nonlinear "free surface" boundary inherent in this type of model (e.g., Neuman and Witherspoon, 1970) requires an iterative solution scheme, much in the manner of a variably saturated flow simulator. Therefore, it is questionable as to whether such non-linear saturated flow codes would be more "efficient" than comparable codes that handle both unsaturated and saturated zones.

Fixed grid, three dimensional, saturated flow codes that exclude elements (or blocks) located above the water table would also appear to be of limited utility in representing stream-aquifer processes when disconnection exists. An example of a commonly used 3-D model that falls into this category is the USGS modular flow code (McDonald and Harbaugh, 1984). In this finite difference simulator, when a block (in the upper layer of blocks) becomes desaturated, it is automatically considered to be nonactive. Consequently, should such a block happen to underlie a losing stream, stream losses in this block that were previously considered a source of recharge to the saturated zone are no longer counted as a source of water. Hence, in this 3-D simulator, the stream becomes artificially severed from the groundwater domain, although this does not happen physically. McDonald and Harbaugh's (1984) modular code provides its users with a stream seepage algorithm like that in (15) for estimating stream fluxes.

From the foregoing paragraphs, one develops the impression that the effects of unsaturated media in the modeling of subsurface water flow should not be overlooked. Yet the development of variably saturated models for regional groundwater analyses currently seems infeasible. Moreover, many of the existing saturated flow models, some of which are widely used, possess shortcomings that tend to limit their application to some of the intrinsic problems exhibited in stream-aquifer systems. It seems, therefore, that improved techniques are needed that can better estimate stream losses for disconnected stream conditions, and that can be easily incorporated into existing flow codes.

Suggestions for Applied Modeling

To help circumvent some of the difficulties that stem from the inability of most conventional flow models to accurately estimate stream losses under disconnection conditions, an approximate technique is proposed here for catching the gross influence of partially saturated media located below a streambed under disconnected conditions. This technique is similar to earlier discussed techniques (Bouwer, 1969; Rovey, 1975; Dillon and Liggett, 1983) in that it assumes the presence of a clogging layer and that seepage across any portion of the clogging layer is at all times represented by fully saturated, one dimensional, steady flow. In addition, it is not entirely novel since previous investigators (e.g., McWhorter and Nelson, 1979) have used methods for determining seepage rates from surface water bodies that jibe with suction heads below flow impeding surface layers. However, the suggested approach does differ from existing schemes in that the stream infiltration rate during

disconnection is allowed to vary with water table depth. Consequently, it is assumed that a means exists to estimate pressure head at the base of the clogging layer (ψ_{sb}) for various values of water table depth and stream stage. Once ψ_{sb} is determined, the stream flux rate is determined by

$$q_s = \frac{K''}{B} (H_s - H_b - \psi_{sb}) \tag{19}$$

where all parameters are as previously defined.

A pictorial representation of the proposed method is provided in Figures 56a and 56b. The first figure consists of a schematic showing the spatial relationship of the parameters that are used in equation (19). The second is a graph of suction head at the base of clogging layer ($-\psi_{sb}$) versus depth to the water table (below the clogging layer) for a specific set of clogging layer and aquifer parameters (see Figure 56b). Three curves have been plotted in this example, each corresponding to a different stream stage. The data for this particular case have been prepared via a series of steady runs with SATURN. Figure 56b is instructive in the sense that it shows there are several factors that ultimately influence the stream seepage rate. Although depth to the water table has been emphasized as being an important parameter (primarily because traditional methods of estimating stream loss rates have ignored it), it should be remembered that other necessary variables include clogging layer and aquifer material properties, as well as the stream stage.

When this proposed method is applied in a saturated flow simulator under disconnected stream/shallow water table conditions, determination of the proper depth to water table becomes part of the solution to the

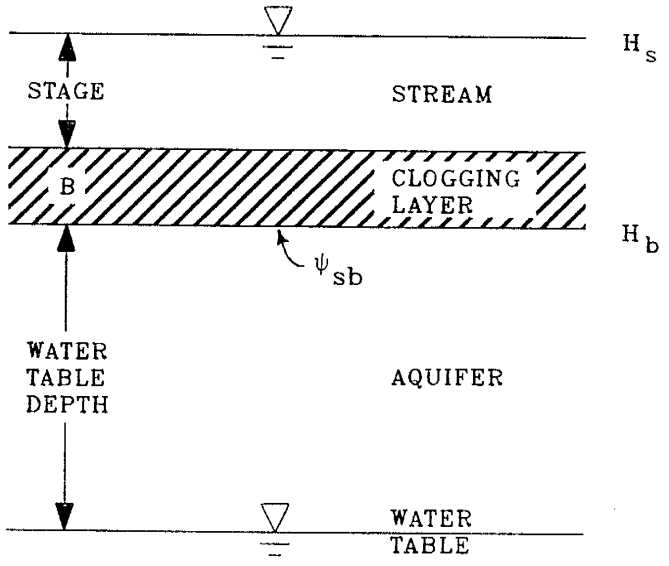

a

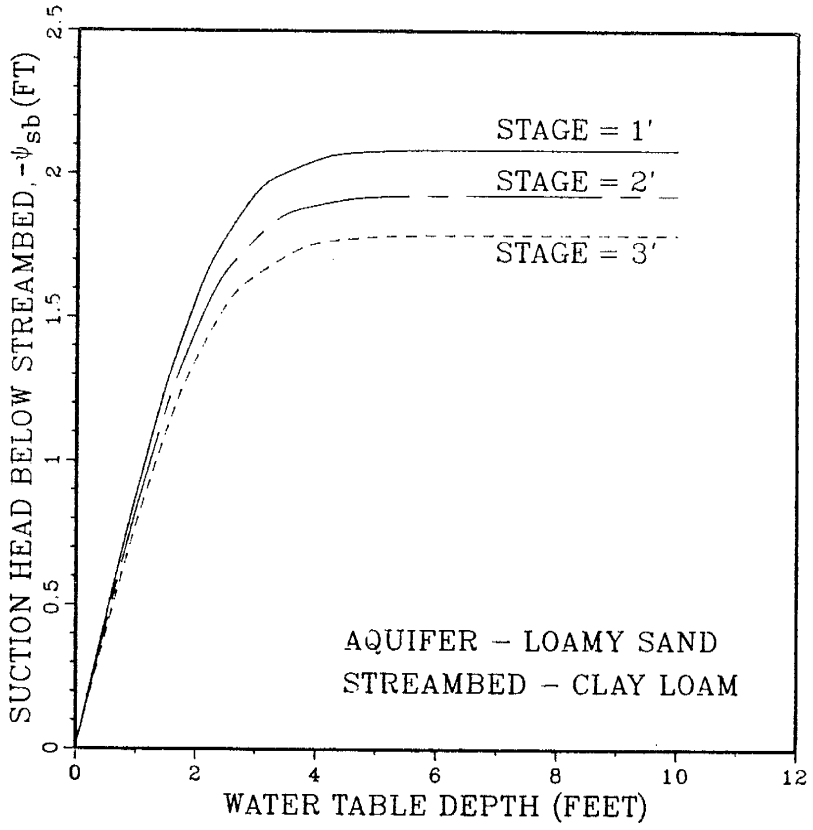

b

Fig. Explanation of proposed method for determining stream loss rate: (a) spatial relationship of parameters and (b) example of suction heads versus water table depth for different stream stages.

nonlinear flow problem. Accordingly, a variety of numerical techniques (e.g., Newton-Raphson iteration, or time extrapolation of head in transient problems) can be implemented in the groundwater flow code to help assure that convergent solutions are achieved. When attempting transient solutions under disconnected stream/deep water table conditions, the proposed method is most appropriate if stream loss rates stabilize quickly relative to the duration over which stream stage is assumed constant. Findings from the transient simulations in this study suggest that stream infiltration rates for deep water table situations stabilize well within a day.

Concerns regarding the proposed algorithm need also be mentioned. For example, this scheme is applicable to surface waterways in which streambed clogging is present. In cases where it is absent, other approaches commonly used in saturated flow models should be considered. Methods falling into this latter category include prescribed head (Dirichlet) boundaries along stream courses, or head-dependent (Cauchy) boundaries that attempt to compensate for additional head losses created by strong vertical flow components near streams that partially penetrate the aquifer (see, e.g., Townley and Wilson, 1980). Unfortunately, the disconnection process in systems unaffected by streambed clogging, along with the formation of a saturated bulb underneath a stream, cannot be easily represented in most saturated flow simulators. In addition, the scheme exemplified by Figures 56a and 56b assumes that the aquifer beneath the streambed is relatively homogeneous for considerable depth below the clogging layer. In a stream-aquifer system wherein intensely stratified alluvium are found immediately below the stream, it is recommended that means be developed

to take into account this heterogeneity when developing graphs similar to those in Figure 56b.

Although the data from which Figure 56b is prepared has been determined from model runs with SATURN, it is not necessary that a numerical simulator be used to develop this information. Governing equations and boundary conditions for one-dimensional flow in a system such as that portrayed in Figure 56a can easily be developed. Accordingly, there is no reason to believe that these equations cannot be solved analytically. An example of one such mathematical analysis is provided by Zaslavsky, in Bear, Zaslavsky and Irmay (1968). Formulae are presented in this reference for determining flux rates and pressure profiles in an aquifer material whose unsaturated hydraulic conductivity varies exponentially with pressure head and in which disconnected stream/maximum flux conditions prevail. Whether such analytical solution approaches are more efficient than one-dimensional numerical simulators is still an issue; comparative testing of the two approaches for the various functional relationships that are commonly employed to characterize hydraulic conductivity of unsaturated soils would help to answer this question.

Regardless of the technique that is ultimately used to determine the pressure head data (ψ_{sb}) utilized in (19), the capacity of a saturated flow code to estimate stream losses is likely to be improved if the proposed method is properly applied. Incorporation of the algorithm for determining the needed pressure data directly into the code, or separate development of this data prior to execution of the saturated flow code, is left up to the code developer and its users.

Implications for the Mesilla Valley

The findings from this research are relevant not only to the generic issues of applied subsurface flow modeling, but also permit several tentative, general conclusions to be made regarding the behavior of Mesilla Valley subsurface hydrology. These conclusions further raise questions as to the applicability of conventional modeling techniques for predicting future groundwater flow in the Mesilla region.

If, as has been suggested by Peterson et al. (1984), groundwater levels in the Rio Grande flood-plain alluvium drop significantly due to proposed increases in regional pumping, it is likely that the influence of unsaturated flow on the valley's hydrologic system will become larger. Deeper water table levels suggest that suction heads beneath the Rio Grande channel and at the base of irrigation canals will generally increase. Accordingly, annual stream losses will probably become larger as the head differences across streambed clogging layers increase. The effects of declining water table levels are likely to be most evident along the Rio Grande as opposed to the numerous irrigation waterways. As was discussed in Chapter III, most irrigation canals in the Mesilla Valley are elevated above local water table levels. In some instances, depths to the saturated zone from canal bed levels appear to exceed ten feet or more. Consequently, disconnected stream/maximum seepage loss conditions probably already exist along many of the canal reaches. On the other hand, many portions of the Rio Grande remain hydraulically connected to saturated zones within the flood-plain alluvium, at least during portions of most years. It is likely, therefore, that the maximum stream infiltration rates associated with deep water table conditions will not be prevalent along

the river until such time that regional groundwater levels are substantially lowered.

Lower regional water table levels also infer that shallow sediments in the Mesilla Valley flood-plain alluvium will tend to impede recharge to the saturated domain. If results from the simple two-layered simulations in Chapters VIII and IX are translatable to the flood-plain alluvium, it is quite possible that disconnected conditions will exist even in areas where streambed clogging is relatively nonexistent. Along stream reaches where flow velocity is large, such as below diversion structures, shallow stratified materials, rather than streambed clogging, could be the major cause of disconnection. At locales where the transition from near-surface, poorly sorted soils to deeper, more uniform materials occurs at relatively shallow depths, disconnection will likely take place at shallower water table depths than would be required in areas where the transition is relatively deep.

Existing models of groundwater flow in the Mesilla Bolson (Gates et al., 1984; Peterson et al., 1984) are based strictly on saturated flow principles and are not explicitly designed to take into account the influence of unsaturated media on stream infiltration. Furthermore, the existing models have been calibrated using hydrologic data from years during which water table levels have remained relatively shallow. As yet, there has been no opportunity to test these models for their ability to simulate groundwater flow for conditions in which regional water levels are substantially lowered. Since it has been demonstrated in Chapter X that saturated flow simulators are susceptible to considerable error in predicting stream losses under disconnected flow conditions, the potential exists for

existing models of the Mesilla region to provide inaccurate estimates of drawdown due to future pumping in the area. This problem is of particular importance in the Mesilla Valley, as it appears (Peterson et al., 1984) that losses from the Rio Grande and appurtenant irrigation canals constitute a major source, if not the largest source, of subsurface water in the Rio Grande flood-plain alluvium.

The quasi 3-D model of Peterson et al. (1984) uses the algorithm represented by equation (15) to compute all stream losses. Since this scheme assumes atmospheric pressures to exist at the base of a streambed clogging layer whenever disconnection occurs, it is probable that predictive simulations with the quasi 3-D model for assessing the effect of a large proposed well field west of the Mesilla Valley tend to underestimate future losses from local surface waterways. Consequently, it is also likely that the rate of drop in local water table levels will not be as rapid as has been indicated in Peterson et al. (1984). To help counteract this possibility, revision of the quasi 3-D code (or any similar type of code) is recommended to take into account increasing suction heads along the channel bottoms of the Rio Grande and neighboring canals. The proposed method described in this chapter (equation (19)) is an example of a technique that would suit this purpose.

The ability of the model of Gates et al. (1984) to accurately predict drawdowns brought about by future pumping is also uncertain. This model of the southern Mesilla Bolson treats the Rio Grande as a prescribed head (Dirichlet) boundary. However, as has been surmised by Peterson et al. (1984), a large portion of the river in the southern Mesilla Valley appears to be occasionally disconnected from the underlying water table due to the presence of a muncipal well field

located near the town of Canutillo (see Figure 6, Chapter III) and considerable evidence of streambed clogging in the valley (New Mexico State University, 1956). Hence, stream loss estimation methods that take into account disconnection, such as those presented in equations (16), (17) and (19), are expected to be more appropriate for groundwater models of the southern Mesilla Valley, rather than the assumed Dirichlet boundaries in Gates et al. (1984).

XII. SUMMARY, CONCLUSIONS AND RECOMMENDATIONS

Two-dimensional (cross-sectional) simulations have been performed of variably saturated (saturated-unsaturated) subsurface flow to examine hydraulic phenomena in stream-aquifer systems. The numerical simulations are of a generic nature in that the domains studied are quite simple, and not, in a strict sense, based on any actual stream-aquifer system. However, many of the generic cases are loosely patterned after conditions frequently observed in the Mesilla Valley flood-plain alluvium aquifer, found in the New Mexico's lower Rio Grande Valley. Therefore, findings from these simulations relate to hydrologic processes of the Mesilla Valley and similar areas. The results of both steady state and transient solutions to variably saturated problems are included in this report. Both types of simulations show that the influence of unsaturated flow is indeed significant in stream-aquifer processes.

All of the simulations have been conducted for losing streams. As a consequence, the simulation results are mostly applicable to systems in which regional water table levels lie below stream levels. Such losing stream conditions may occur because of regional groundwater pumping, or may be due to natural causes. Much of this work is particularly relevant to stream-aquifer systems found in arid to semi-arid regions. Although the analyses in this study deal mostly with perennial streams, many of the findings are relevant to processes occurring near ephemeral watercourses. In addition, despite the fact that simulations are limited to two-dimensional cross sections, much of what is presented also has bearing on the effects of pumping wells near streams.

In an effort to analyze stream-aquifer behavior under a variety of conditions, several hundred simulations have been performed. The number of cases analyzed in this research far exceeds those examined in previous studies of similar nature. Unfortunately, it is impractical to discuss the results from all of the simulations. Instead, the cases examined in this report are limited to those determined by the author to be most descriptive of the influence of unsaturated flow in stream-aquifer domains.

Casual discussion of the simulation results somewhat belies the fact that considerable numerical difficulties have been encountered in attempting to obtain accurate solutions to the highly nonlinear problem of variably saturated seepage. Steady state simulations in two-dimensions are particularly difficult to achieve since the mathematical and numerical formulations for problems of equilibrium flow in unsaturated soils often lead to poorly conditioned series of equations that are not easily solved. Several different numerical codes have been tested for their ability to handle the types of problems dealt with in the stream-aquifer simulations of this study. The variably saturated flow code called SATURN, (Huyakorn et al., 1984) has been selected to conduct both steady state and transient simulations. Features of this code, especially those that enable it to handle the somewhat intractable problems dealt with in this research, are discussed in both the text of this report as well as in an appendix (Appendix A). Explanations of the intrinsic difficulties associated with nonlinear variably saturated flow problems, and the comparative advantages and disadvantages of the codes that have been tested, are also provided.

Two major states of stream-aquifer relationships are distinguished in this study: hydraulic connection and disconnection. The first of these has been defined as the case in which the saturated zone of an aquifer is connected to an overlying stream, at least to some extent, by fully saturated media. Hydraulic disconnection, on the other hand, infers the existence of an unsaturated area that completely separates a saturated zone of soil, located immediately below a stream, from deeper saturated zones. It has been demonstrated, via general hydraulic considerations and the numerical simulations that this study entails, that a variety of factors influence the occurrence of disconnection.

Within the two major classifications of connection and disconnection, four subcategories of stream-aquifer relationships are also defined to help facilitate description of various interactive processes between a surface waterway and an adjoining aquifer. The four, listed in the order in which they are observed with a declining water table, are: (1) connected gaining stream, (2) connected losing stream, (3) disconnected stream with a shallow water table, and (4) disconnected stream with a deep water table. Hydraulic processes associated with each of these stream-aquifer relationships, primarily with respect to steady state flow, have been described in detail. Under the first three relationships, local water table levels have an effect on the steady state seepage either to or from a stream. The fourth and last category, i.e. disconnected stream with a deep water table, signifies conditions in which the steady flow from a stream is a maximum for a given set of stream-aquifer properties, and is independent of depth to the water table.

All of the generic domains considered in the variably saturated analyses have consisted of a stream and an adjoining aquifer, at the

base of which lies an aquitard layer. Some of the simulations also include a streambed clogging layer, which is usually a layer of fine-grained material (silt and/or clay) found on the beds and banks of surface waterways, and that tend to inhibit flow both from and to a stream. Although not considered part of the simulation domain, an additional aquifer has been assumed to underlie the basal aquitard. Hydraulic heads in this "underlying" aquifer (referred to as underlying head) are varied to assess the response of the overlying stream-aquifer system to regional groundwater level declines. A variety of materials have been assumed to comprise the various units making up each simulation domain. Layered aquifer domains have been considered in addition to homogeneous aquifers. As hydraulic heads in the aquifer underlying each simulation domain are incrementally reduced, the conversion from connected losing stream conditions to those of a disconnected/shallow water table case, and from a disconnected stream/shallow water table situation to disconnected stream/deep water table conditions, are observed to take place at a single value of underlying head. These "points" of conversion are referred to as the point of "incipient disconnection" and the point of "incipient maximum flux," respectively.

Results from the variably saturated simulations are analyzed via cross-sectional contour plots of hydraulic head and moisture content, vertical profiles of pressure head, graphs of steady state system flux versus hydraulic head in the underlying aquifer (underlying head), and the behavior of water table levels with reductions in underlying head. Of the above-mentioned stream-aquifer relationships, only those dealing with losing streams (i.e., (2) through (4)) have been examined. The means by which each of these relationships manifest themselves in flow

and water table behavior is illustrated. The variably saturated runs are also used to determine system responses to such factors as aquifer material, streambed clogging (or absence thereof), aquifer dimensions, layering of aquifer materials and depth of flow in a stream (i.e., stream stage).

Subsequent to the generic steady state and transient analyses with the variably saturated flow code, an evaluation has been made of the inherent differences between the approaches taken in variably saturated flow modeling and the more traditional techniques used in conventional saturated flow models. Comparative assessments of the two approaches serve to highlight some of the shortcomings of the traditional modeling schemes. Comparisons are made between actual results (both steady state and transient) from SATURN and a saturated flow simulator (AQUIFEM, Townley and Wilson, 1980) for a few stream-aquifer systems. Disparities in computed fluxes and water table elevations from the two codes help illustrate the degree to which saturated flow models can be in error, which in turn indicates that these models need be improved to make allowances for the effects of unsaturated media. One such improvement, in the form of a revised technique for estimating stream losses under disconnected conditions, is suggested. Comparative analyses of variably saturated and typical saturated simulators, along with the results of the generic simulations made with the variably saturated flow code, help shed light on some of the hydrologic processes now existing and expected to occur in the Mesilla Valley. Concerns are also raised regarding the ability of existing saturated flow models of the Mesilla region to accurately predict stream-aquifer phenomena under future conditions.

Conclusions from Steady State Analyses

The following consists of a brief summary of steady state, variably saturated flow simulations conducted for generic stream-aquifer systems and the conclusions derived there from:

(1) In a series of simulations with a homogeneous aquifer overlain by a stream whose bed and banks are clogged, it has been demonstrated that the clogging layer is capable of inducing hydraulic disconnection. Furthermore, the clogging layer eventually leads to the maximum flux conditions associated with a deep water table if hydraulic heads in the underlying aquifer (underlying head) are sufficiently reduced.

(2) In the above mentioned steady state runs, head and moisture content distributions are observed to become more complex as hydraulic heads in the underlying aquifer (and, therefore, water table levels in the simulation domain) are reduced. In all simulations, flow activity and hydraulic gradients are greatest near the stream, and gradually become less with distance from the stream.

(3) Flow in the unsaturated zone takes place in all of the losing stream situations regardless of the value of underlying head. The effect of the unsaturated zone is relatively minor in connected stream instances, and becomes larger as disconnected stream/deep water table conditions are approached. In the case of steady state flow through a disconnected system, all water infiltrating from the stream, must at some point or another, pass through unsaturated media.

(4) In the case of a disconnected stream with a deep water table, relatively constant pressure heads (and moisture contents) are observed within much of the unsaturated aquifer (homogeneous) material underlying a clogging layer. Constant pressure head infers a vertical pressure head gradient of zero within much of this unsaturated area, which in turn signifies that a constant (maximum) infiltration rate from the stream exists.

(5) The response of steady state (stream-aquifer) system flux to declining underlying head is approximately linear over most of the connected losing stream and disconnected stream/shallow water table phases. System fluxes only show a tendency of leveling out to a constant value just prior to the point at which maximum flux first takes place (i.e., point of incipient maximum flux).

(6) The response of system water table measures to decreasing underlying head can be relatively simple to complex, depending on materials that make up the porous media. In a simple case, two relatively linear slopes are exhibited by the curves that depict water table changes with declining

underlying head. Transition between the two linear segments takes place over the range of underlying heads just prior to the point of incipient maximum flux, and the rate of water table drop with decreasing underlying head is larger after maximum flux conditions are reached. More complex responses, especially for the spatial maximum water table level, are observed in an aquifer material possessing a relatively low saturated hydraulic conductivity. Each of the various stream-aquifer relationships are observed over a larger range of underlying heads in such aquifer materials.

(7) Unsaturated hydraulic conductivities of the aquifer materials affect the rate of seepage loss from a stream, especially in disconnected systems. Flow from a disconnected stream whose streambed is clogged cannot be determined until all properties of the stream-aquifer system have been considered, including the interrelated hydraulic conductivity-pressure head characteristics of the aquifer material, and clogging layer and stream properties.

(8) As expected, the infiltration rate from a stream increases with increasing saturated hydraulic conductivity of the clogging layer. Test simulations with homogeneous aquifers overlain by unclogged streams suggest that flow spreading due to capillarity is not always the sole cause of disconnection in actual stream-aquifer systems. Rather, flow spreading promoted by the combined effects of capillarity and aquifer heterogeneity at shallow depths appears to be a likely cause of disconnection in situations where the streambed is unclogged.

(9) In a homogeneous aquifer overlain by an unclogged stream, the potential for disconnection, induced by capillarity alone, appears to increase as (a) the width of the stream decreases, (b) stream stage is reduced, (c) saturated hydraulic conductivity of the aquifer becomes lower, and (d) the depth over which homogeneity is maintained in the aquifer increases.

(10) For sufficiently wide aquifers, the maximum steady state stream loss rate from a clogged stream is not affected by aquifer width.

(11) Two-layered aquifer systems, in which a relatively nonuniform textured soil overlies a texturally uniform, more permeable material, are conducive to disconnection conditions even if the stream connected to such a system is unclogged. Disconnection under steady state flow conditions takes place after the local water table drops below the material interface separating the two layers. The upper aquifer layer appears to act much like a large clogging layer in the sense that it impedes downward movement of water infiltrated from the stream.

(12) In the two-layered aquifer system, the conversion from connected losing stream conditions to disconnected stream/shallow water table conditions is an abrupt process.

The conversion to disconnection takes place at a single value of underlying head, as is the case for all of the steady state stream-aquifer analyses. Prior to disconnection, a saturated plume of water connects the stream to the underlying water table; after disconnection has taken place, a saturated bulb of water exists below the stream, entirely within the upper layer and separate from the water table.

(13) In the two-layered aquifer system, maximum stream loss rate increases with decreasing thickness of the upper aquifer layer. A system with a shallow interface undergoes disconnection at shallower water table levels than is needed in cases where the interface is deep.

(14) Results of simulations with the two-layered stream-aquifer system can be related to processes that occur in aquifers associated with underfit streams. In such real aquifers, however, it is improbable that two largely homogeneous units, separated by a distinct interface, will exist. Rather a shallower aquifer zone, generally consisting of texturally nonuniform, stratified, and generally low permeability materials, overlies relatively uniform, coarse grained and highly permeable materials at greater depth. In addition, a so-called material interface is replaced by a gradual transition from one general zone of alluvial sediments to another. Nonetheless, it is believed the net effect of systems associated with underfit streams is the same as that observed in the simple two-layered simulations, in that shallow aquifer materials impede the downward movement of stream water, consequently helping to bring about disconnection.

Conclusions from Transient Analyses

Transient simulations have been performed mostly for the purpose of determining temporal response of generic stream-aquifer systems to seasonal changes in stream stage. In each of three separate transient runs, the stream-aquifer systems respond quickly enough such that a "dynamic equilibrium" (e.g., Freeze, 1969) exists in each over the course of the simulation year. For this reason the transient simulations might more appropriately be called "quasi-steady state" simulations. The relatively rapid response of the simulated stream-aquifer systems also allows the long-term behavior of these systems to

be examined through an approximate analysis of successive quasi-equilibrium phases during a 100-year period of progressively declining regional groundwater levels.

Conclusions derived from the transient simulations are:

(1) System inflow (i.e., stream infiltration rate) is strongly influenced by water table elevation in the case of a disconnected stream with a shallow water table. After an initial increase in stream infiltration rate due to a rapid rise in stream stage, the stream loss rate gradually declines in response to water table levels that are rising from increased recharge. The opposite effect is observed after the stream stage quickly drops, i.e., the stream infiltration rate gradually increases (after an initial drop in rate) in response to a steadily dropping water table.

(2) In contrast, the stream infiltration rate in a disconnected stream/deep water table situation stabilizes relatively quickly (<1 day in the runs made in this study) to a constant value after a change in stream stage. This is explained by the speed with which pressure heads beneath the stream (i.e., below a clogging layer or at the base of a saturated bulb in the case of an unclogged stream) reach a constant value after a change in infiltration rate first occurs.

(3) The speed with which a disconnected stream-aquifer system reaches a new equilibrium state after a change in stream stage is heavily dependent on the extent to which the system is unsaturated. For example, equilibrium is usually reached more quickly in a disconnected stream/shallow water table situation than in a case where all conditions are identical other than the fact that the water table is considerably deeper. Despite the fact that system inflow may be greater in the deep water table instance, the larger unsaturated zone across which stream water must flow, and in which hydraulic conductivities and moisture contents are considerably lower than observed in their saturated counterparts, will increase the response time to changes in stream loss rate.

(4) In the case of a disconnected stream with a deep water table, the response time is not necessarily always slow. Using the example of a two-layered aquifer which is overlain by an unclogged stream, it can be demonstrated that a system responds quite rapidly, even under deep water table conditions, because the saturated bulb extending from the base of the stream penetrates deep into the upper aquifer layer. Moreover, high stream loss rates, attributed to the absence of streambed clogging layer, help to maintain relatively high hydraulic conductivities in the unsaturated zone of the lower layer situated below the stream.

(5) In disconnected stream/deep water table situations, wherein the streambed is clogged, the pressure pulse originating at the base of the stream on the underlying saturated zone can

be somewhat delayed. In one of the example simulations in this study, the lag time between an initial increase in stream infiltration rate and concomitant water table rise is on the order of 0.5 days. Significant increases in system outflow (aquitard leakage) are not observed until a full day has elapsed after the initial increase in stream loss. Such delays may be of consequence if a modeling study is concerned with system response over periods spanning several minutes to a few days. In longer duration simulations, however, the effect of these delays is probably of less importance.

(6) Long-term responses of two example simulation domains to steady declines in regional groundwater levels indicates that tens of years may elapse before a system that is currently connected to an overlying stream undergoes the transition to disconnected stream/maximum stream loss rate conditions. After a system enters the so-called maximum flux phase associated with a deep water table, and presuming regional groundwater levels continue dropping at the same rate as prior to this phase, average local water table levels begin dropping at a faster rate than is observed before the phase change.

Model Comparisons and their Implications

Because few saturated flow models fail to take into account the effect of unsaturated media below a stream, serious errors can result in using such models to simulate groundwater flow under deep water table conditions. Findings from the comparisons between simulator types, and the implications that they have for analyses of real stream-aquifer systems are as follows:

(1) Most conventional saturated flow models assume that atmospheric pressures exist at the base of a clogging layer when stream and aquifer are disconnected; consequently, maximum stream loss rates are automatically assumed regardless of depth to the water table. Failure to take into account the suction heads at the base of a clogging layer can cause saturated flow codes to underestimate both the stream infiltration rate and water table levels.

(2) Because of different techniques used to compute stream loss from disconnected streams in variably saturated flow codes and most saturated flow simulators, results from the two model types tend to diverge most greatly from each other when the saturated simulator assumes that disconnection exists.

(3) Potentially serious errors can result if conventional saturated groundwater flow models of stream-aquifer systems are calibrated for connected stream or disconnected

stream/shallow water table conditions and are subsequently used to predict stream losses and head configurations under deep water table conditions.

(4) The greatest cause of disparities between results from variably saturated and saturated simulations of generic stream-aquifer systems can often be attributed to the inability of the strictly saturated simulator to properly estimate stream loss rate, rather than its inability to properly take into account vertical flow when Dupuit flow assumptions are invoked.

(5) An earlier modeling study of groundwater flow in the Mesilla Bolson (Peterson, 1984) suggests that groundwater levels in the Mesilla Valley will show significant declines if proposed groundwater pumping schemes are activated. Lower water table levels suggest that disconnection of the Rio Grande and many irrigation canals in the valley from the underlying water table will become more prevalent. It is likely that the quasi 3-D model of Peterson et al. (1984) underestimates stream losses under future conditions, as this model is calibrated for the shallower groundwater levels observed today, and is incapable of allowing for increased suction heads occurring beneath streams as water levels drop.

(6) Existing groundwater flow models of the Mesilla Valley, or of any similar region, would likely be improved if methods were incorporated into them to make allowances for the effects of unsaturated media beneath a stream. One such method is recommended in this study that attempts to estimate suction heads on the underside of a clogging layer for different streambed properties, aquifer material characteristics, stream stages and depths to the water table.

Recommendations

The finding of this study are based mostly on observations taken from two-dimensional cross-sectional simulations of variably saturated flow in relatively simple systems. Translation of these findings to actual stream-aquifer systems infers that such systems largely obey the assumptions upon which the two-dimensional analyses have been based. In reality, however, these assumptions are never strictly met. For instance, in many stream-aquifer systems, subsurface moisture flow does not lie entirely within a vertical plane lying normal to the stream axis; components of flow oblique to this plane are commonly observed.

Consequently, there is a great need for three-dimensional (3-D) modeling of variably saturated flow in stream-aquifer systems. Generic simulations of a similar nature to those performed in this study would go a long way toward answering questions raised regarding 3-D flow processes in real systems. One phenomenon worthy of investigation would be the tendency of streams, such as the Rio Grande, to exhibit both connected and disconnected zones over a given river reach. Processes affecting the location of the transition line separating the zones and thus, the recharge processes occurring in each, could be examined.

To carry out such a proposed 3-D modeling exercise, a code that includes a robust nonlinear solution algorithm, such as Newton-Raphson techniques, would probably be necessary. Otherwise, the conditions accompanying disconnection combined with a deep water table would be virtually impossible to simulate. As of this writing, the authors are unaware of any public domain codes that possess this feature and that handle variably saturated subsurface seepage.

In addition to the obvious benefits of 3-D codes in attempting to simulate real subsurface flow systems, 3-D simulators also permit study of the effects of varying channel properties along the length of a surface waterway. Recent research by Stephens et al. (1987) has demonstrated that streambed clogging is a highly variable process. The potential exists for a given channel cross-section to exhibit substantial clogging, with other nearby sections being devoid of any such feature. Clogging is also very much a transient phenomenon, with semipermeable streambed layers existing at times and essentially disappearing at others (Stephens et al., 1987). Stream stage is another factor that exhibits considerable spatial and temporal

variability, especially in ephemeral water courses such as arroyos. Other important processes that exhibit complexity in both space and time are infiltration and evapotranspiration. Three-dimensional transient simulators of variably saturated flow would certainly be most suitable for capturing the effects of such spatial and temporal variability.

Along with three-dimensional simulations, continued field investigation of actual stream-aquifer systems is also advised. Much needs to be done to characterize the spatial and temporal variability of sediments underlying stream channels.

Work pertaining to aquifer stratification and the means by which it diminishes downward transport of water that has infiltrated the subsurface from surface waterways is also suggested. This research has only briefly addressed the effects of aquifer layering, primarily with a system containing two layers of quite different aquifer material. Additional simulations involving highly stratified and variable domains, particularly at the shallower depths where such characteristics are apparently common in aquifer systems associated with underfit streams, are recommended. Accordingly, modeling of the effects of moisture dependent anisotropy would also be helpful for better understanding infiltration from surface waterways.

In conjunction with the above-given recommendations to further study the influences of stratification and moisture dependent anisotropy, stochastic modeling (e.g., Monte Carlo simulations) of variably saturated flow in stratified domains would also be beneficial. Carrying out modeling exercises of a stochastic nature would, of course, necessitate synthetic generation of material property fields

that meet the statistical characteristics of typical stratified alluvial domains.

APPENDIX A

CURSORY REVIEW OF TESTED NUMERICAL SIMULATORS

In this appendix, a qualitative analysis is presented for the variably saturated flow codes that have been tested to varying degrees as part of the stream-aquifer project. Five separate computer codes are discussed in this section. The five, listed by their popularly used acronyms, and in the approximate order in which they were examined, are: (1) TRUST, (2) UNSAT2, (3) FEMWATER, (4) T3FEMWATER and (5) SATURN.

It should be noted that several codes other than the five listed above were studied and considered for the stream-aquifer study. However, no further mention is made of these additional simulators, as this writer feels only qualified to discuss codes with which trial simulations have been made.

The following review should not be construed as an objective and exhaustive assessment of the variably saturated flow simulators that have been examined. This appendix can be more appropriately described as a subjective evaluation of existing codes for their capacity to handle saturated-unsaturated problems under largely dessicated conditions and within large domains. This is not meant to cast aspersions upon any of the codes included in the evaluation. Rather, the following essay is merely intended to provide the reader with an account of the advantages and difficulties that have been encountered in attempting to solve stream-aquifer problems.

In the following text, several beneficial (and perhaps deleterious) features of the simulators may be omitted from the analyses, merely because was felt they were irrelevant to this study's

concerns, or were possibly overlooked. It should also be noted that the comments herein have been mostly limited to features that have bearing on either code accuracy or efficiency. Extraneous items such as ease of model use and data input organization, have essentially been avoided.

TRUST

The TRUST simulator is based on the integrated finite difference method (IFDM). The code, written in FORTRAN IV, evolved from an earlier model (TRUMP) authored by Edwards (1968) and designed to accommodate heat transport. TRUST was initially used for unsaturated, porous medium flow problems by Narasimhan (1975). Published information concerning the code, including its underlying theory, details of the model algorithm and code applications were later presented in a series of Water Resources Research (WRR) articles (Narasimhan, 1976; Narasimhan and Witherspoon, 1977; Narasimhan, Witherspoon and Edwards, 1978; Narasimhan and Witherspoon, 1978). Later documentation of the code was provided by Reisenauer et al. (1982), along with a systematic description of data input organization.

Theory of TRUST

Because TRUST is based on the IFDM, the fundamental equation from which the simulator is formulated is not the same as the differential equation (Richard's Equation) for variably saturated flow given in the earlier chapter (Chapter VI, Equation 1) that described major features of SATURN. Instead, as the name of this method infers, an integral form of the governing equation is first developed. That equation, after some alterations, is written as

$$G + \int_{\Gamma} \rho_w \frac{k\rho_w g}{\mu} \nabla(z + \psi) \cdot n \, d\Gamma = M_c \frac{D\psi}{Dt} \qquad \text{(A-1)}$$

where

G = source term

Γ = closed surface of the domain of interest in the flow region

ρ_w = mass density of water

k = intrinsic permeability

g = gravitational constant

μ = coefficient of viscosity

z = elevation

ψ = pressure head

$\vec{n}$ = unit outward vector normal to $d\Gamma$

V = bulk volume

S = saturation

$\frac{D}{Dt}$ = total derivative

The coefficient of the total derivative found on the right-hand side of (A-1) represents the mass of fluid which the volume V can absorb due to a unit change in the average value of ψ over V. Following the mathematical reasoning of Reisenauer et al. (1982), this term, which is called the fluid mass capacity, M_c, can be expanded into three separate components such that

$$M_c = V_s \rho_w [Se\rho_{wo}\beta g + S\gamma_w \chi' a_v + e \, dS/d\psi] \qquad \text{(A-2)}$$

where

V_s = volume of solids

ρ_{wo} = density of water at atmospheric pressure

e = void ratio

β = coefficient of compressibility of water

γ_w = specific weight of water

χ' = parameter correlating change in effective stress and change in pore pressure

a_v = coefficient of compressibility of medium

The three terms on the right-hand side of (A-2) represent, respectively, the compressibility of water, deformability of soil skeleton and desaturability of pores. By taking into account the second of these terms, TRUST therefore attempts to simulate changes in available pore space in a deformable porous medium skeleton. The underpinnings of the deformable medium formulation stem largely from one-dimensional soil consolidation with some adjustments for unsaturated conditions. Deformation of the skeleton may be nonelastic. Although TRUST permits analysis of physical medium deformation, the numerical grid (discretization) remains fixed.

TRUST was originally developed with the idea of making it a versatile flow simulation tool. Besides its previously mentioned ability to account for soil deformation, two other features distinguish this code (Reisenaeur et al., 1982) from comparable simulators: (a) the mathematical model, along with its computational form, considers pressure-dependent density variations of water, and (b) the physical parameters in the governing equation are used in their primitive forms. By the latter, it is meant that, rather than explicitly reading in hydraulic conductivity values and storage parameters, hydraulic conductivities and fluid mass capacities are calculated within the model itself after data for "primitive" parameters such as intrinsic permeability, fluid viscosity, fluid density, gravitational constants, void ratio, and compressibilities

have been read. Thus, the mathematical foundation of TRUST is largely based on fundamental physical concepts rather than secondarily developed parameters evolved from simplified porous medium analysis. TRUST also attempts to represent soil moisture properties as realistically as possible by allowing for hysteresis.

Computational Algorithm of TRUST

TRUST uses a mixed explicit-implicit approach in setting up and ultimately solving the equations that describe flow between subregions of the flow domain. This equation solving scheme recognizes that, in a flow region with volume elements having widely varying time constants, isolated groups of elements with relatively small time constants are only weakly coupled to each other through other elements possessing larger time constants. As a consequence, it is necessary to solve simultaneous equations only for the isolated groups of elements with time constants less than the time step duration (Δt) that is currently being used. The outcome of this observation is that the conductance matrix resulting from equation formulation can be partitioned into one or more submatrices, with iterative computations only being necessary on some of the submatrices. Thus the solution scheme is ostensibly more efficient than other algorithms requiring extensive simultaneous solution of all equations developed by the model.

The mixed explicit-implicit scheme can be explained further by observing Figure A-1, which illustrates a typical model subregion that might be utilized with TRUST. Assume that the variation of ψ over this subregion is not rapid, and that the average properties within it are associated with a representative nodal point ℓ. Assume also that the subregion is chosen so that lines joining the nodal point ℓ to its

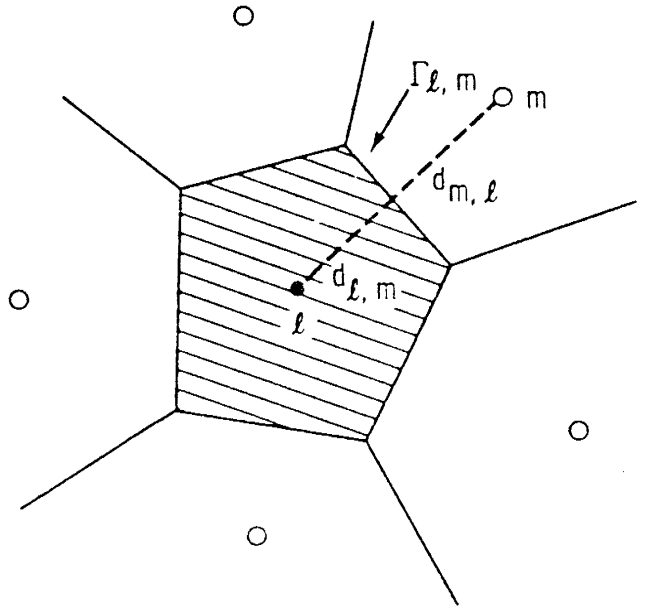

Fig. A-1. Volume element in TRUST associated with nodal point ℓ (after Reisenauer, 1982).

neighbor are normal to the interfaces that define the boundary between subregions. Furthermore, let the average properties associated with each nodal point be functions only of time, and assume that there is a spatially linear variation of these average properties between adjacent nodal points. Upon these premises, Equation A-1 can be applied to Figure A-1 to develop an explicit equation describing flow between two adjacent nodes

$$G_{\ell} + \sum_{m} \rho_{w} \frac{k\rho_{w}g}{\mu} \left[\frac{(z_m + \psi_m) - (z_{\ell} + \psi_{\ell})}{d_{\ell,m} + d_{m,\ell}} \Gamma_{\ell,m} \right] = M_{c,\ell} \frac{\Delta\psi_{\ell}}{\Delta t} \qquad \text{(A-3)}$$

Here, the subscripts ℓ and m are used to denote properties associated with elements ℓ and m, respectively. Note that $\Gamma_{\ell m}$ represents the area of the interface situated midway between elements.

Inspection of (A-3) shows that the quantity within the summation sign is equivalent to the flux across the interface separating elements ℓ and m. In this sense, the quantities k and ρ_w in (A-3) represent inter-element averages of these parameters at the interface $\Gamma_{\ell,m}$ between subregions. In heterogeneous domains, where elements ℓ and m are composed of different materials, TRUST calculates a harmonic mean of these parameters. The harmonic mean is used in order to preserve continuity of flux at the interface.

If we let $U_{\ell,m}$ represent the rate of flux across $\Gamma_{\ell,m}$ due to a unit difference between $(z_m + \psi_m)$ and $(z_{\ell} + \psi_{\ell})$, Equation A-3 can be rewritten as

$$G_{\ell} + \sum_{m} U_{\ell,m}[(z_m + \psi_m) - (z_c + \psi_{\ell})] = M_{c,\ell} \frac{\Delta\psi_{\ell}}{\Delta t} \qquad \text{(A-4)}$$

Equation A-4 can be solved explicitly (Reisenauer, et al., 1982) for $\Delta\psi_\ell$. The resulting equation is

$$\Delta\psi_{\ell,exp} = \frac{\Delta t}{M_{c,\ell}} \left\{ G_\ell + \sum_m U_{\ell,m}[(z_m + \psi_m) - (z_\ell + \psi_\ell)] \right\} \qquad \text{(A-5)}$$

where the subscript exp denotes the explicit nature of the equation.

Equation A-5 is used to solve for changes in ψ at each time step, only for those elements where a local stability criterion is met (Reisenauer et al., 1982). The criterion is stated in terms of a maximum allowable time step for each node. If the model time step is greater than the critical value for a given element, the node associated with the element is termed an implicit node, to which (A-5) cannot be applied. Instead, an augmented form of the equation that includes an implicit correction is used; the implicit equation can be written

$$\Delta\psi_\ell = \Delta\psi_{\ell,exp} + \frac{\lambda\Delta t}{M_{c,\ell}} \left\{ \sum_m U_{\ell,m}(\Delta\psi_m - \Delta\psi_\ell) \right\} \qquad \text{(A-6)}$$

Note that λ is an interpolation (stability) parameter, whose values can range from 0 (forward differencing) to 1 (backward differencing). The local nature of stability and the form of (A-6) suggest that in order to carry out the solution process over the entire simulation domain, one could first compute $\Delta\psi_{\ell,exp}$ for all the nodal points in the flow region and compute the implicit correction only for those elements whose stability limit is exceeded by the time step duration. Indeed, this is the approach taken in TRUST, with a Point-Jacobi type iterative scheme used for evaluating the implicit equations.

All boundaries of a flow domain are handled in TRUST by a general head (see for example, McDonald and Harbaugh, 1984) boundary algorithm. That is, the entire domain boundary is formulated as if it were head dependent. Correspondingly, any boundary type, whether first (Dirichlet), second (Neumann), or third (Cauchy) type, is developed by manipulating a conductance term that comprises the coefficient of the head differential between an interior and exterior node (Reisenauer et al., 1982) located on the boundary. It naturally follows that system mass balance calculations also utilize the general head boundary algorithm.

Advantages of TRUST

It is apparent from the foregoing discussion that TRUST has been designed to be versatile. Incorporation of the IFDM along with a generalized means of inputting geometric data broaden the code's capabilities in the sense that it does not intrinsically differentiate between a one-, two-, or three-dimensional problem. In accordance with this philosophy, the variety of polygonal shapes one may use for subregions, such as the one depicted in Figure A-1, is apparently endless.

TRUST's ability to simulate skeleton deformation is an advantageous feature that many other flow simulators do not possess. The benefit to studies involving the modeling of settlement and consolidation of soils is clear despite the fact that a model grid is nondeformable. Pressure dependent fluid density, and the opportunity to input matrix and water compressibilities separately, rather than combining them in the form of a specific storage parameter, are also features that some modelers may find to their liking.

Another benefit of the TRUST algorithm derives from the general head boundary condition that is used universally along all boundary segments. This approach, when specifically applied to Cauchy conditions, allows boundary influxes and effluxes to vary depending on computed head conditions. In contrast, other simulators frequently permit third-type (Cauchy) boundary conditions only for specialized forms of external flux (e.g., Davis and Neuman, 1983), such as evaporation and/or infiltration. Also included in TRUST is a means of handling seepage face boundaries.

Because possible instability of the numerical solution is a crucial issue in any variably saturated flow simulation, TRUST includes an algorithm for automatically generating successive time step durations (Reisenauer et al., 1982). In the event that convergence within a specified number of iterations is not achieved during a step, the results of the time step are discarded, and a new step with a duration of half the previous one is used in succeeding calculations. The interpolation parameter λ, used in Equation A-6, is also updated at each time step (Reisenauer et al., 1982). The scheme for choosing an optimum λ makes use of rates of changes in pressure head during preceding time steps.

Difficulties and Potential Drawbacks of TRUST

Because steady state simulations were considered crucial in the stream-aquifer study, it was important for the author to be able to obtain steady state results with relative ease. As the original TRUST code was written to exclusively handle transient flow situations, attempts were made via an indirect approach to arrive at equilibrium solutions for two-dimensional flow cases similar to those outlined in

the earlier chapter on steady state modeling. In the indirect approach, the code was operated in its normal manner and was allowed to simulate large periods of time. The intent of this scheme was to extend the total simulation time to the point where a steady state would ultimately be reached. This tactic, however, proved inappropriate, partly due to the excessive CPU times that were required, and partly due to the geometry and model discretization characteristics of the stream-aquifer problem. As may be guessed, computing times became inordinately large primarily because stability criteria severely limited time step durations. Problems with system geometry and discretization were related to more inherent difficulties with the mixed explicit-implicit solver, discussions of which are saved for later paragraphs.

Another difficulty with TRUST appears to be related to the fundamental numerical scheme upon which it is formulated, namely the IFDM. As stated in the development of Equation A-3, inter-element averages of flow rate controlling parameters are a necessary part of the IFDM. In the interest of preserving flux continuity, the original TRUST code uses a harmonic average (Reisenauer, et al., 1982) to compute those mean conductances. However, as reported by Siegel (1980), the harmonic mean conductance can lead to inaccurate solutions, especially near wetting fronts. Indeed, Reisenauer et al. (1982, p. 2.12) have pointed out this potential problem. That same difficulty was encountered in some of the earliest TRUST simulations in this study dealing with mound growth activity. As per Siegel's (1980) recommendation, the authors altered the TRUST code to allow the use of geometric mean conductances between elements. This latter step did somewhat improve the code's accuracy for the mounding problem, but it

did little to overcome the aformentioned difficulties associated with the mixed explicit-implicit solver combined with large system geometry and coarse domain discretization.

By virtue of the fact that the mixed explicit-implicit scheme is a point iterative solver, it is easily seen that it falls far short of being as implicit as a "direct" solver. As a consequence, the potential for the effects of hydraulic "stress" in one part of a domain to be passed on to another portion of the flow system is diminished in the mixed explicit-implicit approach. That is, from a numerical solution perspective, the transmission of distinct properties at one element to contiguous elements is not performed in as direct a manner with the iterative solver as it is with direct solution approaches. The same kind of problem is commonly observed with similar pointwise "relaxation" schemes such as successive over relaxation (SOR), in which computational times for problems involving a moderate number of nodes may far exceed those needed for direct solution.

The upshot of these inherent problems with the mixed explicit-implicit approach, and with any pointwise iterative solver for that matter, is that convergence to an accurate solution is sometimes inachievable. Reisenauer et al. (1982, p. 2.12) make mention of this sometimes troublesome aspect of TRUST, and go on to suggest the use of a direct solver in the code if needed. Through conversations with Dr. T.N. Narasimhan (Narasimhan, personal communication), the authors have learned that a version of TRUST does currently exist in which a direct solver has been incorporated. However, to the author's knowledge, that version has not been released for public use, and will probably not be made available until full testing of the code has been completed.

The above-stated drawback of the TRUST iterative solution scheme becomes compounded when working with domains of large size and containing large elements. Once again, by failing to solve all model equations simultaneously as in a direct solver, stresses in an active part of the system cannot be directly felt (in a numerical sense) in less active areas lying hundreds of feet away.

This problem becomes even more acute for elements with large aspect ratios, in which the largest axis of the element essentially lies parallel to the flow direction. To illustrate this contention, consider the very long rectangular elements used in the SATURN simulation, and that are located within the upper right hand portion of the finite element network shown in Figure 9. Furthermore, refer to the parameters within the summation sign found in Equation A-3. As stated before, these terms are equivalent to the flux across the interface(s) separating elements. Note also that this flux is directly proportional to the area of the interelement interface ($\Gamma_{\ell,m}$), and inversely proportional to the distance ($d_{\ell,m} + d_{m,\ell}$) separating the representative nodes in each element. For the long elements needed in the stream-aquifer simulation, and in cases in which the flow in such areas roughly parallels the longest element axis (see for example, Figures 12, 14 and 16), it can be seen that the interface area is very small relative to the internodal separation. As a consequence, the computed flux across the elements is small relative to calculated fluxes in areas where the aspect ratios of elements are considerably less. The relative disparity in fluxes has a strong impact on the computed numerical solution, as interelement fluxes usually form the most dominant components of $\Delta\psi_{\ell,exp}$ (Equation A-5), an integral and

necessary component of the mixed explicit-implicit (Equation A-6) solution scheme.

In the case of stream-aquifer simulations, such as those attempted in this study, the overall effect of large element aspect ratios was to retard the transmission of recharge effects in areas beneath the stream to areas lying some distance from the stream centerline. In general, this problem became worse as the aspect ratio of outlying elements was increased.

UNSAT 2

UNSAT2 is a two-dimensional finite element flow simulator. The underlying theory and computational scheme for this code was first developed by Neuman (1973). Further documentation and a user's guide for UNSAT2, which is written in FORTRAN IV, are found in Davis and Neuman (1983).

Theory of UNSAT2

The governing equation of two-dimensional flow modeled by UNSAT2 is equivalent to the form of Richard's equation (Equation 1) presented in Chapter VI. For purposes of brevity, that equation is not repeated here.

The type of boundaries handled by UNSAT2 include first type (Dirichlet), second type (Neumann), and seepage face. In addition, algorithms are incorporated to simulate flux processes observed in unsaturated areas of the domain bounded by atmospheric conditions (Davis and Neuman, 1983). These latter boundary types include

evaporation as well as infiltration from rainfall. Both are head-dependent in the sense that neither evaporation nor infiltration fluxes can be determined until the soil pressure head has been calculated.

Unlike TRUST, hysteresis is not represented in UNSAT2. Means of accounting for seepage faces and plant transpiration are, however, included (Davis and Neuman, 1983).

Numerical Methodology of UNSAT2

Like SATURN, UNSAT2 is based upon the Galerkin finite element method. The fundamental mathematical and numerical procedures associated with this method are essentially the same as those described in the text discussion (Chapter VI) of SATURN. The Galerkin approximation procedure used in UNSAT2 produces a matrix equation that is of the same form as equation (2). However, a few minor, yet pertinent, differences are found between the codes. UNSAT2 also differs in important ways from FEMWATER, which is also a Galerkin finite element model.

One of the most notable features of UNSAT2 is the scheme whereby the mass matrix, which forms the coefficient of the time derivative, is mass-lumped. In essence, this means that off-diagonal terms in the element mass matrix are lumped onto the main diagonal. In UNSAT2, this is accomplished as direct consequence of determining a weighted average of the time derivative $\frac{\partial \psi}{\partial t}$ over the entire flow region (see Davis and Neuman, 1983). In some instances this approach leads to a more stable solution (Neuman, 1973) than would occur if a consistent mass matrix (mass matrix without lumping) were used.

UNSAT2 is also distinctive in the sense that the code user is allowed to discretize his flow domain using both quadrilaterals and

triangles. It should be noted, however, that the quadrilaterals are further subdivided within the code into triangles. Thus all computations are ultimately performed using linear triangular elements. The advantage of using simplex elements, as in this approach, is that it avoids the potentially burdensome task of numerical integration normally associated with first order isoparametric (quadrilateral) elements.

The equation solving scheme in UNSAT2 is classified as a bandsolver, as it takes advantage of the banded nature of the global conductance matrix. Because the global matrix is symmetric, computations need only be carried out on the upper triangular portion of the matrix. To handle the nonlinear nature of an unsaturated flow problem, a Picard iteration scheme is employed.

Unlike TRUST, first type (Dirichlet) boundaries are handled in UNSAT2 by transferring all non-diagonal terms of the global conductance matrix affected by the prescribed head node over to the load (right-hand-side) vector. In conjunction, an identity equation is generated for each of the prescribed head nodes, and are included in the global matrix. As a consequence, fixed heads are computed directly from the band-solver calculations and are totally independent of any form of "general head" boundary determinations. Boundary flux at a prescribed head node is determined via back-substitution into the final linearized equation for that node.

Advantages of UNSAT2

Certainly one of the nice features of UNSAT2 is the utilization of linear triangular elements to the exclusion of all other types of elements. The use of these simplex elements voids the need to orient

element sides parallel to domain axes (Segerlind, 1976). Furthermore, sometimes costly numerical integration is completely avoided by using linear triangles. In addition, triangles also allow the boundaries of irregularly shaped domains to be handled quite readily.

Equation back-substitution to determine fluxes at Dirichlet nodes also appears to be a viable means for arriving at accurate global mass balances. In all of the successful runs made with UNSAT2 in this study, mass balance errors were always on the order of 1% or less.

UNSAT2 also employs a dynamic dimensioning algorithm for allocating computer memory (or storage, in the case of a virtual memory system) to the various variables used in the FORTRAN program. This program enhancement eliminates the need to enlarge the size of all arrays used in the code; enlargement, when needed, is simply accomplished by increasing the size of one floating point array and one integer array.

Difficulties Encountered with UNSAT2

Like TRUST, the original UNSAT2 code did not allow a direct steady state solution to be calculated. Once again, it has apparently been assumed that steady state conditions could be arrived at by allowing a simulation to run over very lengthy periods of time. In the interest of circumventing potentially very long transient simulations, a steady state version of the UNSAT2 code was prepared at the New Mexico Institute of Mining and Technology. The author of the steady state simulator was Dr. Jim Yeh (now with the Department of Hydrology and Water Resources, University of Arizona, Tucson) while he was conducting his doctoral research. The approach taken in Yeh's algorithm basically consisted of setting the mass matrix term for all nodes to a value of

zero, while allowing the model to carry out a slightly revised Picard iteration procedure.

Yeh met with considerable success in utilizing his steady state version of UNSAT2. It should be stated, however, that the simulation domains he was working with were quite small (40 feet by 20 feet). In addition, the largest elements that he employed, were also of moderate size (4 feet by 1 foot).

This writer's experience with the steady state version of UNSAT2 has been less successful. Attempts have been made to conduct steady state simulations for the large domain described in Chapter VII. Element sizes were also roughly the same as those used in the SATURN simulations. And, as in the SATURN runs, attempts were made to arrive at equilibrium head profiles resulting from a succession of reduced heads in the aquifer underlying the simulation domain.

Head profiles produced by the steady state model were often in error, although this error was not abundantly clear upon first inspection. In other words, the model seemed to converge, after several iterations, to a solution that appeared reasonable in most areas of the simulation domain. Flow calculations at Dirichlet nodes indicated that fluxes at inflow and outflow boundaries were balanced; thus, it initially appeared that mass was being conserved. Furthermore, computed water table configurations were plausible. However, as hydraulic heads in the underlying aquifer were set at progressively lower values, it became apparent that the maximum flux conditions expected under disconnected cases with deep water table conditions were not being simulated by the model. Rather than stabilizing at a maximum suction level, the computed pressure heads at the base of the clogging layer continued to decline as heads in the

underlying aquifer were continually reduced. Calculated moisture contents at the base of the clogging layer eventually fell to levels at which the aquifer soil was fully incapable of conveying the computed water influx from the stream. Thus, although the model appeared on the surface to be arriving at a solution, this solution was incorrect. Accordingly, the apparent convergence of the solution scheme could be more properly termed a "spurious" convergence. It was also difficult to ascertain if any of the shallow water table runs resulted in correct head configurations.

As the next approach to arriving at steady state solutions, the recommended procedure of simulating over long time durations was implemented. Once again, these simulations were conducted on domains the size of those presented in Chapter VII. It was the intent of these transient runs to establish very wet (high water table) initial conditions and then allow the domain to drain to eventual equilibrium. However, this tactic was also foiled when large instabilities began appearing after a considerable portion of the draining process had elapsed. As might have been expected, most of the instabilities first appeared as infeasible computed heads in the driest zones located far from the stream.

As UNSAT2 does not contain an automatic time stepping algorithm, an attempt was made to minimize stability problems by reducing time step durations manually. This approach met with some measure of success. However, it was eventually discarded as it became necessary to reduce time steps to extremely low values in order that stability could be maintained. CPU times accordingly became prohibitive.

Difficulties in achieving steady state solutions with UNSAT2 are probably reflective of the universally encountered problems with any

simulator of this highly nonlinear form of subsurface water flow. Despite such drawbacks, the code's ability to handle a variety of transient problems (Davis and Neuman, 1983) has been documented. Yet there are a few additional features of UNSAT2 that this writer feels may limit its capacity to handle a variety of simulation conditions, which are mentioned here.

Moisture content values, as they vary with matric potential, are input to the model in tabulated form. Accordingly, specific moisture capacity $\left[C = \frac{d\theta}{d\psi} = \phi \frac{dS_w}{d\psi}\right]$ is determined in the model via linear slopes determined between tabulated data points. It is well known that specific moisture capacity exhibits a maximum value usually at a single value of pressure head ψ. On either side of this maximum, values of C can drop off quickly with changes in pressure head to values of zero. Therefore, the potential exists for large changes in specific moisture capacity to occur over short ranges of pressure variation. It is easy to see then that linearly approximated values of C may not effectively catch important behavior of this parameter during the Picard iteration process. This may help to partly explain why the Picard procedure may fail to converge to a solution in unsaturated zones when large time steps are used. It also serves to illustrate why constitutive mathematical formulae relating moisture content to pressure head are sometimes employed in lieu of tabulated data; i.e., exact values of $d\theta/d\psi$ can usually be obtained by differentiating the functional relationship between the two parameters. An additional technique for handling this potential problem is the chord-slope method (e.g., Huyakorn et al., 1984).

Another concern with the original version of UNSAT2 lies in the fact that is written in single precision FORTRAN. This presumedly is

the case because the code was originally run on computers from Control Data Corporation (CDC), which employ, by default, 64 bit words. The potential exists, therefore, for some roundoff error to exist when the model is executed on computers using smaller word sizes. In the course of running a few example problems on New Mexico Tech's DEC-2060 computer (which uses 36 bit words), this writer found our results to vary slightly, yet noticeably, from those reported for identical problems in the UNSAT2 user's manual (Davis and Neuman, 1983). The need for a double precision version of this code in some situations is clear.

One final concern with UNSAT2 warrants mention. In particular, there is some speculation that the mass-lumping procedure may lead to numerical error when applied to largely saturated domains (Huyakorn and Pinder, 1983). Although this technique apparently enhances the convergence of solution in unsaturated zones, Frind and Verge (1978) report that the accuracy of some of their three-dimensional simulations of mostly saturated flow was adversely affected by the use of mass-lumping.

FEMWATER

The variably saturated flow simulator FEMWATER was developed at Oak Ridge National Laboratory by Yeh and Ward (1980). It is an extension of the work done by Reeves and Duguid (1976). Enhanced features of FEMWATER that specifically address the issue of mass balance computations are discussed by Yeh and Ward (1980) and Yeh (1981).

Theory of FEMWATER

FEMWATER is a Galerkin finite element code designed to simulate two-dimensional variably saturated flow. It is programmed in FORTRAN IV.

As with UNSAT2, the governing equation upon which FEMWATER is predicated is, for all intents and purposes, the same as that (equation (1), Chapter VI) handled by SATURN. However, much in the manner of TRUST, the FEMWATER code has also been designed to determine flow and storage parameters after physical properties have been entered into the model in their primitive forms. Therefore, rather than prompting the code user for a single value of specific storage, compressibilities of both water and media are read in separately. Similarly, hydraulic conductivities are computed from data input of intrinsic permeability, water density, gravitational constant and a fluid viscosity. Unlike TRUST, no attempts are made in FEMWATER to account for pressure effects on fluid density or skeletal deformation. Nor is the ability to account for hysteresis included.

In addition to accommodating first and second type boundaries, FEMWATER allows the use of a so-called rainfall-seepage boundary condition. This last condition is apparently based on a head-dependent algorithm (Yeh and Ward, 1980) and bears some resemblance to the infiltration boundary (Davis and Neuman, 1983) scheme provided in UNSAT2. Seepage faces are also handled by FEMWATER.

Numerical Algorithm of FEMWATER

Spatial discretization of flow domains simulated by FEMWATER is accomplished using quadrilateral elements. Utilization of these first order isoparametric elements is apparently advantageous in two ways:

a) higher order accuracy is presumably achieved (e.g., Tracy and Marino, 1987), than with linear triangular or linear rectangular elements, and b) they easily conform to irregular boundaries of flow domains and subdomains. Being that quadrilaterals are included in the category of complex elements (Segerlind, 1976), there is no restriction as to their orientation; i.e., it is not necessary to align element boundaries parallel to the model coordinate axes. However, the computational burden usually increases when using quadrilaterals when compared with the computational needs associated with linear triangular or rectangular elements.

A direct solver is utilized in FEMWATER which takes advantage of the banded and symmetric nature (Yeh and Ward, 1980) of the model-generated global conductance matrix. Dirichlet (first type) boundary conditions are handled in the same fashion as UNSAT2; i.e., nondiagonal terms in the conductance matrix affected by prescribed head nodes are transferred to the load vector, while identity equations are generated for each Dirichlet node and are included in the global assembly process. The model user has the option of using either a consistent mass matrix or a lumped one. Picard iteration is applied to deal with the nonlinear nature of the variably saturated problem.

Perhaps the one feature of this code that most distinguishes it from other simulators is the means by which it computes Darcy velocities, and, consequently, carries out mass balance calculations. In contrast to other models (e.g., Reeves and Duguid, 1976; Huyakorn et al., 1984) that determines nodal flow velocities by numerically evaluating the spatial derivative ($\partial\psi/\partial x_i$) of the final computed head field, FEMWATER solves for velocity components using an additional finite element formulation (Yeh and Ward, 1980; Yeh, 1981). The

computed velocities are then in turn utilized to compute mass fluxes across boundaries. This last step contrasts with comparable schemes in UNSAT2 and SATURN, wherein mass fluxes at prescribed head nodes are determined via equation back-substitution.

The motivation for applying a separate Galerkin scheme to evaluate Darcy velocities is that such an approach assures continuity of velocity at element boundaries and at nodes. Discontinuity of velocity does occur under the conventional method of evaluating spatial derivatives of the computed head field. This is a natural result of the finite element modeling procedure (Huyakorn and Pinder, 1983) when only one degree of freedom (i.e., head) is included in the numerical formulation of a model. Discontinuity of velocities infers a violation of conservation of mass in a local sense.

Yeh (1981) argues that generation of a continuous velocity field is essential to contaminant transport modeling, as large errors may result when solving the convective-dispersive equation using a discontinuous field. Because the additional Galerkin solution for velocities is an integral part of the FEMWATER code, the computed velocity field is also subsequently used to determine global mass balance during a simulation. Once again, the argument for carrying out this step is premised on the theory that if local mass balance is preserved, so too should global balance be achieved. Yeh and Ward (1981) reported significant reductions in mass balance error using FEMWATER when compared with more conventional schemes (e.g., Reeves and Duguid, 1976; Davis and Neuman, 1983) of computing boundary fluxes.

Pros and Cons of FEMWATER

As stated earlier, FEMWATER allows the opportunity of entering physical flow parameters in their primitive form into the code. This feature no doubt affords a greater interdisciplinary flexibility to some users.

Another feature of FEMWATER that potentially contributes to its simulation versatility is its ability to handle the input of material property information via either tabular form or by constitutive relation. Thus, as mentioned earlier, it is possible to avoid potential discontinuities in the determination of specific moisture capacity C by deriving analytical expression for $d\theta/d\psi$ from the constitutive relationships. Unfortunately, the public version of FEMWATER does not utilize explicit formulae relating intrinsic permeability, moisture content and pressure head. Instead it is left up to the model user to choose his own functional relations, and to add FORTRAN statements to the code which will implement these relations during execution. Correspondingly, it is also necessary to add statements that serve to evaluate specific moisture capacity ($d\theta/d\psi$) as pressure head (ψ) changes. Consequently, although FEMWATER will automatically allow its users to input constitutive formulae parameters, there is some additional work involved in properly making use of those parameters.

FEMWATER does have an option to directly compute steady state solutions. However, as with both TRUST and UNSAT2, the authors ultimately ran into numerical difficulties when attempting to apply the steady state version of the FEMWATER code. Many of the steady state runs with FEMWATER were also conducted on stream-aquifer domains of similar geometry, size and discretization resolution as those presented

in Chapter VII. And, much in the same manner as simulations were made with SATURN, initial runs with the code were done under shallow water table conditions, i.e., uniform head in the underlying aquifer was maintained at a level close to the value needed to maintain hydrostatic conditions. As successive runs were made with gradually reduced heads in the underlying aquifer it was discovered that FEMWATER was capable of arriving at some of the steady state solutions. However, this apparent success was limited to cases wherein the water table remained relatively shallow and within close distance of the streambed. Upon attempting to reduce the underlying aquifer head even more, the numerical solution inevitably became unstable. Thus it appeared that FEMWATER was capable of directly providing feasible steady state solutions during cases of hydraulic connection and disconnection along with a shallow water table; however, when approaching the state of disconnection associated with a deep water table and maximum stream seepage rate, the Picard algorithm was incapable of converging to a solution. No attempts were made with the FEMWATER code to arrive at equilibrium conditions for the deep water table case by running the transient model over extended periods of time.

Aside from simulations of stream-aquifer conditions, the author also made several transient runs with the FEMWATER code for a variety of simple situations. The problems examined ranged from fully saturated one-dimensional cases to unsaturated two-dimensional situations. The same problems were solved with UNSAT2, and the CPU times associated with the respective models were compared. Attempts were made to keep simulation conditions with each of the codes (e.g., discretization, convergence criteria) alike and to force the output from each code to be similar in scope and size. Because these

comparisons were not entirely scientific, nor were intended to be, the exact findings from these simple simulations are not reported here. However, several general observations bear relevance to the respective ability of numerical schemes employed by each code and are worthy of mention.

First, it can be said that the two codes generated essentially the same head configurations for the situations examined. There were a few minor differences, but these were probably attributed to the different numerical approaches (i.e., element type, integration, mass-lumping) taken in each. But the FEMWATER code was consistently the slower of the two. In nearly all cases, FEMWATER CPU times were 5 to 6 times greater than comparable CPU needs of UNSAT2. There are likely a number of reasons for this apparent disparity in code efficiency. The author conjectures as to what the most significant causes are in the following paragraphs.

One of the most probable causes of increased CPU time with FEMWATER stems from the fact that its numerical algorithm is based on four-node quadrilateral elements. Although such elements provide an advantage over multiplex rectangular elements in the sense that their sides need not parallel coordinate axes, it is necessary with quadrilaterals to convert the global coordinates of their corner nodes over to a local, or isoparametric, coordinate system. The use of the resulting so-called isoparametric elements is necessary if continuity (Segerlind, 1976) of the state variable (head) along interelement boundaries is to be maintained. A drawback of this procedure, however, is that necessary integration in the local isoparametric domain is much more complex (e.g., Huyakorn and Pinder, 1983) than when based on global coordinates. Numerical integration (e.g., Gaussian quadrature)

is often required if a numerical solution is to be attained. Consideration of computer operations suggest that the computational times associated with numerical quadrature will commonly exceed those based on direct analytical integration. Huyakorn et al. (1984) indicate that, in some cases, Gaussian quadrature can require more than 20 times the CPU time required by comparable analytical integration.

The difficulties posed by enlarged CPU times when performing numerical integration become even more significant in unsaturated flow simulation. The inherent nonlinearity of this type of problem requires hydraulic conductivities and specific moisture capacities to be updated at each iteration, and values for these parameters must in turn be determined at the Gauss points employed in the numerical quadrature. Functional coefficient schemes do exist (e.g., Frind and Verge, 1978) that remove the need to numerically integrate at each iteration. A disadvantage of these latter approaches, however, is that finer and thus more spatial discretization may become necessary to preserve solution accuracy. The FEMWATER algorithm performs quadrature at each iterative cycle.

Computational time in FEMWATER is also increased if the option to compute velocity components is called upon. According to Yeh (1981), the finite element method of computing velocities with two-dimensional problems enlarges CPU times by a factor of less than 3 compared to the conventional method of determining head gradients.

One may argue that the velocity field is not necessary unless it is to be utilized in succeeding transport simulations. Yet, if mass balance calculations are requested of FEMWATER, velocity determinations are indeed necessary. Furthermore, additional calculations are required to determine the angles at which the horizontal and vertical

components of velocity meet element sides; i.e., mass balance flux evaluations must be done using Darcy velocity components that are normal to element boundaries. In any event, additional calculations, which signify increased CPU time, are unavoidable.

T3FEMWATER

T3FEMWATER is, to a large degree, a three-dimensional version of the original two-dimensional FEMWATER. As of this writing, a formal user's manual for T3FEMWATER has not been placed in the public domain. However, Oak Ridge National Laboratory agreed to let the authors use the three-dimensional code to see if it would suit this study's simulation needs. Although the authors have made a limited number of runs with this simulator, a few comments regarding its philosophy and design are relevant to the stream-aquifer study.

Like the original two-dimensional (2-D) FEMWATER, the three-dimensional (3-D) version is based on isoparametric elements. Rather than 4-node planar quadrilaterals, the 3-D code makes use of 8-node hexahedral elements. Other than this fundamental difference in the dimensionality of each simulator, T3FEMWATER possesses many of the same characteristics as does the 2-D flow code. For example, numerical integration stemming from isoparametric formulation is called for, both during each time step and for each iterative cycle. Similarly, an additional finite element solution is carried out to find the components of a continuous velocity field. These are in turn utilized in mass balance calculations, wherein the velocity components normal to element borders must be determined.

Because some 3-D problems can at times involve large numbers of nodes and elements, two iterative equation solvers have also been made

available in T3FEMWATER. This step helps reduce the computer memory burden, and in certain cases the CPU needs, that are usually required in direct solvers like those applied in the original FEMWATER. One of the iterative solvers provided in the 3-D flow version is based on a block iterative and relaxation method. The other is classified as a point (node) relaxation scheme.

Under the block iterative technique, a three-dimensional domain is perceived as consisting of several interconnected subregions called blocks. During a single iterative cycle, the set of Galerkin equations formulated for each block are solved successively. The effect of an adjacent block on a given block, whose numerical equations are currently being solved, is felt via terms that would normally result from the 3-D Galerkin scheme when applied to that block and its adjacent counterparts. However, instead of those terms being included implicitly in the equations for a given block, they are assumed at each iteration to be known values and are thus incorporated explicitly into the load (right-hand-side) vector that results from Galerkin matrix formulation. The iterative process is carried out from block to block, and is terminated only after the maximum changes in computed head for all nodes during an iterative cycle has been reduced to an acceptable low value.

In T3FEMWATER, the linear equations formulated for each block are solved by a band-solver that takes into account the symmetry of the conductance matrix developed for each block. The entire block iteration method, therefore, results in a significant reduction of bandwidth size and matrix sparseness from that which would occur should the full 3-D set of equations be submitted for solution by a direct solver.

Selection of the nodes to comprise each block subregion is left up to the model user. It is important to choose these blocks such that CPU requirements during the direct solution (band-solver) phase is kept close to minimum possible values.

SATURN

Many of the important features of the two-dimensional finite element simulator SATURN have been previously summarized in Chapter VI. Therefore, the SATURN code is discussed here only in the context that it differs from previously described models. As has been stated, the primary reference for this code is found in Huyakorn et al. (1984).

Trial Runs With SATURN

In a similar fashion to the testing of the other variably saturated flow models, SATURN was assessed for its ability to determine steady state solutions for the stream-aquifer systems and simulation conditions outlined in Chapters VI and VII. The direct steady state solution scheme was invoked rather than attempting to reach equilibrium states by way of long-duration transient runs. Since SATURN provides the model user the option of using either the Picard or Newton-Raphson iteration schemes, the purpose of these trial simulations was to gage the performance of these two approaches in representing stream-aquifer processes associated with various levels of hydraulic disconnection.

In applying the Picard algorithm, it was found that, under shallow water table conditions, a convergent steady state solution was always achieved. Indeed, even for cases of partial connection and disconnection with a shallow water table, the Picard procedure produced a stable solution. However, when heads in the underlying aquifer were

reduced to the extent that the water table was deep enough to no longer affect stream seepage (i.e., disconnected conditions with a deep water table), the code became virtually incapable of converging to a solution. This observation resembled the behavior of FEMWATER under similar situations.

On the other hand, the Newton-Raphson procedure proved much more successful, as it was capable of providing stable simulations under all cases of hydraulic connection and disconnection. For the shallow water table situations in which the Picard scheme converged, comparisons of head configurations produced by each scheme showed that they were virtually identical. In general, the Newton-Raphson procedure required more CPU time than did Picard iteration for identical convergence criteria. This was to be expected, however, since the Newton-Raphson algorithm results in an asymmetric global conductance matrix, which, when solved by a direct elimination method, requires that both upper and lower triangular terms be included in matrix calculations.

The apparent advantages of the nonlinear solution capabilities provided by the Newton Raphson scheme can be better understood by examining the conditions that occur when the deep water table case is reached. When this state exists, the heads at the base of the clogging layer, and, thus the seepage rate from the stream, become constant. If boundary heads elsewhere in the domain, such as those in an underlying aquifer, are perturbed, the model attempts to find changes in head that reflect this perturbation. Yet, because head changes in one part of the system (just beneath the stream) are minuscule when compared with regions where the perturbation effects are quite significant, an algorithm is needed to assist the model in estimating the proportionate changes. The Newton-Raphson scheme apparently meets this need. In

contrast, Picard iteration takes more of a trial-and-error approach to estimating head changes, and unfortunately fails to center in on a workable solution.

SATURN's Numerical Features Compared With Other Simulators

Although the author has not conducted an organized evaluation of SATURN's capabilities as compared with those of other variably saturated flow models, certain features of SATURN have stood out during the course of this study. A few of those items are distinguished below.

It bears repeating that SATURN is the only code, of those that have been applied, that has been able to simulate steady state conditions for the deep water table case sometimes observed in stream-aquifer systems. The one feature that SATURN possesses that appears to make such simulations possible is the Newton-Raphson algorithm. All other simulators that have been tried either do not provide the direct solution of steady state problems (e.g., TRUST, UNSAT2), or use less successful solution schemes classified as Picard iteration methods (e.g., FEMWATER).

Newton-Raphson techniques, when applied to variably saturated numerical models, result in the formulation of an asymmetric conductance matrix. On the other hand, Picard algorithms result in a symmetric conductance matrix. As a natural consequence, the memory requirements are greater for the Newton-Raphson scheme, as are CPU needs in many cases.

Because SATURN uses only linear rectangular and triangular elements, the need for conversion to isoparametric elements and subsequent numerical integration is avoided. In order to preserve

continuity of head, however, it is necessary that the sides of rectangular elements (which are classified as multiplex elements) parallel the coordinate axes utilized in a given simulation. The combined use of rectangular and triangular elements is usually adequate to handle the irregularly shaped subdomains and boundaries sometimes occurring in models of actual situations. Unfortunately, the Newton-Raphson scheme is only usable with rectangular elements in the version of SATURN utilized in this study.

SATURN allows its users to input soil properties (hydraulic conductivity-moisture content-pressure head) either in a tabular format or via constitutive functional relations. Regardless of which of these techniques is applied, specific moisture capacity (C) information is generated by the chord-slope method (see Chapter VI) of estimating derivatives, which has been shown to assist in arriving at stable solutions (Cooley, 1983) for some strongly nonlinear problems. It has been demonstrated that the chord-slope algorithm will in most cases result in better estimates of C (Huyakorn, 1984) than do tabular input approaches where the value of C is simply treated as a piecewise linearly continuous property of pressure head (e.g., UNSAT2).

SATURN does not provide the option of inputting physical parameters in their so-called primitive forms, as is allowed in TRUST (e.g., Reisenauer, 1982) and FEMWATER (Yeh and Ward, 1980). Rather than asking for separate values of water and media compressibility, SATURN looks for a single value of specific storage to be entered into the model. Unlike TRUST, it cannot represent skeletal deformation of porous media that may result from aquifer dewatering. To some extent, SATURN is restricted by its ability to solve only two-dimensional or axisymmetric problems. In addition, hysteresis of soil properties is

not taken into account. The SATURN code does contain an algorithm for modeling seepage faces.

REFERENCES

Bachmat, Y., Brehehoeft, B., Andrews, B., Holt, D. and Sebastian, S., 1980. Ground-water management: the use of numerical models. American Geophysical Union, Water Resources Monograph 5.

Baumann, P., 1952. Groundwater movement controlled through spreading. Transactions, American Society of Civil Engineers, v. 114, pp. 1024-1074.

Bear, J., Zaslavsky, D. and S. Irmay, 1968. Physical principles of water percolation and seepage. UNESCO, Paris.

Bear, J., 1972. Hydraulics of porous media, Academic Press.

Bear, J., 1979. Hydraulics of groundwater, McGraw-Hill.

Behnke, J.J., 1969. Clogging in surface spreading operations for artificial groundwater recharge. Water Resources Research, v. 5, pp. 870-876.

Bouwer, H. 1964. Unsaturated flow in groundwater hydraulics. American Society of Civil Engineers, Journal of the Hydraulics Division, 90, HY 5, pp. 121-144.

Bouwer, H., 1969. Theory of seepage from open channels. In Advances in hydroscience, vol. 5, V.T. Chow (ed.), Academic Press, Inc., New York, pp. 121-172.

Bouwer, H., 1978. Groundwater hydrology. McGraw-Hill.

Brockway, C.E. and Bloomsburg, G.L., 1968. Movement of water from canals to groundwater table. Water Resources Research Institute, University of Idaho, Research Technical Completion Report, Project A-009-IDA.

Brooks, R.H. and Corey, A.T., 1966. Properties of porous media affecting fluid flow. American Society of Civil Engineers, Journal of the Irrigation and Drainage Division, 92, IR2, pp. 61-68.

Brutsaert, W., 1966. Probability laws for pore size distribution. Soil Science, v. 101, pp. 85-92.

Byers, E. and Stephens, D.B., 1983. Statistical and stochastic analyses of hydraulic conductivity and particle-size in a fluvial sand. Soil Science Society of America Journal, v. 47, pp. 1072-1081.

Chow, V.T., 1959. Open-channel hydraulics. McGraw-Hill.

Clapp, R.B. and Hornberger, G.M., 1978. Empirical equations for some soil hydraulic properties. Water Resources Research, v. 14, no. 4, pp. 601-604.

Cooley, R.W., 1971. A finite difference method for unsteady flow in variably saturated porous media: Application to a single pumping well. Water Resources Research, v. 7, no. 6, pp. 1607-1625.

Cooley, R.L. and Westphal, J.A., 1974. An evaluation of the theory of ground-water and river-water interchange, Winnemucca reach of the Humboldt River, Nevada. Center for Water Resources Research, Desert Research Institute, University of Nevada. Technical Report Series H-W, Publication No. 19.

Cooley, R.L., 1983. Some new procedures for numerical solution of variably saturated flow problems. Water Resources Research, v. 19, no. 5, pp. 1271-1285.

Davis, L.A. and Neuman, S.P., 1983. Documentation and user's guide: UNSAT2 - variably saturated flow model. U.S. Nuclear Regulatory Commission, NUREG/CR-3390, WWL/TM-1791-1.

Day, P.R. and J.N. Luthin, 1954. Sand model experiments on the distribution of water-pressure under an unlined canal. Soil Science Society of America Proceedings, v. 18, pp. 133-136.

DeWiest, R.J.M., 1962. Free surface flow in homogeneous porous medium. American Society of Civil Engineers Transactions, 127, pp. 1045-1089.

Dillon, P.J. and Liggett, J.A., 1983. An ephemeral stream-aquifer interaction model. Water Resources Research, v. 19, pp. 621-626.

Edwards, A.L., 1968. TRUMP: A computer program for transient and steady-state temperature distributions in multidimensional systems. National Technical Information Service, Springfield, VA., Report UCRL-14754.

Finlayson, B.A., 1977. Water movement in dessicated soils. In Finite Elements in Water Resources, edited by W.G. Gray, G.F. Pinder and C.A. Brebbia, pp. 3.91-3.106.

Freeze, R.A., 1969. The mechanism of natural ground-water recharge and discharge, 1. One-dimensional, vertical, unsteady, unsaturated flow above a recharging or discharging groundwater flow system. Water Resources Research, v. 5, pp. 153-171.

Freeze, R.A., 1971. Three-dimensional, transient, saturated-unsaturated flow in a groundwater basin. Water Resources Research, v. 7, pp. 347-366.

Freeze, R.A. and Cherry, 1979. Groundwater. Prentice-Hall, Inc., Englewood Cliffs, New Jersey, 604 pp.

Freyberg, D.L., Reeder, J.W., Franzini, J.B., and Remson, I., 1980. Application of the Green-Ampt model to infiltration under time-dependent surface water depths. Water Resources Research, v. 16, no. 3, pp. 517-528.

Frind, E.O. and Verge, M.J., 1978. Three-dimensional modeling of groundwater flow systems. Water Resources Research, v. 14, pp. 844-856.

Gates, J.S., White, D.E., and Leggat, E.R., 1984. Preliminary study of the aquifers of the Lower Mesilla Valley in Texas and New Mexico by model simulation. U.S. Geological Survey, Water-Resources Investigations Report 84-4317.

Glover, R.E., 1960. Mathematical derivations as pertain to groundwater recharge. U. S. Department of Agriculture, Agricultural Research Service, Fort Collins, Colorado.

Green, W.H. and Ampt, G.A., 1911. Studies on soil physics, 1, The flow of air and water through soils. Journal of Agricultural Science, 4, pp. 1-24.

Gunaji, N.N., 1961. Groundwater conditions in Elephant Butte Irrigation District. Engineering Experiment Station, New Mexico State University, Las Cruces, New Mexico.

Hantush, M.S., 1965. Wells near streams with semipervious beds. Journal of Geophysical Research, v. 70, no. 12, pp. 2829-2838.

Hantush, M.S., 1967. Growth and decay of groundwater-mounds in response to uniform percolation. Water Resources Research, v. 3, pp. 227-234.

Harms, J.D. and Fahnestock, R.K., 1965. Stratification, bed forms, and flow phenomena (with an example from the Rio Grande). In Primary Sedimentary Structures and Their Hydrodynamic Interpretation. Society of Economic Paleontologists and Mineralogists, Special Publication No. 12, Tulsa, OK.

Harr, M.E., 1962. Groundwater and seepage. McGraw-Hill, New York.

Haverkamp, R. and M. Vauclin, 1979. A note on estimating finite difference interblock hydraulic conductivity values for transient unsaturated flow problems. Water Resources Research, v. 15, no. 1, pp. 181-187.

Heermann, S.E., 1986. A laboratory experiment of axisymmetrical infiltration into a layered soil. Unpublished M.S. independent study, New Mexico Institute of Mining and Technology.

Heermann, S.E. and Stephens, D.B., 1986. A laboratory experiment of axisymmetrical infiltration into a layered soil. Transactions, American Geophysical Union, v. 67, no. 16.

Hillel, D., 1964. Infiltration and rainfall runoff as affected by surface crusts. Trans. Int. Soil Sci. Congr., 8th, Bucharest, v. 2, pp. 53-62.

Hillel, D. and Gardner, W.R., 1969. Steady infiltration into crust-topped profiles. Soil Science, v. 108, pp. 137-142.

Hillel, D. and H. Talpaz, 1976. Simulation of soil water dynamics in layered soils. Soil Science, v. 123, no. 1, pp. 54-62.

Hunt, B.W., 1971. Vertical recharge of unconfined aquifer. American Society of Civil Engineers, Journal of the Hydraulics Division, 97, HY7, pp. 1017-1020.

Huyakorn, P.S., Jones, B.G., Parker, J.C., Wadsworth, T.D., and White, H.O., 1986. Finite element simulation of moisture movement and solute transport in a large caisson. Report submitted to Environmental Science Group, HSE-12, by GeoTrans, Inc., Herndon, Virginia.

Huyakorn, P.S. and Pinder, G.S., 1983. Computational methods in subsurface flow. Academic Press.

Huyakorn, P.S., Thomas, S.D., Mercer, J.W., and Lester, B.H., 1983. SATURN: A finite element model for simulating saturated-unsaturated flow and radionuclide transport. Report prepared for Electric Power Research Institute, Palo Alto, California.

Huyakorn, P.S., Thomas, S.D. and Thompson, B.M., 1984. Techniques for making finite elements competitive in modeling flow in variably saturated porous media. Water Resources Research, v. 20, no. 8, pp. 1099-1115.

Jenkins, C.T., 1968. Techniques for computing rate and volume of stream depletion by wells. Ground Water, v. 6, no. 2, pp. 37-46.

Jeppson, R. and Nelson, R., 1970. Inverse formulation and finite difference solution to partially saturated seepage from canals. Soil Science Society of America Proceedings, 34, pp. 9-14.

Kazmann, R.G., 1948. The induced infiltration of river water to wells. Transactions of the American Geophysical Union, 29, pp. 85-92.

King, J.D., Hawley, J.W., Taylor, A.M., and Wilson, R.P., 1971. Geology and groundwater resources of central and western Dona Ana County, New Mexico. New Mexico Water Resources Research Institute, Hydrologic Report 1.

Lee Wilson and Associates, 1981. Water supply alternatives for El Paso. Prepared for El Paso Water Utilities Public Service Board, El Paso, Texas.

Leggat, E.R., Lowry, M.E., and Hood, J.W., 1963. Ground-water resources of the lower Mesilla Valley, Texas and New Mexico. U.S. Geological Survey, Water Supply Paper 1669-AA.

Longenbaugh, R.A., 1967. Mathematical simulation of a stream-aquifer system. Paper presented at the Third American Water Resources conference, San Francisco, California.

Marino, M.A., 1967. Hele-Shaw model study of the growth and decay of groundwater ridges. Journal of Geophysical Research, v. 72, pp. 1195-1205.

Marino, M.A., 1973. Water-table fluctuations in semipervious stream-unconfined aquifer systems. Journal of Hydrology, no. 19, pp. 43-52.

Matlock, W.G., 1965. The effect of silt-laden water on infiltration in alluvial channels. Ph.D. Dissertation, University of Arizona, Department of Civil Engineering.

McCord, J.T. and Stephens, D.B., 1987. Lateral moisture flow beneath a sandy hillslope without an apparent impeding layer. Hydrological Processes, v. 1, pp. 225-238.

McDonald, M.G. and Harbaugh, A.W., 1984. A modular three-dimensional finite-difference groundwater flow model. U.S. Geological Survey, Open File Report 83-875.

McLin, S.G., 1981. Validity of the generalized lumped parameter hydrosalinity model in predicting irrigation return flow. Ph.D. Dissertation, New Mexico Institute of Mining and Technology, Socorro, New Mexico.

McWhorter, D.B. and Sunada, D.K., 1979. Ground-water hydrology and hydraulics. Water Resources Publications, Fort Collins, Colorado, 290 pp.

McWhorter, D.B. and Nelson, J.D., 1979. Unsaturated flow beneath tailings impoundments. American Society of Civil Engineers, Geotechnical Division, 105, GT 11, pp. 1317-1334.

Moore, J.E., and Jenkins, C.T., 1966. An evaluation of the effect of groundwater pumpage on the infiltration rate of a semipervious streambed. Water Resources Research, v. 2, pp. 691-696.

Mualem, Y., 1984. Anisotropy of unsaturated soils. Soil Science Society of America Journal, 48, pp. 505-509.

Narasimhan, T.N., 1975. A unified numerical model for saturated-unsaturated groundwater flow. Ph.D. dissertation, University of California, Berkeley, CA.

Narasimhan, T.N. and Witherspoon, P.A., 1976. An integrated finite difference method for analyzing fluid flow in porous media. Water Resources Research, v. 12, no. 1, pp. 57-64.

Narasimhan, T.N. and Witherspoon, P.A., 1977. Numerical model for saturated-unsaturated flow in deformable porous media, 1. Theory. Water Resources Research, v. 13, pp. 657-664.

Narasimhan, T.N. and Witherspoon, P.A. 1978. Numerical model for saturated-unsaturated flow in deformable porous media, 3. Applications. Water Resources Research, v. 14, no. 6, pp. 1017-1034.

Narasimhan, T.N., Witherspoon, P.A. and Edwards, A.L., 1978. Numerical model for saturated-unsaturated flow in deformable porous media, 2. The algorithm. Water Resources Research, v. 14, pp. 255-261.

Neuman, S.P. and Witherspoon, P.A., 1970. Finite element method of analyzing steady seepage with a free surface. Water Resources Research, v. 6, pp. 889-897.

Neuman, S.P. and Witherspoon, P.A., 1971. Analysis of nonsteady flow with a free surface using the finite element method. Water Resources Research, v. 7, pp. 611-623.

Neuman, S.P., 1973. Saturated-unsaturated seepage by finite elements. American Society of Civil Engineers, Journal of the Hydraulics Division, 99, HY 12, pp. 2233-2250.

New Mexico State University (NMSU), Civil Engineering Department, 1956. Flow of Rio Grande River, Mesilla Valley, New Mexico, 1955. Unpublished report submitted to the Elephant Butte Irrigation District.

Newsom, J.M. and Wilson, J.L., 1987. The effect of ambient flow direction on pumping near a stream. Transactions, American Geophysical Union, v. 68, no. 67.

Ortiz, N.V., Duke, H.R., Sunada, D.K., and McWhorter, D.B., 1978. Artificial ground-water recharge with capillarity. American Society of Civil Engineers, Irrigation and Drainage Division, 104, I1, pp. 79-93.

Ortiz, N.V., McWhorter, D.B., Sunada, D.K., and Duke, H.R., 1978. Growth of groundwater mounds affected by in-transit water. Water Resources Research, v. 14, no. 6, pp. 1084-1088.

Oster, C.A., 1982. Review of ground-water flow and transport models in the unsaturated zone. Battelle Memorial Institute, Pacific Northwest Laboratory, NUREG/CR-2197, PNL-4427.

Palmquist, W.N. and A.I. Johnson, 1962. Vadose flow in layered and nonlayered materials. U.S. Geological Survey Prof. Paper 450-C, pp. C142-C143.

Peterson, D.M., Khaleel, R. and J. Hawley, 1984. Quasi three-dimensional modeling of groundwater flow in the Mesilla Bolson, New Mexico and Texas. New Mexico Water Resources Research Institute, Project No. 1-3-45645.

Philip, J.R., 1984. Steady infiltration from circular cylindrical cavities. Soil Science Society of America Proceedings, v. 48, pp. 270-278.

Philip, J.R., 1985. Scattering functions and infiltration. Water Resources Research, v. 21, no. 12, pp. 1889-1894.

Polubarinova-Kochina, P. Ya., 1962. Theory of ground water movement. Enlish translation by R.J.M. DeWiest, Princeton University Press, Princeton, N.J.

Prickett, T.A. and Lonnquist, C.G., 1971. Selected digital computer techniques for groundwater resource evaluation. Illinois State Water Survey, Bulletin 55.

Rao, N.H. and Sarma, P.G.S., 1980. Growth of ground-water mound in response to recharge. Ground Water, v. 18, no. 6, pp. 587-595.

Reeder, J.W., Freyberg, D.L., Franzini, J.B., and Remson, I., 1980. Infiltration under rapidly varying surface water depths. Water Resources Research, v. 16, no. 1, pp. 97-104.

Reeves, M., and Duguid, J.O., 1976. Water movement through saturated-unsaturated porous media: A finite-element Galerkin model. Oak Ridge National Laboratory Report ORNL-4927.

Reisenauer, A.E., 1963. Methods for solving problems of multidimensional, partially saturated steady flow in soils. Journal of Geophysical Research, v. 68, no. 20, pp. 5725-5733.

Reisenauer, A.E., Key, K.T., Narasimhan, T.N., and Nelson, R.W., 1982. TRUST: A computer program for variably saturated flow in multidimensional, deformable media. U.S. Nuclear Regulatory Commission, NUREG/DR-2360, PNL-3975.

Rorabaugh, M.I., 1956. Groundwater in northeast Louisville and Kentucky with reference to induced infiltration. U.S. Geological Survey Water Supply Paper 1369-B.

Rovey, C.E.K., 1975. Numerical model of flow in a stream aquifer system. Hydrology Paper 74, Colorado State University, Fort Collins, Colorado.

Schumm, S.A., 1961. Effect of sediment characteristics, on erosion and deposition in ephemeral stream channels. U.S. Geological Survey Prof. Paper 352-C.

Segerlind, L.J., 1976. Applied finite element analysis. John Wiley and Sons.

Sharp, J.M., 1977. Limitations of bank-storage model assumptions. Journal of Hydrology, 35, pp. 31-47.

Siegel, J., 1980. Numerical simulation of seepage beneath lined ponds. New Mexico Institute of Mining and Technology, unpublished M.S. independent study.

Sophocleus, M., 1985. The role of specific yield in groundwater recharge estimations: A numerical study. Ground Water, v. 23, no. 1, pp. 52-58.

Spalding, C.P., 1985. An evaluation of analytical methods to estimate drawdown and stream depletions by wells. New Mexico Institute of Mining and Technology, unpublished M.S. independent study.

Stephens, D.B., Cox, W. and Havlena, J., 1987. Field study of ephemeral stream infiltration and recharge. New Mexico Water Resources Research Institute, Project Nos. 1423655, 1423658.

Streltsova, T.D., 1974. Method of additional seepage resistances - theory and application. American Society of Civil Engineers, Journal of the Hydraulics Division, 100, HY8, pp. 1119-1131.

Tagaki, 1959. Analysis of the vertical downward flow of water through a two-layered soil. Soil Science, 90, pp. 98-103.

Taylor, R.L. and Brown, C.B., 1967. Darcy flow solutions with a free surface. Proceedings of the American Society of Civil Engineers, Hydraulics Division, v. 93, HY2, pp. 25-33.

Todd, D.K., 1980. Groundwater hydrology. Wiley and Sons, 535 pp.

Townley, L.R., and Wilson, J.L., 1980. Description of and user's manual for a finite element aquifer flow model, AQUIFEM-1. Ralph M. Parsons Laboratory for Water Resources and Hydrodynamics, Massachusetts Institute of Technology, Report No. 252.

Tracy, J.D. and Marino, M.A., 1987. Seepage into variably saturated porous medium. American Society of Civil Engineers, Journal of Irrigation and Drainage Engineering, v. 113, pp. 198-212.

Trescott, P.C., Pinder, G.F., and Larson, S.P., 1976. Finite difference model for aquifer simulation in two dimensions with results of numerical experiments. Techniques of Water-Resources Investigations of the U. S. Geological Survey, Book 7, Chapter C1.

Vauclin, M., Khanji, D. and G. Vauchard, 1979. Experimental and numerical study of a transient, two-dimensional unsaturated-saturated water table recharge problem. Water Resources Research, v. 15, no. 5, pp. 1089-1011.

Waechter, R.T. and J.R. Philip, 1985. Steady two- and three-dimensional flows in unsaturated soil: The scattering analog. Water Resources Research, v. 21, no. 12, pp. 1875-1887.

Warrick, A.W. and Nielsen, D.R., 1980. Spatial variability of soil physical properties in the field. In Application of Soil Physics, D. Hillel editor, Chapter 13, pp. 319-344, Academic Press.White, D.E., 1983. Summary of hydrologic information in the El Paso, Texas area, with emphasis on ground-water studies, 1903-1980. U.S. Geological Survey, Open File Report 83-775.

Wilson, C.A., White R.R., Orr, B.R. and Roybal, R.G., 1981. Water resources of the Rincon and Mesilla Valleys and adjacent areas, New Mexico. New Mexico State Engineer, Technical Report No. 43, 514 pp.

Wilson, C.A. and White, R.R., 1984. Geohydrology of the central Mesilla Valley, Dona Ana County, New Mexico. U.S. Geological Survey, Water-Resources Investigations Report 82-555, 144 pp.

Wilson, J.L., 1981. Analytical methods in groundwater hydrology. Boston Society of Civil Engineers - ASCE, Geotechnical Lecture Series for 1981, Groundwater Hydrology.

Winter, T.C., 1983. The interaction of lakes with variably saturated porous media. Water Resources Research, v. 19, no. 5, pp. 1203-1218.

Yeh, G.T., and Ward, D.S., 1980. FEMWATER: A finite element model of water flow through saturated-unsaturated porous media. Oak Ridge National Laboratory Report ORNL-5567.

Yeh, G.T., 1981. On the computation of Darcian velocity and mass balance in the finite element modeling of groundwater flow. Water Resources Research, v. 17, no. 5, pp. 1529-1534.

Yeh, T.C. Jim and Gelhar, L.W., 1983. Unsaturated flow in heterogeneous soils. In Role of the Unsaturated Zone in Radioactive and Hazardous Waste Disposal, ed. J. W. Mercer et al., pp. 71-79, Butterworth, Stoneham, Mass.

Yeh, T.C.J., Gelhar, L.W., and Gelhar, A.L., 1985a. Stochastic analysis of unsaturated flow in heterogeneous soils, 1. Statistically isotropic media. Water Resources Research, v. 21, no. 4, pp. 447-456.

Yeh, T.C.J., Gelhar, L.W., and Gutjahr, A.L., 1985b. Stochastic analysis of unsaturated flow in heterogeneous soils, 2. Statistically anisotropic media with variable α. Water Resources Research, v. 21, no. 4, pp. 457-464.

Yeh, T.C.J., Gelhar, L.W., and Gutjahr, A.L., 1985c. Stochastic analysis of unsaturated flow in heterogeneous soils, 3. Observations and applications. Water Resources Research, v. 21, no. 4, pp. 465-471.

Zaslavsky, D., 1964. Theory of unsaturated flow into a non-uniform soil profile. Soil Science, v. 97, pp. 400-410.

Zaslavsky, D. and G. Sinai, 1981. Surface Hydrology: IV-Flow in sloping layered soil. American Society of Civil Engineers, Journal of the Hydraulics Division, 107, HY1, pp. 53-64.